Reviews of Plasma Physics 24

Reviews of Plasma Physics

The series Reviews of Plasma Physics, founded in 1963, covers complex problems of modern theoretical plasma physics. It contains reviews presented by the leading Russian researchers in this field.

Reviews of Plasma Physics

Volume 24

Contributions to this Volume:

V. Rozhansky
Mechanisma of Transverse Conductivity and Generation
of Self-consistent Electric Fields
in Strongly Ionized Magnetized Plasma

O.G. Bakunin
Correlations and Anomalous Transport Models

Springer

Contributors:

Dr. V. Rozhansky
St. Petersburg State Polytecnical University
Polytechnicheskaya 29
195251 St. Petersburg, Russia
E-mail: rozhansky@phtf.stu.neva.ru

Dr. Oleg G. Bakunin
Kurchatov Institute
Nuclear Fusion Institute
Kurchatov sq. 1
123182 Moscow, Russia
E-mail: oleg_bakunin@yahoo.com

ISSN 0080-2050 e-ISSN 1574-8952
ISBN 978-0-387-71088-4 e-ISBN 978-3-540-74576-1

Library of Congress ControlNumber: 2008927236

Typesetting by VTEX using a Springer LaTeX macro
Cover design: eStudio Calamar Steinen

SPIN 12024315 57/3180/vtex
Printed on acid-free paper

9 8 7 6 5 4 3 2 1 0

springer.com

Preface

The “Reviews of Plasma Physics”, Vol. 24, contains two reviews. This book, as well as the previous volumes, presents reviews for specialists interested in plasma physics theory. In the review by V.A. Rozhansky, the problem of currents and self-consistent electric fields in the magnetized fully ionized plasma is considered. The situation in fully ionized plasma is completely different from that in solid state, gases, or partially ionized plasmas, where the current density is proportional to the electric field. In contrast, in a fully ionized magnetized plasma, a homogeneous electric field causes drift both for electrons and ions, while a current in the direction of the electric field is absent. A perpendicular current arises when the electric field is temporary or spatially dependent. Various mechanisms, when the perpendicular currents are driven by inertia, collisions with neutrals and different components of viscosity tensor are analyzed in the review. Current systems in a vicinity of a biased electrode are studied in connection with such applications as probes, unipolar arc formation, pellets, where two-dimensional or three-dimensional currents systems determine plasma dynamics, shielding properties, and current–voltage characteristics.

Since the end of 80th it became clear that self-consistent electric fields play the key role in the formation of improved confinement regimes (H-regimes) in tokamaks and stellarators. The poloidal drifts suppress the turbulence and hence the turbulent transport coefficients so that the transport barriers with steep density and temperature gradients and reduced transport coefficients are created. It is demonstrated that the electric field structure is consistent with the experimental observations.

More complicated issues when a radial current is generated in fusion devices are also considered. In a group of experiments performed on several tokamaks, an electrode was installed into the plasma (inside the separatrix or last closed flux surface), and the voltage was applied between this electrode and limiter or divertor plates. The current–voltage characteristic of such a system, the value of the effective transverse conductivity, and related problem of toroidal rotation generation in the plasma are analyzed in the review. In the last few years, new methods of radial current generation are widely discussed. One of them is connected with the formation of a stochastic magnetic layer in a separatrix vicinity by special coils (resonance magnetic perturbations). The aim is to suppress the edge localized modes, and this issue is rather critical for the successful operation of the International Thermonuclear Experimental Reactor (ITER). A radial current of electrons in a stochastic magnetic field should be accompanied by the same radial current of ions similar to the biasing experiments. As a result, the radial electric field, density, and temperature profiles are significantly modified, and edge modes are stabilized. The effective electron perpendicular conductivity in a stochastic magnetic field and the ion perpendicular conductivity, which are the key players in this situation, are also discussed in the review.

In the second review “Correlations and anomalous transport models” by O.G. Bakunin, numerous aspects of turbulent transport are considered. This review is intended to summarize the recent results from the multidisciplinary field of anomalous diffusion in turbulent plasma. A description of turbulent transport in the presence of coherent structures, convective rolls, zonal flows, and stochastic magnetic fields is a very complex problem.

From the methodological point of view, this review focuses on the general use of correlation estimates, quasilinear equations, and continuous-time random walk approach. The structure of some derivations, when they may be useful for more general purposes, is given in detail. Thus, the review provides a fairly informative treatment of seed diffusion effects in the framework of the correlation description. The relationship between Lagrangian and Eulerian correlation functions is discussed, and the problem of relations between stochastic instability and transport effects in a stochastic magnetic field is analyzed.

The author reviews in details the percolation approach to turbulent transport. Both the monoscale representation and multiscale approach are considered. The relationships between the transport and correlation exponents are derived. Nonlocal and memory effects in the framework of the continuous-time random walk model are treated. The kinetic (phase-space) approach describing ballistic modes of anomalous transport in complex systems is studied.

The topics to be discussed include renormalized quasi-linear equations, the Levy–Khintchine distributions, and intermittency effects. The author focuses on scaling arguments that play an important role in obtaining estimates of transport effects. A careful analysis of more important results obtained in this field is presented in this review.

Moscow, V.D. Shafranov
June 2008

Contents

1

Mechanisma of Transverse Conductivity and Generation of Self-Consistent Electric Fields in Strongly Ionized Magnetized Plasma

V. Rozhansky

1.1 Introduction

In many areas of plasma physics a problem of currents flowing perpendicular to a magnetic field in the presence of an electric field arises. This is also typical for fully ionized plasmas. However, the situation in fully ionized plasma is completely different from that in a solid state, gases, or partially ionized plasmas, where current is simply proportional to the applied electric field and the corresponding conductivity is determined by the collisions between charged particles and neutrals. In fully ionized plasmas, a homogeneous electric field causes $\vec{E} \times \vec{B}$ drift both for electrons and ions perpendicular to the electric field and no current in the direction of the electric field is generated.

On the other hand, perpendicular current is observed in many experiments. Among the examples are the so-called biasing experiments in tokamaks and other magnetic traps, where an electrode is installed into the plasma [inside the separatrix or last closed flux surface (LCFS)] and the voltage is applied between this electrode and the limiter or divertor plate. The whole flux surface is biased to the same potential due to extremely large parallel conductivity and the radial current flows from the core through the LCFS to another electrode (limiter). The current–voltage characteristic, which is measured in these experiments, corresponds to effective plasma resistance on the order of 1 Ω; such resistance was observed in experiments on CCT, TEXTOR, Tuman-3M, and other machines. So effective perpendicular conductivity exists and should be explained theoretically.

This issue is closely connected with the problem of the self-consistent radial electric field in tokamaks and other fusion devices since the self-consistent electric field corresponds to the particular point of the current–voltage characteristic, i.e., to the condition of zero net radial current flowing through the flux surfaces. And according to the modern conception the self-consistent electric field is a key element in the formation of transport barriers in the core and edge tokamak plasmas and in the transition to high confinement regimes.

At present, a theoretical understanding of the mechanisms responsible for the formation of the radial electric field in a tokamak and the radial current in the biasing experiments has been reached. The radial current in the presence of a poloidal component of the magnetic field accelerates plasma in the toroidal direction. The acceleration force is balanced by the radial transport of the toroidal momentum, which to a large extent is determined by turbulent (anomalous) mechanisms. Fortunately, from the parallel momentum balance the force associated with radial transport of toroidal momentum may be expressed through the parallel viscosity, which is connected, as known from neoclassical theory, with the radial electric field. As a result, in some important cases the radial effective conductivity, as well as the radial electric field in the absence of current, may be expressed through the pure classical or neoclassical viscosity coefficients.

The calculation of radial current and the self-consistent electric field in a cylinder whose axis is parallel to the magnetic field is significantly simpler than for a tokamak. Here, the first estimate of the self-consistent electric field has been done in the review by Braginskii; however, the case of nonuniform temperature adds complexity and the final result is not widely known in the thermonuclear community.

2D current systems in fully ionized plasma, where current flows both along and across the magnetic field, are important in many applications. Among them are probes in the magnetic field, which are used to measure local plasma parameters, in particular flush mounted probes in the divertor region of a tokamak. Their current–voltage characteristics, especially their slope, are determined by the mechanisms of the perpendicular conductivity. Similar 2D current systems in the vicinity of unipolar arcs are responsible for the ignition of the arcs and determine the dynamic of the arc, the value of the return current to the electrode, and other parameters. This area of plasmaphysics, in spite of its importance, is not very well developed and only several publications on the subject exist.

The 2D problem of currents and self-consistent electric fields is typical for edge tokamak plasma, including the divertor region, scrape-off layer, and vicinity of a separatrix. In recent years, numerical 2D fluid codes have been developed, where the self-consistent electric field is treated in detail and corresponding plasma fluxes across and along the magnetic field, caused by this field, have been analyzed. The structure of the electric field in the scrape-off layer is responsible for plasma flows to the divertor plates, while the radial field near the separatrix determines the transition to the regime of improved confinement. The theoretical progress in understanding these important issues is also the subject of this review.

Situations where perpendicular currents in fully ionized plasmas determine the whole dynamic are too diverse to consider in one review. Therefore, we tried to focus on the basic mechanisms and principles. In addition to those mentioned above, considered are polarization currents in the Alfven wave, which might often act as an effective wave conductivity, currents in a braided magnetic field, and few other typical cases. The main characteristic and practically important situations in strongly ionized plasma in the homogeneous magnetic field are considered, as well as more complicated effects in the inhomogeneous magnetic field, which are typical for magnetic traps.

Conductivity in gases or solids is a tensor, which links electric field and current density. In partially ionized plasmas this tensor can be easily calculated, and expressions for conductivity are widely used in many applications. In contrast, in fully ionized magnetized plasmas a homogeneous electric field causes $\vec{E} \times \vec{B}$ drift of electrons and ions with a common velocity. Such electric field does not create current at all. Therefore, in fully ionized plasma in the steady state case the current arises only along the inhomogeneous electric field (there is also polarization current, which is proportional to the temporal derivative of the electric field). The inhomogeneous $\vec{E} \times \vec{B}$ drifts produce different types of forces associated with inertia and viscosity, which in turn cause the current in the direction of the electric field. As a result, the current density in the steady state case is not directly proportional to the electric field itself but to its spatial derivatives. Hence, generally speaking, in the fully ionized plasma it is impossible to introduce the conductivity tensor as in the partially ionized plasma. One can talk only about an "effective" conductivity, which can be introduced analogously, using dimensional arguments.

In the presence of a strong turbulence (the situation typical for many plasma devices), the transport coefficients (diffusion, heat conductivity, and viscosity) become anomalous. There are many phenomenological approaches, in which an ad hoc anomalous conductivity is also introduced to explain experimentally observed transverse currents. However, due to the ambipolar character of plasma motion, which is connected with momentum conservation in Coulomb collisions, such anomalous conductivity does not exist. It can be shown rigorously that the only remaining currents are those controlled by inertia and viscosity with anomalous values of diffusion and viscosity coefficients.

The transverse currents in fully ionized plasma are rather small, since they contain a small parameter: the ratio of ion gyroradius to the plasma spatial scale. However, they are extremely important since the condition $\nabla \cdot \vec{j} = 0$ determines the distribution of self-consistent electric fields in the plasma and the corresponding $\vec{E} \times \vec{B}$ drifts, which to a large extent control plasma dynamics. The problems of calculating these perpendicular currents in strongly ionized plasmas, closing currents in the plasma, and generating self-consistent electric fields is analyzed in detail below.

In Sect. 1.2 a conductivity tensor in partially ionized plasma is derived and Einstein relations between mobility and diffusion tensors are discussed. In Sect. 1.3 an expression for the perpendicular current is derived from the momentum balance equations, and the contrast between the fully and partially ionized plasmas is emphasized. In Sect. 1.4 the effects of plasma acceleration, which are closely connected with the combination of polarization and ∇B currents, are considered. Acceleration of plasma clouds in space and in magnetic traps is discussed. The phenomenon of Alfven conductivity, where the polarization currents in the Alfven wave close a current circuit and compensate current inside the plasma inhomogeneity, is analyzed in Sect. 1.5. In Sect. 1.6 the simplest 1D situation of a plasma cylinder in the homogeneous magnetic field where the perpendicular viscosity determines the radial current is considered. Expressions for effective conductivity and for the ambipolar electric field, which corresponds to zero radial current, are derived. In Sect. 1.7 a more complicated 2D problem of the current systems in the vicinity of a biased electrode or spot of emission is studied. It is demonstrated that the current–voltage characteristics and potential and current distribution in the plasma is controlled by different mechanisms of effective transverse conductivity. Application to the problems of interpretation of the characteristics of flush-mounted probes and unipolar arc formation is analyzed. The specific question of currents closing when the perpendicular scale of the electrode is smaller than the ion gyroradius is studied in Sect. 1.8. Section 1.9 is devoted to the complicated problem of transverse currents in a tokamak. It is demonstrated that the parallel component of a viscosity tensor and the radial transport of toroidal momentum control transverse current. Interpretation of tokamak biasing experiments is also given. A similar analysis for reversed field pinch is presented in Sect. 1.10. In Sect. 1.11 the problem of electric fields and currents in the tokamak edge plasma is studied numerically, and the results of different transport codes are analyzed both for core and divertor plasmas. The key parameters which are responsible for the transition into the improved confinement regime (L–H transition) are investigated. A comparison with tokamak experiments is also presented in this section. Section 1.12 is devoted to the analysis of the perpendicular anomalous viscosity and corresponding transverse currents, which are generated by an electrostatic turbulence. The absence of ad hoc anomalous current is demonstrated. A quasilinear expression for the anomalous viscosity coefficient and effective perpendicular conductivity is analyzed for specific types of instabilities. The transverse conductivity in a braided magnetic field is calculated in Sect. 1.13. Here, the self-consistent electric field in systems with a stochastic magnetic field is also analyzed. In Sect. 1.14, electric fields which are generated in a shielding layer between a hot plasma and a solid state are considered. The plasma drifts there may significantly change the shielding properties of the cold ablated plasma, and may increase the ablation rate of the surface during such events as hard disruptions in a tokamak.

1.2 Conductivity Tensor in Partially Ionized Plasma

Consider magnetized partially ionized plasma with a homogeneous magnetic field $\vec{B}$ parallel to the z-axis and an electric field $\vec{E}$ parallel to the y-axis, Fig. 1.1. Let us assume for simplicity that cyclotron frequencies ω_{ce}, ω_{ci} of electrons and ions are much higher than the corresponding collision frequencies between the charged particles and neutrals ν_{eN}, ν_{iN}. In the strong magnetic field both electrons and ions drift in the crossed $\vec{E} \times \vec{B}$ fields in the x (Hall) direction with almost equal velocities $u_{\mathrm{e}x} = u_{\mathrm{i}x} = E/B$ and the current in the Hall direction is negligible. Collisions with neutrals produce friction forces $R_{\alpha x} = -\mu_{\alpha\mathrm{N}} n \nu_{\alpha\mathrm{N}} u_{\alpha x}$ in the reference frame where neutrals are at rest [α corresponds to the ions and electrons, respectively, $\mu_{\alpha\mathrm{N}} = m_\alpha m_{\mathrm{N}}/(m_\alpha + m_{\mathrm{N}})$]. These friction forces in their turn cause the drift of electrons and ions in the y direction, i.e., along the electric field, with the velocity $u_{\alpha y} = \pm R_{\alpha x}/eB$

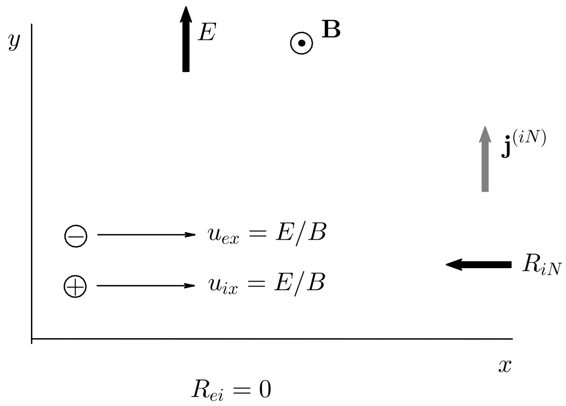

Fig. 1.1.

(the charge number of the ions is put to unity for simplicity). Finally,

$$u_{\alpha y} = \pm b_{\alpha\perp} E; \quad b_{\alpha\perp} = \frac{e\nu_{\alpha \mathrm{N}}}{\mu_{\alpha \mathrm{N}}\omega_{\mathrm{c}\alpha}^2}. \tag{1.1}$$

Here, $\omega_{\mathrm{c}\alpha} = eB/\mu_{\alpha\mathrm{N}}$. The coefficient $b_{\alpha\perp}$ is the mobility of a particle perpendicular to the magnetic field. Since the ion mobility is much larger than that of electrons, the conductivity is determined by the ion mobility:

$$\vec{j} = \sigma_{\mathrm{iN}} \vec{E}; \quad \sigma_{\mathrm{iN}} = \frac{ne^2\nu_{\mathrm{iN}}}{\mu_{\mathrm{iN}}\omega_{\mathrm{ci}}^2}. \tag{1.2}$$

The general expression for the mobility tensor for an arbitrary ratio between cyclotron and collision frequencies can be found in [1]. In the so-called elementary approximation, when collision frequencies are supposed to be independent of charged particle velocities, the mobility tensor has the form

$$\widehat{b}_\alpha = \begin{pmatrix} b_{\alpha\perp} & \pm b_{\alpha\wedge} & 0 \\ \mp b_{\alpha\wedge} & b_{\alpha\perp} & 0 \\ 0 & 0 & b_{\alpha||} \end{pmatrix}, \tag{1.3}$$

where

$$b_{\alpha||} = \frac{e}{m_\alpha \nu_{\alpha\mathrm{N}}}, \qquad b_{\alpha\perp} = \frac{e\nu_{\alpha\mathrm{N}}}{m_\alpha(\omega_{\mathrm{c}\alpha}^2 + \nu_{\alpha\mathrm{N}}^2)}, \qquad b_{\alpha\wedge} = \frac{e\omega_{\mathrm{c}\alpha}}{m_\alpha(\omega_{\mathrm{c}\alpha}^2 + \nu_{\alpha\mathrm{N}}^2)}.$$

The conductivity tensor is

$$\widehat{\sigma} = ne(\widehat{b}_{\mathrm{i}} - \widehat{b}_{\mathrm{e}}). \tag{1.4}$$

In the partially ionized plasmas, the mobility tensor is linked to the diffusion tensor by an Einstein relation [1]. In particular,

$$b_{\alpha\perp} = \frac{e}{T_\alpha} D_{\alpha\perp}, \tag{1.5}$$

where $D_{\alpha\perp}$ is the diffusion coefficient perpendicular to the magnetic field.

1.3 Main Mechanisms of Perpendicular Conductivity in Fully Ionized Plasma: Currents Caused by Viscosity, Inertia, Collisions with Neutrals, and ∇B, and Mass-Loading Currents

If a constant homogeneous electric field is applied perpendicular to $\vec{B}$ in fully ionized magnetized plasmas, the transverse conductivity in a steady state is zero, in contrast to the situation discussed in the previous section. Indeed, since the drift velocities of electrons and ions in the $\vec{E} \times \vec{B}$ direction coincide, the friction force between electrons and ions is absent and hence no particle fluxes and no currents along the electric field are generated. This result can easily be obtained in the reference frame moving with the drift velocity E/B: in this reference frame the electric field is absent due to the Lorentz transformation, and hence the current is also absent. Therefore, to obtain a finite transverse current in fully ionized plasmas in a steady state it is necessary to consider a nonuniform electric field or to take into account collisions with neutrals.

There have been several publications, in which the authors introduced an ad hoc anomalous conductivity for turbulent plasma in a manner similar to the case of slightly ionized plasma,

$$\vec{j} = \sigma_\perp \vec{E} = neb_\perp \vec{E} = ne^2 (D/T)\vec{E},$$

where D is the anomalous diffusion coefficient. However, it is clear that this expression in the fully ionized plasma is erroneous, independent of the question of whether anomalous transport is important or not. Indeed, in fully ionized plasmas, by changing the reference frame to that moving with $\vec{E} \times \vec{B}$ velocity, one can cancel the homogeneous electric field. Consequently, perpendicular current, which is proportional to the electric field itself, does not exist, and only current that is caused by the temporal or spatial derivatives of the electric field remains.

To obtain the expression for the perpendicular current we start with the momentum balance equation, which is the sum of the momentum balance equations for the ions and electrons:

$$m_\mathrm{i} \frac{dn\,\vec{u}_\mathrm{i}}{dt} = -\nabla p - \nabla \cdot \overleftrightarrow{\pi} + \vec{R}_\mathrm{iN} + [\vec{j} \times \vec{B}] + \vec{S}^{(\mathrm{M})}. \tag{1.6}$$

Here, $p = p_\mathrm{i} + p_\mathrm{e}$ is the total pressure, $\vec{R}_\mathrm{iN}$ is the ion–neutral friction force, and $\vec{S}^{(\mathrm{M})}$ are other momentum sources and sinks. Resolving the perpendicular current from this equation, we find

$$\vec{j} = \left[\vec{B} \times m_\mathrm{i} \frac{dn\,\vec{u}_\mathrm{i}}{dt}\right] \Big/ B^2 + [\vec{B} \times \vec{R}_\mathrm{iN}]/B^2 + [\vec{B} \times \nabla p]/B^2$$
$$+ [\vec{B} \times \nabla \cdot \overleftrightarrow{\pi}]/B^2 + \left[\vec{B} \times \vec{S}^{(\mathrm{M})}\right]/B^2. \tag{1.7}$$

1.3.1 Inertia Currents

The fourth term on the r.h.s. of (1.7) is a current caused by ion motion due to inertia forces, which we shall denote as $\vec{j}^{(\mathrm{in})}$. The corresponding velocities are usually much smaller than the velocities of the diamagnetic and $\vec{E} \times \vec{B}$ drifts, with small parameter proportional to the ratio of the ion gyroradius to the plasma spatial scale, and the ratio of inverse ion cyclotron frequency proportional to the time scale. Velocities associated with other currents in (1.7), i.e., with viscosity-driven currents and currents driven by ion–neutral collisions, are also small. Therefore, in the $d\vec{u}_\mathrm{i}/dt$ term it is possible to keep only the diamagnetic and $\vec{E} \times \vec{B}$ drifts and the parallel velocities. The exception is the drift caused by gyroviscosity, which is approximately the same as diamagnetic drift. In turbulent plasmas anomalous diffusive flux should also be taken into account, since anomalous diffusion represents averaged $\vec{E} \times \vec{B}$ drifts in stochastic electric fields. Thus, the expression for the ion velocity to be inserted into the $d\vec{u}_\mathrm{i}/dt$ term is

$$\vec{u}_\mathrm{i} \approx \vec{u}_{\mathrm{i}||} + \vec{u}_\mathrm{i}^{(\mathrm{dia})} + \vec{u}^{(\mathrm{E})} + \vec{u}^{(\mathrm{D})} + \vec{u}^{(\mathrm{vis})}, \tag{1.8}$$

where

$$\begin{aligned} \vec{u}_\mathrm{i}^{(\mathrm{dia})} &= \frac{[\vec{B} \times \nabla p_\mathrm{i}]}{enB^2}; \qquad & \vec{u}_\mathrm{i}^{(\mathrm{E})} &= \frac{[\vec{E} \times \vec{B}]}{B^2}; \\ \vec{u}_\mathrm{i}^{(\mathrm{D})} &= -D\nabla \ln n; \qquad & \vec{u}_\mathrm{i}^{(\mathrm{vis})} &= \frac{[\vec{B} \times \nabla \cdot \overset{\leftrightarrow}{\pi}_\mathrm{i}]}{enB^2}. \end{aligned} \tag{1.9}$$

Here, we use the simplest expression for anomalous diffusive flux. More detailed expressions will be given below for special cases. In the homogeneous magnetic field, the expression for the inertia current can thus be reduced to the form

$$\vec{j}^{(\mathrm{in})} = \frac{m_\mathrm{i}}{B^2}\left[\frac{\partial(n\vec{E} - \nabla p_\mathrm{i}/e)}{\partial t} + \vec{u}_\mathrm{i}^{(0)}\nabla(n\vec{E} - \nabla p_\mathrm{i}/e)\right], \tag{1.10}$$

where

$$\vec{u}_\mathrm{i}^{(0)} = \vec{u}_\mathrm{i}^{(\mathrm{E})} + \vec{u}_\mathrm{i}^{(\mathrm{D})}.$$

Here, the Braginskii expression for gyroviscosity [2] is used to cancel the contribution from the diamagnetic drift. For a more sophisticated expression in the inhomogeneous magnetic field see Sect. 1.11.

1.3.2 Currents Caused by Ion–Neutral Collisions

These currents might be important in strongly ionized plasmas in spite of the small density of neutral particles because other currents are also rather small. If neutral gas velocity may be neglected with respect to the ion velocity we have the same expression for the perpendicular mobility as in partially ionized plasmas, (1.1). In general, when the neutral gas velocity is taken into account, inserting expressions for the perpendicular ion velocity, (1.8) and (1.10), into the perpendicular friction force, we find

$$\vec{j}^{(\mathrm{iN})} = \sigma_{\mathrm{iN}}\big(\vec{E} + [\vec{u}_{\mathrm{N}} \times \vec{B}]\big) - \sigma_{\mathrm{iN}}\nabla p_{\mathrm{i}}/en \tag{1.11}$$

for the second term on the r.h.s. of (1.7), where σ_{iN} is the ion–neutral perpendicular conductivity, (1.2). For the important case of charge exchange collisions [1],

$$\sigma_{\mathrm{iN}} = \frac{nm_{\mathrm{i}}\langle V_{\mathrm{iN}}\sigma_{\mathrm{ex}}\rangle n_{\mathrm{N}}}{2B^2}.$$

1.3.3 Diamagnetic Currents

The third term on the r.h.s. of (1.7) is a diamagnetic current, which is almost divergence free. Indeed, its divergence is proportional to ∇B and equals zero in a homogeneous magnetic field. Sometimes, besides the diamagnetic current

$$\vec{j}^{(\mathrm{dia})} = [\vec{B} \times \nabla p]/B^2, \tag{1.12}$$

it is convenient to introduce the divergent part of the diamagnetic current [2]

$$\vec{\tilde{j}}^{(\mathrm{dia})} = p\left[\frac{[\vec{B} \times \nabla B]}{B^3} + \frac{\vec{B} \times (\vec{B}\nabla)(\vec{B}/B)}{B^3}\right], \tag{1.13}$$

which produces the same divergence as the diamagnetic current. This current corresponds to the guiding center drifts of charged particles in inhomogeneous magnetic fields and is responsible for plasma polarization. Other currents should balance the divergence of the diamagnetic current to provide quasineutrality. The corresponding example is discussed in the next section.

1.3.4 Viscosity-Driven Currents

The fourth term on the r.h.s. of (1.7) represents the viscosity-driven current:

$$\vec{j}^{(\mathrm{vis})} = [\vec{B} \times \nabla \cdot \overleftrightarrow{\pi}]/B^2. \tag{1.14}$$

In various situations this current can be caused by different components of ion viscosity tensor: by perpendicular viscosity, by gyroviscosity, or by parallel viscosity. Electron viscosity is much smaller and may usually be neglected.

The simplest case in which the perpendicular viscosity causes a current is illustrated by Fig. 1.2. Here, an inhomogeneous electric field is applied in the y direction perpendicular to the magnetic field. This field generates inhomogeneous $\vec{E} \times \vec{B}$ drifts in the x-direction $u_{\mathrm{i}x}^{(\mathrm{E})} = E_y(y)/B$. A similar contribution form ion pressure gradient comes from diamagnetic velocity $u_{\mathrm{i}x}^{(\mathrm{dia})} = -(\partial p_{\mathrm{i}}/\partial y)(enB)^{-1}$. Inhomogeneous velocities produce viscous force in the x-direction [2]:

$$-(\nabla \cdot \overleftrightarrow{\pi})_x = \frac{\partial}{\partial y}\eta_1\frac{\partial u_{\mathrm{i}x}}{\partial y}, \tag{1.15}$$

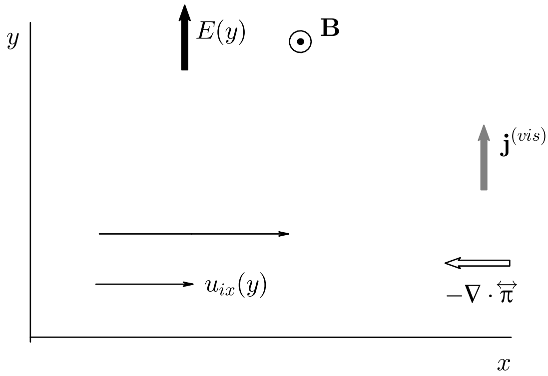

Fig. 1.2.

where $\eta_1 = 0.3nT_i\nu_i/\omega_{ci}^2$ is the classical perpendicular viscosity coefficient. In turbulent plasmas the perpendicular viscosity coefficient similar to the diffusion and heat conductivity coefficients may be anomalous. The connection between this coefficient and the spectrum of turbulent oscillations is analyzed in Sect. 1.12. However, for applications one can simply use the anomalous value η for the viscosity coefficient instead of the classical value η_1, where roughly $\eta = nm_iD$, with D being the anomalous diffusion coefficient.

Combining (1.14) and (1.15), we obtain

$$j_y^{(\mathrm{vis})} = -\frac{1}{B^2}\frac{\partial}{\partial y}\eta_1\frac{\partial}{\partial y}\left(E_y - \frac{\partial p_i}{en\partial y}\right). \tag{1.16}$$

The corresponding particle flux $\Gamma_y^{(\mathrm{vis})} = j_y^{(\mathrm{vis})}/e$ is rather small. Indeed, assuming $E_y \sim T/eL$, where L is the spatial scale, for the case of anomalous transport we have $\Gamma_y^{(\mathrm{vis})}/\Gamma_y^{(\mathrm{D})} \sim \rho_{ci}^2/L^2$ (ρ_{ci} is the ion gyroradius), i.e., anomalous viscous flux is much smaller than the anomalous diffusive flux. In the classical case the situation is quite different: this ratio is $(m_i/m_e)^{1/2}$ times larger, since classical diffusive flux is caused by the electron–ion collisions and the classical viscosity-driven current is proportional to the ion–ion collision frequency.

In the classical case (1.16) is strictly valid only for constant ion temperature. The reason consists in the fact that in general the ion temperature gradients and the corresponding heat fluxes cause additional viscosity (thermostress terms) [3], which in turn produce additional current proportional to the ion temperature gradient. We shall not consider this effect in detail and only present some results for special cases, see below.

Gyroviscosity terms in some cases may be combined with inertial terms, the corresponding example considered in Sect. 1.11. In many situations gyroviscosity produce divergence-free currents.

The contribution of the parallel viscosity to the perpendicular current is rather important. It is well known that the parallel viscosity is responsible for the difference between the perpendicular and parallel pressures. Physically, the perpendicular pressure should contribute to the diamagnetic current in (1.12) instead of the full pressure. Therefore, the viscosity-driven current $\vec{j}^{(\mathrm{vis})} = [\vec{B} \times (\nabla \cdot \overleftrightarrow{\pi}_{||})]/B^2$ should be added to the diamagnetic current in (1.12), and their sum represents the current caused by the perpendicular pressure. Furthermore, similarly to the diamagnetic current, current caused by the parallel viscosity is almost divergence-free. One can check this using the Braginskii expression for the parallel viscosity in a homogeneous magnetic field parallel to the z-axis:

$$\pi_{||xx} = \pi_{||yy} = -\eta_0 \left(\frac{\partial u_{\mathrm{i}x}}{\partial x} + \frac{\partial u_{\mathrm{i}y}}{\partial y} - \frac{2}{3} \nabla \cdot \vec{u}_{\mathrm{i}} \right), \tag{1.17}$$

where $\eta_0 = 0.96 n T_{\mathrm{i}} / \nu_{\mathrm{i}}$ is the parallel viscosity coefficient. Inserting (1.17) into (1.14) and taking the divergence, one obtains zero for the constant magnetic field. In the more complicated geometry it is convenient to use the following expression for the parallel viscosity tensor:

$$\pi_{||\alpha\beta} = (p_{||} - p_{\perp}) \left(\frac{B_\alpha}{B} \frac{B_\beta}{B} - \frac{1}{3} \delta_{\alpha\beta} \right). \tag{1.18}$$

This expression can be applied not only in the fluid case when the value $(p_{||} - p_{\perp})$ is known from the Braginskii expression, but also in low collisionality regimes when the viscosity tensor must be calculated using a kinetic approach. Analogously to the diamagnetic current, (1.13), in the inhomogeneous magnetic field it is convenient to introduce a divergent part of the current driven by the parallel viscosity

$$\vec{j}^{(\mathrm{vis}||)} = -\frac{\pi_{||}}{2} \frac{[\vec{B} \times \nabla B]}{B^3} + \pi_{||} \frac{\vec{B} \times (\vec{B} \nabla)(\vec{B}/B)}{B^3}, \tag{1.19}$$

where $\pi_{||} = 2/3(p_{||} - p_{\perp})$.

1.3.5 Mass-Loading Current

This current, which corresponds to the last term on the r.h.s. of (1.7), arises in the presence of a plasma source, for example in the ionization process, when the ionized particles move due to $\vec{E} \times \vec{B}$ drift. Injected ions or ions which are created during ionization do not have momentum in the $\vec{E} \times \vec{B}$ direction at first. They start to move over a cycloid in the crossed fields, and their average shift in the $\vec{E}$ direction is given by the cycloid radius $E/(\omega_{\mathrm{ci}} B)$. Therefore, the mass-loading current is proportional to the ion source intensity S [4, 5] (S is the number of ionized particles created per second):

$$j^{(\mathrm{ml})} = \frac{n m_{\mathrm{i}} S}{B^2} \vec{E}. \tag{1.20}$$

This current is important in space physics and in some situations in laboratory plasmas.

1.4 Inertial (Polarization) and ∇B Currents. Acceleration of Plasma Clouds in an Inhomogeneous Magnetic Field

Diamagnetic currents in an inhomogeneous magnetic field can produce strong polarization of plasma. Let us start with the classical example of acceleration of a plasma cloud by ∇B [6]. Consider a plasma cloud in the xy plane in a magnetic field parallel to the z-axis, which decreases in the x direction: $B = B_0(1 - x/R)$. The magnetic pressure is assumed to be much larger than that of the plasma so that the magnetic field is not perturbed by the plasma motion. Since the cloud is restricted in the z direction, the Boltzmann potential on the order of T_e/e should arise to prevent electrons from running along $\vec{B}$. We shall neglect this potential with respect to that caused by the ∇B current.

The physical picture of the acceleration is quite simple. The divergent part of the diamagnetic current in (1.13), which is responsible for polarization of the cloud, is directed vertically:

$$\tilde{j}^{(\mathrm{dia})} = -\frac{n(T_\mathrm{e} + T_\mathrm{i})}{BR}. \tag{1.21}$$

This current creates an electric field, which can roughly be considered to be vertical and homogeneous. The inertial current produced by this field is

$$j^{(\mathrm{in})} = \frac{nm_\mathrm{i}}{B^2}\frac{\partial E_y}{\partial t}. \tag{1.22}$$

This current compensates the vertical ∇B current and from the condition $j^{(\mathrm{in})} = -\tilde{j}^{(\mathrm{dia})}$ it follows that the vertical electric field increases with time:

$$E_y = \frac{Bc_\mathrm{s}^2}{R}t, \tag{1.23}$$

where $c_\mathrm{s} = \sqrt{(T_\mathrm{e} + T_\mathrm{i})/m_\mathrm{i}}$ is the speed of sound. The corresponding $\vec{E} \times \vec{B}$ velocity in the x direction also grows linearly with time:

$$u_x = gt; \qquad x = gt^2/2; \qquad g = c_\mathrm{s}^2/R. \tag{1.24}$$

Therefore, a simple estimate predicts acceleration of the plasma cloud towards the low field side.

However, this picture is oversimplified. In reality, charged particles move along equipotentials. Since there exist two potential extrema, plasma at the top and at the bottom of the cloud move in the negative x direction opposite to the center of the cloud and cloud acceleration is accompanied by its deformation. To describe this it is necessary to solve current continuity equation $\operatorname{div}\vec{j} = 0$. This has been done in [7]. For the inertial current, (1.10) is to be used, where the pressure gradient contribution is neglected with respect to the electric field term. After integrating the current continuity equation along the magnetic field we find [7]

$$\frac{\partial \Delta\varphi}{\partial t} + J(\varphi, \Delta\varphi) + \left[\frac{\partial \nabla\varphi}{\partial t} + J(\varphi, \nabla\varphi)\right]\nabla \ln N + \frac{\partial \ln N}{\partial y} = 0, \tag{1.25}$$

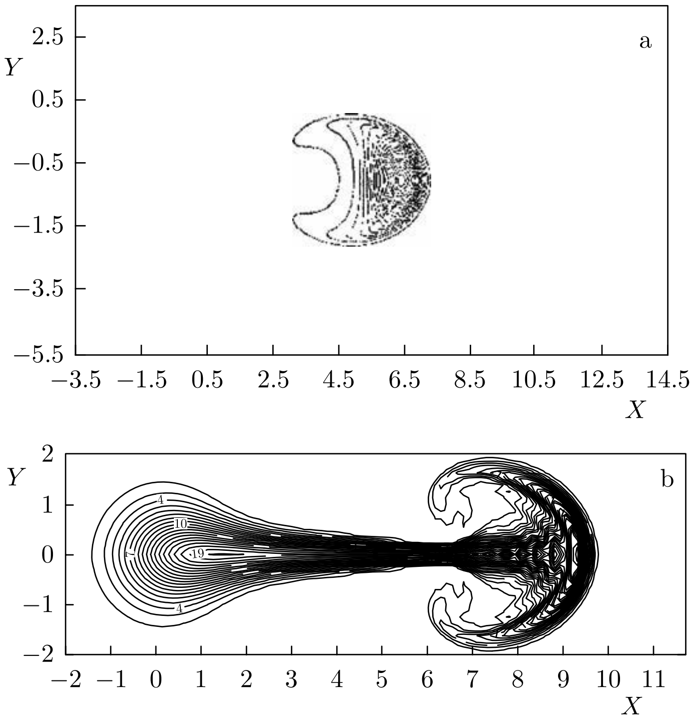

Fig. 1.3. **a** The isodensities for initially Gaussian cloud $N \sim \exp[-(x^2 + y^2)/a^2]$ at the moment $t = 4(aR)^{1/2}/c_s$. Coordinates are in the units of a; **b** The isodensities for the case of a constant plasma source $Q \sim \exp[-(x^2 + y^2)/a^2]$, which was switched on at $t = 0$, at $t = 5(aR)^{1/2}/c_s$

where $J(\alpha, \beta) = \frac{\partial\alpha}{\partial x}\frac{\partial\beta}{\partial y} - \frac{\partial\beta}{\partial x}\frac{\partial\alpha}{\partial y}$ and N is the cloud density integrated along the magnetic field, $N = \int_{-\infty}^{\infty} n\, dz$. The continuity equation for the particles is reduced to the form

$$\frac{\partial N}{\partial t} + J(\varphi, N) = 0. \tag{1.26}$$

Results of the numerical simulation of (1.25) and (1.26) with the boundary conditions $N \to 0$, $\varphi \to 0$ at infinity are shown in Fig. 1.3a [7]. The initial cloud moves in the x direction with an acceleration on the order of g, (1.24). The front of the cloud becomes much steeper because the vertical electric field and corresponding drift in the x direction are larger in the center of the cloud and smaller at its front. The sides of the cloud are left behind since particles rotate around potential extrema. The typical shape of the cloud resembles the cap of a mushroom.

The evolution of the plasma created by a constant plasma source is shown in Fig. 1.3b. To obtain this result one has to add particle source Q to the r.h.s. of particle continuity equation (1.26) and the term $-N^{-1}\nabla \cdot (Q\nabla\varphi) = 0$ to the r.h.s. of current continuity equation (1.25). The shape of the plasma cloud resembles a mushroom. Plasma density in the vicinity of the source and in the stem remains approximately constant. Here, the vertical ∇B current is balanced by the stationary part of the inertial current [the second term on the l.h.s. of (1.10)]. Hence, the charged particles are spatially accelerated in the inhomogeneous electric field and equipotentials converge along x in the stem region. As a result, the stem becomes thinner for larger values of x, while the vertical electric field becomes stronger. In the region of the cap, where the electric field is the largest and increases with time, plasma evolution is similar to that of a single cloud, so that the cap accelerates along x according to (1.24). At later stages the cloud is split into separate striations [7]. Such processes (albeit more complicated) are responsible for the acceleration of the evaporated plasma during pellet injection into a tokamak. Note that in tokamak geometry, due to the curvature of the magnetic field line, the nondivergent free part of the diamagnetic current is

$$\tilde{j}^{(\mathrm{dia})} = -\frac{2n(T_\mathrm{e} + T_\mathrm{i})}{BR}$$

instead of that given by (1.21). Hence, $g = 2c_\mathrm{s}^2/R$ in (1.24). Plasma acceleration in the tokamaks, predicted in [7], has been observed in several pellet experiments on ASDEX-Upgrade, DIII–D, and others [8–11]. Density perturbations (blobs), which have a similar mushroom shape, are also discussed as candidates for enhanced transport in the edge plasma of tokamaks [12, 13].

1.5 Alfven Conductivity

In the previous case we neglected currents in the ambient plasma surrounding a cloud. In reality, polarization of the cloud, which is caused by ∇B drifts or by cloud motion across a magnetic field, propagates along magnetic field lines with Alfven velocity. Inertial (polarization) currents of the Alfven wave flow perpendicular to the magnetic field and, together with parallel currents, close the currents inside the cloud. Parameters of the ambient plasma may be characterized by the so-called Alfven conductivity, which determines the ability of the ambient plasma to reduce polarization of the cloud and thus to reduce its $\vec{E} \times \vec{B}$ velocity.

This effect can be illustrated by considering deceleration of plasma inhomogeneity, which is infinite in the x direction and has initial velocity u_0 in this direction with respect to the ambient plasma [14], Fig. 1.4. Initial velocity u_0 is caused by $\vec{E} \times \vec{B}$ drift of the cloud in the x direction: $\vec{u}_0 = [\vec{E}_0 \times \vec{B}]/B^2$. The kinetic energy of the cloud is assumed to be small with respect to the magnetic energy so that the magnetic field is only slightly perturbed. Polarization of the cloud tends to spread along the magnetic field lines, thus creating an electric field in places where the ambient plasma was initially at rest. Hence, momentum is transferred from the cloud to the ambient plasma. If the skin time $\tau_\mathrm{s} = L_y^2 \sigma \mu_0$, where σ is the Spitzer conductivity and L_y is the cloud size in the y direction, is large with respect to the typical timescale of the problem, the polarization and the plasma drift velocity are spread along the magnetic field as an Alfven wave:

$$\frac{\partial^2 u_x}{\partial t^2} = c_\mathrm{A}^2 \frac{\partial^2 u_x}{\partial z^2}; \quad c_\mathrm{A}^2 = \frac{B^2}{\mu_0 m_\mathrm{i} n}. \tag{1.27}$$

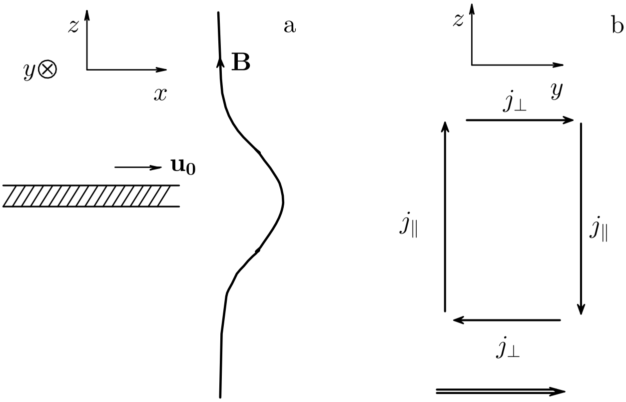

Fig. 1.4. Cloud (infinite in the x direction) in the zx (**a**) and zy (**b**) planes

The cloud itself also expands along $\vec{B}$ with a velocity on the order of the speed of sound. Since the Alfven wave is assumed to propagate over a much larger distance $L_A = c_A t$, it is possible to multiply (1.27) by $m_i n$ and integrate it along the magnetic field to the distance $\pm\delta$, which is much larger than the cloud size but is much smaller than L_A. Considering u_x as constant under the integral and taking into account the symmetry over z, after neglecting δ with respect to L_A we obtain

$$M \frac{\partial^2 u_x}{\partial t^2}\bigg|_{z=0} = \frac{B^2}{\mu_0} \frac{\partial u_x}{\partial z}\bigg|_{z=0}, \tag{1.28}$$

where $M = \int_{-\infty}^{\infty} n m_i \, dz$ is the integrated cloud mass.

Equation (1.28) can be used as a boundary condition for (1.27). The solution for $z \geq 0$ has the form

$$\begin{aligned} u_x &= u_0 \exp\left[\frac{2B^2}{\mu_0 M c_A^2}(z - c_A t)\right], \quad z \leq c_A t; \\ u_x &= 0, \quad z \geq c_A t, \end{aligned} \tag{1.29}$$

where the Alfven velocity is calculated for the ambient plasma. The velocity of the cloud at $z = 0$ decreases exponentially with the time scale $\tau_A = \mu_0 M c_A / 2B^2$. On the other hand, the distance over which the ambient plasma moves in the x direction increases as $c_A t$.

Since the electric field in the cloud and in the ambient plasma up to distances $z = \pm c_A t$ decreases with time, there is a negative inertial current flowing in the y direction. The net negative current (for positive z) is obtained by integrating along the magnetic field:

$$I = I_c + I_0 = \int_0^{c_A t} \frac{n m_i}{B^2} \frac{\partial E_y}{\partial t} \, dz = -\frac{2}{\mu_0 c_A} E_y,$$

where $E_y \equiv E_y(z=0) = u_0 B \exp(-t/\tau_A)$. There are two equal contributions to the current I. The first one, I_c, arises from integrating over the cloud itself, when E_y is taken at $z=0$ and the integral over $n(z)m_i$ gives $M/2$. This contribution corresponds to the current flowing inside the cloud. The second contribution, $I_0 = I_c$, is obtained by integrating the inertial current in the ambient plasma with constant density and electric field, which is determined by (1.29). This part of the current flows in the region $0 \le z \le c_A t$. From the current continuity equation it follows that the net current perpendicular to the magnetic field should be zero. Consequently, there should exist a third positive contribution to cancel current I. This current $I_F = -I$ flows at the front of the Alfven wave, where the plasma is accelerated from zero velocity up to u_0. Finally, we separate zero net transverse current into two different parts: the negative current of the cloud $I_c = -E_y/\mu_0 c_A$ and the positive net current of the ambient plasma $I_W = I_0 + I_F = E_y/\mu_0 c_A$. The latter can be rewritten in the form

$$I_W = \Sigma_W E_y; \quad \Sigma_W = \frac{1}{\mu_0 c_A}, \tag{1.30}$$

where the net conductivity Σ_W is called the Alfven conductivity.

In other words, ambient plasma with a propagating Alfven wave may be replaced by a simple resistance determined by (1.30) (one has to keep in mind that the same current flows on the other side of the cloud at negative z). The Alfven conductivity Σ_W may be used in many other problems to determine electric fields and current systems inside plasma clouds in the ionosphere and magnetosphere [14] and during pellet injection in tokamaks [7, 15, 16].

1.6 Perpendicular Viscosity, Radial Current, and Radial Electric Field in an Infinite Cylinder

In this section we demonstrate how the self-consistent electric field is formed in the simplest geometry. Consider a cylinder of low β fully ionized plasma infinite in the z direction, which is parallel to a homogeneous magnetic field. Neglecting viscosity, one can obtain from the perpendicular components of the momentum balance equations for electrons and ions the well-known classical result [2, 3], radial diffusion of a plasma column with the velocity

$$u_r^{(D)} = -D\frac{dn}{n\,dr} + \frac{D}{T_e + T_i}\left(\frac{1}{2}\frac{dT_e}{dr} - \frac{dT_i}{dr}\right). \tag{1.31}$$

This radial diffusion and thermodiffusion are often known as "automatically ambipolar" processes, which means that the radial velocities of electrons and ions are equal to each other and are given by (1.31) independently of the radial electric field. This result can be understood if the radial velocities of the charged particles are considered as drifts produced by azimuth friction forces, which are caused by azimuth particle diamagnetic fluxes and a radial temperature gradient (thermal force). Since friction forces acting on ions and electrons have the same value and different signs, they produce the same drift for electrons and ions in the radial direction.

In other words, the ambipolar character of the classical diffusion in the absence of viscosity is the result of momentum conservation during the collisions of charged particles. However, the azimuth component of perpendicular viscosity, in accordance with (1.6), produces radial current. Indeed, azimuth viscosity corresponds to the transfer of azimuth momentum in the radial direction due to ion–ion collisions. Hence, an inhomogeneous radial electric field and ion pressure gradient, which produce inhomogeneous azimuth $\vec{E} \times \vec{B}$ and ion diamagnetic drifts, cause the azimuth force applied to ions only. This viscosity force creates radial current, which, in accordance with (1.7) [similar to (1.16) for the slab case], is

$$j_r = -\frac{1}{B^2}\frac{d}{dr}\left[\eta_1 \frac{1}{r}\frac{d}{dr}\left(r\left(E_r - \frac{dp_\mathrm{i}}{en\,dr}\right)\right)\right]. \tag{1.32}$$

Here, the Braginskii expression for the perpendicular viscosity is used, which is valid for constant ion temperature.

In the absence of an electrode in the center of the plasma column the net radial current should be zero, as follows from the current continuity equation. Therefore, the ambipolar radial electric field corresponds to the Boltzmann distribution for ions:

$$E_r = \frac{T_\mathrm{i}}{e}\frac{d\ln n}{dr}. \tag{1.33}$$

In other words, the plasma center is biased negatively with respect to its periphery. This electric field causes such a rotation whereby the ion diamagnetic drift is canceled and thus the perpendicular viscosity force is turned to zero.

A more complicated situation with inhomogeneous ion temperature was analyzed in [17]. In this case, the additional perpendicular viscosity caused by the azimuth ion heat flux should be taken into account. It is proportional to the first and second derivatives of the ion temperature and density. The ambipolar radial electric field, which is calculated from the zero current condition, might be obtained using the expression for the viscosity tensor from [17, 18]:

$$E_r = \frac{T_\mathrm{i}}{e}\left\{\frac{d(nT_\mathrm{i})}{nT_\mathrm{i}\,dr} + \frac{19}{12}\frac{r}{T_\mathrm{i}}\int_0^r T_\mathrm{i}\frac{d}{dr'}\left(\frac{1}{r'}\frac{d\ln T_\mathrm{i}}{dr'}\right)dr' \right.$$
$$\left. + \frac{5}{12}\frac{r}{T_\mathrm{i}}\int_0^r \frac{1}{r'T_\mathrm{i}}\left(\frac{dT_\mathrm{i}}{dr'}\right)^2 dr' + \frac{11}{3}\frac{r}{T_\mathrm{i}}\int_0^r \frac{1}{r'}\frac{dT_\mathrm{i}}{dr'}\frac{d\ln n}{dr'}dr'\right\}. \tag{1.34}$$

The value and even the sign of the radial electric field generally depend on the ratio of the density and the ion temperature gradients.

1.7 Current Systems in Front of a Biased Electrode (Flush-Mounted Probe) and Spot of Emission

Perpendicular currents determine the structure of the current systems in magnetized plasma. Among the simplest 2D problems is that of closing currents in front of a biased electrode. The current distribution determines, for example, the current–voltage

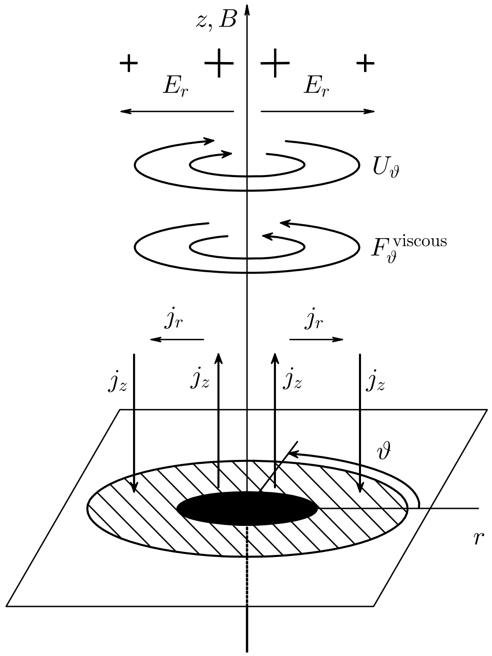

Fig. 1.5. Schematic of electric fields and currents generated by the viscosity mechanism in front of a biased electrode. The radial electric field E_r is caused by the potential rise in front of a positively biased electrode, u_ϑ is the azimuth $\vec{E} \times \vec{B}$ drift velocity, j_r is the viscosity driven current, j_z is the Spitzer current

characteristics of an electrostatic probe, which is a very simple diagnostic tool for investigating fully ionized plasma. In particular, electrostatic probes (especially so-called flush-mounted probes [19]) are widely used for the study of edge plasma in fusion devices, where they are often considered to be a standard diagnostic. Similar current systems exist in front of a spot of emission, which can transform under certain conditions into a unipolar arc [20].

We shall demonstrate the principles of current closing for the simplest geometry. Consider non-uniform plasma with density $n(z)$ restricted by a conductive surface. Electrons and ions are created in pairs by a source $S(z)$ and are driven towards the wall by a pressure gradient. Electron and ion temperatures are assumed to be constant. An infinite conductive surface is situated at $z = L$, while $z = 0$ is a plane of symmetry where the z-component of plasma velocity equals zero, Fig. 1.5. The magnetic field is parallel to the z-axis and is normal to the surface. An electrode with radius a centered at $r = 0$ and at $z = L$ is biased (for example, positively) to potential $V > 0$ with respect to the conductive surface. The longitudinal size of the electrode is unimportant because it is always smaller than the longitudinal scale of the potential perturbation. We assume that for modest applied voltages the plasma density in the vicinity of the electrode is only slightly perturbed due to the strong ambipolar anomalous diffusion across the magnetic field. The transverse diffusion can "wash out" the density perturbations caused by relatively small transverse currents.

1.7.1 Viscosity-Driven Perpendicular Currents

Let us start with the situation where the perpendicular viscosity determines the perpendicular current. In the absence of biasing (for $V = 0$) the plasma potential near the surface is equal to the floating potential, which equalizes electron and ion fluxes to the surface [21],

$$\varphi_{\mathrm{s}} = \varphi_{\mathrm{f}} = \frac{T_{\mathrm{e}}}{e} \ln \sqrt{\frac{m_{\mathrm{i}} T_{\mathrm{e}}}{2\pi m_{\mathrm{e}} (T_{\mathrm{e}} + \gamma T_{\mathrm{i}})}}. \tag{1.35}$$

When the electrode is biased positively with respect to the surface, the potential in the channel in front of it becomes larger than the floating potential, while at $r \to \infty$ the potential remains unperturbed. As a result, a radial electric field emerges, as shown in Fig. 1.5. This electric field produces $\vec{E} \times \vec{B}$ plasma drift in the azimuth direction. The plasma rotation is differential, because the radial electric field is a function of r. Therefore, the azimuth component of the ion perpendicular viscosity causes the radial ion current from the channel to compensate the space charge of electrons collecting by the probe. This mechanism was discussed in the previous section. The potential perturbation is spread along the magnetic field over a distance $l_{||}$ and the potential perturbation also causes longitudinal currents to the biased electrode and to the grounded surface. These currents are governed by the classical Spitzer conductivity. Due to the ion perpendicular current the zone of enhanced potential becomes much larger than the channel with the radius $r = a$, and, as a result, a return current to the surface is created to close the circuit. In this zone, $a < r \leq R$ plasma potential at the sheath edge is larger than φ_{f} and the ion flux to the surface exceeds that of the electrons.

The following boundary conditions should be imposed at the sheath edge:

$$\begin{aligned} j_{||}|_{z=L,\, r\leq a} &= e(\Gamma_{\mathrm{i}||} - \Gamma_{\mathrm{e}||}) = e\left[n_{\mathrm{s}} c_{\mathrm{s}} - n_{\mathrm{s}} \sqrt{\frac{T_{\mathrm{e}}}{2\pi m_{\mathrm{e}}}} \exp\left(-\frac{e(\varphi_{\mathrm{s}} - V)}{T_{\mathrm{e}}} \right) \right], \\ j_{||}|_{z=L,\, r> a} &= e(\Gamma_{\mathrm{i}||} - \Gamma_{\mathrm{e}||}) = e\left[n_{\mathrm{s}} c_{\mathrm{s}} - n_{\mathrm{s}} \sqrt{\frac{T_{\mathrm{e}}}{2\pi m_{\mathrm{e}}}} \exp\left(-\frac{e\varphi_{\mathrm{s}}}{T_{\mathrm{e}}} \right) \right]. \end{aligned} \tag{1.36}$$

Here, n_{s} and φ_{s} denote the density and the potential in plasma at the sheath edge, respectively, c_{s}, according to the Bohm criterion, is the speed of sound, $c_{\mathrm{s}} = \sqrt{(T_{\mathrm{e}} + \gamma T_{\mathrm{i}})/m_{\mathrm{i}}}$, and $\gamma = 1$ or $5/3$ for isothermal or adiabatic ions, respectively. For a floating electrode $V = 0$ the unperturbed density $n(z)$, the parallel velocity V_z, and the potential distribution in plasma should be calculated from the 1D momentum balance equations. In particular, the potential corresponds to the Boltzmann distribution for electrons: $\varphi = (T_{\mathrm{e}}/e) \ln(n/n_{\mathrm{s}}) + \varphi_{\mathrm{f}}$.

We shall now consider the transitional part of the I–V characteristic, where the applied potential is modest so that the current is far from the saturation current $I_i^{sat} < I \ll I_e^{sat}$. From the parallel component of the momentum balance equation for electrons we have

$$j_{||} = -\sigma\left(\frac{\partial\varphi}{\partial z} - \frac{T_e}{e}\frac{\partial \ln n}{\partial z}\right), \tag{1.37}$$

where $\sigma_{||} = 1.96ne^2/m_e\nu_{ei}$ is the Spitzer conductivity. The perpendicular current is given by (1.32). Neglecting the density perturbations, from the current continuity equation it is easy to obtain [22, 23]

$$\frac{\eta_1}{B^2}\frac{1}{r}\frac{\partial}{\partial r}\left(r\Delta^*\frac{\partial\psi}{\partial r}\right) = \sigma_{||}\frac{\partial^2\psi}{\partial z^2}, \tag{1.38}$$

where the perturbed potential ψ is defined as $\psi = \varphi - (T_e/e)\ln(n/n_s) - \varphi_f$, and

$$\Delta^* = \frac{1}{r}\frac{\partial}{\partial r}\left(r\frac{\partial}{\partial r}\right) - \frac{1}{r^2}.$$

Equation (1.38) should be solved with the boundary conditions in plasma

$$\left.\frac{\partial\psi}{\partial z}\right|_{z=0}, \qquad \psi|_{r\to\infty} \to 0, \tag{1.39}$$

and the boundary conditions at the sheath edge adjacent to the material surface, which is obtained by combining (1.36) and (1.37),

$$\begin{aligned} -\sigma_{||}\left.\frac{\partial\psi}{\partial z}\right|_{z=L,\, r\le a} &= e\left[n_s c_s - n_s\sqrt{\frac{T_e}{2\pi m_e}}\exp\left(-\frac{e(\psi_s+\varphi_f-V)}{T_e}\right)\right], \\ -\sigma_{||}\left.\frac{\partial\psi}{\partial z}\right|_{z=L,\, r> a} &= e\left[n_s c_s - n_s\sqrt{\frac{T_e}{2\pi m_e}}\exp\left(-\frac{e(\psi_s+\varphi_f)}{T_e}\right)\right]. \end{aligned} \tag{1.40}$$

When the applied voltage is small, $|V| < T_e/e$, boundary condition (1.40) can be linearized:

$$\begin{aligned} -\sigma_{||}\left.\frac{\partial\psi}{\partial z}\right|_{z=L,\, r\le a} &= en_s c_s\frac{e(\psi_s - V)}{T_e}, \\ -\sigma_{||}\left.\frac{\partial\psi}{\partial z}\right|_{z=L,\, r> a} &= en_s c_s\frac{e\psi_s}{T_e}. \end{aligned} \tag{1.41}$$

The longitudinal scale $l_{||}$ of the potential perturbation can be estimated from this condition. Estimating $\partial\psi/\partial z$ as $\psi/l_{||}$, we find

$$l_{||} = \frac{\sigma T_e}{n_s c_s e^2} = \frac{\sqrt{T_e/m_e}\sqrt{m_i/m_e}}{0.51\nu_{ei}\sqrt{1+T_i/T_e}}. \tag{1.42}$$

The longitudinal scale of potential perturbation is determined by the Spitzer conductivity and is independent of the viscosity coefficient.

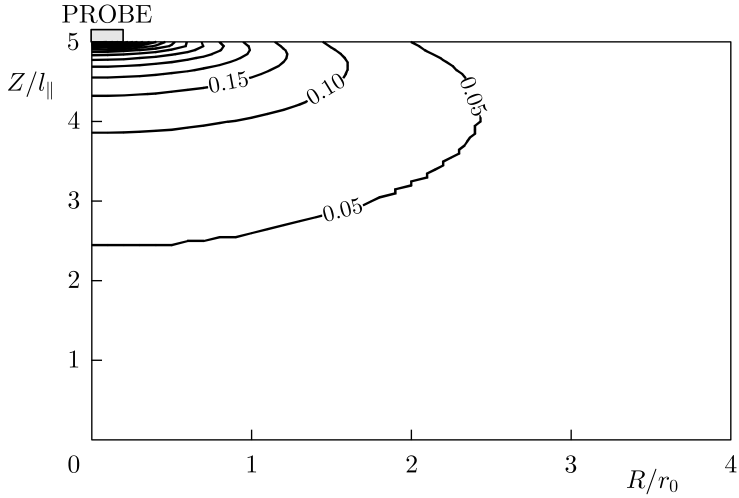

Fig. 1.6. Equipotentials for normalized perturbed potential $\Phi = e\psi/T_{\mathrm{e}}$, $a/R_0^{(\mathrm{vis})} = 0.2$, $L/l_{||} = 5.0$. The potential perturbation is normalized to unity at $r = 0$, $z = L$

The perpendicular scale $R_0^{(\mathrm{vis})}$ of the potential perturbation can be obtained from (1.38) and (1.42). For the Braginskii viscosity coefficient η_1 in (1.38)

$$R_0^{(\mathrm{vis})} = \left(\frac{3}{5}\frac{T_{\mathrm{e}}/T_{\mathrm{i}}}{1 + T_{\mathrm{i}}/T_{\mathrm{e}}}\right)^{1/4} \frac{\sqrt{T_{\mathrm{i}}/m_{\mathrm{i}}}}{\omega_{\mathrm{ci}}} \left(\frac{m_{\mathrm{i}}}{m_{\mathrm{e}}}\right)^{1/8}. \tag{1.43}$$

If η_1 is replaced by anomalous viscosity coefficient η, we have

$$R_0^{(\mathrm{vis})} = \left(\frac{3}{5}\frac{T_{\mathrm{e}}/T_{\mathrm{i}}}{1 + \gamma T_{\mathrm{i}}/T_{\mathrm{e}}}\right)^{1/4} \frac{\sqrt{T_{\mathrm{i}}/m_{\mathrm{i}}}}{\omega_{\mathrm{ci}}} \left(\frac{m_{\mathrm{i}}}{m_{\mathrm{e}}}\right)^{1/8} \left(\frac{\eta_1}{\eta}\right)^{1/4}. \tag{1.44}$$

For the small applied potentials, (1.38) was solved both analytically and numerically in [22, 23]. The calculated normalized potential perturbation $\Phi = e\psi/T_{\mathrm{e}}$ is shown in Figs. 1.6 and 1.7 for the case when the electrode radius a is smaller than $R_0^{(\mathrm{vis})}$. It can be clearly seen that the longitudinal scale of the potential perturbation is $l_{||}$, while the transverse scale is on the order of $R_0^{(\mathrm{vis})}$. The variation of the mean free path does not change the transverse scale of the perturbation, which remains the same for both Figs. 1.6 and 1.7. On the contrary, the longitudinal scale increases with λ_{mfp} in the more collisionless regime. The scale $R_0^{(\mathrm{vis})}$ determines the radius of the return current to the conductive surface.

For the electrode, which is small with respect to the current collecting zone radius ($a < R_0^{(\mathrm{vis})}$), and for the small applied voltages V, the current I to the electrode can be easily calculated. Indeed, since the net current to the electrode and to the conductive surface is zero, the perturbed potential ψ_{s} is small with respect to V. Hence, according to (1.41)

$$I = \pi e n_{\mathrm{s}} c_{\mathrm{s}} a^2 eV/T_{\mathrm{e}} = I_{\mathrm{i}}^{\mathrm{sat}} eV/T_{\mathrm{e}}. \tag{1.45}$$

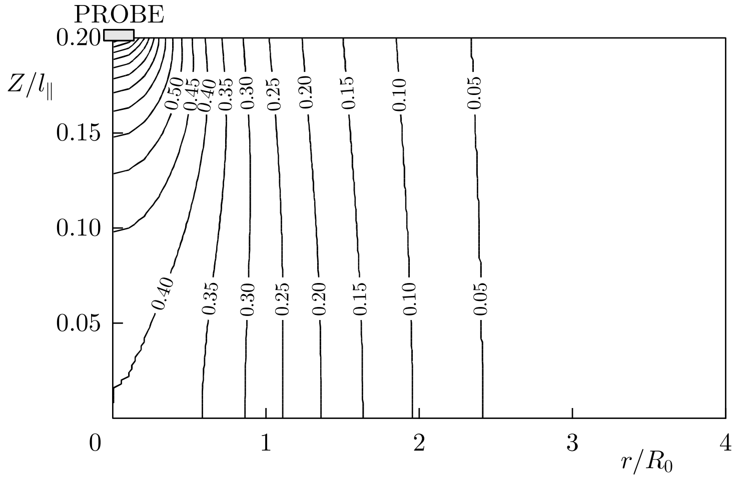

Fig. 1.7. Equipotentials for normalized perturbed potential $\Phi = e\psi/T_e$, $a/R_0^{(vis)} = 0.2$, $L/l_{||} = 0.2$. The potential perturbation is normalized to unity at $r = 0$, $z = L$

This expression justifies the widely used method of determining the electron temperature from the slope of current voltage characteristic (see, e.g., [24] and the literature therein)

$$T_e^{s\tan d} = eI_i^{sat}\frac{dV}{dI}\bigg|_{V=0}. \tag{1.46}$$

The situation when the electrode radius a is larger than $R_0^{(vis)}$ is quite different. In this case, electron current to the electrode is collected not by the whole electrode area but by the band of width $R_0^{(vis)}$ at its periphery. Due to the finite transverse conductivity, the return current collecting zone at the surface and the band at the electrode have the same scale $R_0^{(vis)}$. The potential perturbation is, therefore, on the order of V to cancel the current to the center of the electrode [see (1.35)]. The remaining part of the current to the electrode, as well as the current with the opposite sign to the conductive surface, can be estimated as

$$I \sim \frac{\sigma_{||}V}{l_{||}}S^{return} \sim en_s c_s \frac{eV}{T_e}S^{return} = kI_i^{sat}\frac{eV}{T_e}\frac{S^{return}}{S^{electrode}}. \tag{1.47}$$

Numerical simulations [22, 23] support this estimate and, moreover, give the exact value of the numerical coefficient $k = 0.5$. We can conclude that the current to the large electrode [see (1.47)] is significantly smaller than that given by (1.45). The electron temperature calculated from the slope of the I–V characteristic is

$$T_e = keI_i^{sat}\frac{dV}{dI}\bigg|_{V=0}\frac{S^{return}}{S^{electrode}}. \tag{1.48}$$

It is significantly smaller than the standard expression (1.46). This fact can explain some unrealistic values of electron temperature measured in several regimes in tokamak edge plasma using standard expression (1.46); for more details see [25].

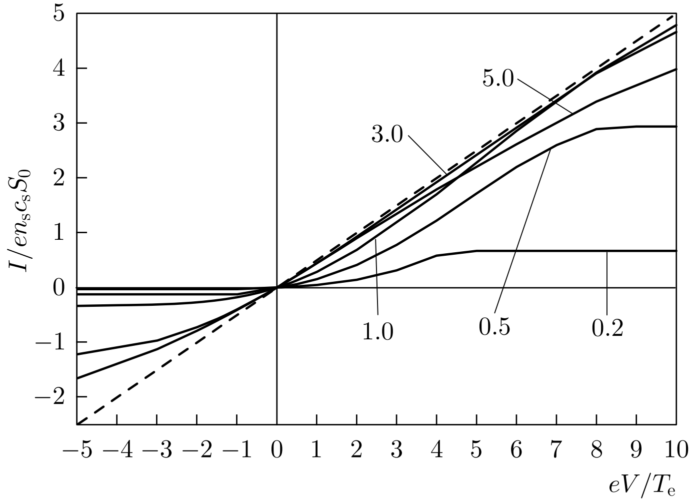

Fig. 1.8. Calculated I–V characteristics for different electrode sizes (the ratio $a/R_0^{(\mathrm{vis})}$ is specified in the rectangle for each plot). The broken line corresponds to (1.47) with $k = 0.5$

When the applied positive voltage V is on the order of or larger than T_e/e, one has to impose nonlinear boundary conditions, (1.40). The nonlinear regime was simulated in [22, 23]. The potential in front of the electrode remains on the order of V, since the potential difference between the plasma and the electrode should be on the order of the floating potential, otherwise large electron thermal current would flow to the electrode. This potential decreases with the scale $R_0^{(\mathrm{vis})}$ and, therefore, the return current and the current to the electrode are given by (1.47). In other words, the transitional part of the current–voltage characteristic of the electrode is close to the linear function of the applied potentials. An example of the simulation is shown in Fig. 1.8.

For very large positive applied potentials, the perpendicular ion flux, which is proportional to the viscosity driven current, becomes close to the particle diffusive flux and the density in front of the electrode is depleted. This situation corresponds to the electron saturation current. In fact, electron saturation current can be calculated as diffusive flux to a depleted channel of length $l_{||}$ in front of the electrode [26]. It should be noted that an attempt to estimate electron saturation current as maximal possible return current, which is proportional to the ion thermal flux to the area of radius $R_0^{(\mathrm{vis})}$ [27], is erroneous. The reason consists in the fact that the radius of the current-collecting zone increases with applied voltage [22, 23], and the resulting current is significantly larger.

1.7.2 Currents Driven by Ion–Neutral Collisions

When this mechanism dominates the perpendicular current is proportional to the electric field itself. Neglecting density perturbations and assuming small neutral velocity, according to (1.11) we have

$$\vec{j}^{(\mathrm{iN})} = -\sigma_{\mathrm{iN}}\nabla_{\perp}\varphi = -\sigma_{\mathrm{iN}}\nabla_{\perp}\psi. \tag{1.49}$$

Substitution of this current into the current continuity equation yields the Laplace equation

$$\frac{n_0\mu_{\mathrm{iN}}\nu_{\mathrm{iN}}}{B^2}\Delta_{\perp}\psi + \sigma_{||}\frac{\partial^2\psi}{\partial z^2} = 0. \tag{1.50}$$

Since the longitudinal scale of the potential perturbation is determined by the boundary conditions (1.40), (1.41), it remains the same as in the previous case and is given by (1.42). The perpendicular scale, which can be estimated from (1.50), is

$$R_0^{\mathrm{i-N}} = \sqrt{\frac{n_0\mu_{\mathrm{iN}}\nu_{\mathrm{iN}}l_{||}^2}{B^2\sigma_{||}}} \sim \rho_{\mathrm{ci}}\sqrt{\frac{\nu_{\mathrm{iN}}}{\nu_{\mathrm{ii}}}}\left(\frac{m_{\mathrm{i}}}{m_{\mathrm{e}}}\right)^{1/4}. \tag{1.51}$$

Equation (1.50) has been solved analytically in [23, 25] with the linearized boundary conditions from (1.41), and with the nonlinear boundary conditions in [23]. It was demonstrated that the results of the previous section remain valid after the substitution $R_0^{\mathrm{i-N}} \to R_0^{(\mathrm{vis})}$.

1.7.3 Inertia Currents

If a global convective flux across the magnetic field exists in the plasma, inertia currents arise. Such a flux may be produced by $\vec{E} \times \vec{B}$ drift in a global electric field or by low frequency large-scale turbulent electric fields. In [23, 25] a 2-D case with a biased electrode being a band of width $2a$ infinite in the y direction is considered. A constant plasma velocity u_{d} in the x direction is responsible for the transverse current

$$j_x = -\frac{n_0 m_{\mathrm{i}} u_{\mathrm{d}}}{B^2}\frac{\partial^2\varphi}{\partial x^2}. \tag{1.52}$$

Substitution of this expression into the current continuity equation yields

$$\frac{n_0 m_{\mathrm{i}} u_{\mathrm{d}}}{B^2}\frac{\partial^3\psi}{\partial x^3} + \sigma_{||}\frac{\partial^2\psi}{\partial z^2} = 0. \tag{1.53}$$

Again, as in the previous two cases, the longitudinal scale is given by (1.42), while the perpendicular scale of the potential perturbation should be estimated from (1.53):

$$R_0^{\mathrm{inertia}} = \left(\frac{n_0 m_{\mathrm{i}} u_{\mathrm{d}} l_{||}^2}{B^2\sigma_{||}}\right)^{1/3} \sim \rho_{\mathrm{ci}}\left(\frac{u_{\mathrm{d}}\lambda_{\mathrm{mfp}}}{c_{\mathrm{s}}\rho_{\mathrm{ci}}}\sqrt{\frac{m_{\mathrm{i}}}{m_{\mathrm{e}}}}\right)^{1/3}. \tag{1.54}$$

Equation (1.53) has been solved analytically in [23, 25]. An example of the potential perturbation distribution in the plasma is shown in Fig. 1.9. In contrast to the previous two cases, the potential perturbation is asymmetric in the direction of the convection. However, the expression for the I–V characteristic again has the universal character of (1.47) with the substitution $R_0^{\mathrm{inertia}} \to R_0^{(\mathrm{vis})}$ (for further details see [23]).

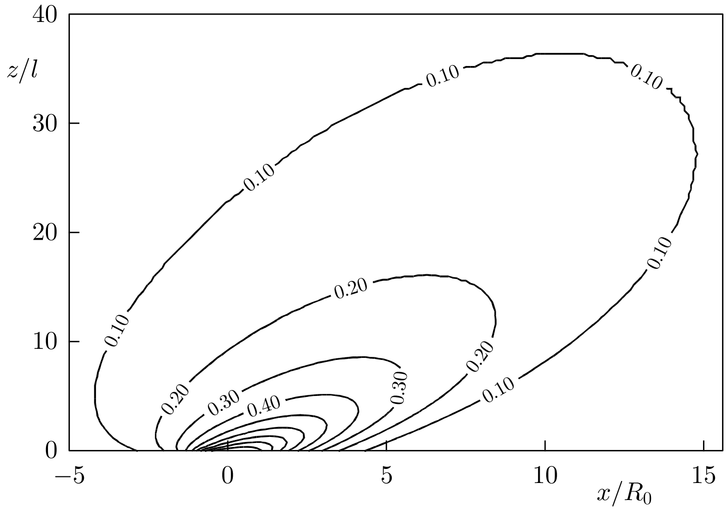

Fig. 1.9. Example of the equipotentials for normalized perturbed potential $\Phi = e\psi/T_e$, when the transverse current is caused by inertia for $a/R_0^{(\text{inertia})} = 0.2$, $L/l_{||} = 5.0$. The perturbed potential is normalized to unity at the middle of the probe

1.7.4 General Situation

Under real conditions three mechanisms of the effective transverse conductivity may act simultaneously. To choose the dominating mechanism it is necessary to compare the three perpendicular scales of the current-collecting zone given by (1.43), (1.44), (1.51), and (1.54). The largest value of R_0 corresponds to the largest perpendicular current in the system, which closes the current loop. The corresponding criteria can be found in [23, 25].

The model described above can be easily generalized to the case of an inclined magnetic field [23]; it is only necessary to replace the electrode size by its projection across the magnetic field.

One more condition is connected with the assumption of the unperturbed plasma density. This assumption remains valid if the perpendicular diffusive flux $\delta n D/R_0$ (for $a \sim R_0$), which balances the perpendicular flux associated with current $j_\perp/e$ in the particle continuity equation, corresponds to small $\delta n/n_0$. In the case of a viscosity dominated mechanism of the effective transverse conductivity, for example, this condition is violated even for applied voltages on the order of T_e/e if both perpendicular viscosity and diffusion coefficients are classical. In contrast, for the anomalous coefficients $\eta \sim m_i n D$ and $V \sim T_e/e$ the value $\delta n/n_0 \sim \rho_{ci}^2/R_0^2$ is small. However, for sufficiently large positive applied voltage δn becomes close to n_0 and it is necessary to solve both current and particle continuity equations simultaneously. This situation corresponds to the electron saturation current, which has been calculated in [26].

1.7.5 Spot of Emission

Spots of enhanced emission in a magnetic field are often observed on the metal surfaces and walls of fusion devices (see, e.g., [28]). Under some conditions a unipolar arc can be ignited in these places. The term unipolar arc was first introduced by Robson and Thoneman [29] to describe an arc discharge with a metal surface as a cathode and plasma as an anode, which is ignited without applying any external voltage. Many authors have reported arcing of the walls of fusion machines, limiters, or divertor plates; see, for example, [30, 31]. The surface erosion produced by arcs is one of the serious factors that restrict reactor operation, especially during disruptions when dense and hot plasma is brought in contact with the surface.

It is well understood that unipolar arcs can exist only when there is a return current flowing from the plasma to the surface to close the current circuit. Before the ignition of an arc, the potential perturbation in the plasma in front of a spot of enhanced emission and the corresponding current system are quite similar to those discussed in the previous sections for the biased electrode. Indeed, electron current from the spot of emission reduces the potential in front of it with respect to the floating potential. Furthermore, the radial electric field arises and causes the radial current to be dependent on the dominating mechanism of effective perpendicular conductivity. The reduced potential also creates the return current to the electrode. The potential perturbation is thus described by one of (1.38), (1.50), or (1.53). The boundary condition at the surface should be replaced by

$$-\sigma \frac{\partial \psi}{\partial z}\bigg|_{z=L} = e\left(n_{\mathrm{s}} c_{\mathrm{s}} - n_{\mathrm{s}} \sqrt{\frac{T_{\mathrm{e}}}{2\pi m_{\mathrm{e}}}} \exp\left(-\frac{e(\psi_{\mathrm{s}} + \varphi_{\mathrm{f}})}{T_{\mathrm{e}}} \right) + \Gamma_{\mathrm{em}} \right). \tag{1.55}$$

Here, Γ_{em} is the flux of emitted electrons, which is a function of the radius. For example, one can choose

$$\Gamma_{\mathrm{em}}(\rho) = \frac{I_{\mathrm{em}}}{e\pi a^2} \exp\left(-\frac{r^2}{a^2} \right).$$

In the linear case, when the potential perturbation is small, the solution is the same as for the case of a biased electrode [20].

When the emission current is large and the unipolar arc is ignited, the solution obtained is still valid outside the arc where the plasma is unperturbed and the return current is collected. On the basis of the solution obtained a criterion of unipolar arc formation has been put forward in [20]. The criterion is based on two experimental parameters, which are usually known for each material: the cathode voltage drop of the arc and the minimal current typical for the arc. When the reduced potential in front of the emitting surface is larger than the cathode voltage drop of the arc and the return current exceeds the minimal current typical for the arc, then ignition of the arc is possible. The potential drop between the plasma and the spot of emission as a function of emission current is calculated numerically as in the previous sections. In this criterion, in contrast to previous estimates, the return current, which is determined by the perpendicular viscosity, is properly calculated.

1.8 Currents in the Vicinity of a Biased Electrode That is Smaller Than the Ion Gyroradius

When the transverse size of an electrode a is smaller than the ion gyroradius ρ_{ci} (but still larger than the electron gyroradius ρ_{ce}), the effective transverse current is quite different from that considered in the previous section. Now ions can move freely across the magnetic field and the parallel electron current, which should be closed in the plasma, restricts the perpendicular current. The I–V characteristic of a small electrode (probe) in fully ionized plasmas was calculated numerically by Sanmartin [32]. However, his results were seldom used. One reason consists in the fact that the perpendicular diffusivity in the fusion plasmas is anomalous while calculations in [32] were performed for the classical case.

The problem was analytically approached recently in [33]. It was demonstrated that, on one hand, the I–V characteristic could be represented by a simple analytical expression, which coincides with simulation [32], and, on the other hand, experiments on the TdeV tokamak [34] with small probes can be described by the theory with the classical diffusion coefficient. The approach of [33] is similar to that used for weakly ionized plasma by Bohm [35] (saturation currents) and Rozhansky and Tsendin [36] (whole characteristics), where the ion mobility across the magnetic field is much larger than that of the electrons. Similar ideas were also discussed in [37], however the erroneous attempt has been made to apply this approach to the case of fully ionized plasma and a large electrode, which is analyzed in the previous section.

Let us consider a homogeneous plasma of density n_0. When the electrode is biased positively it collects electrons and the plasma density is reduced in an ellipsoidal zone having characteristic dimensions a and $l_{||}$, Fig. 1.10. In contrast to the previous case, we assume the classical type of diffusivity, since at scales a smaller than the ion gyroradius it is unlikely to have intensive plasma fluctuations. Therefore, perpendicular diffusion is unable to compensate plasma depletion in front of the electrode. The ions can move freely across $\vec{B}$ substantially faster than the electrons. Thus, the ions should be trapped in the electron ellipsoid, i.e., the electric field should be balanced by the ion pressure gradient, and the Boltzmann distribution is established for the ions:

$$\varphi = -\frac{T_i}{e}\ln\frac{n}{n_0} + \varphi_f. \tag{1.56}$$

The electron fluxes can be obtained from the parallel and perpendicular projections of the momentum balance equation for electrons:

$$\Gamma_{e||} = \Gamma_{i||} - D^*_{e||}\frac{\partial n}{\partial z}, \qquad \vec{\Gamma}_{e\perp} = -D_{e\perp}\nabla_\perp n, \tag{1.57}$$

where $D^*_{e||} = (T_e + T_i)/(0.51 m_e \nu_{ei})$ is the effective parallel diffusion coefficient of electrons and $D_{e\perp} = (T_e + T_i)\nu_{ei}/(m_e\omega_{ce}^2)$ is the classical perpendicular diffusion coefficient.

The ions are gathered to the electrode from the other region whose size is on the order of the ion gyroradius ρ_{ci}, Fig. 1.10, where (1.56) and (1.57) are violated.

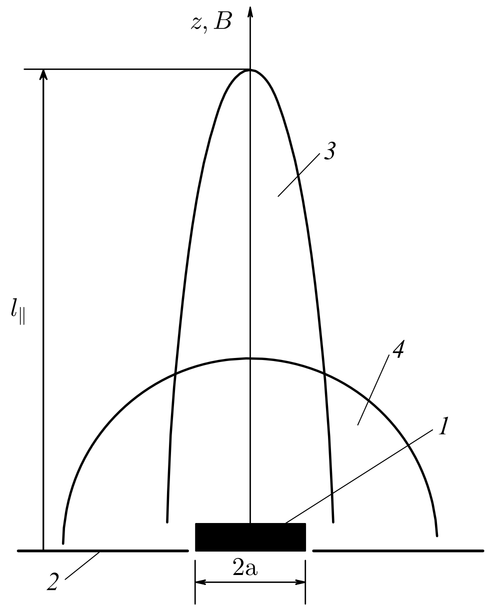

Fig. 1.10. Structure of electron and ion current collection regions for a small probe: *1*—electrode, *2*—conductive surface, *3*—electron collection region, *4*—ion collection region

Substituting (1.57) into the electron particle continuity equation yields

$$\frac{1}{r}\frac{\partial}{\partial r}\left(r\frac{n}{n_0}\frac{\partial n}{\partial r}\right)+\frac{\omega_{\mathrm{ce}}^2}{0.51\nu_{\mathrm{ei}}^2(n_0)}\frac{\partial}{\partial z}\left(\frac{n_0}{n}\frac{\partial n}{\partial z}\right)=0. \tag{1.58}$$

We neglected here the divergence of the parallel ion flux, which is directed out of the zone of the ion collection. From (1.58) it follows that the characteristic longitudinal dimension of the electron ellipsoid is

$$l_{||}=a(\omega_{\mathrm{ce}}/\nu_{\mathrm{ei}}). \tag{1.59}$$

In contrast to the case of the large electrode, (1.42), this scale depends on the electrode size a.

If the electron current to the electrode is smaller than the saturation electrode current, the longitudinal potential profile in the plasma should be nonmonotonic (see Fig. 1.11). This effect is known as potential overlap [33, 36]. In most parts of the electron ellipsoid the potential corresponds to the Boltzmann distribution for the ions, (1.56). The potential in this region increases from the plasma potential φ_{f} at infinity to its maximum φ^*, which is related to the plasma density n^* at this point according to (1.56). Near the probe, however, there must be a region where the electrons are trapped along $\vec{B}$, since their flux to the electrode must be less than the thermal flux. Consequently, in this region the potential profile should correspond to the Boltzmann distribution for the electrons and should therefore decrease on approaching the probe.

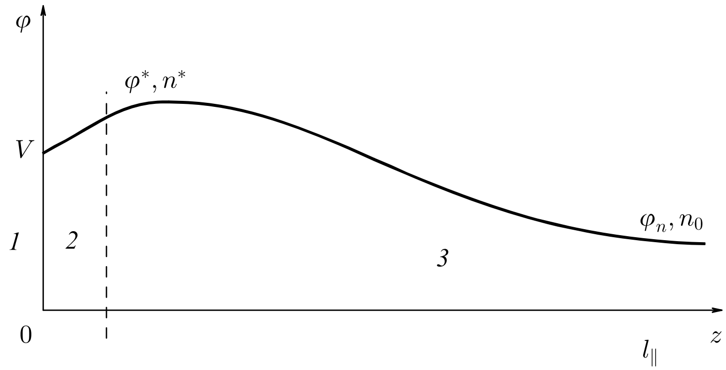

Fig. 1.11. Potential distribution along a magnetic field: *1*—electrode, *2*—sheath, *3*—electron collection region

The electron flux to the probe can be expressed in terms of the potential difference $\varphi^* - V$ (V is the electrode potential)

$$\Gamma_{\mathrm{e}||} = n^* \sqrt{\frac{T_\mathrm{e}}{2\pi m_\mathrm{e}}} \exp\left(-\frac{e(\varphi^* - V)}{T_\mathrm{e}}\right). \tag{1.60}$$

Then, substituting the maximum of the potential φ^* from (1.56) into (1.60), we obtain

$$-\frac{T_\mathrm{i}}{e} \ln\left(\frac{n^*}{n_0}\right) - \frac{T_\mathrm{e}}{e} \ln\left(\frac{n^*}{\Gamma_{\mathrm{e}||}} \sqrt{\frac{T_\mathrm{e}}{2\pi m_\mathrm{e}}}\right) = V - \varphi_\mathrm{f}. \tag{1.61}$$

Most of the electron current I_e to the electrode is collected far from the electrode where the plasma density is weakly perturbed. Thus, to obtain the analytical expression for the electron current, we replace the nonlinear equation (1.58) by the corresponding linear Laplace equation

$$\frac{1}{r}\frac{\partial}{\partial r}\left(r\frac{\partial n}{\partial r}\right) + \frac{D^*_{\mathrm{e}||}(n_0)}{D_{\mathrm{e}\perp}(n_0)}\frac{\partial^2 n}{\partial z^2} = 0. \tag{1.62}$$

The problem may be solved analytically by imposing the boundary condition $n = n^*$ at the surface of the electrode (thus neglecting the longitudinal dimension of the ion ellipsoid compared with the longitudinal dimension of the electron ellipsoid). In this linearized case, the electron current I_e should be a linear function of the plasma density n^*,

$$\frac{n^*}{n_0} = 1 - \frac{I_\mathrm{e} - I_\mathrm{i}(n^*)}{I_\mathrm{e}^\mathrm{sat}}. \tag{1.63}$$

We shall assume the ion current to a positively charged electrode to be $I_\mathrm{i} = en^* c_\mathrm{s} \times S^\mathrm{electrode} = I_\mathrm{i}^0 n^*/n_0$. The electron current to the electrode is $I_\mathrm{e} = e\Gamma_{\mathrm{e}||} S^\mathrm{electrode}$. The electron saturation current $I_\mathrm{e}^\mathrm{sat}$ is calculated by solving the Laplace equation (1.62) with zero boundary conditions at the electrode surface, similar to the case of weakly

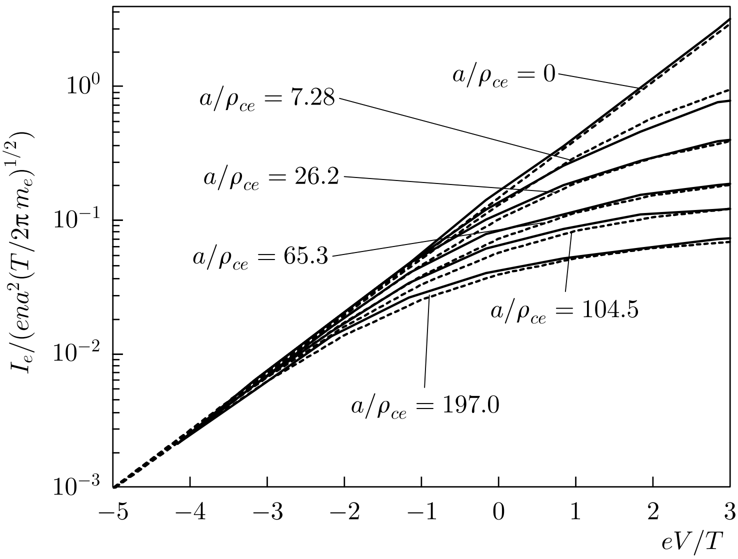

Fig. 1.12. Electron current to the electrode I_e versus applied potential V for various magnetic fields, $T_e = T_i = T$. Results of the numerical calculations of Sanmartin [32] (*dashed curves*) are compared with those obtained by analytic expression (1.65) (*solid curves*)

ionized plasma [35]

$$I_e^{sat} = k2\pi e n_0 \sqrt{D^*_{e||} D_{e\perp}} C = k2.8\pi e n_0 \rho_{ci} c_s C, \quad \rho_{ci} = c_s/\omega_{ci}. \tag{1.64}$$

The nonlinearity of the initial equation (1.58) is taken into account by introducing a coefficient k on the order of unity. The function C is a geometric factor determined by the size and shape of the electrode and corresponds to the capacity of a conductor of the same shape as the electrode but whose longitudinal dimension is $(D^*_{e||}/D_{e\perp})^{1/2}$ times shorter. For a disk electrode of radius a the coefficient is $C = 2a/\pi$. Other cases are considered in [33].

An expression for the transition part of the I–V characteristic is obtained by substituting (1.63) into (1.61). For example, if $T_e = T_i = T$ we find

$$\left(1 - \frac{I_e}{I_e^{sat}}\right)^2 \frac{e n_0 S^{\text{electrode}}}{I_e} \sqrt{\frac{T}{2\pi m_e}} = \left(1 - \frac{I_i^0}{I_e^{sat}}\right)^2 \exp\left(\frac{e(\varphi_f - V)}{T}\right). \tag{1.65}$$

In Fig. 1.12 the I–V characteristics obtained from (1.65) are compared with the numerical solution of the nonlinear problem of (1.58). Good agreement is achieved over a wide range of magnetic fields for $k = 0.7$. For $T_e \neq T_i$ one should use the more complicated expression which follows from (1.61), (1.63).

In [33] other geometries are considered, including the case of inclined magnetic field lines. It is also demonstrated there that (1.65) can describe the I–V characteristics of a small probe obtained on TdeV [34]. Therefore, in contrast to the case of a large electrode, the model with a classical diffusion coefficient gives results close to the experimental ones.

1.9 Neoclassical Perpendicular Conductivity in a Tokamak

1.9.1 Steady State Current

The problem of a self-consistent radial electric field in an installation with an inhomogeneous magnetic field such as a tokamak is much more complicated than that considered in Sect. 1.6 for the cylinder. As in the cylinder, the radial electric field is determined by the condition $I = 0$ or $I = \text{const}$ in the biasing experiments, where I is the net current through the flux surface. However, the contributions from the other radial currents, in particular from the diamagnetic current and current caused by the parallel viscosity, are more important than those from the perpendicular viscosity driven current. It is also necessary to take into account the possibility of toroidal rotation caused by external forces or generated by internal torque.

We consider the general toroidal geometry where the x and y coordinates correspond to the directions along and across flux surfaces, respectively, and z is the toroidal direction. The metric coefficients are

$$h_x = \frac{1}{\|\nabla x\|}, \qquad h_y = \frac{1}{\|\nabla y\|}, \qquad h_z = \frac{1}{\|\nabla z\|}, \qquad \sqrt{g} = h_x h_y h_z.$$

One can also replace $h_z \to 2\pi R$, where R is the major radius. The physical components of a vector are used. Subscript "$\perp$" denotes the direction perpendicular both to the magnetic field $\vec{B}$ and to the y-axis, $b_x = B_x/B, b_z = B_z/B$.

The surface averaged radial current is

$$I \Big/ \oint h_x h_z \, dx = \langle\langle j_y \rangle\rangle = \left\langle\left\langle \tilde{j}_y^{(\text{dia})} + j_y^{(\text{vis})} + j_y^{(\text{in})} + j_y^{(\text{iN})} \right\rangle\right\rangle, \tag{1.66}$$

where $\langle\langle f \rangle\rangle = \oint f h_x h_z \, dx / \oint h_x h_z \, dx$. The diamagnetic current here is taken in the divergent form of (1.13). In the tokamak geometry

$$\tilde{j}_y^{(\text{dia})} = -\frac{n(T_\text{e} + T_\text{i}) B_z}{h_x} \frac{\partial}{\partial x}\left(\frac{1}{B^2}\right). \tag{1.67}$$

We separate the viscosity driven current into currents caused parallel, perpendicular, and gyroviscosity. The divergent part of the current driven by the parallel viscosity, (1.19), is

$$\tilde{j}_y^{(\text{vis}||)} = -\frac{(1/4)\pi_{||} B_z}{h_x} \frac{\partial}{\partial x}\left(\frac{1}{B^2}\right). \tag{1.68}$$

In the fluid or Pfirsch–Schlueter regime, an expression for the parallel viscosity current may be found in [38]. It is also demonstrated there that other currents in (1.66) are significantly smaller in the core region of a tokamak.

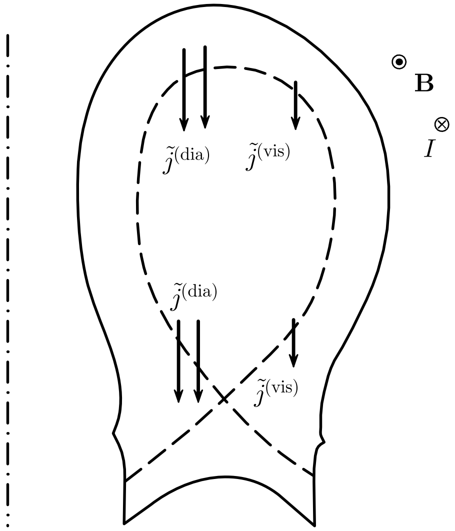

Fig. 1.13. Divergent part of the diamagnetic and parallel viscosity-driven currents in a tokamak

The diamagnetic and parallel viscosity currents are shown in Fig. 1.13. Both currents are directed vertically, as follows from (1.67) and (1.68). The diamagnetic current is the largest in the system since in the fluid regime the parallel viscosity, which depends on the parallel velocity and parallel ion heat flux distribution over the flux surface, is a small correction to the pressure. However, the contribution from the viscosity driven current to the average radial current equation (1.66) is on the same order as the contribution from the diamagnetic current. The reason is connected with the fact that the pressure is almost constant on the flux surface. Hence, the averaged diamagnetic current is much smaller than its local value.

An arbitrary radial electric field causes poloidal $\vec{E} \times \vec{B}$ drift. In the inhomogeneous magnetic field the poloidal drifts are not divergence free and hence the parallel flux is generated to satisfy the particle continuity equations. The ion parallel flux, which closes the diamagnetic poloidal flux and poloidal $\vec{E} \times \vec{B}$ drift, is known as Pfirsch–Schlueter flux; see, e.g., [39–41]. The net parallel velocity is

$$
\begin{aligned}
V_{||} &= V_{||}^{\text{P.S.}} + \frac{\langle V_{||} B \rangle}{B};\\
V_{||}^{\text{P.S.}} &= \left[\left(\frac{\partial p_{\text{i}}}{en\partial y} + \frac{\partial \varphi}{\partial y} \right) \frac{B_z}{h_y B_x B} - \frac{\langle V_{||} B \rangle}{B} \right] \left(1 - \frac{B^2}{\langle B^2 \rangle} \right),
\end{aligned}
\tag{1.69}
$$

where $\langle f \rangle = \oint f h_x h_y h_z \, dx / \oint h_x h_y h_z \, dx$. This parallel flux is driven by the parallel pressure gradient and hence the poloidal pressure is perturbed on the flux surface. The parallel viscosity also arises due to this parallel flux and due to the similar ion parallel heat flux [39–41]. The diamagnetic and the parallel viscosity-driven currents, (1.67) and (1.68), which depend on the radial electric field, do not satisfy the condition $I = 0$ (or I equal to a given value in the biasing experiments) for an arbitrary radial electric field. Therefore, the self-consistent radial electric field is determined by the ambipolarity condition $I = 0$ and the parallel momentum balance equation.

The parallel momentum balance equation in a simplified form contains the pressure gradient, parallel viscosity, an external force in the case of unbalanced neutral beam injection (NBI), and a term responsible for the radial transport of parallel momentum (for details see [38]):

$$-b_x \frac{\partial p}{h_x \partial x} - (\nabla \cdot \vec{\pi}_{||})_{||} + F^{(\mathrm{ex})} = \frac{d(m_\mathrm{i} n V_{||})}{dt}, \tag{1.70}$$

where

$$\frac{d(m_\mathrm{i} n V_{||})}{dt} = \frac{1}{h_z \sqrt{g}} \frac{\partial}{\partial y} \left[\frac{h_z \sqrt{g}}{h_y} \left(m_\mathrm{i} \Gamma_y V_{||} - \frac{\eta}{h_y} \frac{\partial V_{||}}{\partial y} \right) \right]. \tag{1.71}$$

Here, Γ_y is the radial particle flux, $\Gamma_y = -D \frac{\partial n}{h_y \partial y} + Vn$ with D and V being the anomalous coefficients of diffusion and convection, and η is the anomalous viscosity coefficient. We neglect here the ion–neutral friction with respect to the radial transport of parallel momentum in accordance with the results of numerical simulation [38]. The parallel momentum balance equation may be averaged over the flux surface with the weight B to cancel the pressure gradient contribution:

$$-\langle \vec{B} \cdot \nabla \cdot \overleftrightarrow{\pi}_{||} \rangle + \langle \vec{B} \cdot \vec{F}^{(\mathrm{ex})} \rangle = \left\langle B n m_\mathrm{i} \frac{dV_{||}}{dt} \right\rangle. \tag{1.72}$$

The averaged parallel viscosity may be expressed through the radial electric field. In the collision-dominated regime this can be done using the Braginskii viscosity and additional viscosity, which is proportional to the parallel heat flux. In the collisionless case one has to solve the drift kinetic equation. The general expression, which is valid in all regimes, was calculated in the neoclassical theory (see reviews [39–41]):

$$\langle \vec{B} \cdot \nabla \cdot \overleftrightarrow{\pi}_{||} \rangle = -\nu^{(\mathrm{mp})} n m_\mathrm{i} \left(\frac{B}{h_y B_x} \left(\frac{\partial \varphi}{\partial y} + \frac{T_\mathrm{i}}{en} \frac{\partial n}{\partial y} + k_\mathrm{T} \frac{\partial T_\mathrm{i}}{e \partial y} \right) - \langle B V_{||} \rangle \right). \tag{1.73}$$

The magnetic pumping frequency is

$$\nu^{(\mathrm{mp})} = \frac{3 \langle (\frac{\vec{B}}{B} \nabla B)^2 \rangle}{\langle B^2 \rangle} \frac{\mu_{\mathrm{i}1}}{n m_\mathrm{i}}, \tag{1.74}$$

where the viscosity coefficient $\mu_{\mathrm{i}1}$is calculated in [40]. In the collision dominated regime viscosity coefficient $\mu_{\mathrm{i}1}$ coincides with Braginskii parallel viscosity coefficient $\eta_0 = 0.96 n T_\mathrm{i} / \nu_\mathrm{i}$. For the tokamak with a circular cross section and small $\varepsilon = r/R$, where r and R are the radius of flux surface and the major radius, respectively, the magnetic pumping frequency is

$$\nu^{(\mathrm{mp})} = \frac{3 b_x^2}{2 R^2} \frac{\mu_{\mathrm{i}1}}{n m_\mathrm{i}}. \tag{1.75}$$

The numerical coefficient k_T is 2.7, 1.5, and −0.17 in the collision dominated, plateau, and banana regimes, respectively.

The parallel momentum balance equation contains two unknown variables: the radial electric field and the average toroidal rotation. As a second equation it is convenient to use the toroidal component of the momentum balance equation [41, 42]

$$-j_y B_x - (\nabla \cdot \vec{\pi}_{||})_z + F^{(\mathrm{ex})} = n m_{\mathrm{i}} \frac{dV_z}{dt}. \tag{1.76}$$

There is no pressure gradient in (1.76) due to the toroidal symmetry. The parallel and toroidal velocities are almost the same, $V_z \approx V_{||}$, and we shall neglect the small correction cased by the projection of the poloidal velocity to the parallel direction. The surface averaged radial current, as follows from (1.76), is

$$\langle\langle j_y \rangle\rangle = \left\langle\!\!\left\langle \frac{1}{B_x} \left[F^{(\mathrm{ex})} - m_{\mathrm{i}} n \frac{dV_z}{dt} \right] \right\rangle\!\!\right\rangle. \tag{1.77}$$

The parallel viscosity does not contribute to this equation. This fact may be shown using the parallel viscosity in the form of (1.18).

Two equations, (1.72) and (1.77), determine the radial current as a function of the radial electric field and also determine the average toroidal rotation for the given radial current. Combining (1.72) and (1.77), we find

$$\langle\langle j_y \rangle\rangle = \frac{\langle \vec{B} \cdot \nabla \cdot \overleftrightarrow{\pi}_{||} \rangle}{\langle B B_x \rangle} + \left\langle\!\!\left\langle \frac{1}{B_x} \left[F^{(\mathrm{ex})} - m_{\mathrm{i}} n \frac{dV_z}{dt} \right] \right\rangle\!\!\right\rangle - \frac{\langle \vec{B} \cdot [\vec{F}^{(\mathrm{ex})} - m_{\mathrm{i}} n \frac{d\vec{V}_{||}}{dt}] \rangle}{\langle B B_x \rangle}. \tag{1.78}$$

Let us start with the simplest situation of the absence of biasing, when $I = \langle\langle j_y \rangle\rangle = 0$. We introduce the parameter

$$\kappa = \frac{\nu^{(\mathrm{mp})} L^2}{D}, \tag{1.79}$$

where L is the radial scale for the toroidal velocity. The mean toroidal velocity is canceled in the last two terms on the r.h.s of (1.78) and only the Pfirsch–Schlueter part contributes to the difference of the second and the third terms in the r.h.s. Inserting (1.73) and (1.69), we see that the term with the parallel viscosity dominates in (1.78) when

$$\kappa = \frac{\nu^{(\mathrm{mp})} L^2}{D} > \varepsilon^2. \tag{1.80}$$

If this condition is satisfied, then the radial electric field is determined by the neoclassical expression $\langle \vec{B} \cdot \nabla \cdot \overleftrightarrow{\pi}_{||} \rangle = 0$ [39–41]:

$$E^{(\mathrm{NEO})} = \frac{T_{\mathrm{i}}}{e} \left(\frac{1}{h_y} \frac{d \ln n}{dy} + k_{\mathrm{T}} \frac{1}{h_y} \frac{d \ln T_{\mathrm{i}}}{dy} \right) - \frac{B_x}{B} \langle B V_{||} \rangle. \tag{1.81}$$

The profile of the average toroidal velocity may be obtained from (1.77). Note that in the absence of NBI, when the toroidal rotation is small, mainly the density and temperature radial profiles determine the radial electric field. If $\kappa < \varepsilon^2$, the radial electric

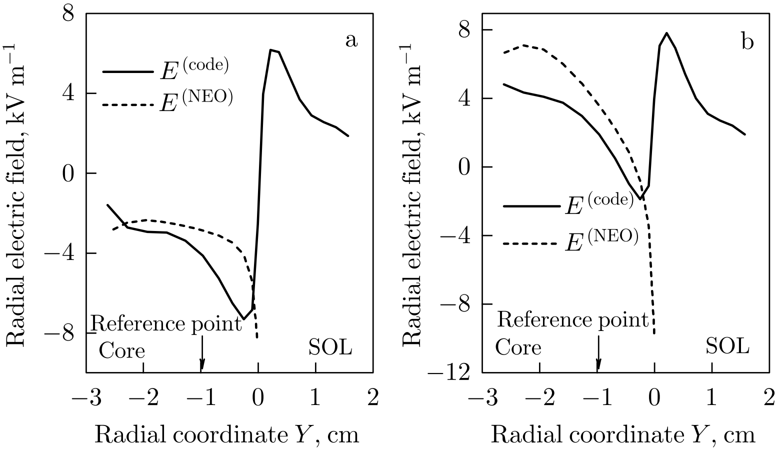

Fig. 1.14. The radial electric field in the equatorial midplane calculated by B2SOLPS5.0 fluid code in the absence of NBI (**a**) and for NBI in the co-current direction (**b**)

field profile differs significantly from the neoclassical expression. In Fig. 1.14 the radial electric field in the separatrix vicinity calculated by means of the B2SOLPS5.0 fluid code [43] is shown and compared with the neoclassical electric field, (1.81). With the exclusion of a small region at the separatrix vicinity on the order of 1 cm, where the condition in (1.80) is violated, the radial electric field is close to the neoclassical electric field and its dependence on the local parameters coincides with that of the neoclassical electric field. Such an electric field has been observed in experiments on tokamaks; see reviews [44–46] both for low (L) and high (H) confinement regimes.

On several tokamaks (CCT [47, 48], TUMAN-3 [49], TEXTOR [50] and others) the biasing experiments were performed where a biased electrode was inserted into the core plasma. Thus, a potential on the order of a few hundred eV was applied to the core flux surface with respect to the limiter, and the current–voltage characteristic was measured. The typical I–V characteristic is shown in Fig. 1.15. To calculate the I–V characteristic and to obtain local effective perpendicular conductivity of the tokamak plasma it is necessary to keep the net radial current in (1.77) and (1.78) as a prescribed value. According to the toroidal momentum balance of (1.77), the radial current accelerates plasma in the toroidal direction due to the $\vec{j} \times \vec{B}$ force. The toroidal velocity may be calculated from (1.77). Furthermore, if the condition in (1.80) is satisfied, the radial current in (1.78) may be expressed through the parallel velocity [42, 49]

$$\langle\langle j_y \rangle\rangle = \frac{\langle \vec{B} \cdot \nabla \cdot \overset{\leftrightarrow}{\pi}_{||} \rangle}{\langle B B_x \rangle}. \tag{1.82}$$

The parallel velocity depends both on toroidal rotation and radial electric field. If

$$1 > \kappa = \frac{\nu^{(\mathrm{mp})} L^2}{D} > \varepsilon^2, \tag{1.83}$$

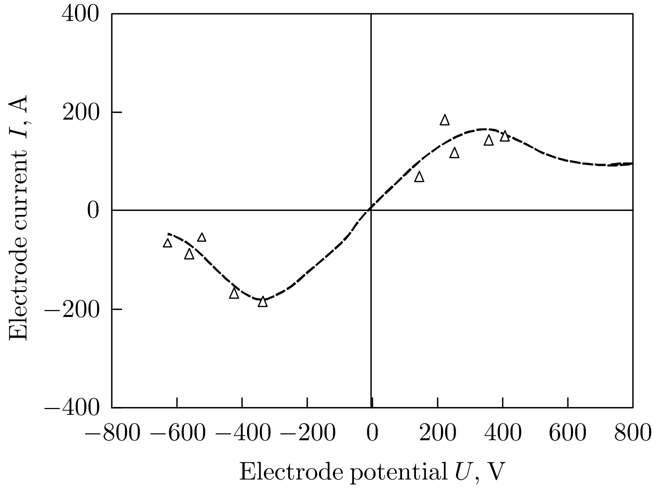

Fig. 1.15. Typical current–voltage characteristic during the biasing experiment in the Tuman-3 [49]

then from the parallel momentum balance in (1.72) it follows that the toroidal rotation velocity $\langle V_{||}\rangle \sim \kappa E_y/B_x$ is small and thus may be neglected in the expression for the parallel viscosity (1.73). Equation (1.82) in this case yields [42, 49]

$$\langle\langle j_y\rangle\rangle = -\nu^{(\mathrm{mp})} n m_\mathrm{i} \frac{B}{\langle B B_x\rangle B_x h_y}\left[\frac{\partial\varphi}{\partial y} - \frac{T_\mathrm{i}}{e}\left(\frac{\partial \ln n}{\partial y} + k_\mathrm{T}\frac{\partial \ln T_\mathrm{i}}{\partial y}\right)\right]. \tag{1.84}$$

The average radial current in this regime is the linear function of the electric field.

In contrast, the situation in the case

$$\kappa > 1 \tag{1.85}$$

is quite different. The radial current still might be expressed through the parallel viscosity according to (1.82), but the contribution of the toroidal rotation term to the parallel viscosity of (1.73) is quite significant. Indeed, since $\kappa > 1$, the parallel momentum balance, (1.72), may be satisfied only if the sum in the r.h.s. of (1.73) is close to zero. In other words, the poloidal rotation in this regime is close to the neoclassical poloidal rotation and the radial electric field is given by the neoclassical expression in (1.81). To calculate the radial current one has to use (1.77) where the radial current is expressed through the toroidal velocity. Neglecting the difference in averaging of the toroidal velocity in (1.81) and (1.77), which is equivalent to neglecting the Pfirsch–Schlueter velocities with respect to the main toroidal velocity, and expressing the toroidal velocity in (1.81) through the radial electric field and inserting it into (1.77), we find

$$\langle\langle j_y\rangle\rangle = \left\langle\!\!\left\langle \frac{1}{B_x}\frac{d}{dt}\left\{m_\mathrm{i} n\left[-\frac{E_y}{B_x} + \frac{T_\mathrm{i}}{e}\left(\frac{1}{h_y}\frac{d\ln n}{dy} + k_\mathrm{T}\frac{1}{h_y}\frac{d\ln T_\mathrm{i}}{dy}\right)\right]\right\}\right\rangle\!\!\right\rangle. \tag{1.86}$$

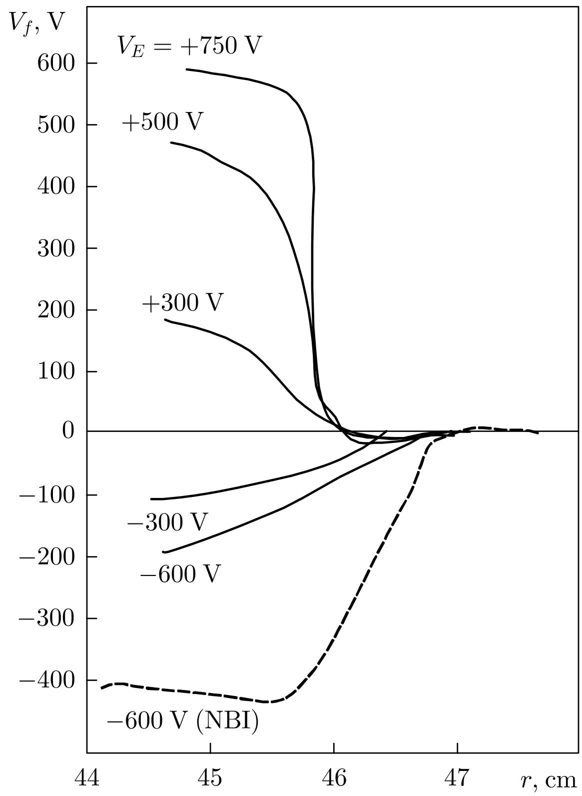

Fig. 1.16. Radial profiles of the potential measured for different applied voltages in the biasing experiment in TEXTOR

The profile of the radial electric field and the effective perpendicular conductivity in this case is quite different from that given by (1.84). Finally, for $\kappa < \varepsilon^2$ the radial current cannot be expressed through the parallel viscosity and the corresponding equation is more complicated [51].

The analytical expressions in this section were checked by comparison with the results of numerical simulation for ASDEX Upgrade performed by means of the B2SOPS5.0 code [51]. The electric field observed on TEXTOR [52, 53], Fig. 1.16, may also be understood from the analytical results (see [51]).

In some publications [50, 52, 53] it was suggested that the $\vec{j} \times \vec{B}$ force, which accelerates plasma in the toroidal direction, is balanced by ion–neutral friction. However, the simulation results demonstrate that this force is an order of magnitude smaller than the anomalous radial transport of toroidal momentum.

In experiments [47–49] it was observed that at large applied voltages the radial current started to decrease. The current drop is usually accompanied by turbulence suppression and transition to the regime of improved confinement (L–H transition). In [42, 49, 54] this effect was associated with the decrease in the parallel viscosity when the poloidal drift velocity becomes near the poloidal speed of sound $b_x c_s$. Indeed, as is known (see, for example, review [41] and references therein), (1.73) is valid only in the linear case if the poloidal velocity $|V_x| \ll b_x c_s$. In [54] it was suggested that the radial profile of the electric field for large applied voltages may be discontinuous. In [55] the radial current was taken in the form

$$\begin{aligned}\langle\langle j_y \rangle\rangle = -\nu^{(\mathrm{mp})} n m_{\mathrm{i}} \frac{B}{\langle B B_x \rangle B_x h_y} \\ \times \left[\frac{\partial \varphi}{\partial y} - \frac{T_{\mathrm{i}}}{e} \left(\frac{\partial \ln n}{\partial y} + k_{\mathrm{T}} \frac{\partial \ln T_{\mathrm{i}}}{\partial y} \right) \right] f \left(\left| \frac{\partial \varphi}{b_x c_{\mathrm{s}} h_y \partial y} \right| \right) \\ + \left\langle\left\langle \frac{1}{B^2} \left[\frac{\partial}{h_y \partial y} \eta_1 \frac{\partial}{h_y \partial y} \left(\frac{\partial \varphi}{h_y \partial y} + \frac{\partial p_{\mathrm{i}}}{e n h_y \partial y} \right) \right] \right\rangle\right\rangle,\end{aligned} \tag{1.87}$$

where f is a decreasing function (e.g., $\exp(-|\partial\varphi/\partial y/(h_y b_x c_s)|$ in the plateau regime). It was shown that for large applied voltages, (1.87) has the soliton-like solution, where a narrow region of a large electric field was localized somewhere between the biased electrode and the separatrix. Such a profile was also obtained in the numerical simulations [56, 57] by the Monte-Carlo code. However, for large applied voltages the criterion of validity of (1.83) is rather severe. Indeed, the solitary structure for an electric field also implies the solitary structure for Pfirsch–Schlueter parallel flux, which results in strong radial transport of parallel momentum (the scale L in (1.83) becomes small). Hence, the neoclassical part of the radial current, which corresponds to the fist term in (1.87), cannot be expressed through the parallel viscosity and is given by the more complicated equation (1.78). In the simulations with full fluid code [51] the formation of a solitary structure was not observed.

The current drop for large applied voltages and the details of the radial electric field profile observed in [58, 59] may be explained by the transition to the H-mode. Due to the drop in the diffusion and the perpendicular viscosity coefficient, in the H-mode the radial transport of toroidal momentum is strongly reduced and the condition in (1.85) $\kappa > 1$ is more likely fulfilled even if it was not satisfied in the L-regime. Therefore, assuming that radial current is given by (1.86), we see that the current is proportional to the anomalous transport coefficients and hence should drop in the H-mode.

1.9.2 Time-Dependent Current

The time-dependent radial current in a tokamak is quite different from the inertia (polarization) current in the straight magnetic field of (1.10). The time-dependent radial electric field creates Pfirsch–Schlueter time-dependent parallel flux and time-dependent average toroidal rotation, which causes the parallel and toroidal inertia terms. According to (1.78), these forces lead to an additional time-dependent current. Combining (1.78) with (1.69) and (1.72) after adding the normal inertia current from (1.10), we find the time-dependent part of the radial current,

$$\langle\langle j_y^{(\mathrm{t})} \rangle\rangle = -\left\langle\left\langle \frac{\langle B^2 \rangle}{\langle B \rangle \langle B_x \rangle \langle\langle B/B_x \rangle\rangle} \left(1 - \frac{B^2}{\langle B^2 \rangle} \right) \frac{1}{h_y B_x^2} + \frac{1}{h_y B^2} \right\rangle\right\rangle n m_{\mathrm{i}} \frac{\partial^2 \varphi_y}{\partial t \partial y}. \tag{1.88}$$

For circular cross section, (1.88) is reduced to

$$\langle\langle j_y^{(\mathrm{t})}\rangle\rangle = -\left(1+2q^2\right)\left\langle\!\left\langle \frac{1}{B^2 h_y}\right\rangle\!\right\rangle n m_{\mathrm{i}} \frac{\partial^2 \varphi_y}{\partial t \partial y}, \tag{1.89}$$

where q is the safety factor. Thus, the polarization current is enhanced by a factor of $(1+2q^2)$. In the plateau and banana regimes the corresponding factor is larger; see, e.g., [41]. In the banana regime the factor $(1+2q^2)$ should be replaced by $\sqrt{\varepsilon}/b_x^2$.

1.10 Transverse Conductivity in a Reversed Field Pinch

The radial current in the reversed field pinch (RFP) has much in common with that in the tokamak, in spite of the fact that in the RFP the main component of the magnetic field is the poloidal magnetic field. Therefore, in contrast to the tokamak situation, the radial electric field and the radial pressure gradient generate the toroidal $\vec{E}\times\vec{B}$ drift

$$E_y = -V_z B_x + \frac{\partial p_{\mathrm{i}}}{e n h_y \partial y} \tag{1.90}$$

instead of the poloidal $\vec{E}\times\vec{B}$ drift.

The toroidal projection of the momentum balance equation then gives the current voltage characteristic, which practically coincides with (1.86) (the coefficient k_{T} is replaced by 1). The radial profiles of the radial electric field and the toroidal velocities were measured in RFP [60] during the biasing experiments. The profiles are in good agreement with those calculated according to (1.86) and (1.90), Fig. 1.17.

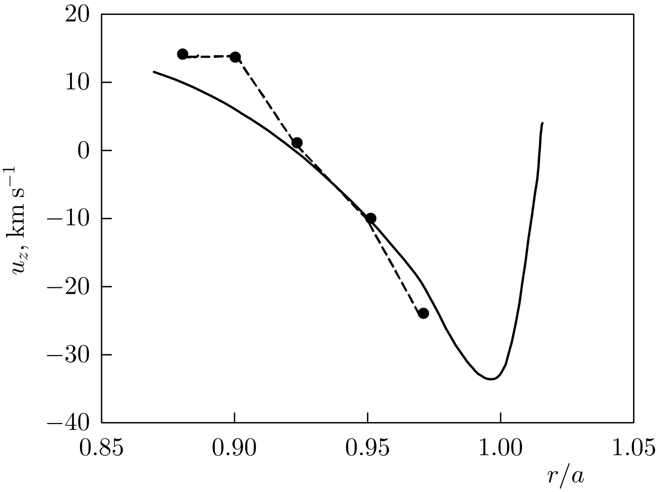

Fig. 1.17. Toroidal velocity in RFX calculated according to (1.86) and the measured density, temperature, and radial electric field profiles (*continuous line*) and according to (1.90) and the measured electric field profile

Hence we can conclude that in the absence of strong magnetic turbulence, which may modify the perpendicular conductivity (see Sect. 1.13), the perpendicular current in the RFP is determined by the expression in (1.86).

1.11 Modeling of Electric Field and Currents in the Tokamak Edge Plasma

Such modeling was performed by two-dimensional transport fluid codes such as B2SOLPS5.0 [38], UEDGE [61–64], EDGE2D [65], and TECXY [66]. Typical radial electric field profiles calculated by B2SOLPS5.0 [38] in the absence of biasing are shown in Fig. 1.14. Similar radial profiles were obtained by UEDGE [67] and TECXY [68]. In [43] the dependence of the radial electric field on the plasma parameters was studied in detail. It was demonstrated that with the exception of a small region in the separatrix vicinity the radial electric field depends on parameters like the neoclassical electric field. As an example, Fig. 1.18 illustrates the weak dependence on the toroidal and poloidal magnetic fields in the absence of NBI in accordance with (1.81). The deviation from the neoclassical expression in

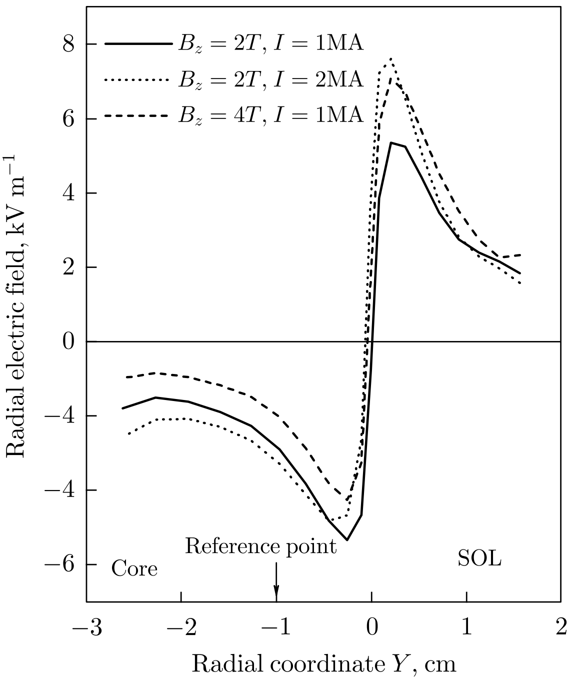

Fig. 1.18. The radial electric field profiles at the outer midplane for discharges with different toroidal magnetic fields B and different plasma currents I. No NBI, normal direction of the magnetic field, $n = 2 \times 10^{19}$ m^{-3}, $T_\mathrm{i} = 80$ eV in the reference point

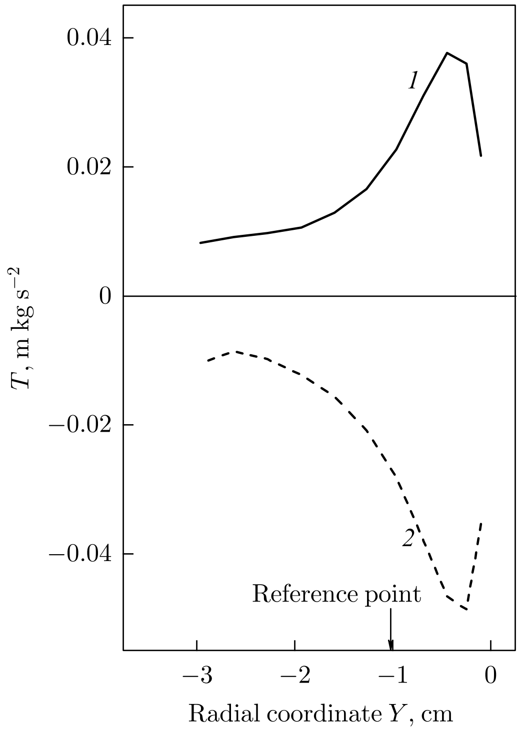

Fig. 1.19. Different components of the parallel momentum balance equation averaged over the flux surface: *1*—perpendicular anomalous viscosity and inertia [r.h.s. of (1.72)], *2*—parallel viscosity $\langle \vec{B} \cdot \nabla \cdot \overset{\leftrightarrow}{\pi}^{(\mathrm{NEO})} \rangle$ [l.h.s. of (1.72)]. No NBI, reversed magnetic field, $n = 2 \times 10^{19}\ \mathrm{m}^{-3}$, $T_\mathrm{i} = 98$ eV in the reference point 1 cm inside the separatrix, $I = 1$ MA, $B = 2$ T

the separatrix vicinity in Fig. 1.14 may be explained by the fact that the parameter κ here becomes smaller than ε^2 due to the small scale L of the variation of the plasma parameters. In Fig. 1.19, the parallel viscosity $\langle \vec{B} \cdot \nabla \cdot \overset{\leftrightarrow}{\pi}_{||} \rangle$ averaged over the flux surface and the r.h.s. of (1.72), which corresponds to the radial transport of toroidal momentum, are shown. One can see that the parallel viscosity decreases towards the core with the scale δ which in the Pfirsch–Schlueter regime is estimated [43] as $\delta \sim (B^2 a^2 D \nu_{\mathrm{ii}} / B_x^2 c_\mathrm{s}^2)^{1/2}$, where a is the minor radius. Therefore, the numerical modeling supports the conclusion that the radial electric field in the core region in the absence of biasing is given by the neoclassical expression even in the presence of anomalous transport. On the basis of the simulations a scaling for the threshold of the transition to the high confinement regime (L–H transition) has been put forward [43, 69]. A similar radial electric field and scaling has been obtained by Monte-Carlo simulations using ASCOT code [56, 70]. The predicted radial electric field and L–H transition threshold are consistent with experimental observations [69, 71].

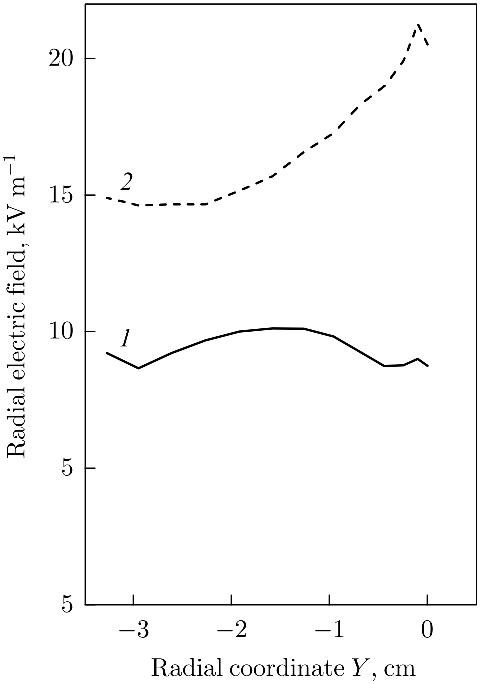

Fig. 1.20. The radial electric field profile at the outer midplane for $\kappa = 0.1$ (discharge parameters $\varphi|_{\text{electrode}} = 400$ V, $n|_{-1\,\text{cm}} = 2.7 \times 10^{19}$ m^{-3}, $T_{\text{i}}|_{-1\,\text{cm}} = 32$ eV): *1*—calculated profile; *2*—theoretical prediction

Outside the separatrix the radial electric field is quite different and is governed by the parallel momentum balance equation [38]. A detailed study of the electric fields and current system outside the separatrix was done in [72].

The simulations of biasing experiments were performed by means of B2SOL-PS5.0 transport code in [51] for the real divertor geometry. It was demonstrated that there indeed exist three regimes which correspond to the different values of the effective perpendicular conductivity and to different profiles of the radial electric field. As an example, in Figs. 1.20 and 1.21 is shown the radial electric field calculated according to equations (1.84) and (1.86). The case in Fig. 1.20 corresponds to inequality (1.83) and in Fig. 1.21 to the case when κ is close to unity.

1.12 Mechanisms of Anomalous Perpendicular Viscosity and Viscosity-Driven Currents

In turbulent plasma the current driven by the perpendicular viscosity (or by the corresponding component of the Reynolds stress tensor) can be obtained by direct averaging over the fluctuations. For example, in accordance with (1.15) and (1.16), in

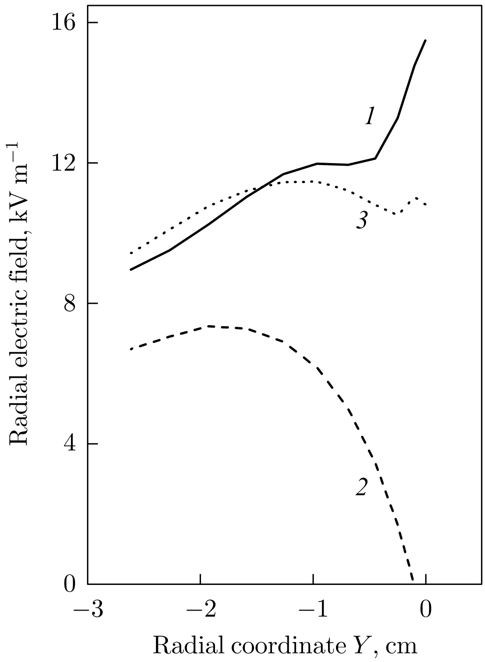

Fig. 1.21. The radial electric field profile at the outer midplane for $\kappa = 0.7$ (discharge parameters $\varphi|_{\text{electrode}} = 400$ V, $n|_{-1\,\text{cm}} = 5 \times 10^{18}$ m^{-3}, $T_\text{i}|_{-1\,\text{cm}} = 35$ eV): *1*—calculated profile; *2*—theoretical prediction for the boundary condition at the separatrix $V_{||} = 0$; *3*—theoretical profile for the boundary condition for velocity taken from the code

slab geometry

$$j_y^{(\text{visan})} = \left\langle \frac{\partial}{\partial y} m_\text{i} n \tilde{V}_x \tilde{V}_y \right\rangle \Big/ B, \tag{1.91}$$

where $\tilde{V}_{x,y}$ are the fluctuating velocities. For the electrostatic turbulence

$$j_y^{(\text{visan})} = -\frac{\partial}{\partial y} \sum_{\vec{k}} m_\text{i} n k_x k_y |\varphi_{\vec{k}}|^2 / B^3. \tag{1.92}$$

As was mentioned in [73], the radial current driven by the turbulent viscosity is not automatically zero for waves propagating in the direction of the main inhomogeneity (the y direction). In other words, the viscosity-driven current of (1.92) is nonzero if the radial wave numbers have a finite real part. For drift waves in the cylinder, where in the absence of the radial electric field the eigenfunctions are of the form $\varphi_{\vec{k}} = \varphi_{\vec{k}}^{(0)} \exp[-i\mu_{\vec{k}}(y - y_r)^2/2]$, where y_r is the coordinate of the resonance surface for the given k_y and k_z and $\mu_{\vec{k}} = (L_\text{n}/L_\text{s})/\rho_\text{ci}^2$ with L_n and L_s being the density and the magnetic shear radial scales. The radial current is thus [73]

$$j_y^{(\text{visan})} = \frac{\partial}{\partial y} \sum_{\vec{k}} m_\text{i} n k_x \mu_{\vec{k}} (y - y_r) |\varphi_{\vec{k}}|^2 / B^3. \tag{1.93}$$

Since modes from different resonance surfaces contribute to (1.92) and the spectrum depends on the global plasma parameters, which vary slowly, it is convenient to average equation (1.92) over the distance L larger than the mode radial width but smaller than the radial scale of plasma parameters

$$j_y^{(\mathrm{visan})} = -\frac{\partial}{\partial y} \sum_{\vec{k}} \int_{-L}^{L} m_{\mathrm{i}} n k_x k_y |\varphi_{\vec{k}}|^2 \, dy' / \big(2LB^3\big). \tag{1.94}$$

The integral in (1.94) remains nonzero only if the spectrum depends on y due to a change in the density or temperature gradient, otherwise it is zero. Hence, the sum is the linear function on density and temperature gradients and the viscosity-driven current has the form of (1.16).

In the presence of the radial electric field the eigenfunctions become asymmetric with respect to the resonance surface and the integral in (1.94) becomes a linear function of the radial electric field. For the case of the ITG mode the normalized sum in (1.94) was calculated numerically in [74] in the quasilinear approach. Therefore, the viscosity coefficient in (1.94) was calculated for this case. It may be shown that the viscosity coefficient η is on the order of $m_{\mathrm{i}} n D$ with D being the quasilinear diffusion coefficient $D = \sum_{\vec{k}} \int_{-L}^{L} k_x^2 |\varphi_{\vec{k}}|^2 \, dy' \, \mathrm{Im}(\omega)/|\omega|^2/(2LB^2)$. For strong turbulence the calculation of the perpendicular viscosity still remains an open question. Note that in the turbulent plasma, besides the viscosity-driven current, there exists the inertia current of the form given by (1.10) with the anomalous radial particle flux. Both currents are generally of the same order.

1.13 Transverse Conductivity in a Stochastic Magnetic Field

The perturbation of the magnetic field may change the average conductivity across the main magnetic field and, therefore, may influence the value of the self-consistent electric field. On some tokamaks (TM-4 [75], TEXT [76], Tore Supra [77]) electric fields less negative than the neoclassical or even positive were observed for special regimes. A tentative explanation is connected with an intrinsic magnetic field stochasticity, which can create an additional current of electrons thus reducing the negative neoclassical electric field. On TEXT and Tore Supra the extrinsic stochasticity was created by an ergodic magnetic limiter. As a result, a strong reduction in the negative electric field was observed [78]. This effect should be interpreted in terms of a modified transverse conductivity associated with the perturbations of the magnetic field.

The simplest approach to calculate the current in a braided magnetic field is to calculate the current of test particles, as was done in [79–81] for the collisionless case similar to the calculation of the heat conductivity [82]. However, in reality the motion of electrons in the braided magnetic field is accompanied by the emergence of the potential, density, and temperature perturbations, which arise to provide local quasineutrality. These perturbations strongly affect the motion of charged particles, generate the local perturbed currents, and, as a result, significantly change the physical picture and the averaged cross-field current. The effective perpendicular conductivity taking into account these effects has been calculated in [83] for the case of an externally perturbed magnetic field. More complicated situations, when the perturbations of the magnetic field are generated self-consistently by plasma turbulence [84, 85], are not considered here.

Let us analyze the case of uniform density and temperatures to focus attention on the effects caused by the electric field perpendicular to the flux surface. Slab geometry is chosen for simplicity with the plasma parameters depending on the y-coordinate normal to the flux surfaces. The unperturbed magnetic field is given by $\vec{B} = B_z\vec{e}_z + B_x(y)\vec{e}_y = B[\vec{e}_z + b_x\vec{e}_y]$. The x-axis corresponds to the poloidal direction in a tokamak, the z-axis to the toroidal direction, and the y-axis to the radial direction. The unperturbed potential is denoted as $\varphi_0(y)$, and the corresponding electric field is E_0. Toroidal effects are neglected here. The perturbed magnetic field is taken in the form $\vec{B}' = \sum_{\vec{k}} \vec{B}'_{0\vec{k}} \exp(i\vec{k}\vec{r})$, where $|k_z| \ll |k_x|, |k_y|$. The magnetic field perturbations are assumed to be sufficiently small, so that the following conditions are fulfilled: $|k_y b'_y/k_{||}| \sim |k_x b'_x/k_{||}| \ll 1$, $k_y L \ll 1$, where $b'_{x,y} = B'_{x,y}/B$, $L = |d \ln \varphi_0/dy|^{-1}$, and $k_{||}(y) = [k_x B_x(y) + k_z B_z]/B$ is the parallel wave vector. Therefore, we can apply the quasilinear theory based on the small parameter $|k_y b'_y/k_{||}| \sim |k_x b'_x/k_{||}| \ll 1$. This condition means that the displacement of the point at the magnetic field line in the y or x directions is smaller than the transverse spatial scale of the perturbations provided the point passes a distance $k_{||}^{-1}$ along the magnetic field.

1.13.1 Nonstochastic Magnetic Field

The main effect is more transparent in the simplest collisional case when the mean-free path $\lambda_{\mathrm{mfp}} \ll k_{||}^{-1}$ in the absence of the resonance where $k_{||} = 0$ [83]. The analysis is based on the Braginskii fluid equations. If one neglects for a while the perpendicular currents, then from the current continuity equation, which in this case is reduced simply to $ik_{||} j_{||\vec{k}} = 0$, it follows that the parallel current should be zero. Since $j_{||\vec{k}} = -\sigma_{||}[b'_{y\vec{k}}(d\varphi_0/dy) + ik_{||}\varphi^1_{\vec{k}}] = 0$, we find the potential perturbations:

$$\varphi^{(1)}_{\vec{k}} = -\frac{b'_{y\vec{k}}}{ik_{||}}\frac{d\varphi_0}{dy}. \tag{1.95}$$

In other words, the perturbed magnetic field line remains equipotential due to the emergence of the perturbations of the potential. The potential perturbations change the drift velocity and the inhomogeneous part of the drifts cause viscosity and inertia forces and, consequently, perpendicular currents.

The potential perturbations, calculated taking into account perpendicular currents from the full current continuity equation, are

$$\varphi^{(1)}_{\vec{k}} = \left(1 - \frac{\sigma_{\perp\vec{k}}k_\perp^2}{\sigma_{\perp\vec{k}}k_\perp^2 + \sigma_{||}k_{||}^2}\right)\frac{ib'_{y\vec{k}}}{k_{||}}\frac{d\varphi_0}{dy}, \tag{1.96}$$

where

$$\sigma_{\perp\vec{k}} = -\nabla \cdot \vec{j}_{\perp\vec{k}}/\Delta_\perp \varphi_{\vec{k}} = \sigma_{\perp\vec{k},\mathrm{i}} + \sigma_{\perp\vec{k},\mathrm{v}} = i m_\mathrm{i} V_0 k_x n/B^2 + \eta_1 \left(k_\perp^2 + 4k_z^2\right)/B^2.$$

Here, $V_0 = E_0/B$ is the velocity of unperturbed $\vec{E} \times \vec{B}$ drift in the x direction and η_1 is the Braginskii viscosity coefficient (or anomalous coefficient in the turbulent plasma). The deviation from the equipotential magnetic field line, i.e., the difference between (1.95) and (1.96) determines the parallel current

$$j_y = \left\langle j_{||} b'_y \frac{1}{2} \operatorname{Re} \sum_{\vec{k}} j_{||} b_{y\vec{k}} \right\rangle \frac{\sigma_{||} E_0}{2} \times \sum_{\vec{k}} \frac{|\sigma_{\perp\vec{k},\mathrm{i}} k_\perp^2|^2 + \sigma_{\perp\vec{k},\mathrm{v}} k_\perp^2 (\sigma_{||} k_{||}^2 + \sigma_{\perp\vec{k},\mathrm{v}} k_\perp^2)}{|\sigma_{\perp\vec{k},\mathrm{i}} k_\perp^2|^2 + (\sigma_{||} k_{||}^2 + \sigma_{\perp\vec{k},\mathrm{v}} k_\perp^2)^2} |b_{y\vec{k}}|^2. \tag{1.97}$$

We see that the radial current is proportional to the effective perpendicular conductivity and is quadratic with respect to magnetic field perturbations.

In the presence of resonance surfaces $k_{||} \to 0$ the expression for the current has singularity and the radial current increases. This situation is analyzed in [83].

1.13.2 Stochastic Magnetic Field

When the width of the magnetic island, which is formed near the resonance flux surface where $k_{||} \to 0$, exceeds the distance between the neighboring islands, the magnetic field becomes stochastic. The stochasticity of magnetic field lines in this case is characterized by the Kolmogorov length of exponential divergence L_k of two neighboring magnetic lines being initially at distance δ_0: $\delta = \delta_0 \exp(z/L_k)$. In the stochastic magnetic field the local transverse transport is strongly amplified because the magnetic field lines approach each other very close at distances larger than L_k due to the conservation of the magnetic flux in the magnetic flux tube. This fact strongly effects the final expression for the perpendicular current. Let us consider the flux tube of initial size δ_0. Due to the stochastic instability the average distance between the neighboring lines increases exponentially. But, the cross-section of a flux tube conserves. Therefore, since the distance between the neighboring magnetic field lines exponentially diverges in one direction, in the other direction it decreases exponentially: $\delta = \delta_0 \exp(-z/L_k)$. So, if the distance between the two magnetic field lines at $z = 0$ is δ_0, it becomes equal to $\delta_0 \exp(-z/L_k)$ at $z > L_k$. Due to rather small cross-field conductivity, the equipotentials almost coincide with the magnetic field lines. Hence, an initial potential drop $\delta_0 E_0$ between the two magnetic field lines is applied to the very small distance δ at $z > L_k$. As a result, a large electric field on the order of $E_0 \exp(z/L_k)$ arises. At such places where the magnetic field lines approach each other close, the parallel current is short-circuited by the ion transverse current in spite of the low value of the cross-field conductivity (see Fig. 1.22).

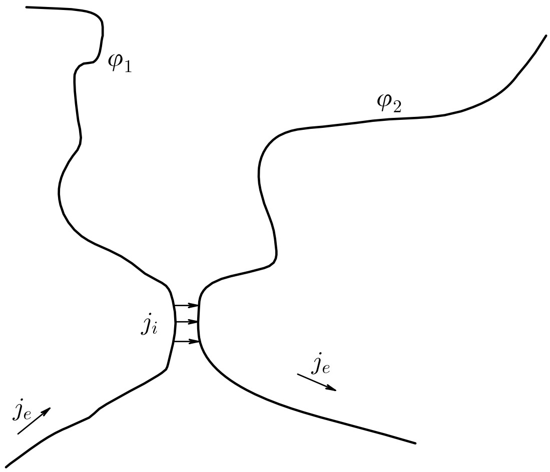

Fig. 1.22. Schematic of the currents for the stochastic magnetic field lines

In the collisionless case, where the mean free path is much larger than L_k, the new longitudinal scale L may be introduced. This is the scale at which the divergences of the perpendicular and the parallel currents become similar: $\sigma_{||}/L^2 \sim \sigma_{\perp \bar{k}} k_\perp^2 \exp(2L/L_k)$. The corresponding scale is

$$L = 2L_k \ln \frac{\sigma_{||}}{\sigma_{\perp k} k_\perp^2 L_k^2}. \tag{1.98}$$

The perpendicular current is thus reduced by a factor L_k/L with respect to the current of the test particles because the potential perturbation that makes the magnetic field line equipotential [see (1.95)] is "washed out" at a distance L larger than L_k. According to [83],

$$j_x \approx e^2 D_{\mathrm{st}} n E_0 \sqrt{\frac{2}{\pi m_{\mathrm{e}} T_{\mathrm{e}}}} \frac{L_k}{L}, \tag{1.99}$$

where D_{st} is the stochastic diffusion coefficient of the magnetic field lines. This model is consistent with experimental observations of the radial electric field in the plasma edge of TEXTOR tokamak with ergodic magnetic limiter [86].

1.14 Electric Fields Generated in the Shielding Layer between Hot Plasma and a Solid State

The self-consistent electric fields may be generated in plasmas by injection of a beam, which causes the return plasma current. A typical example is the contact between solid state and hot plasma in an inclined magnetic field. Such contact takes place, for example, during hard disruptions in tokamaks, when the hot plasma from

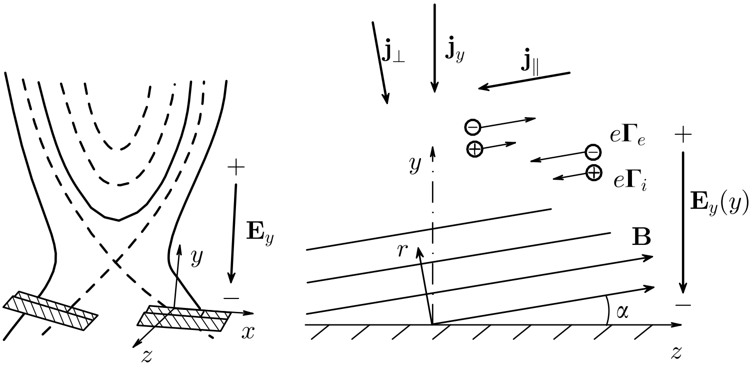

Fig. 1.23. The geometry considered

the core region is moving towards the divertor plates. During hard disruptions, an intense vaporization of the divertor plates takes place. The process is accompanied by the formation of a dense and partially ionized shielding layer in front of the plates, which significantly reduces the particle and heat fluxes reaching the divertor tiles and thus determines the evaporation rate of the surface.

The energetic plasma particles moving along the skewed magnetic field lines are stopped inside the layer at different depths as in Fig. 1.23. Hence, in order to produce a return current that compensates the current carried by the plasma particles, a self-consistent electric field is generated (ambipolarity constraint). Since the temperature of the vapor plasma is on the order of a few eV-s, the electrical conductivity is rather low and the resulting electric field is of considerable strength. In a tokamak with conducting divertor plates, the local electric field has to be normal to the plates, thus creating plasma drift across the flux surfaces [87, 88].

The electric field and the resulting drift motion were modeled self-consistently in [87, 88]. In the applied code, the deceleration of hot particles of different energy groups is calculated, while the cold layer is described by means of fluid equations by taking into account all important elementary processes taking place in the plasma. The electric field is calculated from the condition of zero net current through the plates.

The 1D geometry is considered in Fig. 1.23, $\partial/\partial z = \partial/\partial x = 0$, B_x assumed to be zero. The current of hot particles $e\Gamma_{\mathrm{i}}(y) - e\Gamma_{\mathrm{e}}(y)$ is antiparallel to $\vec{B}$, and its projection in the y-direction is $e(\Gamma_{\mathrm{i}} - \Gamma_{\mathrm{e}})\sin\alpha$. It is calculated by tracing the depletion of particle groups of different energies. The potential drop between the cold and the hot plasmas is also taken into account. The current has to be balanced by the return current $\vec{j}$, created by the self-consistent electric field E_y. The return current j_y is the sum of the projections of the B-parallel current $j_{||}\sin\alpha$ and the B-perpendicular current $j_\perp\cos\alpha$ ($j_\perp$ belongs to the plane yz, and there is also another projection j_x). The parallel current is primarily the electron current driven by the parallel projection of electric field $E_{||} = E_y\sin\alpha$. The perpendicular current $j_\perp$ is associated with $E_\perp$. The condition of vanishing net current $j_\sum$ in the y-direction throughout the vapor layer can be written as

$$j_{\sum y} = j_{||}\sin\alpha + j_{\perp}\cos\alpha + e(\Gamma_{\rm i} - \Gamma_{\rm e})\sin\alpha = 0. \tag{1.100}$$

The component $j_{||}$ is determined from the parallel projection of the electron momentum balance equation

$$j_{||} = \sigma_{||}\sin\alpha(E_y + eT_{\rm e}\partial\ln n_{\rm e}/\partial y + g_{\rm T}e\partial T_{\rm e}/\partial y), \tag{1.101}$$

where $\sigma_{||}$ is the electrical conductivity which depends both on Coulomb and electron-neutral collisions [1], and the coefficient $g_{\rm T}$ is larger than unity due to the thermal force. From the perpendicular component of the electron momentum balance equation (neglecting the perpendicular thermal force), we have

$$\vec{j} + \beta_{\rm e}\left[\vec{j} \times \frac{\vec{B}}{B}\right] = \sigma_{\perp}\left(\vec{E} + [\vec{V} \times \vec{B}] + \frac{\nabla p_{\rm e}}{en_{\rm e}}\right), \tag{1.102}$$

where the Hall parameter $\beta_{\rm e} = \omega_{\rm ce}/\nu_{\rm e}$, $\omega_{\rm ce}$ is the electron cyclotron frequency, $\nu_{\rm e}$ is the electron collision frequency, and $\vec{V}$ is the ion velocity, $\sigma_{\perp} = 2\sigma_{||}$. Due to the high collision rate, the ion and neutral gas velocities are assumed to be equal. Another relation between the perpendicular current and plasma velocity is given by the x-component of the momentum balance equation

$$\frac{d\rho V_x}{dt} \equiv \frac{\partial\rho V_x}{\partial t} + \frac{\partial(\rho V_x V_y)}{\partial y} = [\vec{j}_{\perp} \times \vec{B}]_x. \tag{1.103}$$

The velocity component V_y is calculated from the y-component of the momentum equation by simultaneously solving the complete set of fluid equations, thus determining the evolution of the vapor layer. The electric field component E_x is assumed to be zero.

A typical result for a scenario in which a carbon divertor plate is exposed to a thermal disrupting plasma at $t = 0$. The following input parameters were assumed: $T_{\rm e0} = 5$ keV, $n_{\rm e0} = 5.5 \times 10^{18}$ m^{-3}, $B = 6$ T, $\alpha = 5°$. A cold and dense shielding layer evolves at the surface. The potential distribution at $t = 50$ μs is shown in Fig. 1.24. At this time instant, ionization degrees significantly less than unity only exist in a narrow vapor layer adjacent to the surface (y less than 2 cm) in which the neutral atom density is on the order of 10^{24} m^{-3}. The divertor plate, as well as the vapor layer, is biased negatively with respect to the hot plasma. The potential difference is on the order of the energy of the incident hot electrons. Large lateral velocities may exist. Outside of the weakly ionized region the value of V_x practically coincides with the drift velocity $V_{\rm drift} = E_{\perp}/B \approx E_y/B$.

The perpendicular to magnetic field currents $j_{\perp}$ and j_x, which are generated in the cold plasma, are determined by the general Ohm's law, (1.102). On the other hand, current $j_{\perp}$ results in plasma acceleration in the x-direction, according to (1.103), while current j_x is connected with the $V_{\perp}$ component of the plasma velocity. Plasma motion reduces the r.h.s. of (1.102) with respect to $\sigma_{\perp}\vec{E}$, thus also reduc-

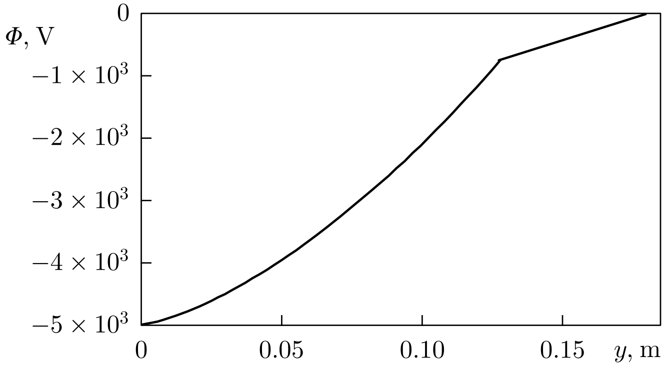

Fig. 1.24. The 5 keV disrupting plasma: potential distribution across the vapor layer, $t = 50\ \mu s$

ing the current values. Therefore, a self-consistent analysis of (1.102) and (1.103) is necessary. Evaluating the components $j_\perp$, j_x from the two projections of (1.102) and substituting them into the two projections of the momentum conservation equation, we find

$$\begin{aligned} \frac{d\rho V_x}{dt} &= \frac{\sigma_\perp B^2}{1+\beta_e^2}\big[(E_\perp/B - V_x) + \beta_e V_\perp\big]; \\ \frac{d\rho V_\perp}{dt} &= -\frac{\sigma_\perp B^2}{1+\beta_e^2}\big[-\beta_e(E_\perp/B - V_x) + V_\perp\big]. \end{aligned} \tag{1.104}$$

The pressure gradient term is neglected here with respect to the electric force term. Let us introduce the parameter

$$q_r = \frac{V_y}{\omega_{ci} L_y}\frac{1+\beta_e^2}{\beta_e}\frac{n}{n_e}, \tag{1.105}$$

where L_y is the characteristic scale of the cold plasma, ω_{ci} is the ion cyclotron frequency, n is the density of the heavy component (ions plus neutrals). We assume here $\partial/\partial t \sim V_y \partial/\partial y \sim V_y/L_y$. For $q_r \ll 1$, excluding $E_\perp$ from (1.104) and (1.105) and making ordering, we find

$$V_\perp \sim q_r \frac{\beta_e}{1+\beta_e^2} V_x \ll V_x. \tag{1.106}$$

Furthermore, neglecting $\beta_e V_\perp$ with respect to V_x in (1.104), we can conclude that (1.104) can be satisfied only if

$$V_x \approx E_\perp/B; \qquad (V_x - E_\perp/B) \sim q_r E_\perp/B \ll E_\perp/B. \tag{1.107}$$

In the opposite case, $q_r \gg 1$, the result depends on the β_e value. For $\beta_e \ll 1$ we have $V_\perp \sim \beta_e V_x$, and hence $V_\perp$ again can be neglected in (1.104). In this situation, as follows from (1.104), the lateral velocity is strongly reduced with respect to the drift velocity $E_\perp/B$:

$$V_x \sim q_r^{-1} E_\perp/B. \tag{1.108}$$

The results of the calculations are in agreement with this qualitative analysis. Close to the surface in the low ionization high collision region we have $\beta_e < 1$ and $q_r > 1$; here, the calculated lateral velocity V_x is much smaller than the drift velocity.

References

[1] V.A. Rozhansky, L.D. Tsendin, *Transport Phenomena in Partially Ionized Plasma* (Taylor & Francis, London, 2001)
[2] S.I. Braginskii, in *Reviews of Plasma Physics*, vol. 1, ed. by M.A. Leontovich (Consultants Bureau, New York, 1965), p. 205
[3] V.M. Zhdanov, *Transport Processes in Multicomponent Plasma* (Taylor & Francis, London, 2002)
[4] C.K. Goertz, J. Geophys. Res. **85**, 2949 (1980)
[5] V.A. Rozhasnkii, Sov. J. Plasma Phys. **16**, 483 (1990)
[6] C.L. Longmire, in *Elementary Plasma Physics* (Interscience, New York, 1963), p. 341
[7] V. Rozhansky, I. Veselova, S. Voskoboynikov, Plasma Phys. Control. Fusion **37**, 399 (1995)
[8] P.T. Lang et al., Phys. Rev. Lett. **79**, 1487 (1997)
[9] J. de Kloe, E. Noordermeer, N.J. Lopes Cardozo, A.A.M. Oomens, Phys. Rev. Lett. **82**, 2685 (1999)
[10] L.R. Baylor et al., in *26th EPS Conference on Controlled Fusion and Plasma Physics*, ed. by R.M. Pick. Maastricht, The Netherlands, 14–18 June 1999. Europhysics Conference Abstracts, vol. 23J (European Physical Society, Geneva, 1999), p. 297
[11] L.R. Baylor et al., Phys. Plasmas **7**, 1878 (2000)
[12] S.I. Krasheninnikov, Phys. Lett. A **283**, 368 (2001)
[13] Y. Sarazin, P. Ghendrih, G. Attuel et al., J. Nucl. Mater. **313–316**, 796 (2003)
[14] M. Scholer, Planet. Space Sci. **18**, 977 (1970)
[15] P.B. Parks, Nucl. Fusion **32**, 2137 (1992)
[16] V. Rozhansky, I. Senichenkov, I. Veselova, R. Schneider, Plasma Phys. Control. Fusion **46**, 575 (2004)
[17] S.M. Dikman, L.P. Pitaevskii, Sov. Phys. JETP **51**, 879 (1980)
[18] A.B. Mikhailovskii, *Electromagnetic Instabilities in an Inhomogeneous Plasma* (IOP, Bristol, 1992)
[19] M. Weinlich, A. Carlson, Contrib. Plasma Phys. **36S**, 53 (1996)
[20] V.A. Rozhanskij, A.A. Ushakov, S.P. Voskobojnikov, Nucl. Fusion **36**, 191 (1996)
[21] F.F. Chen, *Introduction to Plasma Physics and Controlled Fusion*, vol. 1, 2nd edn. (Plenum, New York, 1984)
[22] V.A. Rozhanskii, A.A. Ushakov, S.P. Voskoboynikov, Plasma Phys. Rep. **24**, 777 (1998)
[23] V.A. Rozhanskij, A.A. Ushakov, S.P. Voskoboynikov, Nucl. Fusion **39**, 613 (1999)
[24] P.C. Stangeby, *The Plasma Boundary of Magnetic Fusion Devices* (IOP, Bristol, 2000)
[25] A. Carlson, Contrib. Plasma Phys. **38S**, 38 (1998)
[26] V. Rozhansky, A. Ushakov, I. Veselova, in *26th EPS Conference on Controlled Fusion and Plasma Physics*, ed. by R.M. Pick. Maastricht, The Netherlands, 14–18 June 1999. Europhysics Conference Abstracts, vol. 23J (European Physical Society, Geneva, 1999), p. 841

[27] M. Weinlich, A. Carlson, Phys. Plasmas **4**, 2151 (1997)
[28] M.Z. Tokar, A.V. Nedospasov, A.V. Yarochkin, Nucl. Fusion **32**, 15 (1992)
[29] A.E. Robson, P.C. Thonemann, Proc. Phys. Soc. **73**, 508 (1959)
[30] G.M. McCracken, P.E. Stott, Nucl. Fusion **19**, 889 (1979)
[31] K. Erdl, B. Juttner, Nucl. Fusion **25**, 1413 (1985)
[32] J.R. Sanmartin, Phys. Fluids **13**, 103 (1970)
[33] V.A. Rozhanskii, A.A. Ushakov, Tech. Phys. Lett. **24**, 869 (1998)
[34] P. Gunn, C. Boucher, B.L. Stansfield, C.S. MacLatchy, Contrib. Plasma Phys. **36**, 45 (1996)
[35] D. Bohm, in *The Characteristics of Electrical Discharges in Magnetic Fields*, ed. by A. Guthrie, R.K. Wakerling (McGraw-Hill, New York, 1949), Chaps. 1, 2, 9
[36] V.A. Rozhanskii, L.D. Tsendin, Sov. Phys. Tech. Phys. **23**, 932 (1978)
[37] P.C. Stangeby, J. Phys. D: Appl. Phys. **15**, 1007 (1982)
[38] V.A. Rozhansky, S.P. Voskoboynikov, E.G. Kaveeva, D.P. Coster, R. Schneider, Nucl. Fusion **41**, 387 (2001)
[39] F.L. Hinton, R.D. Hazeltine, Rev. Mod. Phys. **48**, 239 (1976)
[40] S.P. Hirshman, D.J. Sigmar, Nucl. Fusion **21**, 1079 (1981)
[41] V. Rozhansky, M. Tendler, in *Reviews of Plasma Physics*, vol. 19, ed. by B.B. Kadomtsev (Consultants Bureau, New York, 1996), p. 147
[42] V. Rozhansky, M. Tendler, Phys. Fluids B **4**, 1877 (1992)
[43] V. Rozhansky, E. Kaveeva, S. Voskoboynikov, D. Coster, X. Bonnin, R. Schneider, Nucl. Fusion **42**, 1110 (2002)
[44] R.J. Groebner, Phys. Fluids B **5**, 2343 (1993)
[45] K.H. Burrel, Phys. Plasmas **4**, 1418 (1997)
[46] V. Rozhansky, Contrib. Plasma Phys. **46**, 103 (2006)
[47] R.J. Taylor, M.L. Brown, B.D. Fried et al., Phys. Rev. Lett. **63**, 2365 (1989)
[48] R.R. Weynants, R.J. Taylor, Nucl. Fusion **30**, 945 (1990)
[49] L.G. Askinazi, V.E. Golant, S.V. Lebedev, V.A. Rozhanskij, M. Tendler, Nucl. Fusion **32**, 271 (1992)
[50] R.R. Weynants, G. van Oost, G. Bertschinger et al., Nucl. Fusion **32**, 837 (1992)
[51] V. Rozhansky, E. Kaveeva, S. Voskoboynikov, D. Coster, X. Bonnin, R. Schneider, Phys. Plasmas **9**, 3385 (2002)
[52] J. Cornelis, R. Sporken, G. van Oost, R.R. Weynants, Nucl. Fusion **34**, 171 (1994)
[53] M. Van Schoor, R. Weynants, Plasma Phys. Control. Fusion **40**, 403 (1998)
[54] T.E. Stringer, Nucl. Fusion **33**, 1249 (1993)
[55] K. Itoh, S.-I. Itoh, M. Yagi, A. Fukuyama, Phys. Plasmas **5**, 4121 (1998)
[56] J.A. Heikkinen, T.P. Kiviniemi, A.G. Peeters, Phys. Rev. Lett. **84**, 487 (2000)
[57] J.A. Heikkinen, S. Jachmich, T.P. Kiviniemi, T. Kurki-Suonio, A.G. Peeters, Phys. Plasmas **8**, 2824 (2001)
[58] R.R. Weynants, S. Jachmich, G. Van Oost, Plasma Phys. Control. Fusion **40**, 635 (1998)
[59] S. Jachmich, G. Van Oost, R.R. Weynants, J.A. Boedo, Plasma Phys. Control. Fusion **40**, 1105 (1998)
[60] D. Desideri et al., Czech. J. Phys. **49**(Suppl. S3), 119 (1999)
[61] T.D. Rognlien, D.D. Ryutov, Contrib. Plasma Phys. **38**(1–2), 152 (1998)
[62] T.D. Rognlien, D.D. Ryutov, Plasma Phys. Rep. **25**, 943 (1999)
[63] T.D. Rognlien, D.D. Ryutov, N. Mattor, Czech. J. Phys. **48**(Suppl. S2), 201 (1998)
[64] T.D. Rognlien, D.D. Ryutov, N. Mattor, G.D. Porter, Phys. Plasmas **6**, 1851 (1999)
[65] G.J. Radford et al., Contrib. Plasma Phys. **36**(2–3), 187 (1996)
[66] R. Zagorski, H. Gerhauser, H.A. Claasen, Contrib. Plasma Phys. **38**(1–2), 61 (1996)
[67] T.D. Rognlien, Plasma Phys. Control. Fusion **47**, A283 (2005)

[68] R. Zagorski et al., in *28th EPS Conference on Controlled Fusion and Plasma Physics*, ed. by C. Silva, C. Varandas, D. Campbell. Madeira, Portugal, 18–22 June 2001. Europhysics Conference Abstracts, vol. 25A (European Physical Society, Geneva, 2001), p. 2069
[69] V. Rozhansky, Plasma Phys. Control. Fusion **46**, A1 (2004)
[70] T.P. Kiviniemi et al., Phys. Plasmas **10**, 2604 (2003)
[71] Y. Andrew et al., Plasma Phys. Control. Fusion **46**, 337 (2004)
[72] V. Rozhansky, E. Kaveeva, S. Voskoboynikov, D. Coster, X. Bonnin, R. Schneider, Nucl. Fusion **43**, 614 (2003)
[73] P.H. Diamond, Y.B. Kim, Phys. Fluids B **3**, 1626 (1991)
[74] G.M. Staebler, R.R. Dominguez, Nucl. Fusion **33**, 77 (1993)
[75] V.I. Bugarya, A.V. Gorshkov, S.A. Grashin et al., Nucl. Fusion **25**, 1707 (1985)
[76] D.L. Brower, W.A. Peebles, N.C. Luhman, Nucl. Fusion **27**, 2055 (1987)
[77] P. Ghendrih, A. Grosman, H. Capes, Plasma Phys. Control. Fusion **38**, 1653 (1996)
[78] X.Z. Yang, B.Z. Zhang, A.J. Wooton et al., Phys. Fluids B **3**, 3448 (1991)
[79] R.W. Harvey, M.G. McCoy, J.Y. Hsu, A.A. Mirin, Phys. Rev. Lett. **47**, 102 (1981)
[80] A. Gurevich, K. Zybin, Y.N. Istomin, Nucl. Fusion **27**, 453 (1987)
[81] T. Kubota, S.-I. Itoh, Phys. Plasmas **2**, 3368 (1995)
[82] A.B. Rechester, M.N. Rosenbluth, Phys. Rev. Lett. **40**, 38 (1978)
[83] I. Kaganovich, V. Rozhansky, Phys. Plasmas **5**, 3901 (1998)
[84] R.E. Waltz, Phys. Fluids **25**, 1269 (1982)
[85] P.W. Terry, P.H. Diamond, T.S. Hahm, Phys. Rev. Lett. **57**, 1899 (1986)
[86] C. Busch et al., in *33rd EPS Conference on Control Fusion and Plasma Physics*, Rome. ECA, vol. 30I (2006), p. 2.167
[87] L. Lengyel, V.A. Rozhansky, I. Veselova, P. Lalousis, Contrib. Plasma Phys. **38**, 124 (1998)
[88] L.L. Lengyel, K. Lackner, P.J. Lalousis, P.N. Spathis, V.A. Rozhanskij, I.Y. Veselova, P.B. Parks, Nucl. Fusion **38**, 1435 (1998)

2

Correlations and Anomalous Transport Models

O.G. Bakunin

2.1 Introduction

At present, the major obstacle on the way to the realization of controlled thermonuclear fusion in closed magnetic configuration devices is commonly attributed to the existence of anomalous energy losses due to particle and energy transport across a confining magnetic field. The anomalous transport of particles is usually related to the turbulent character of plasma behavior [1–5]. In spite of considerable effort, this problem still remains to be solved [6–12].

The equations describing diffusion phenomena [13–16] are among the key tools for investigating transport processes in plasmas. The ever-increasing complexity of the problems requires the development of more and more elaborate and diverse diffusion models [17–22]. The relation between heat conduction and random walk processes was established as early as the beginning of the 20th century [13]. At the first stage of research in this field, the main problem was that of calculating the diffusion coefficient (thermal conductivity). The investigation of turbulent diffusion in the atmosphere had led to the use of scalings, correlation functions, and new equations that differ substantially in structure from the conventional diffusion equation [18–20]. The research on atmospheric turbulence alone allows one to understand the hierarchic nature of turbulent scales and the importance of accounting for anisotropy. The intensive investigation of processes in strongly magnetized plasma, which was started in the middle of 20th century, essentially expands the notion about both transport processes and the nature of turbulence. Thus, transport models in stochastic magnetic fields and two-dimensional turbulent models were developed. It was revealed that transport processes in turbulent plasmas are often nondiffusive in nature. New forms of equations describing transport processes have constantly been searched for since the first studies on quasi-linear theory [23, 24]. The description of diffusion under strongly nonequilibrium conditions in highly turbulent plasma required the use of equations that take into account memory effects and the nonlocal nature of transport processes [18–20].

The objective of this paper is to consider various methods for constructing such equations, ranging from those in the quasi-linear approximation [23, 24] to those with fractional derivatives [19–22]. The topics to be discussed include the telegraph equation, the Levy–Khintchine distribution, and the Kohlrausch slow relaxation law and continuous time random walks. Use will be made of some important notions belonging to theoretical probabilistic analysis: the return probability, the self-intersection probability, and the probability of staying in a trap.

Another important aspect of the problem of describing turbulent transport is using the correlation methods of analysis [25–30]. Even from the common point of view, one can see that the correlation function is a more relevant tool to investigate a constant diffusion coefficient. Long-range correlations are responsible for anomalous transport. The methods of direct calculations and the diffusive approximation of the correlation effects are represented. One can see that the analysis of correlation effects and the interrelation between the diffusion coefficient and the autocorrelation function have been of major importance. It would therefore be instructive to trace the relation between Taylor's paper [31] that introduced the autocorrelation function and the papers on percolation diffusion [17], which are new trends of the turbulent transport theory.

It is well known that scaling representation, which was initially developed by Richardson and Kolmogorov, plays an important role in turbulence. A large number of researchers have used the ideas of scaling laws and fractality [32–48] to describe properties of turbulent transport. This is not surprising, because turbulent diffusion models differ significantly from one-dimensional transport models. Thus, the presence of vortex structures in turbulent flows and plasma requires the consideration of hierarchies of spatial and correlation scales. The system of convective cells is one of the typical examples of quasi-regular vortex structures. On the one hand, the space between convective rolls is responsible for convective transport. On the other hand, in vortex structures trapping leads to subdiffusive transport. Therefore, obtaining the expression for the effective diffusion coefficient is a nontrivial problem. Often, several different types of transport are present simultaneously in turbulent diffusion [38, 39, 48], making it important to take into account initial diffusivity and anisotropy. The anisotropy of the medium is thought to be due to the presence of a strong magnetic field or shear convective flows.

The sealing approach to describe long-range correlation was essentially developed in papers on the theory of phase transitions and critical phenomena [49–57]. Thus, the power form dependence of correlation scale on the small parameter, which describes the closeness of a system to the percolation threshold, is a fairly universal model to describe anomalous transport. In such an approach, the existence of very long (percolation) streamlines in two-dimensional random flows allows one to use the well-developed mathematical methods of transport analysis in percolation systems [17]. A detailed analysis of the more important results obtained in this field is presented in this chapter.

The review is structured as follows. It contains essentially seven parts. The first part covers Sects. 2.1 and 2.2. Here, the diffusion equations for the description of nonlocal effects are considered.

Section 2.1 is devoted to the consideration of models using the conventional representation of the diffusion equations and the definition of the correlation representation of the turbulent diffusion coefficient. Thus, the models by Richardson [58] and Batchelor [59] are based on diffusion coefficient approximations that are in agreement with the scaling for relative diffusion [58]. The Davydov idea [60] to describe the turbulent transport of a passive scalar by a telegraph equation is treated in this section.

In Sect. 2.2, the importance of using integral representation for the description of nonlocal effects is pointed out. The Levy–Khintchine approach based on the power representation of the Fourier-transformation of the nonlocal functional kernel is considered [61]. The Monin idea [62] of agreement between the transport equations in the Levy–Khintchine form and the Kolmogorov law [63] for isotropic turbulence is discussed in Sect. 2.2.

The second part consists of Sects. 2.3–2.8. Here, we deal with the initial diffusivity effects and the quasi-linear approximation of the nonlinear equations.

The Corrsin conjecture to describe the relationship between Lagrangian and Eulerian correlation functions is introduced in Sect. 2.3 [28]. It is an important aspect of the problem that the Corrsin conjecture relates correlation effects to the seed diffusion nature of transport. Later, this idea was developed in Dupree's and Kadomtsev–Pogutse's papers [64–67]. Then in Sect. 2.4 we consider the effects of molecular diffusion, which lead to the power approximation of the correlation function [68]. Another important aspect is anisotropy effects. In this connection, the double diffusion regime in a stochastic magnetic field is considered [69]. The Howell representation [73] of the effective coefficient of diffusion is observed.

In Sect. 2.5, the heuristic Taylor method to obtain such an equation is considered. The approximation suggested in [117] has become an important step in the development of description methods of anomalous transport and complex correlation effects.

In Sect. 2.6, we consider anomalous transport in the system of random shear flows [72] where the nontrivial character of diffusivity in an anisotropic system is manifested. The quasi-linear equations are derived in Sect. 2.7 [23, 24]. We then discuss the short-range and long-range effects in terms of the quasi-linear approach [20]. The possibility of using the quasi-linear approximation for the description of stochastic magnetic field diffusion is discussed [67, 70].

Section 2.8 treats the diffusive renormalization of correlation effects. We will consider the direct calculations of the correlation function [71], the Corrsin conjecture [72], and the renormalized quasi-linear equations [67]. The focus of Sect. 2.9 is the derivation of the expression for the effective diffusion coefficient, which is based on the balance of convective and diffusive fluxes, in the convective cell system.

The third part covers Sect. 2.10, where the problems of relations between stochastic instability [74] and transport effects in the stochastic magnetic field are analyzed on the basis of Rechester and Rosenbluth's models [75]. The relations between the Rechester–Rosenbluth model and the Kadomtsev–Pogutse approach are treated here.

The fourth part consists of Sects. 2.11 and 2.12. This part deals with the fractal and percolation approaches to describe the transport effects.

Several important definitions from fractal theory [56, 57] are introduced in Sect. 2.11. We then consider the fractal interpretation of Richardson's [58] and Kolmogorov's [63] laws by using the notion of fractal dimensionality [76–78].

Section 2.12 is devoted to the consideration of percolation methods for describing transport effects. Here we discuss the fractal representations of important formulas of transport theory, the percolation renormalization technique [79], and the convective cells problem [33, 80, 81] as the simplest examples to describe transport effects in the presence of the structure.

The fifth part covers Sects. 2.13–2.17. Here, percolation methods for describing the anomalous transport in random two-dimensional flows are observed on the grounds of both the monoscale and multiscale approaches [17]. We point out the importance and universality of renormalization methods to describe turbulent transport in terms of percolation theory. The model of steady flow percolation [82], time-dependent percolation [83], and the influence of drift effects [84] are considered.

Section 2.17 of this review deals with the multiscale approach [85, 86] that is applied to the description of percolation effects. The relationships between the exponents (the hull exponent, the correlation exponent, the Hurst exponent) are considered [17].

The sixth part consists of Sects. 2.18–2.20. Here, the memory and trap effects are represented on the basis of both fractal and continuous time random walk approaches.

Section 2.18 treats the problem of subdiffusive regimes and the trap approximation to describe anomalous transport effects [18–20]. The Balagurov–Vaks trap model is considered [87]. The simplest fractal representation of subdiffusive behavior is explored, as are comb structures. Section 2.19 describes the continuous time random walk approach for the description of nonlocal and memory effects [18–20]. Using the relaxation function in the power form leads to the consideration of transport fractional differential equations. Fractional differential equations with the correlation exponent as a parameter are derived and the relationships between the correlation exponent and the Hurst exponent are obtained in Sect. 2.20.

The last part consists of Sect. 2.21. Here, we discuss the relationship between the conventional space approach to transport and the phase-space approach. The Hamiltonian approach gives the advantage of using degrees of freedom to treat nonlocality and memory effects in the framework of phase-space. The kinetic model provides the possibility of describing ballistic modes and establishing the relationship between different exponents and distributions [96]. We consider the phase-space modification of the Corrsin conjecture, sticky island exponent, and nonlocal velocity distribution function.

2.2 Turbulent Diffusion and Transport

In spite of considerable progress in the understanding of anomalous transport, many aspects of the first papers in this region remain present-day. Thus, at the first stages of research on turbulent diffusion processes it was proposed using correlation functions, modifying the conventional diffusion equation, and searching scaling laws that describe nondiffusive transport. In this section we will discuss the aforementioned ideas using the classical papers by Taylor [31], Richardson [58], Davydov [60] and Batchelor [59].

2.2.1 The Correlation Function and the Taylor Diffusivity

In this section we briefly consider defining the turbulent diffusion coefficient. Taylor published a paper [31] (1921) in which he suggested a formula showing a direct relationship between the diffusion coefficient and the autocorrelation function of velocity. Actually, a new "tool" was suggested for the analysis of diffusion processes.

Following ideas in Langevin's and Einstein's papers [88, 89], Taylor wrote a stochastic equation of motion of a test Lagrangian particle in a random field,

$$x(t) = \int_0^t V(x_0, \tau)\, d\tau, \tag{2.1}$$

where $x(t)$ is the coordinate of the particle at time t, $V(x_0, t)$ is the random function of Lagrangian velocity, and x_0 is the initial coordinate of the Lagrangian particle. The purpose of his calculation was the mean square of a random displacement of the particle

$$\langle x^2 \rangle = \langle x(t)x(t) \rangle = \left\langle \int_0^t V(t_1)\, dt_1 \int_0^t V(t_2)\, dt_2 \right\rangle. \tag{2.2}$$

The brackets $\langle\rangle$ indicate an average over the ensemble of Lagrangian trajectory. Here, we omit the calculations described in detail in [27–29]. The final result of the calculations can be written in the form

$$\langle x^2 \rangle = 2 \int_0^t dt_1 \int_0^{t_1} C(\tau)\, d\tau, \tag{2.3}$$

where $C(\tau)$ is the Lagrange correlation function,

$$C(\tau) = \langle V(x_0, t) V(x_0, t + \tau) \rangle. \tag{2.4}$$

A somewhat different form of this formula was suggested by Kampe de Feriet in [90]:

$$\langle x^2 \rangle = 2 \int_0^t (t - \tau) C(\tau)\, d\tau. \tag{2.5}$$

Here, the symmetry of integral expression (2.3) is used to simplify the representation of the formula. Estimates of the turbulent diffusion coefficient in the Taylor approach lead to the expression

$$D_T = \frac{1}{2} \frac{d}{dt} \langle x^2 \rangle = \frac{d}{dt} \int_o^t (t - t') C(t')\, dt' = \int_0^t C(\tau)\, d\tau \approx V_0^2 \tau. \tag{2.6}$$

Here, V_0 is the characteristic velocity and τ is the correlation time. The specific form of the expression for the turbulent diffusion coefficient $D_T(t)$ depends on the behavior of the correlation function $C(t)$. This differs significantly from the "graded" representation of the familiar Fick's Law [7–9] with $D_0 \propto \Delta_{\mathrm{COR}}^2/\tau$. Here, Δ_{COR} is the spatial correlation scale. Usually, the exponential form is used:

$$C(t) = V_0^2 \exp\left(-\frac{|t|}{\tau}\right), \tag{2.7}$$

where V_0 is the characteristic velocity and τ is the characteristic correlation time. Such a representation of the correlation function for $t \gg \tau$ is in agreement with the rigorous results from the stochastic equation theory [13, 14, 16].

There are two asymptotic cases of significance. In the first, when $t \gg \tau$, upon substitution of (2.7) into (2.5) and simple transformations one can easily obtain

$$\left\langle x^2 \right\rangle = 2V_0^2 t\tau - 2\int_0^{\infty} \tau C(\tau)\, d\tau \approx 2V_0^2 \tau t. \tag{2.8}$$

This expression coincides with the well-known Einstein law for the root-mean-square displacement, $R^2 \propto t$.

In the second case, when $t \to 0$, we can use the simplest approximation of the correlation function in the form

$$C(t) \approx V_0^2 \left(1 - \frac{t^2}{\tau^2}\right). \tag{2.9}$$

This is an important correction of representation (2.7), from a formal point of view, because we have to take into account the rigorous condition of applicability of correlation approximations [27],

$$\left.\frac{d}{dt} C(t)\right|_{t\to 0} \to 0. \tag{2.10}$$

Upon substitution of (2.9) into formula (2.5), one obtains the ballistic motion law in the form

$$\left\langle x^2 \right\rangle = 2V_0^2 t^2. \tag{2.11}$$

Another important relationship, which will be used in the subsequent discussions, is the expression

$$\left.\frac{d^2}{dt^2}\left\langle x^2 \right\rangle\right|_{t=\tau} = 2C(\tau). \tag{2.12}$$

This formula can be obtained by differentiation of expression (2.6).

Even from general considerations, it is clear that the correlation function is a more relevant tool of investigation than the constant diffusion coefficient. In the next sections, we will show that the development of correlation ideas had an essential influence on the form of diffusion equations.

2.2.2 The Richardson Law

The problem formulated by Taylor [31] appears to be especially actual in relation to the Richardson investigations of turbulent diffusion that were carried out in 1926 [58]. The author of [58] discovered that the laws of atmospheric diffusion essentially differ from conventional expression (2.8). An analysis of experimental results has led to the expression for the mean square separation of a pair of marked particles,

$$\frac{1}{2}\frac{d}{dt}\left\langle Y^2(t)\right\rangle \approx \text{const}\cdot\left\langle Y^2(t)\right\rangle^{2/3}. \tag{2.13}$$

Here, $Y(t)$ is the separation between two particles that are situated at the points $x_1(t)$ and $x_2(t)$,

$$Y(t) = x_2(t) - x_1(t). \tag{2.14}$$

Dependence (2.13) shows the accelerating character of particle relative motion. The expression can be represented in the scaling form:

$$\left\langle Y^2(t)\right\rangle \propto t^3. \tag{2.15}$$

Result (2.15) is not trivial because it differs significantly even from the ballistic scaling (2.11). Indeed, from the formal standpoint we can expect that

$$\left\langle Y^2(t)\right\rangle = \left\langle x_1^2(t)\right\rangle - 2\left\langle x_1(t)x_2(t)\right\rangle + \left\langle x_2^2(t)\right\rangle. \tag{2.16}$$

Destroying correlations in time leads to the result that is in accord with the following estimates:

$$\left\langle Y^2(t)\right\rangle \approx 2(2D_T)t. \tag{2.17}$$

However, from the point of view of the scaling law (2.13) we deal with the dependence

$$D_R \approx \left\langle Y^2(t)\right\rangle^{2/3}. \tag{2.18}$$

This expression, in fact, mirrors the nonlocal character of transport effects in the conditions of atmospheric turbulence, since the separation between the diffusing particles significantly changes only under the influence of eddies comparable in size to interparticle separation.

Richardson suggested using the diffusion equation for the description of the probability density evolution F to find two initially close particles at a distance l from one another at the moment t:

$$\frac{\partial F(l,t)}{\partial t} = \frac{\partial}{\partial l} D_R \frac{\partial F(l,t)}{\partial l}. \tag{2.19}$$

In the framework of the offered scaling law (2.13), the expression for $D_R(l)$ takes the form

$$D_R(l) \approx l^{4/3}. \tag{2.20}$$

This result was later confirmed in the framework of the theory of uniform isotropic turbulence [63]. Kolmogorov and Obuchov showed in their articles [63, 91] that the rate of energy dissipation ε_K is the only dimensional characteristic in a wide interval of scales l. Then it is possible to compose the scaling laws based on the dimensional character of the value $\varepsilon_K = [L^2/T^3]$ and the variable k that characterizes the spatial scale $k \approx 1/l(k) = [1/L]$. Simple calculations then yield the dimensional estimate for the Richardson coefficient:

$$D_R(l) = \left[\frac{L^2}{T}\right] \approx \varepsilon_K^{1/3}\frac{k^{2/3}}{k^2} \approx \varepsilon_K^{1/3}\frac{1}{k^{4/3}} \approx \varepsilon_K^{1/3} l^{4/3}. \tag{2.21}$$

Thus, the idea of describing turbulence by the hierarchy of eddies of different scales [63] has obtained its first experimental confirmation.

It is important to note that expression (2.13) suggested by Richardson is in accord with the experimental data in a wide spectrum of parameters. This quite justifies the usage of the expression “the Richardson law”. The papers by Taylor and Richardson undoubtedly opened up a fundamentally new avenue for research and had a profound effect on the subsequent development of the theory of transport processes.

2.2.3 The Davydov Model of Turbulent Diffusion

The nonlocal character of transport that has been investigated by Richardson is manifested not only for the relative diffusion of particles. The problem of the diffusion description of a single test particle in the field of turbulence also leads to the necessity to take into account the interaction between different scales $l(k)$. Such an approach naturally requires considerable modification of Fick’s diffusion equation:

$$\frac{\partial n}{\partial t} = D\frac{\partial^2 n}{\partial x^2}. \tag{2.22}$$

Here, n is the particle density and D is the conventional coefficient of diffusion. One of the first models to describe turbulent diffusion is the Davydov model [60], which is based on the telegraph equation

$$\frac{1}{\tau}\frac{\partial n}{\partial t} + \frac{\partial^2 n}{\partial t^2} = V^2\frac{\partial^2 n}{\partial x^2}, \tag{2.23}$$

where V is the velocity scale and τ is the correlation time. From the dimensional standpoint, the use of this expression permits one to obtain scaling laws for the mean square displacement of a particle in the ballistic form

$$\left\langle x^2 \right\rangle \propto t^2. \tag{2.24}$$

Note that Maxwell [18] was the first to suggest the hyperbolic model of heat-conductivity for the description of the finite velocity of perturbation spreading. This corresponds fairly well to his investigations of electromagnetic theory.

Davydov used the phenomenological set of equations for the particle density $n(x,t)$:

$$\frac{\partial n(x,t)}{\partial t} + \frac{\partial q(x,t)}{\partial x} = 0; \tag{2.25}$$

$$\frac{\partial q}{\partial t} = \frac{q_0 - q}{\tau}. \tag{2.26}$$

Here, q is the particle flux. It is natural to use the classical expression for the particle initial flux:

$$q_0(x,t) = -D\frac{\partial n(x,t)}{\partial x}. \tag{2.27}$$

Formal manipulations with this set of equations yield telegraph equation (2.23). The author of [60] suggested using (2.23) to take into account the finite particle velocity V during the molecular diffusion. The classical parabolic diffusion equation follows from telegraph equation (2.23) in the limit

$$\tau \to 0; \qquad D \approx V^2\tau \to \text{const}. \tag{2.28}$$

The physical meaning of the representation proposed by Davydov for the particle flux q can be easily clarified by writing the formal solution

$$q(x,t) = \int_0^t q_0(x,t')\exp\bigl(-(t-t')\bigr)\frac{dt'}{\tau} = -\int_0^t D\frac{\partial n}{\partial x}\exp\bigl(-(t-t')\bigr)\frac{dt'}{\tau}. \tag{2.29}$$

Obviously, such an expression for the particle flux contains memory effects. After Davydov, this formula was generalized in many studies in such a way as to replace the exponential function by an arbitrary memory function $M(t-t')$,

$$q(x,t) = \int_0^t q_0(x,t')M(t-t')\frac{dt'}{\tau}. \tag{2.30}$$

In this general case one obtains the diffusion equation in the form

$$\frac{\partial n(x,t)}{\partial t} = \int_0^t D\frac{\partial^2 n(x,t')}{\partial x^2}M(t-t')\frac{dt'}{\tau}. \tag{2.31}$$

Later, the telegraph equation in the form (2.23) was often applied to describe turbulent diffusion [27, 92–95].

From the modern point of view such an approach looks fairly naive. However, in essence, the idea of using the additional derivative in the equations describing the anomalous character of turbulent diffusion was clearly formulated by Davydov as early as 1934 [60]. At present, not only are conventional partial derivatives used, but fractional derivatives are also used, better mirroring the essence of the nonlocality and memory effects because they have the integral character of the operator [18–22]

$$\frac{\partial^\xi n}{\partial x^\xi}, \qquad \frac{\partial^\zeta n}{\partial t^\varsigma}, \qquad \ldots. \tag{2.32}$$

Here, ξ and ζ are the fractional parameters of the problem. Moreover, this approximation method is also applied to the description of strong nonequilibrium processes in the framework of kinetic equation [96, 97] for the distribution function $f(V, x, t)$. Here, V is the velocity. Thus, it is suggested replacing the Fokker–Planck diffusive operator $\partial^2 f/\partial V^2$ by the fractional derivatives $\partial^\xi f/\partial V^\xi$ that reflect the nonlocal character of relaxation in the phase space. In the next sections of the paper we will discuss these problems in detail.

2.2.4 The Batchelor Approximation for the Diffusion Coefficient

The approximation suggested by Richardson (2.20) corresponds to his ideas about the hierarchical and nonlocal character of turbulent transport. Thus, he related nonlocality to the increasing scale of eddies taking part in transport processes. Therefore, in his approach the diffusion coefficient D_R is the function of the interparticle distance l. However, there exist alternative possibilities. Batchelor [59] considered the problem from a different point of view. In his model the diffusion coefficient D_R is the result of statistical averaging over the ensemble of different scales. Hence, he proposed using the temporal dependence for the definition of D_R. In the framework of this approach the dimensional consideration yields the expression

$$D_R(t) \approx \frac{\langle Y^2(t)\rangle}{t} \approx \left\langle l^2(t)\right\rangle^{2/3} \propto t^2. \tag{2.33}$$

The equation for the probability density then takes the following form, which is similar to the conventional one (2.22) but with the time-dependent coefficient of diffusion:

$$\frac{\partial F(l,t)}{\partial t} = D_R(t)\frac{\partial}{\partial l}\frac{\partial F}{\partial l}. \tag{2.34}$$

After the simplest analysis it becomes clear that the Richardson model and the Batchelor model lead to different results in spite of the underlying law (2.13). Thus, in the conventional diffusion equation (2.22) the law of temporal relaxation of the function F in the Fourier form corresponds to

$$\tilde{F}_k(t) \propto \exp(-t), \tag{2.35}$$

whereas in the Batchelor model we deal with stronger damping:

$$\tilde{F}_k(t) \propto \exp\left(-t^3\right). \tag{2.36}$$

Here, $\tilde{F}_k(t)$ is the Fourier transformation of the function $F(x, t)$ over the variable x. It is obvious that the characters of the solutions suggested by Richardson and Batchelor describing the probability density evolution are also different. Considering the model with a point-source of particles, one can obtain for the Richardson model [58]

$$F(l,t) = \frac{8}{315\pi^{8/2}}\left(\frac{9}{4t}\right)^{9/2}\exp\left(-\frac{9l^{2/3}}{4t}\right). \tag{2.37}$$

Under analogous conditions (the model with a point-source) for the Batchelor model one obtains [59]

$$F(l,t) = \left(\frac{1}{2\pi\langle l^2(t)\rangle}\right)^{3/2} \exp\left(-\frac{l^2}{2\langle l^2(t)\rangle}\right). \tag{2.38}$$

Note that the arguments in favor of one type or another of the diffusion coefficient have a qualitative character in both these cases. Moreover, the "combination" of both these approaches is possible, if one supposes that D_R can depend on both the interparticle distance l and time t:

$$D_R(t,l) \approx t^{\phi} l^{\varphi}. \tag{2.39}$$

To save the Richardson law we need to take into account the relationship between exponents ϕ and φ:

$$2\phi + 3\varphi = 4. \tag{2.40}$$

Then, the case $\phi = 0$, $\varphi = 4/3$ corresponds to the Richardson law and the case $\phi = 2$, $\varphi = 0$ corresponds to the Batchelor supposition. Thus, Okubo [98] suggested a mixed algebraic representation for the diffusion coefficient:

$$D_R(t,l) \approx t l^{2/3}. \tag{2.41}$$

The three-dimensional solution for the point-source at $t = 0$ is given by [98]

$$F(l,t) = \text{const} \cdot t^{-\frac{3(1+\phi)}{2-\varphi}} \exp\left(-\text{const} \cdot \frac{l^{2-\varphi}}{t^{1+\phi}}\right). \tag{2.42}$$

Unfortunately, it is impossible to decide what is a correct equation, if one looks at this problem from the conventional diffusion point of view, because the physical arguments from Kolmogorov and Obukhov lead to an explanation in terms of the hierarchy of scales, whereas Richardson and Batchelor deal with the local diffusive equation with partial differentials. However, these classical papers [58–60] formulated problems that allow us to develop theoretical methods of anomalous transport description that are based on the analysis of correlation effects and scaling laws.

2.3 Nonlocal Effects and Diffusion Equations

The nonlocal nature of relative diffusion has stimulated the search for equations that differ significantly from conventional diffusion equations. An elegant integral equation corresponding to this problem was suggested by Einstein [89]. The use of this equation in combination with the scaling ideas has led to the necessity to consider a distribution function that differs essentially from the Gauss function. A new type of distribution, called the Levy–Khintchine distribution, is now one of the basic tools for researching anomalous transport.

2.3.1 The Functional Equation for Random Walks

For the Richardson law Kolmogorov and Obuchov [63, 91] obtained dimensional estimates, which give qualitative explanations of the nonlocality transport effects of turbulent diffusion in terms the interaction of different scales. However, the nonlocal effects can also be described by means of the random walk model. Thus, besides the different phenomenological methods of improvement of the diffusion equation, there exists a possibility to use the integral equation to describe the random walk processes.

As early as 1905, Albert Einstein obtained a functional equation for the particle density solely on the basis of the general ideas about the process of random walk [89]:

$$n(x, t+\tau) = \int_{-\infty}^{+\infty} W(y) n(x-y, t)\, dy, \tag{2.43}$$

where $W(y)$ is the probability density of undergoing a jump y. This fundamentally nonlocal equation can be made local by reducing it to a diffusion equation. Assuming that the time scale τ is short and the jump y is small, Einstein arrived at the classical diffusion equation. In this way, he used the expansions

$$n(x, t+\tau) = n(x, t) + \frac{\partial n}{\partial t}\tau + \cdots, \tag{2.44}$$

$$n(x+y, t) = n(x, t) + \frac{\partial n}{\partial x} y + \frac{y^2}{2}\frac{\partial^2 n}{\partial x^2} + \cdots. \tag{2.45}$$

Simple calculations yield

$$n + \frac{\partial n}{\partial t}\tau = n \int_{-\infty}^{\infty} W(y)\, dy + \frac{\partial n}{\partial x}\int_{-\infty}^{\infty} W(y) y\, dy + \frac{\partial^2 n}{\partial x^2}\int_{-\infty}^{\infty} W(y)\frac{y^2}{2} + \cdots. \tag{2.46}$$

Assuming that the function W is symmetric, $W(y) = W(-y)$, and specifying the normalization condition

$$\int_{-\infty}^{+\infty} W(y)\, dy = 1, \tag{2.47}$$

one obtains the conventional diffusion equation

$$\frac{\partial n}{\partial t} = D\frac{\partial^2 n}{\partial x^2}, \quad \text{where } D = \frac{1}{\tau}\int_{-\infty}^{+\infty} W(y)\frac{y^2}{2}\, dy. \tag{2.48}$$

Note that the number of terms in expansions (2.44), (2.45) was chosen in a physically meaningful way. Based on the relationship characterizing the average behavior of Brownian particles, $\langle x^2 \rangle \approx R^2 \propto t$. We can estimate the orders of the terms for $t \to \infty$ in the expansions as follows: $n \propto 1/R$. This corresponds to the one-dimensional case. Then one can obtain

$$\begin{aligned} &n \propto t^{-1/2}, \qquad \frac{\partial n}{\partial t} \propto \frac{n}{t} \propto t^{-3/2}, \qquad \frac{\partial^2 n}{\partial t^2} \propto \frac{n}{t^2} \propto t^{-5/2}, \\ &\frac{\partial n}{\partial x} \propto \frac{n}{R} \propto t^{-1}, \qquad \frac{\partial^2 n}{\partial x^2} \propto t^{-3/2}. \end{aligned} \tag{2.49}$$

Retaining only two terms in expansions (2.44) and (2.45) each results in a telegraph equation. However, this does not indicate that the telegraph equation is invalid. The reason is that, in this case, the effects of the finite propagation velocity of the perturbations come into play, which are absent in the classical diffusion model.

The integral approach was further developed in the papers by Smoluchowski, Chapman, and Kolmogorov [99–101]. A key element in their approach is Markov's postulate [13, 14] that the length of the jump y is independent of the prehistory of motion. To describe the nonlocal effects, just the integral form of the equations is important.

Using expansion (2.44) of functional (2.43), we can readily obtain the Smoluchowski equation [99]

$$\frac{\partial n(x,t)}{\partial t} = \int_{-\infty}^{+\infty} \left[K(x',x)n(x',t) - K(x,x')n(x,t)\right] dx'. \tag{2.50}$$

Here, $K(x,x')\,dx\,dx'$ is the probability for a particle at position x at time t to pass over to the interval $x' + dx'$ during the time interval dt. We introduce the functional

$$G(x',x) = K(x',x) - \delta(x-x') \int_{-\infty}^{+\infty} K(x,x')\,dx'. \tag{2.51}$$

For a uniform isotropic medium, we have $G(x'-x) = G(|x-x'|)$. In the simplest case under consideration, this functional has the form

$$\frac{\partial n}{\partial t} = \int_{-\infty}^{+\infty} G(x-x')n(t,x')\,dx'. \tag{2.52}$$

This representation reflects the nonlocal character of transport and at the same time it has a close relation to the conventional diffusion equation (2.22). It is possible to consider several analytical functions $G(x)$ to find some solution of this equation [15]. As an example, one can form such an approximation on the basis of Poisson's probabilistic law [13, 14]. But there is another good way that leads to new and very fruitful research trends, which are especially relevant for turbulent diffusion problems.

2.3.2 Nonlocality and the Levy Distribution

Functional (2.52) is linear and it is more convenient to switch to the Fourier representation for $n(x,t)$ with respect to the variable x. Formal manipulations yield

$$\frac{\partial \tilde{n}_k(t)}{\partial t} = \tilde{G}_k \tilde{n}_k(t), \tag{2.53}$$

which indicates the absence of memory effects for the Fourier harmonics. Here, $\tilde{G}_k$ and $\tilde{n}_k(t)$ are the Fourier transformations of the functions $G(x)$ and $n(x,t)$ with respect to the variable x. The expression

$$\tilde{G}_k \tilde{n}_k = -Dk^2 \tilde{n}_k \tag{2.54}$$

corresponds to the classical diffusion equation, where D is the conventional diffusion coefficient. In the case of telegraph equation (2.23), the memory effects were taken into account (see (2.31)):

$$\frac{\partial \tilde{n}_k(t)}{\partial t} = -k^2 \int_0^t \tilde{n}_k(t) M(t-t') \frac{dt'}{\tau} = -k^2 M(t) * \tilde{n}_k(t), \tag{2.55}$$

where the asterisk indicates the convolution operation.

Applying the Laplace transformation in time, we obtain the following expression for the telegraph equation with memory:

$$\tilde{\tilde{G}}(k,s) = -\frac{Dk^2}{1 - is\tau}. \tag{2.56}$$

Hereafter, $\tilde{\tilde{G}}(k,s)$ will denote both the Fourier and Laplace transformations of the function $G(x,t)$ with respect to the variables x and t. It is an easy matter to combine the memory and nonlocality effects into a common expression containing a convolution:

$$\frac{\partial \tilde{n}_k(t)}{\partial t} = -k^2 \int_0^t \tilde{n}_k(t) \tilde{D}_k(k, t-t') \frac{dt'}{\tau} = -k^2 \tilde{D}_k(k,t) * \tilde{n}_k(t). \tag{2.57}$$

Performing the Laplace transformation in time gives the transition from the conventional result to the new one:

$$-Dk^2 \to -k^2 \tilde{\tilde{D}}_{k,s}(k,s). \tag{2.58}$$

In the theoretical probabilistic approach, however, this heuristic method is unsatisfactory. Below, we will consider this point in more detail.

The approach based on (2.53) was developed by Levy and Khintchine [61], who used the approximate equation of the form

$$\frac{\partial \tilde{n}_k(t)}{\partial t} = -k^{\alpha_L} \tilde{n}_k(t), \quad 0 < \alpha_L \leq 2. \tag{2.59}$$

It is easy to see that, for $\alpha_L = 2$, we are dealing with a Gaussian distribution (corresponding to a conventional diffusion equation). Some other analytic distributions are also known.

For the case $\alpha_L = 1$, we obtain the Cauchy distribution [102].

For the case $\alpha_L = 3/2$, one arrives at the familiar Holtsmark distribution [13].

For the case $\alpha_L = 1/2$, we have the Levy–Smirnov distribution [18].

For the case $\alpha_L = 2/3$, we obtain the Smirnov distribution [18]. In this context, it is important to note that all the probability densities with $\alpha_L < 2$ have power-law tails. Another important feature is that the second and higher order of moments of the distributions with $1 \leq \alpha_L < 2$ and all moments of the distributions with $0 < \alpha_L < 1$ diverge.

Representation (2.59) is sufficient to consider the important models of anomalous diffusion, which are often described by the scaling law,

$$\langle x^2 \rangle^{1/2} \approx R \propto t^H. \tag{2.60}$$

Here, H is the Hurst exponent [18–22]. In the case of classical diffusive behavior we find $H = 1/2$. The cases $0 < H < 1/2$ correspond to the subdiffusive behavior. The cases $1/2 < H < 1$ correspond to the superdiffusive behavior. There is a relationship between the Hurst exponent H and the Levy–Khintchine exponent a_L that is the parameter of the power approximation (2.59):

$$H = \frac{1}{\alpha_L}. \tag{2.61}$$

There is also a very interesting result which follows from the Fourier representation of density $n(x,t)$:

$$\langle x^2 \rangle^{1/2} = -\frac{\partial}{\partial k}\left(\frac{\partial}{\partial k} \tilde{n}_k(t) \bigg|_{t=0} \right). \tag{2.62}$$

This expression is very useful for relating scaling laws to probabilistic approximations in the Levy–Khintchine term.

2.3.3 The Monin Fractional Differential Equation

Monin [62] used the Einstein–Smoluchowski functional given in (2.52) and (2.59) to describe turbulent diffusion in the atmosphere. That paper anticipated the development of modern ideas of using additional fractional partial derivatives in diffusion equations.

Monin was guided by Kolmogorov's ideas about the universal properties of well-developed isotropic turbulence [63]. In the corresponding formulation of the problem, all statistical parameters are determined exclusively by the scale length $l_k \approx 1/k \approx [L]$ and the mean energy dissipation rate $\varepsilon_K = [L^2/T^3]$. Here, L and T characterize the physical dimensionality of space and time. In the framework of Fourier's representation (2.59) there is a single "uncertain parameter" a_L, which defines the power form of the kernel of the nonlocal functional. Based on dimensional considerations, it is possible to compose the approximation for function $\tilde{G}(k)$, which has $[1/T]$ order that is in agreement with relaxation law (2.35). Monin obtained the following expression for the kernel of the nonlocal functional describing turbulent diffusion:

$$\tilde{G}(k) \propto \tilde{G}(\varepsilon_K, k) = \varepsilon_K^{1/3} k^{2/3}. \tag{2.63}$$

The expression used by Monin has a dimensionality that is inversely proportional to time. This fact reflects the essential difference of such a model from the Batchelor approach [59]. This representation is consistent with the results derived in 1926 by Richardson [58] under the assumption

$$\tilde{G}(k) = -D(k)k^2, \tag{2.64}$$

where $D(k) \approx \frac{l^2}{t} \propto l^{4/3} \propto k^{-4/3}$. Also, in modern terminology [20–22], the equation

$$\frac{\partial \tilde{n}_k(t)}{\partial t} = -\varepsilon_K^{\frac{1}{3}} k^{\frac{2}{3}} \tilde{n}_k(t) \tag{2.65}$$

is the one with the fractional derivative with respect to x,

$$\frac{\partial^{\alpha_L} n}{\partial x^{\alpha_L}} \propto \frac{n}{(\Delta x)^{\alpha_L}} \propto k^{\alpha_L} n, \tag{2.66}$$

where $\alpha_L = 2/3$ [see formula (2.59)]. Monin was the first to obtain this equation for the probability density on the basis of physical considerations. He solved this equation and wrote the solution in terms of the Whittaker functions. The solution behaves asymptotically as $n(x \to \infty) \propto x^{-11/13}$. The problem of the relaxation in a self-similar regime was discussed in detail in [27, 62].

However, Monin was unsatisfied with the above form of the equation. In fact, he derived the following equation with fractional derivatives:

$$\frac{\partial n}{\partial t} = \varepsilon_K^{1/3} \frac{\partial^{2/3} n}{\partial x^{2/3}}. \tag{2.67}$$

It is only recently that the idea of using fractional derivatives has come to be recognized [18–22]. In an effort to derive an equation that would be as clear as the telegraph equation, Monin differentiated his equation twice with respect to time and obtained the expression

$$\frac{\partial^3 n}{\partial t^3} = \varepsilon_K \frac{\partial^2 n}{\partial x^2}. \tag{2.68}$$

Note that Monin suggested his equation to describe the diffusing particle probability density evolution n. However his idea can be used to describe the probability density evolution F, which describes relative diffusion. Such a version was considered in [103, 104]. But in those papers [103, 104] use was made of the modern terminology and the fractional differential is represented as nonlocal integral operator

$$\frac{\partial F(\vec{l}, t)}{\partial t} = \Gamma(2/3) \frac{\sqrt{3}}{4\pi^2} \Delta_L \int \frac{F(\vec{l}, t)}{|\vec{l} - \vec{l}'|^{5/3}} d^3 \vec{l}'. \tag{2.69}$$

Here, Γ is the Gamma function and Δ_L is the Laplace operator.

It is natural that the use of nonlocal operator (2.69) leads to the distribution function, which differs significantly from the Richardson and Batchelor models. Nevertheless, convincing arguments in favor of the choice of the specific type of equation describing the behavior of the distribution function are absent and the search for adequate models and experimental proofs has been continued. Note that in spite of the assumptions of isotropy and the relative simplicity of experiments, these problems remain acute. From this standpoint, the absence of a detailed pattern of anomalous transport in high-temperature plasma does not look so catastrophic.

2.4 The Corrsin Conjecture

The classical correlation definition of Taylor's coefficient of turbulent diffusion does not contain any information on molecular diffusion. It is obvious that a serious problem arises when we analyze the passive tracer transport. In this section we will consider several important models in which the effects of molecular (seed) diffusion and correlation effects play a significant role. The scaling arguments are presented.

2.4.1 The Corrsin Independence Hypothesis

The definition of the correlation function suggested by Taylor [31] is based on using Lagrangian velocities $V(x_0, y)$, but their experimental determination is a serious problem. That is why use is made of the Eulerian representation for the correlation function, which takes into account the velocity correlation at points separated by a distance λ:

$$C_E(\lambda, t) = \langle u(x_0, T) u(x_0 + \lambda, T + t) \rangle. \tag{2.70}$$

This form of the correlation function is more convenient for experimenters. We can also express the Lagrangian correlation function through the Eulerian velocity,

$$C(t) = \langle u(x_0; T) u\big(x(x_0, T + t); T + t\big) \rangle. \tag{2.71}$$

Here, $U(x_0, T)$ is the Eulerian velocity at point x_0 and time T. However, there is no simple relation between the Lagrangian correlation function and the Eulerian one. Actually, there is no Lagrangian relation between the points x_0 and $x_0 + \lambda$ in expression (2.70). Here, λ is merely some arbitrary displacement.

Corrsin [28] suggested an approximation formula in terms of the randomization of the Lagrange correlation function with the probability density $\rho(x, t)$,

$$C(t) = \int_{-\infty}^{\infty} \rho(\lambda, t) C_E(\lambda, t)\, d\lambda, \tag{2.72}$$

in which he expressed the Lagrangian correlation function through the Eulerian one [25–30]. However, a more important point is the idea of the diffusion nature of the displacement λ, because for $\rho(\lambda, t)$ Corrsin used the classical solution of the diffusion equation in a three-dimensional space,

$$\rho(\lambda, t) = \frac{1}{(4\pi D_0 t)^{3/2}} \exp\left(-\frac{\lambda^2}{4 D_0 t}\right). \tag{2.73}$$

This formula also includes the molecular diffusion coefficient D_0. Hence, one can consider both the turbulent transport and the molecular diffusion. Finally, Corrsin obtained the integral expression

$$C(t) = \int_{-\infty}^{\infty} \frac{C_E(\lambda, t)}{(4\pi D_0 t)^{3/2}} \exp\left(-\frac{\lambda^2}{4 D_0 t}\right) d\lambda. \tag{2.74}$$

From this point of view, one can note that λ is the distance and the diffusive displacement at the same time. In fact, instead of formal averaging in the form

$$\langle V(x(0))V(x(t))\rangle = \int_{-\infty}^{\infty} \langle V(0)V(y)\delta(y - x(t))\rangle\, dy, \tag{2.75}$$

the factorization approach was used (the "independence hypothesis"):

$$\langle V(0)V(y)\delta(y - x(t))\rangle = \langle V(0)V(x)\rangle\langle\delta(y - x(t))\rangle. \tag{2.76}$$

Moreover, Corrsin used Gaussian distribution (2.73) to describe trajectory correlations:

$$\langle\delta(y - x(t))\rangle \approx \rho(y, t). \tag{2.77}$$

Using rigorous analysis, Weinstock [105] and Kraichnan [106] showed that the Corrsin conjecture is equivalent to a first-order truncation of the renormalization expansion, which can be considered systematically.

The Corrsin conjecture has been tested against kinetic simulations of two- and three-dimensional flows with an energy spectrum sharply peaked about one well-determined length scale [105, 107, 108] with the conclusion that it is valid for all times (not only for large times) provided that there is no helicity and that the flow is not frozen in time.

2.4.2 The Simplified Corrsin Conjecture

The interesting paper by Hay and Pasquill [109] was written almost simultaneously with the Corrsin paper [28]. They taken into account that Eulerian and Lagrangian correlation functions have similar shapes; but at the same time, their characteristic scales are different. Thus, the characteristic temporal scale, which corresponds to the Lagrangian correlation function, is defined by the expression

$$\tau_L = \frac{1}{\langle V^2\rangle} \int_0^{\infty} C_L(t)\, dt. \tag{2.78}$$

The characteristic Eulerian temporal and spatial scales are defined analogously

$$\tau_E = \frac{1}{\langle U^2\rangle} \int_0^{\infty} C_E(\Delta, t)\, dt, \tag{2.79}$$

$$l_E = \frac{1}{\langle U^2\rangle} \int_0^{\infty} C_E(\Delta, t)\, d\Delta. \tag{2.80}$$

The authors of [109] supposed that there exists a certain universal constant β_C that allows us to relate Lagrangian and Eulerian scales,

$$\tau_L = \beta_C \tau_E, \tag{2.81}$$

$$l_L(\beta_C t) = \beta_C l_E(t). \tag{2.82}$$

The variety of turbulence types leads to the fact that the values of β_C defined experimentally lie in a wide interval:

$$1 \leq \beta_C < 8.5. \tag{2.83}$$

In spite of the obvious simplicity of the approach suggested by Hay and Pasquill, in recent papers it was shown that in the framework of the consideration of one-particle vertical diffusion in strongly stratified turbulence, the Eulerian and Lagrangian velocity correlation functions are almost the same:

$$\langle V_i(0)V_j(t)\rangle = \langle U_i(x,0)U_j(x,t)\rangle. \tag{2.84}$$

Thus, Kaneda and Ishida [110] considered the Fourier transformation of the Corrsin conjecture (2.76) in the form

$$\langle V_i(t)V_j(t')\rangle = \int d^3\vec{k}\, \tilde{R}_{ij}(\vec{k},t,t')\langle e^{-i\vec{k}(x(t')-x(t))}\rangle, \tag{2.85}$$

where

$$\tilde{R}_{ij}(\vec{k},t,t') = \frac{1}{(2\pi)^3}\int \langle U_i(\vec{x}+\vec{r},t)U_j(\vec{x},t')e^{-i\vec{k}\vec{r}}\, d^3\vec{r}\rangle. \tag{2.86}$$

From the physical point of view the Eulerian velocity correlations must be dominated by large eddies (see [107]). This corresponds to small values of $\vec{k}$. Therefore, for $\vec{k} \approx 0$ one can expect that

$$\langle e^{-i\vec{k}(x(t')-x(t))}\rangle \approx 1. \tag{2.87}$$

This simple estimate gives the simplified Corrsin conjecture

$$\langle V_i(t)V_j(t')\rangle = \langle U_i(\vec{x},t)U_j(\vec{x},t')\rangle. \tag{2.88}$$

This new representation

$$C_L(\tau) \approx C_E(\lambda,\tau)|_{\lambda=0} \tag{2.89}$$

was first discussed by the author of [107]. In the framework of the Boussinesq approximation of strongly stratified flows, the validity of the simplified Corrsin conjecture (2.88) was checked by direct numerical simulations [110, 112]. It was shown that the simulation results agree well with the hypothesis (2.88).

2.4.3 The Correlation Function and Scalings

The Corrsin conjecture looks fairly formal; however, it allows us to visualize correlation effects and to take into account the effects of molecular diffusion. Note that the definition of Taylor's coefficient of turbulent diffusion does not contain any information on molecular diffusion. It is obvious that a serious problem arises when analyzing the passive tracer transport [27, 28]. Moreover, the Corrsin representation offers an additional possibility of developing the scaling approximation of transport by the power approximations of the Eulerian correlation function and different kinds of probability density [18–22].

The effective use of scaling laws will be considered here. Thus, the authors of [113] made a rigorous analysis of equations for a random noncompressible flow where the mean velocity is zero and the spatial correlation function decays as

$$C_E(\lambda) \propto \frac{1}{\lambda^{\alpha_C}}. \tag{2.90}$$

Koch and Brady used a continuum nonlocal advection–diffusion theory (the direct-interaction approximation) and obtained an expression which connects the Hurst exponent H that describes the transport character with the correlation exponent α_C:

$$H = \frac{2}{2+\alpha_C}. \tag{2.91}$$

Here, α_C describes the power behavior of the spatial correlation function of velocity

$$C(\lambda) = \langle V(x)V(x+\lambda) \rangle \propto V_0^2 \left(\frac{\lambda_0}{\lambda} \right)^{\alpha_C}. \tag{2.92}$$

Here, V_0 and λ_0 are the dimensional parameters of the model. Note that this relationship can be obtained by simple calculations based on both the dimensional consideration of the correlation function

$$C \approx V^2 \approx \frac{\lambda^2}{t^2} \tag{2.93}$$

and the power dependence (2.92). Then, the comparison of (2.93) with (2.92) yields

$$\frac{\lambda^2}{t^2} \approx V_0^2 \left(\frac{\lambda_0}{\lambda} \right)^{\alpha}. \tag{2.94}$$

If we suppose that the spatial scale λ is the correlation scale and the diffusive displacement at the same time (as in the Corrsin conjecture), then it is possible to treat (2.94) as the transport scaling. Now, one can obtain the diffusive estimate:

$$\lambda \propto \left(V_0^2 \lambda_0^{\alpha_C} \right)^{\frac{1}{2+\alpha_C}} t^{\frac{2}{2+\alpha_C}} \tag{2.95}$$

and

$$H = \frac{2}{2+\alpha_C}, \tag{2.96}$$

where $0 < \alpha_C < 2$ since the result (2.95) was obtained for incompressible flow, where the subdiffusive transport is absent [17, 114]. Later, relationship (2.96) was repeatedly discussed in connection with the analysis of more complex models of turbulent transport [17, 85, 86].

2.5 Effects of Seed Diffusivity

Corrsin was one of the first to understand the importance of accounting for seed diffusivity effects to describe correlations. Further investigation of turbulent transport led the appearance of numerous estimates and scalings based on diffusive estimates. Thus, in the framework of diffusive approximations it is possible to consider not only transport of a passive tracer but also anomalous diffusion of particles in a braided magnetic field.

2.5.1 Seed Diffusivity and Correlations

It is well known that interactions both create and destroy correlations. There is a useful estimate which illustrates this in terms of the correlation function. It was assumed [16, 68] that the number of interactions N_I is proportional to the number of particles that are located in the correlation region W_D:

$$N_I \approx n W_D \approx n R_D^d. \tag{2.97}$$

Here, n is the density of particles in this region, R_D is the spatial scale of this region, and d is the space dimensionality. Then, from the dimensional point of view, the correlation effects can be expressed in the form

$$C(t) = \langle V(0)V(t)\rangle \approx V_0 \frac{V_0}{N_I} \approx \frac{V_0^2}{n W_D}, \tag{2.98}$$

where $V(t)$ is the velocity at the moment t and V_0 is the characteristic scale of the velocity. The estimate of W_D can be obtained from the conventional Gaussian distribution

$$\rho(x,t) = \frac{1}{(4\pi D_0 t)^{d/2}} \exp\left(-\frac{x^2}{4D_0 t}\right). \tag{2.99}$$

Here, D_0 is the molecular coefficient of diffusion. To derive the estimate it was supposed that correlation scale R_D has the diffusion nature

$$R_D \propto (D_0 t)^{1/2} \quad \text{for } t \to \infty. \tag{2.100}$$

This corresponds to the Corrsin assumptions. Simple calculations then yield

$$C(t) = \langle V(0)V(t)\rangle \approx \frac{V_0^2}{n(D_0 t)^{d/2}} \propto \frac{1}{t^{d/2}}. \tag{2.101}$$

In spite of the difference between this result and the exponential form (2.7), the obtained power approximation of the correlation function is not senseless. The "long tails" of correlation functions $C(t) \propto t^{-3/2}$ are being investigated in molecular dynamics and are related to "the collective" (hydrodynamic) nature of the evolution of a system [16, 68]. The correlation function is related to diffusion coefficient (2.6), which in our case leads to the estimate

$$C(t) \propto \frac{d}{dt} D_T \propto \frac{R^2}{t^2} \propto \frac{1}{t^{d/2}}. \tag{2.102}$$

This yields the transport scaling, which differs significantly from the classical diffusive one.

2.5.2 "Returns" and Correlations

In the previous sections we touched on some questions concerning the relationship between the diffusion coefficient and correlations. Now, we analyze the effect underlying the notion of correlations—return of a randomly moving particle to the initial point. This is best illustrated by considering the problem of one-dimensional random walks at the very beginning of the process. In the problem as formulated, the particle can definitely return to its initial position, thereby providing a clear realistic interpretation of the abstract notion of correlations. Rigorous analysis of returns on complicated spatial grids is necessarily based on the chain functional equation for the return probability $P_0(t)$ [18, 19]. Recall that most of the fundamental problems in the theory of random-walk processes can be formulated in terms of chain functional equations [18, 19]. However, we restrict ourselves here to considering the effects of returns.

Simple estimates for these effects can be obtained from the classical solution to the equation for the probability density function describing the random walks of a particle. For a space of dimensionality d, one obtains the distribution

$$P(x,t) = \rho(x,t)(\delta x)^d = \frac{(\delta x)^d}{(4\pi Dt)^{d/2}} \exp\left(-\frac{x^2}{4Dt}\right). \tag{2.103}$$

Here, $(\delta x)^d$ is the small area around the point x. The probability of a particle returning to point $x = 0$ at time t has the form

$$P_0(t) \propto \frac{(\delta x)^d}{(4\pi Dt)^{d/2}}. \tag{2.104}$$

Generally, this simple (although rather efficient) formula serves merely to obtain estimates [18, 19]. It has the same drawbacks as the simple diffusion model, namely, those associated with the infinite propagation velocity of perturbations and the presence of a point-source term. However, for our purposes here, this solution is important because it provides evidence that the dimensionality of the space, d, which was used above as a formal parameter, plays a significant role. It turns out [18, 19] that, for grids of dimensionality $d \le 2$, the particle will inevitably return to its initial position. For grids with $d > 2$, the particle can execute random walks without returning. We thus see that the case $d = 2$ is intermediate and, as such, attracts much attention of mathematicians. Note that the correct dependence for P_0 for $d = 2$ and $d = 3$ is

$$P_0(N) \propto \frac{1}{N^2} \ll \frac{1}{N^{d/2}}. \tag{2.105}$$

Along with the return probability P_0, use is made of the number of returns and the number of visited grid points. Usually, the task is to express these numbers as certain scaling laws and to establish their relationships to other scaling laws.

Using approximation (2.104), we derive an important scaling relation for particles executing random motion with no self-intersections (self-avoiding random walk). We introduce the probability $p(N)$ of self-intersection after N random walks,

$$p(N) \approx \frac{N}{R^d}, \tag{2.106}$$

where $R^2(N)$ is the root-mean-square displacement, d is the dimension of the space, and $N = t/\tau$ is the number of random walks. Here, t is the time and τ is the correlation time. In fact, we are assuming that the probability of the particle trajectory intersecting itself is proportional to the number density of visited grid points within the region of random particle motion. Then, the probability for a particle to execute N self-avoiding random walks can be estimated as

$$P_S(N) \approx (1-p)^N\big|_{N\to\infty} \approx \exp(-pN) \approx \exp\left(-\frac{N^2}{R^d}\right). \tag{2.107}$$

Taking into account the fact that the relationship between the quantities R and N is of a diffusive nature, we can estimate the effective probability of self-avoiding random walks by averaging the probability $P_S(N)$ with the Gauss distribution:

$$P_S(t) = \int_{-\infty}^{\infty} \exp\left(-\frac{1}{R^d}\left(\frac{t}{\tau}\right)^2\right)\frac{1}{(4\pi Dt)^{d/2}}\exp\left(-\frac{R^2}{4Dt}\right)(dR)^d. \tag{2.108}$$

We assume that the main contribution to the integral comes from the extremum of the integrand,

$$\min\left(\frac{1}{R^d}\left(\frac{t}{\tau}\right)^2 + \frac{R^2}{4Dt}\right), \tag{2.109}$$

and perform simple manipulations to obtain the scaling law:

$$R(t) \propto t^{3/(2+d)} \gg t^{1/2}, \qquad H = \frac{3}{2+d} \tag{2.110}$$

for $d \le 3$. Here, we must take into account the fact that, in a space of dimensionality $d = 1$, nonself-intersecting random walks can occur only for the particles moving in one direction, which indicates that $R \propto t$. We see that estimate (2.110) satisfies this condition automatically.

This scaling, which was first obtained in the theory of polymers by Flory [18], is very important in describing the properties of different systems with nonconventional correlation properties and complex topology.

2.5.3 The Stochastic Magnetic Field and Scalings

The description of the interaction of different scales in turbulent transport can also be considered in another aspect. Thus, the analysis of transport in an anisotropic medium leads to the necessity of considering the interplay of both the longitudinal and transverse correlation mechanisms. This problem is particularly relevant in connection with investigations of the processes of turbulent diffusion of plasma in a

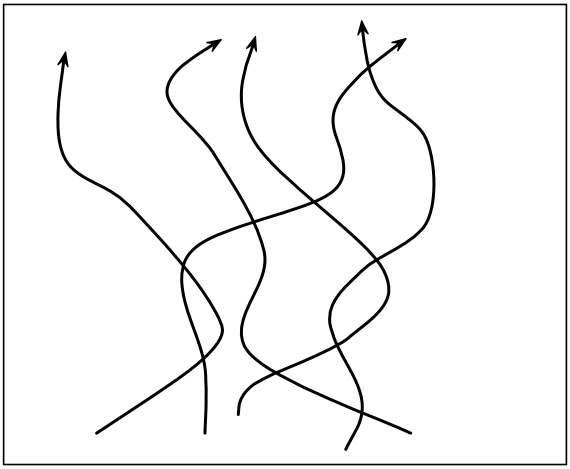

Fig. 2.1. Force lines random walk

stochastic magnetic field. Many papers are devoted to this problem, but its complete solution is still a long way off. In this section, we consider one of the first models of particle transport in a "braided" magnetic field. This problem was formulated in connection with the description of cosmic ray diffusion in a galactic magnetic field [69, 70]. But this is a relevant model for some mechanisms of anomalous diffusion in magnetized plasma [5–8]. The concept of random walks of magnetic force lines in the transverse direction was the basis of this consideration (see Fig. 2.1). In this case, it is convenient to introduce a magnetic diffusion coefficient of streamlines

$$D_m \propto \frac{\Delta_\perp^2}{L_\parallel}. \tag{2.111}$$

Here, $\Delta_\perp$ is the displacement of the perturbed force line in the transverse direction under the condition of displacement along the streamline on the length $L_\parallel$. If we assume that particles in their motion strictly follow the displacement of the force line, which was initially chosen by them (particles are skewed on the streamline similar to beads), then it is easy to obtain the expression for the coefficient of the transverse diffusion of particles,

$$D_\perp \propto \frac{\Delta_\perp^2}{L_\parallel}\frac{L_\parallel}{t} \approx D_m \frac{L_\parallel}{t}. \tag{2.112}$$

In the case of ballistic motion of particles along the streamline, the estimate of the transverse diffusion coefficient has the form

$$D_\perp \approx D_m V_\parallel. \tag{2.113}$$

Here, $V_\parallel$ is the particle velocity under the condition of motion along the force line.

A nonstandard situation arises when we consider collisions between particles which are located in the "braided" field under consideration. Then it is natural to suppose that the motion in the longitudinal direction has a diffusive character (random walks along the force line):

$$D_{\|} \approx \frac{L_{\mathrm{cor}}^2}{2\tau} \approx \frac{L_{\|}^2}{2t}. \tag{2.114}$$

Here, L_{cor} is the particle longitudinal correlation length and τ is the correlation time. Then the estimate of longitudinal displacement is the value

$$L_{\|} \approx \sqrt{2D_{\|}t}. \tag{2.115}$$

The substitution of (2.115) into (2.112) yields

$$D_{\perp} \approx D_m \frac{\sqrt{2D_{\|}t}}{t} \approx \sqrt{2D_{\|}} \frac{D_m}{\sqrt{t}}. \tag{2.116}$$

This result demonstrates an essential deviation of the transverse transport from the classical diffusion transport, since

$$\Delta_{\perp}^2 \approx D_m \sqrt{2D_{\|}} \sqrt{t} \propto t^{1/2} \ll t. \tag{2.117}$$

This corresponds to the subdiffusive character of transport with the Hurst exponent $H = 1/4$. Note that in this model particles never leave the force line of the magnetic field in which they were initially situated. The result obtained shows the nontrivial character of the relation between longitudinal and transverse correlation effects in the case of the description of transport in the stochastic magnetic field. Another important aspect of this problem is the necessity to consider the essentially nondiffusive character of transport.

Note that double diffusion is one of the simplest models of anisotropic anomalous transport in the stochastic magnetic field. This mechanism is destroyed under the influence of time-dependent perturbations and the effect of stochastic instability of nearby streamlines [3, 5, 17]. These effects will be considered in the next section of this paper.

2.5.4 The Howells Result

The "seed diffusivity" concept is very effective and allows the consideration of fairly complex correlation effects. The natural generalization of this approach is the application of the "self-consistent" diffusion coefficient that describes both turbulent transport and molecular diffusion effects. Here, we consider very briefly the Howells model [73] that will be repeatedly discussed in the context of scaling arguments. A more detailed consideration of this problem can be found in the well-known Moffat reviews [32, 33].

The Howells model of turbulent transport is based on the spectral energy function $E(k)$ that plays a significant role in the framework of the Kolmogorov theory of isotropic turbulence [27, 29, 30]:

$$\frac{\langle V^2 \rangle}{2} = \int_0^{\infty} E(k)\, dk. \tag{2.118}$$

Here, V is the velocity scale and k is the wave number. From this point of view the Kolmogorov–Obukhov law has the form

$$E(k) \propto \frac{V_k^2}{k} \propto \frac{1}{k^{5/3}}. \tag{2.119}$$

Howells [73] obtained an important relationship between the turbulent diffusion coefficient D_T and the energy spectrum $E(k)$. He considered a "local" diffusion coefficient $\delta D(k)$ related to the specific scale length $l_k \approx 1/k$ of eddies with the characteristic velocity V_k, $\delta D(k) \approx V_k^2 \tau_0$, where $V_k^2 \approx E(k)\delta k$. Here, δk is a small interval of wave numbers and τ_0 is the characteristic correlation time. We will consider that τ_0 is related to the molecular diffusion D_o, $\tau_0 \approx 1/k^2 D_0$. We obtain the expression that is differential in form:

$$\frac{\delta D(k)}{\delta k} = \frac{E(k)}{k^2 D_0}. \tag{2.120}$$

Note that the value of $D(k)$ should be taken into account along with molecular diffusion D_0. This is the simplest example of renormalization by "seed" diffusivity. One then obtains

$$\frac{dD(k)}{dk} = \frac{E(k)}{k^2 (D_0 + D(k))}. \tag{2.121}$$

Upon solving this equation, we obtain the expression for the turbulent diffusion coefficient. This expression describes the influence of different scales,

$$\big(D(k) + D_0\big)^2 = \int_k^{\infty} \frac{E(k)}{k^2}\, dk + D_0^2. \tag{2.122}$$

Here, it is assumed that $D(\infty) = 0$. In this expression the integral term plays the main role for scales that are larger than the characteristic turbulent scale l_T, which enters into the expression for the Reynolds number: $Re = V_0 l_T/\eta$. Here, V_0 is the characteristic velocity and η is the coefficient of viscosity. Therefore, neglecting the molecular diffusion effects (on the right-hand side), the Howells expression can be derived:

$$D_H^2 = \int_k^{\infty} \frac{E(k)}{k^2}\, dk. \tag{2.123}$$

From the standpoint of dimensional estimates, the expression obtained differs significantly from the Taylor definition for D_T (2.6). The classical dimensional estimate of the diffusion coefficient is a formula closely associated with the model of random walk, $D_0 \approx \Delta^2/\tau$. Here, Δ is the characteristic spatial correlation scale length and τ is the characteristic correlation time. An analogous estimate in the Taylor formula is $D_T \approx V_0^2 \tau$. The formula suggested by Howells yields a different (kinetic) type of estimates for the diffusion coefficient,

$$D_H \approx V_0 \varDelta. \tag{2.124}$$

It is possible to determine a relationship between these expressions. Let us consider the Peclet number [17, 32, 33],

$$Pe = \frac{V_0 \varDelta}{D_0}. \tag{2.125}$$

This dimensionless quantity reminiscent of the Reynolds number has the same significance. The Peclet number allows the estimation of the fraction of convective transport and its comparison with the diffusion one. In terms of the Peclet number we obtain

$$D_0 = D_0 Pe^0 \equiv D_0, \qquad D_T = D_0 Pe^2, \qquad D_H = D_0 Pe. \tag{2.126}$$

The result presented in this form with different exponents ϑ is now in wide use [17, 32, 33]:

$$D_{\text{eff}} = D_0 Pe^{\vartheta}. \tag{2.127}$$

Here, D_{eff} is the effective diffusion coefficient. It permits us to describe transport in terms of the exponent ϑ, and such a representation reflects the nature of the dependence on the velocity amplitude. Of course, there is no unique recipe to obtain the estimates of turbulent transport. Thus there is an important example that was obtained by Dykhne, Isichenko, and Horton [116] for anomalous transport enhancement due to the hexagonal cells controlled by the boundary tubes:

$$D_{\text{eff}} \approx D_0 \ln Pe, \quad \text{where } Pe \gg 1. \tag{2.128}$$

The detailed analysis and scaling estimates for this nontrivial model can be found in [17, 116].

2.6 The Diffusive Tracer Equation and Averaging

In spite of the effectiveness of diffusive estimates to describe correlation effects and transport, the equations describing the evolution of tracer distribution density play an important role in the description of anomalous diffusion effects. In this section, the heuristic Taylor method of obtaining such an equation is considered. The approximation suggested in [117] has become an important step in the development of description methods of anomalous transport and complex correlation effects.

2.6.1 The Taylor Shear Flow Model

In this section, we consider the description of the effective diffusion of a passive scalar in a shear flow in the presence of seed diffusivity. In his paper [117] Taylor suggested a new method to obtain the effective diffusion coefficient, which is based on averaging the convection–diffusion equation

$$\frac{\partial n}{\partial t} + V(y,z)\frac{\partial n}{\partial x} = D_0 \nabla^2 n. \tag{2.129}$$

Here, n is the scalar density, V is the longitudinal (along the x-axis) velocity, and D_0 is the seed diffusivity. Actually, in the Taylor model the influence of transverse molecular diffusion on longitudinal convective transport was considered.

The paper [117] deals with Poiseuille (parabolic) flow in a cylindrical tube, but in order to simplify calculations we will analyze a flat model. Considering the profile of the longitudinal flow in the form

$$V(y) = \frac{V_0}{L^2}\left(L^2 - y^2\right), \tag{2.130}$$

we can learn the scalar transport problem in the framework of the decomposition method

$$n = \langle n \rangle + n_1(x,y,t) = n_0 + n_1(x,y,t), \tag{2.131}$$

$$V = \langle V \rangle + V_1(y) \equiv V_0 + V_1, \tag{2.132}$$

where V_0 is the characteristic velocity and L is the characteristic spatial scale. Here, use is made of the expression for mean values

$$\langle n \rangle \equiv \frac{1}{2L}\int_{-L}^{L} n(x,y,t)\,dy \equiv n_0(x,t), \tag{2.133}$$

$$\langle V \rangle = \frac{1}{2L}\int_{-L}^{L} V(y)\,dy = \frac{2}{3}V_0. \tag{2.134}$$

Hence, one obtains

$$V_1 = V_0\left[\frac{1}{3} - \left(\frac{y}{L}\right)^2\right]. \tag{2.135}$$

The substitution of the expression for n and V into the initial equation (2.139) yields

$$\frac{\partial}{\partial t}n_0 + \frac{\partial}{\partial t}n_1 + (V_0 + V_1)\frac{\partial}{\partial x}(n_0 + n_1) = D_0\nabla^2[n_0 + n_1]. \tag{2.136}$$

Taking the average of this equation, it is easy to obtain an expression for the mean density evolution,

$$\frac{\partial}{\partial t}n_0 + V_0\frac{\partial}{\partial x}n_0 + \left\langle V_1\frac{\partial}{\partial x}n_1\right\rangle = D_0\frac{\partial^2 n_0}{\partial x^2}. \tag{2.137}$$

Actually, in order to obtain a closed-equation for the mean density of the scalar, it is necessary to find an expression for $n_1(x,y,t)$. Subtracting (2.137) from (2.136), one obtains the equation for the evolution of density perturbation n_1:

$$\frac{\partial n_1}{\partial t} + V_1 \frac{\partial n_0}{\partial x} + V_0 \frac{\partial n_1}{\partial x} + V_1 \frac{\partial n_1}{\partial x} - \left\langle V_1 \frac{\partial n_1}{\partial x} \right\rangle = D \left(\frac{\partial^2 n_1}{\partial x^2} + \frac{\partial^2 n_1}{\partial y^2} \right). \tag{2.138}$$

The expression obtained is too complex; therefore, Taylor suggested the heuristic method to obtain the estimates of effective diffusion, which is based on some hypotheses:

- quasi-steadiness of n_1, i.e., $\frac{\partial n_1}{\partial t} \approx 0$;
- smallness of $\frac{\partial n_1}{\partial x}$ and $\frac{\partial^2 n_1}{\partial x^2}$ in comparison with $\frac{\partial n_0}{\partial x}$ and $\frac{\partial^2 n_1}{\partial y^2}$.

Taylor kept the term $\partial^2 n_1/\partial y^2$, basing this on the necessity of taking into account the density gradient in the direction of the walls, which has to be greater to satisfy the no flux condition $\partial n_1/\partial y = 0$ at $y = L$ and $y = -L$. Then, solving the equation obtained from (2.138),

$$D_0 \frac{\partial^2 n_1}{\partial y^2} = Q(x, y, t), \tag{2.139}$$

where $Q = V_1(y)\partial n_0(x, t)/\partial x$, it is easy to find

$$n_1 = \frac{\partial n_0}{\partial x} \frac{V_0}{3D_0} \left[\frac{y^2}{2} - \frac{y^4}{4L^2} \right] + \mathrm{const}(x, t). \tag{2.140}$$

Applying the condition $\langle n_1 \rangle = 0$ we arrive at const $= (\partial n_0/\partial x) \times (V_0/3D_0) \times (-7L^2/60)$,

$$\frac{\partial n_1}{\partial x} = \frac{\partial^2 n_0}{\partial x^2} \frac{V_0}{3D_0} \left[\frac{y^2}{2} - \frac{y^4}{4L^2} - \frac{7}{60} L^2 \right]. \tag{2.141}$$

The expression $\langle V_1 \partial n_1/\partial x \rangle$, which defines an additional contribution in longitudinal diffusive transport, can be rewritten in the form

$$\left\langle V_1 \frac{\partial n_1}{\partial x} \right\rangle = -D_1 \frac{\partial^2 n_0}{\partial x^2} = -\frac{8}{945} \frac{(V_0 L)^2}{D_0} \frac{\partial^2 n_0}{\partial x^2}. \tag{2.142}$$

The result obtained is not trivial, because the additional diffusive contribution depends inversely on seed diffusivity D_0. The physical interpretation of this result is the limitation of the influence of nonuniformity of the longitudinal velocity profile $V(y)$ by transverse diffusion. Hence, nonuniform longitudinal convection in combination with transverse diffusion leads to longitudinal diffusion. Naturally, the new diffusive mechanism manifests itself at a large distance downstream only, since the equation obtained is correct only for $t \gg \tau_D \approx L^2/D$. On the other hand, use was made of the condition of the smallness of the transverse spatial scale in comparison with the longitudinal one l: $L \ll l$. The effective diffusion coefficient obtained can be rewritten in terms of the Peclet number

$$D_{\mathrm{eff}} = D_0 + \left(\frac{8}{945} \right) \frac{V_0^2 L^2}{D_0} = D_0 + D_0 \left(\frac{8}{945} \right) Pe^2. \tag{2.143}$$

Note that the author of [117, 118] did not use any restriction on the Peclet number.

2.6.2 Generalization of the Taylor Model

The flow model considered in the previous section is fairly simple, however, the method suggested by Taylor allows one to apply an analogous approach for the description of different shear flows [118, 119]. Thus, from the formal standpoint, the equation describing density perturbation

$$D_0 \frac{\partial^2 n_1}{\partial y^2} = V \frac{\partial n_0}{\partial x} \tag{2.144}$$

can easily be supplemented with the terms omitted before in order to describe more complex situations. Thus, including the term describing the time dependent character of density perturbations $\partial n_1/\partial t$ or using the Laplace operator, which characterizes diffusion on the plane of a transverse cross-section of a canal in the form

$$D_0 \left(\frac{\partial^2 n_1}{\partial y^2} + \frac{\partial^2 n_1}{\partial z^2} \right) \tag{2.145}$$

keeps the advantages of the algorithm of the solution suggested by Taylor; since the equation for density perturbation n_1 has, as before, a linear form,

$$\frac{\partial n_1}{\partial t} = D_0 \nabla^2 n_1 - V_1 \frac{\partial n_0}{\partial x}. \tag{2.146}$$

It is necessary to note that there is also some arbitrariness in the choice of conditions for solving the partial differential equation. The solutions founded in the framework of a more precise formulation of the problem allow us to see that the nontrivial dependence (2.143) obtained by Taylor of the effective diffusion D_{eff} on the flow parameters D_0 and L is correct. The nontrivial character of effective diffusivity behavior in the Taylor model impels us to use the heuristic methods of including nonlocal effects and memory effects into the initial local equation. In the framework of the heuristic approach, it is easy to include memory effects in the equation under analysis (2.129). This allows us to analyze trapping effects, which play an important role in tracer transport. Thus, one can represent the total concentration of tracer $n(x,t)$ as two parts,

$$n(x,t) = p(x,t) + q(t), \tag{2.147}$$

where $p(x,t)$ corresponds to actively transporting particles and $q(x,t)$ describes trapping. In the simplest case the relationship between p and q is given by

$$\frac{\partial q}{\partial t} = \alpha_T (\beta_T p - q). \tag{2.148}$$

Here, α_T and β_T are the parameters of the problem. If all the particles are released in the untrapped region at $t = 0$, one obtains

$$q(x,t) = \alpha_T \beta_T \int_0^t p(x,\tau) e^{-\alpha_T (t-\tau)} \, d\tau. \tag{2.149}$$

Here, $\alpha_T \beta_T \exp[-\alpha_T(t-\tau)]$ is the memory function. In general, we can rewrite the expression in the form with an arbitrary memory function M:

$$q(x,t) = \int_0^t p(x,t) M(t-\tau)\, d\tau. \tag{2.150}$$

Then, based on tracer conservation, it is possible to describe transport by

$$\frac{\partial p}{\partial t} + \frac{\partial q}{\partial t} + V\frac{\partial p}{\partial x} = D\frac{\partial^2 p}{\partial x^2}. \tag{2.151}$$

Using the Taylor method, the modified equation for the mean density can be rewritten in the form

$$\frac{\partial n_0}{\partial t} = \int_0^t M(t-\tau)\frac{\partial^2 n_0(x,\tau)}{\partial x^2}\, d\tau. \tag{2.152}$$

The expression for the effective diffusion coefficient, which takes into account memory effects, is then given by

$$D_{\text{eff}} = \int_0^\infty M(\tau)\, d\tau. \tag{2.153}$$

Here, we consider the behavior over a long time period.

Another aspect of the problem considered in [117] is the possibility of analyzing more complex profiles of shear flow V. Thus, in the next parts we will consider the model profiles $V_x = V_x(y,t)$, which allow us to understand time periodic velocity fields and tracer diffusivity in the turbulent Poiseuille flow [35]. On the other hand, the use of randomly distributed stream functions $\Psi(z)$ makes it possible to describe the system of random shear flows [72] $\vec{V}_x = -[\nabla_z \times \Psi(z)]$ based on their correlation properties.

2.6.3 The Zeldovich Flow and the Kubo Number

The time-dependence of a flow is an important factor that has an influence on transport processes. This leads to reconstruction of the streamline topology. To describe this situation we need a new dimensionless parameter, which includes the characteristic time $T_0 \approx 1/\omega$. In the case of high frequencies ω, the path of a test particle can be estimated using the ballistic method as $l_\omega \approx V_0/\omega$. Then the convective fraction of transport can be characterized by the dimensionless Kubo number

$$Ku = \frac{l_\omega}{\lambda} \approx \frac{V_0}{\omega\lambda}, \tag{2.154}$$

where λ is the spatial scale of the flow under consideration. In the conventional situation (the quasi-linear limit), we obtain the estimate of the diffusivity in the form $D_T \approx V_0^2 \tau_c \approx V_0^2/\omega$. However, in the case of high frequencies it is necessary to use the path $l_\omega = V_0/\omega$ as the correlation length:

$$D \approx \frac{l_\omega^2}{\tau_c} \approx \frac{V_0^2}{\omega^2}\frac{1}{\tau_c}. \tag{2.155}$$

For $\tau_c \approx 1/\omega$ one then obtains the quasi-linear estimate. There is also another possible method. We can relate the correlation time to the diffusive mechanism of the particle escape from streamlines $1/\tau_c \approx D_0/\lambda^2 \approx 1/\tau_D$, where D_0 is the seed diffusion coefficient. Then the new estimate of the effective diffusion coefficient takes the form

$$D \approx \frac{D_0 V_0^2}{\lambda^2 \omega^2} \approx D_0 Ku^2. \tag{2.156}$$

These simple estimates can be validated by considering Zeldovich's model of two-dimensional flow. Zeldovich considered [35] turbulent diffusion in a system of regular but time-dependent flows (compare with the Taylor model). The solved equation has the form

$$\frac{\partial n}{\partial t} + V_X(z,t)\frac{\partial n}{\partial x} = D_0 \Delta n. \tag{2.157}$$

The expression for the velocity of flows is given by

$$V_X(z,t) = 2V_0 \cos(kz)\cos(\omega t). \tag{2.158}$$

Zeldovich suggested finding the solution as follows:

$$n(z,t) = n_0 + n_1 = n_0 + \sin(kz)(n_S \sin \omega t + n_C \cos \omega t + \cdots). \tag{2.159}$$

The amplitudes of the harmonics n_S, n_C can be defined as a result of the solution of (2.157). It was suggested that

$$n_0 = \langle n \rangle = a + bx. \tag{2.160}$$

The values V_0, a, b are the flow characteristics. Substitution of (2.159) into (2.157) with allowance for the assumption $n_1 \ll n_0$ yields the equation for the average density n_0,

$$\frac{\partial n_0}{\partial t} = -\left\langle V_X \frac{\partial n_1}{\partial x} \right\rangle + D_0 \frac{\partial^2 n_0}{\partial x^2}. \tag{2.161}$$

The equations for the amplitudes of the harmonics n_S, n_C have the form

$$n_S + \frac{2V_0}{w}\frac{\partial n_0}{\partial x} = -\frac{D_0 k^2}{\omega} n_C, \quad n_C = \frac{D_0 k^2}{\omega} n_S. \tag{2.162}$$

Simple calculations allow us to obtain

$$\frac{\partial n_0}{\partial t} = D_0 \left[\frac{V_0^2 k^2}{\omega^2 + D_0^2 k^4} \right] \frac{\partial^2 n_0}{\partial x^2} + D_0 \frac{\partial^2 n_0}{\partial x^2}. \tag{2.163}$$

In terms of the Kubo number we get the expression for the effective diffusion coefficient,

$$D_{\text{eff}}(k,\omega) = D_0 \left[\frac{Ku^2}{1 + (\omega \tau_D)^{-1}} + 1 \right], \tag{2.164}$$

where $\tau_D = 1/(D_0 k^2)$. For high frequencies $\omega > 1/\tau_D$ we arrive at the formula

$$D \approx D_0 \left[\frac{V_0^2 k^2}{\omega^2} \right] \approx D_0 K u^2. \tag{2.165}$$

In the case of linear dispersion $\omega^2 \approx \beta V_0^2 k^2$, Zeldovich obtained the expression for $\beta \to 0$: $D \approx V_0^2 / D_0 k^2$. The effective coefficient of diffusion takes the form of the Howells diffusion coefficient [72] $D D_0 \approx D_{\text{eff}}^2 \approx V_0^2 / k^2$. However, in contrast to Howells' paper, where an isotropic model was considered, the Zeldovich case is essentially anisotropic.

2.6.4 Advection and Zeldovich Scaling

Based on the Taylor renormalization method, it is appropriate to raise a question about the estimation of effective transport in a turbulent flow. Zeldovich [35, 36] suggested the phenomenological method to estimate scalar transport in a turbulent flow in the presence of seed diffusion based on

$$\frac{\partial n}{\partial t} = \nabla (D_0 \nabla n) - \vec{V}(t) \nabla n. \tag{2.166}$$

Here, $\vec{V}(t)$ is the velocity field. The terms describing effects that are important for us here enter into the left-hand side of this equation; therefore, multiplying the equation by n and using the Gaussian theorem, we can omit the term describing density evolution,

$$0 = \frac{1}{2} \frac{\partial}{\partial t} \int_W n^2 \, dW = \int_S n D_0 (\nabla n)_N \, dS - \int_W D_0 (\nabla n)^2 \, dW, \tag{2.167}$$

since in the framework of quasi-steady turbulence it is natural to omit the term on the left-hand side of (2.167). The expression for $D_0 (\nabla n)_N$ characterizes the contribution of external sources inside the volume W, which is bounded by the surface S, whereas the term $D_0 (\nabla n)^2$ is related to the scalar redistribution inside the considered volume W. It is convenient to introduce here the effective diffusive coefficient in the form

$$D_{\text{eff}} = \frac{1}{n^2 L_0} \int_W D_0 (\nabla n)^2 \, dW, \tag{2.168}$$

where L_0 is the system characteristic size. Then the minimum condition for D_{eff} (the condition of minimizing functional) comes to a purely diffusive equation

$$\nabla (D_0 \nabla n) = 0, \quad \text{where } \min D_{\text{eff}} = D_0. \tag{2.169}$$

Applying a method analogous to the above-considered Taylor approach, it is easy to obtain the upper estimate of the effective diffusion coefficient in a quasi-steady turbulent flow. Consider the steady scalar density equation

$$D_0 \Delta n - \vec{V} \nabla n = 0 \tag{2.170}$$

using the perturbation method:

$$n = \langle n \rangle + n_1 = n_0 + n_1, \tag{2.171}$$

$$V = \langle V \rangle + v_1 = v_1, \tag{2.172}$$

where $\langle V \rangle = 0$, $n_1 \ll n_0$, and $D_0 \Delta n_0 = 0$. Simple calculations lead to the equation for density perturbation n_1 which actually coincides with the Taylor "renormalization" formulated now for a turbulent velocity field:

$$D_0 \frac{\partial^2 n_1}{\partial x^2} = v_1 \frac{\partial n_0}{\partial x}. \tag{2.173}$$

For the sake of simplicity, this equation is presented in the one-dimensional form. In the framework of the dimensional estimate, we obtain

$$n_1 \approx v_1 L n_0 / D_0 \approx Pe n_0, \tag{2.174}$$

where $Pe \ll 1$, which corresponds to weak turbulence regimes. In obtaining (2.174) we use the condition of smallness of the term $v_1 \nabla n_1$ in comparison with $v_1 \nabla n_0$. The definition of the effective diffusion coefficient in terms of $(\nabla n)^2$ yields

$$D_{\text{eff}} \approx \frac{1}{n_0^2 L} \int_W D_0 (\nabla n_0)^2 \left(1 + A \cdot Pe^2\right) dW \approx D_0 \left(1 + A \cdot Pe^2\right), \tag{2.175}$$

where A is the dimensionless constant. Note that the term $\nabla n_0 \nabla n_1$ is illuminated because of the extremal properties of the distribution n_0. This upper estimate of transport D_{eff} in the steady turbulent flow coincides with the quasilinear scaling $D_{\text{eff}} \approx V_0^2 \tau$ when the correlation time τ has the diffusive meaning

$$\tau \approx \tau_D \approx L_0^2 / D_0. \tag{2.176}$$

At the same time, there is certainly a strong relation between the Taylor approach to transport in a laminar shear flow and the Zeldovich general estimate of turbulent diffusivity [40]. In the next sections we consider how different modifications of the diffusive term in the equation for density perturbations n_1 make it possible to move from the quasi-linear description of transport to nonlocal models with complex topology.

2.7 The System of Random Shear Flows

The problem of calculating the turbulent diffusion coefficient is closely related to the character of the correlation function. In "common language", the correlation means a relation between events. The return of a walking particle to the initial point [18, 19] is a good example of this relationship. Corrsin [34] was probably the first to suggest using the return probability to describe turbulent diffusion. He formulated several other probabilistic problems in the framework of turbulent diffusion in [34]. In this section, we consider anomalous transport in the system of random shear flows where the nontrivial character of diffusivity in anisotropic systems is manifested.

2.7.1 The Dreizin–Dykhne Superdiffusion Regime

A physically transparent model was suggested and considered in Dreizin and Dykhne's paper [72] related to the incorporation of the influence of returns. The action of "seed" diffusion in the longitudinal direction (which relates to the magnetic field direction) with the diffusion coefficient D_0 was considered. Random fluctuations creating narrow convective flows of width a and velocity V_0 act in the transverse direction on the diffusing test particle (see Fig. 2.2). A simple model was proposed [72] for the calculation of the transverse diffusion coefficient $D_\perp$:

$$D_\perp \approx \frac{\lambda_\perp^2}{t}, \quad \text{where } \lambda_\perp \approx V_0 t P_\infty, \; P_\infty = \frac{\delta N}{N}. \tag{2.177}$$

Here $\lambda_\perp$ is the transverse displacement during time t and P_∞ is the relative number of the small fraction of "noncompensated" fluctuations δN. The value $N \approx \sqrt{2D_0 t}/a$ is the number of shear flows intersected by the particle during its longitudinal motion. Using the Gauss representation $\delta N \approx \sqrt{N}$, the following formula was obtained in [72]:

$$D_\perp \propto V_0^2 a \sqrt{\frac{t}{D_0}}. \tag{2.178}$$

In the superdiffusive case under consideration, it was found that $H = 3/4 > 1/2$.

To explain this result, the correlation function in the following form was considered in [72]:

$$C(t_1, t_2) = \int_{-\infty}^{\infty} \langle V_x(0) V_x(z) \rangle \rho(z, t_2 - t_1)\, dz. \tag{2.179}$$

The probability density has the Gaussian form:

$$\rho = \frac{1}{(4\pi D_0(t_2 - t_1))^{1/2}} \exp\left(-\frac{z^2}{4D_0(t_2 - t_1)}\right). \tag{2.180}$$

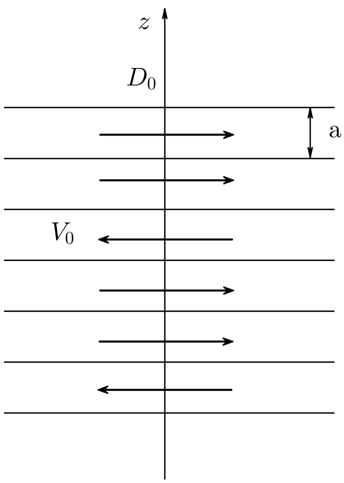

Fig. 2.2. Shear flows model

Here, $V_x(z)$ is the velocity of the flow at the point z. This approach corresponds exactly to the Corrsin idea about the diffusive nature of decorrelation [28] with allowance for the anisotropy of the model. However, using the conjecture about the significant role of returns has become the main step in the description of anomalous diffusion, since the condition $z \to 0$ for (2.179) corresponds to the return to the initial point. Thus, we have the expression

$$C(t_1, t_2) = C(\tau) \approx \frac{V_0^2 a}{\sqrt{4\pi D_0 \tau}}, \quad \tau = t_2 - t_1. \tag{2.181}$$

Using the classical expression from the turbulent diffusion theory (2.6), estimate (2.181) was obtained as

$$\langle \lambda_\perp^2 \rangle \approx \frac{V_0^2 a}{\sqrt{4\pi D_0}} \int_0^t \int_0^t \frac{dt_1\, dt_2}{\sqrt{t_1 - t_2}} \approx \frac{V_0^2 a}{\sqrt{4\pi D_0}} t^{3/2}. \tag{2.182}$$

Here $\langle\,\rangle$ denotes the averaging symbol.

It is important that representation (2.182) be valid only if the perpendicular spatial displacement is no larger than the perpendicular correlation length $\Delta_\perp \approx a$: $\lambda_\perp < a$. This restriction has the form

$$\lambda_\perp^2 \approx \frac{V_0^2 a}{\sqrt{D_0}} \tau_C^{3/2} \le a^2, \quad \tau_C \approx \left(\frac{D_0 a^2}{V_0^4} \right)^{1/3}. \tag{2.183}$$

If time scales $t > \tau_C$, then we are dealing with classical diffusion, $D_\perp \propto a^2/2\tau_C$.

We see that Dreizin and Dykhne suggested a fairly simple and, at the same time, nontrivial model of anisotropic transport. Later, the analogous problem was considered by Matheron and De Marsily [120] in the context of transport effects in porous media. Avellaneda and Majda [41, 42] treated this model in detail in the framework of the renormalization theory. Analyses carried out in [41, 42, 72, 120] show that if the value $\langle V \rangle$ is not strictly parallel to the "layers" and if the sample is finite in the longitudinal directions then the superdiffusion regime (2.182) is destroyed. Nevertheless, the anomalous regime exists for intermediate times [see (2.183)].

2.7.2 The Matheron–de Marsily Model

In spite of the detailed physical analysis of the shear flows model, which was carried out by Dreizin and Dykhne, this result became well known after the paper [120] by Matheron and de Marsily in connection with learning transport in a porous media. Their analysis is based on the consideration of stochastic equations of motion in longitudinal and transverse directions:

$$\frac{dx}{dt} = V_X\big(z(t)\big), \tag{2.184}$$

$$\frac{dz}{dt} = \eta(t). \tag{2.185}$$

Here, $\langle V_x \rangle$ and the shear velocity distribution are taken to be white noise:

$$\left\langle V_X(z)V_X(z')\right\rangle = \sigma_V \delta(z-z'). \tag{2.186}$$

At the same time, the motion along the z-axis is the conventional Brownian motion:

$$\left\langle \eta(t)\eta(t')\right\rangle = 2D_0\delta(t-t'). \tag{2.187}$$

Note that in the framework of the consideration of the Dreisin–Dykhne superdiffusive regime, the Brownian motion in the transverse direction can be neglected. Then, longitudinal and transverse displacements can be rewritten in the form

$$z(t) = \int^t \eta(t')\,dt' \quad \text{or} \quad \left\langle \Delta z^2 \right\rangle = 2D_0 t, \tag{2.188}$$

$$x(t) = \int^t V_X\big(z(t')\big)\,dt'. \tag{2.189}$$

To obtain the scaling describing transport in the transverse direction, let us introduce a distribution function $J(z,t)$ of the number of visits that were made by a test particle into different "jets" by the moment t,

$$J(z,t) = \int_0^t \delta\big(z - z(t')\big)\,dt. \tag{2.190}$$

The formal expressions for the displacement $x(t)$ can then be represented in the form

$$x(t) = \int_{-\infty}^{\infty} V_x(z)J(z,t)\,dz. \tag{2.191}$$

Since in the transport analysis the mean values play the main role, consider the simplest Gaussian approximation of the mean probability density J,

$$J(z,t) = \int_0^t \rho(z,t')\,dt' = \frac{|z|}{4\sqrt{\pi}D_0}\Gamma\left(-\frac{1}{2}; \frac{z^2}{4D_0 t}\right), \tag{2.192}$$

where $\Gamma(-\frac{1}{2}; x)$ is the incomplete gamma function. Then the mean displacement is given by the expression

$$\left\langle x(t)\right\rangle = \frac{1}{4\sqrt{\pi}D_0}\int_{-\infty}^{\infty} dz\,|z|\Gamma\left(-\frac{1}{2}; \frac{z^2}{4D_0 t}\right)V_x(z). \tag{2.193}$$

Using the averaging over environments we obtain the expression for the mean-squared displacement that takes into account the statistical properties of the field $V_x(z)$,

$$\left\langle\left\langle x(t)\right\rangle^2\right\rangle = \int dz \int dz' \left\{\left\langle V_X(z)V_X(z')\right\rangle J(z,t)J(z',t)\right\}. \tag{2.194}$$

Applying the statistical properties of the velocity field $\langle V(z)V(z')\rangle = \sigma_V \delta(z-z')$ it is easy to find a final solution:

$$\langle\langle x^2(t)\rangle\rangle = \sigma_V \int dz\, J(z,t)^2 = \frac{\sigma_V}{\sqrt{D_0}} \frac{t^{3/2}}{\pi} \int_0^\infty s^2 \Gamma\left(-\frac{1}{2}; s^2\right)^2 ds$$
$$= \frac{4}{3\sqrt{\pi}}(\sqrt{2}-1)\frac{\sigma_V}{\sqrt{D_0}} t^{3/2}. \qquad (2.195)$$

The averaging method that was used here is not traditional, however, the scaling obtained is correct, $R^2 \propto t^{3/2}$.

The authors of [120] repeatedly pointed out the nontrivial character of the different possible ensemble averages. Thus, the alternative possibility is the definition of $\langle\langle x^m(t)\rangle\rangle$ by the expression

$$\langle\langle x^m(t)\rangle\rangle = m! \int_0^t dt_1 \int_0^{t_1} dt_2 \int_0^{t_{m-1}} dt_m \,\langle\langle V_X\big(z(t_1)\big)\cdots V_X\big(z(t_m)\big)\rangle\rangle, \qquad (2.196)$$

where

$$\langle\langle V_X\big(z(t_1)\big)\cdots V_X\big(z(t_m)\big)\rangle\rangle$$
$$= \int_{-\infty}^{\infty} dz_1 \cdots dz_{m-1}\, dz_m \big\langle V_X(z_1)\cdots V_X(z_{m-1})V_X(z_m)\big\rangle$$
$$\times \rho(z_m, t_m)\rho(z_{m-1}-z_m, t_{m-1}-t_m)\cdots\rho(z_1-z_2, t_1-t_2). \qquad (2.197)$$

To calculate $\langle x^m\rangle$ it is convenient to use the Laplace transformation in time:

$$\langle\langle x^m(s)\rangle\rangle = \frac{m!}{s}\int_{-\infty}^{\infty} dz_1\cdots dz_m \big\langle V_X(z_1)\cdots V_X(z_m)\big\rangle$$
$$\times \rho(z_m, s)\rho(z_{m-1}-z_m, s)\cdots\rho(z_1-z_2, s). \qquad (2.198)$$

Using the Gaussian representation for $\rho(z,t)$ allows us to carry out the necessary calculations. Thus, for the mean-squared displacement one obtains [120]

$$\langle\langle x^2(s)\rangle\rangle = \frac{2\sigma_V}{s}\int_{-\infty}^{\infty}\int_{-\infty}^{\infty} dz_1\, dz_2\, \delta(z_1-z_2)\rho(z_2,s)\rho(z_1-z_2,s)$$
$$= \frac{2\sigma_V}{s}\rho(0,s)\int_{-\infty}^{\infty} dz\,\rho(z,s) = \frac{\sigma_V}{\sqrt{D_0}}\left(\frac{1}{s^{5/2}}\right) \qquad (2.199)$$

which by the Laplace inversion yields

$$\langle\langle x^2(t)\rangle\rangle = \frac{4\sigma_V}{3\sqrt{\pi D_0}} t^{3/2}. \qquad (2.200)$$

Actually, in such an approach we consider the averages, which are first taken over the walks $\langle\cdots\rangle_W$ and then over the shear flow configurations $\langle\cdots\rangle_C$, i.e., $\langle\langle\cdots\rangle\rangle \equiv \langle\langle\cdots\rangle_W\rangle_C$.

2.7.3 The "Manhattan Grid" Flow and Transport

The Dreizin–Dykhne renormalization (6.1) shows that even a small fraction of non-compensated flows

$$P_\infty(t) = \frac{\delta N}{N} \propto 1/\sqrt{N(t)} \tag{2.201}$$

leads to a considerable deviation in transport from the diffusive behavior. Moreover, several other important models of anomalous and percolation transport can be described in the framework of a similar approach. Thus, the formula for correlation function (2.181) includes the number of returns N_B or the number of intersected flows N_I for the particle walking along a straight-line trajectory for time t as

$$N(t) \propto \frac{\sqrt{2D_0 t}}{a}. \tag{2.202}$$

Indeed, the number of returns N_B in the interval δz can be estimated after we assume that the return probability $\rho(0,t)\delta z \approx \rho(0,t)a$. Thus, we obtain the estimate

$$N_B^{(t)} \propto \frac{t}{\tau_\|}\rho(0,t)a \propto \frac{\sqrt{D_0 t}}{a}. \tag{2.203}$$

Here, $\tau_\| \propto D_0/a^2$ is the longitudinal correlation time. In the case of one-dimensional longitudinal diffusion ($d = 1$), which we are considering, we have $N_B(t) \propto N_I(t)$. There exists an opportunity to generalize the Dreizin–Dykhne result for the case of a more complex "topology" of flows with the value $d > 1$ as follows:

$$C(t) \propto \frac{V_0^2}{N_I(t)} \quad \text{or} \quad C(t) \propto \frac{V_0^2}{N_B(t)}. \tag{2.204}$$

A similar formula is used in analyzing correlation effects in statistical physics [16] as the simplest correlation estimate (2.98).

In the isotropic case, for a system of random flows, it is possible to use the Alexander–Orbach conjecture for the number of visited sites, $N_I(t) \propto t^{2/3}$, for $2 \le d \le 6$ [17, 18]. Hence, we obtain the following scaling law for the displacement R of the particle:

$$\frac{R^2}{t} \propto \int C(t)\,dt, \qquad R \propto t^{2/3}. \tag{2.205}$$

Here, the Hurst exponent is denoted by $H = 2/3$. Indeed, Redner [122] and Bouchaud et al. [123] obtained such a superdiffusion regime for the "Manhattan-grid" flow, which is a generalization of the shear flows model [72, 120, 124]. Thus, from the formal standpoint a shear flow system is described by the velocity field

$$\vec{V} = -\big[\nabla_z \times \Psi(z)\big] = \big(u(z), 0\big), \tag{2.206}$$

where $u(z)$ is a random function. A flow with the stream function $\Psi = \Psi(x) + \Psi(z)$ is then a two-dimensional generalization of the shear flows model (see Fig. 2.3). The authors of [22] assumed that in the case under consideration transport is described

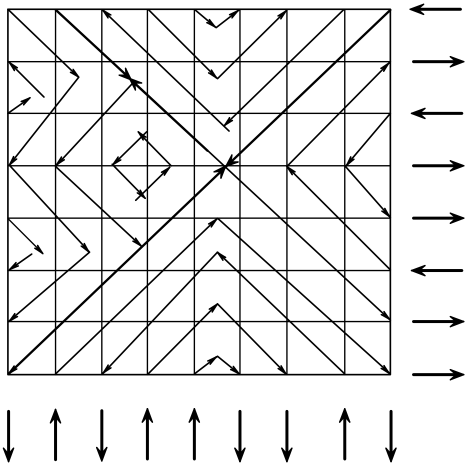

Fig. 2.3. "Manhattan-grid" flow

by the Hurst scaling $R \approx t^H$. On the other hand, scaling arguments yield

$$R \approx \langle V \rangle t. \tag{2.207}$$

The expression for $\langle V \rangle$ for the case of Gaussian statistics has the form

$$\langle V \rangle = \frac{1}{N} \sum_{i=1}^{N} V_i = \frac{V_0 \delta N}{N} \approx \frac{V_0}{N^{1/2}}. \tag{2.208}$$

Here, the value N corresponds to the number of "layers" intersected by the test particle. The authors of [122] suggested the simplest approximation (analogous to the one-dimensional case) $N \propto R \propto t^H$, which leads to the scaling

$$R \approx V_0 t^{1-H/2}. \tag{2.209}$$

A comparison between the last expressions yields the Hurst exponent $H = 2/3$.

Note that expression (2.209) implies that the auto-correlation function of velocity has the power tail $C(t) \approx 1/t^H$, which is in accordance with estimate (2.204). Redner [122] supposed a "hyper scaling" for models with the dimensionality $d \leq 3$,

$$H = \frac{2}{d+1}, \tag{2.210}$$

which implies the accuracy of the result obtained for both the one-dimensional ($d = 1$) and the isotropic three-dimensional ($d = 3$) cases. The "Manhattan-grid" flow could be a simple model for two-dimensional turbulent transport. Thus, the analysis of the experimental data of turbulent transport in a tokamak (where turbulence can be considered two-dimensional due to the presence of a strong magnetic field) yields the following estimate of the Hurst exponent: $0.6 < H < 0.75$, which approximately corresponds to $H = 2/3$.

2.8 The Quasi-Linear Approximation

The quasi-linear approximation has become widely popular due to its exceptional efficiency and close relation to hydrodynamic models. However, an analysis shows that quasi-linear equations are also closely related to correlation concepts. Thus, the dimensional estimate of the Taylor coefficient of turbulent diffusion D_T is usually called the quasi-linear expression for the diffusivity. In this section, we consider a derivation of the quasi-linear equation and a simple quasi-linear model of the stochastic magnetic field diffusivity.

2.8.1 Quasi-Linear Equations

From the formal standpoint, the construction of perturbation theory based on the continuity equation is more correct than the consideration of equations, where seed diffusion is incorporated. However, historically the paper by Taylor [117], which shows the nontrivial character of calculations of mean magnitudes, has played an important role, since the heuristic arguments used in [117] are the basis of many papers where use is made of the simplification of equations by the elimination of "fast modes". Note that quasi-linear equations were first considered in [23, 24] in connection with the description of the phase space consideration of the interaction between waves and particles. For our purposes here, it is sufficient to consider only some of the ideas advanced in the cited papers, namely, those associated with an averaging of the quasi-linear equations [123–125].

We consider the continuity equation for the density of a passive scalar in an incompressible flow:

$$\frac{\partial n}{\partial t} + V\frac{\partial n}{\partial x} = 0, \tag{2.211}$$

where $n(x,t)$ is the spatial density of the passive scalar and $V(t)$ is the random velocity field. We use the method of averaging over the ensemble of realizations for (2.211), assuming that the density field can be represented as a sum of the mean density n_0 and the fluctuation component $n_1 = n - \langle n \rangle$,

$$n = n_0 + n_1. \tag{2.212}$$

We also set $\langle n_1 \rangle = 0$ and $V = v_0 + v_1$, where $v_0 = \text{const}$ and $\langle v_1 \rangle = 0$. As a result, after simple manipulations (which are frequently used in the literature [123–125]), we arrive at the following two equations:

$$\frac{\partial n_0}{\partial t} + v_0\frac{\partial n_0}{\partial x} + \left\langle v_1\frac{\partial n_1}{\partial x}\right\rangle = 0; \tag{2.213}$$

$$\frac{\partial n_1}{\partial t} + v_0\frac{\partial n_1}{\partial x} + v_1\frac{\partial n_0}{\partial x} + v_1\frac{\partial n_1}{\partial x} - \left\langle v_1\frac{\partial n_1}{\partial x}\right\rangle = 0. \tag{2.214}$$

We assume that the fluctuations n_1 and v_1 are as small as ε in comparison with the mean density n_0. The quasi-linear character of the approximation indicates that, in the equation for n_0, we keep the nonlinear term on the order of ε^2 but, in the equation for n_1, we keep only the terms that are of the first order in ε. As a result, the transformations put the equation for n_1 into the form

$$\frac{\partial n_1}{\partial t} + v_0 \frac{\partial n_1}{\partial x} = -v_1 \frac{\partial n_0}{\partial x}. \tag{2.215}$$

We solve this equation by the method of Green functions. We consider (2.215) to be a first-order linear hyperbolic equation with the source term $I(x,t) = -v_1 \partial n_0/\partial x$, where the derivative $\partial n_0/\partial x$ is the parameter of the equation. We also supplement the equation with the uniform initial condition $n_1(x,0) = 0$. We then consider the equation for the Green function G:

$$\frac{\partial G}{\partial t} + v_0 \frac{\partial G}{\partial x} = \delta(x - x_1)\delta(t - t_1). \tag{2.216}$$

It is easy to solve this equation by applying the Laplace transformation in time t and the Fourier transformation in the spatial coordinate x:

$$\tilde{\tilde{G}}_{k,s} = \frac{\exp(-t_1 s)}{s + ikv_0} \exp(ikx). \tag{2.217}$$

Here and below, the tildes mark the Fourier or Laplace-transformed quantities. The solution has a simple physical meaning: it describes a perturbation propagating along the characteristic $z = x - v_0(t - t_1)$:

$$G(x,t,x_1,t_1) = \delta\big(x - x_1 - v_0(t - t_1)\big)\Theta(t - t_1), \tag{2.218}$$

where we have used $\Theta(t)$ to denote the Heaviside function. The solution for $n_1(x,t)$ has the form

$$n_1(x,t) = -\int_0^t v_1(t_1) \frac{\partial_0^n(z,t)}{\partial z}\, dt_1. \tag{2.219}$$

We substitute this expression for n_1 into (2.213) and perform simple manipulations [123, 124] to obtain

$$\frac{\partial n_0}{\partial t} + v_0 \frac{\partial n_0}{\partial x} = \int_0^t \big\langle v_1(t) v_1(t_1)\big\rangle \frac{\partial^2 n_0(z,t_1)}{\partial z \partial x}\, dt_1. \tag{2.220}$$

The integral nature of this equation reflects the Lagrangian character of the relationships between the derivatives of $n_0(x,t)$. In this respect, the continuity equation at hand is quite different from the fundamentally local continuity equation. The characteristic that appeared in our analysis relates the derivatives at different times. The left-hand side of (2.220) contains the partial derivatives with respect to x and t. On the right-hand side, we sum the values of the derivative $\partial^2 n_0/\partial x^2$ calculated along the characteristic with a weighting factor, which is the autocorrelation function of velocity, $C(t,t_1) = \langle v_1(t) v_1(t_1)\rangle$. Thus, in the case of a steady random process, the function $C(t,t_1) \approx C(t - t_1)$ in the equation under analysis plays the role of the memory function. The final form of the transport equation in the framework of the quasi-linear approach depends on the correlation function approximation.

2.8.2 Short-Range and Long-Range Correlations

The particular form of the equation is governed by the choice of the correlation function $C(\tau)$. In the simplest physically meaningful case, (2.220) reduces to the classical diffusion equation

$$\frac{\partial n_0}{\partial t} + v_0 \frac{\partial n_0}{\partial x} = D \frac{\partial^2 n_0(x,t)}{\partial x^2}. \tag{2.221}$$

This is possible only if the main contribution to the integral on the right-hand side of (2.220) comes from a short interval $(t - t_0; t)$ such that $t_0 \ll t$. If the second derivative changes insignificantly over the short interval, we obtain

$$\int_0^t \langle v(t)v(t_1)\rangle \frac{\partial^2 n_0(z,t)}{\partial z \partial x}\, dt_1 \approx \frac{\partial^2 n_0(x,t)}{\partial x^2} \int_{t-t_0}^{t} C(t-t_1)\, dt_1. \tag{2.222}$$

In fact, we are assuming that the correlations are short-range. Thus, in this approximation, we arrive at the familiar Kubo–Green formula for the diffusion coefficient [16, 20]:

$$D = \int_0^\infty C(\tau)\, d\tau. \tag{2.223}$$

In terms of the δ-correlations [18–20], $C(t - t_1) \approx C_0 \tau \delta(t - t_1)$, the quasi-linear equation (2.220) takes the conventional form with the Taylor estimate of diffusivity $D \approx V_0^2 \tau \approx C_0 \tau$:

$$\frac{\partial n_0}{\partial t} + v_0 \frac{\partial n_0}{\partial x} = C_0 \tau \frac{\partial^2 n_0(x,t)}{\partial x^2}. \tag{2.224}$$

In the case of long-range correlations, we could assume that $C \approx \text{const}$ for $t_1 \gg 0$, and (2.220) reduces to

$$\frac{\partial n_0}{\partial t} + v_0 \frac{\partial n_0}{\partial x} = C_0 \int_0^t \frac{\partial^2 n_0(z,t_1)}{\partial z \partial x}\, dt_1. \tag{2.225}$$

This equation can be further simplified by using the properties of the characteristic z. Differentiating (2.225) with respect to x gives

$$\frac{\partial^2 n_0}{\partial t \partial x} + v_0 \frac{\partial^2 n_0}{\partial x^2} = C_0 \int_0^t \frac{\partial^3 n_0(z,t_1)}{\partial x^3}\, dt_1. \tag{2.226}$$

Differentiating (2.225) with respect to t gives

$$\frac{\partial^2 n_0}{\partial t^2} + v_0 \frac{\partial^2 n_0}{\partial x \partial t} = C_0 \frac{\partial^2 n_0}{\partial x^2} - v_0 \int_0^t \frac{\partial^3 n_0(z,t_1)}{\partial x^3}\, dt_1. \tag{2.227}$$

Eliminating the integral in (2.226) and (2.227) yields

$$\frac{\partial^2 n_0}{\partial t^2} + 2 v_0 \frac{\partial^2 n_0}{\partial x \partial t} + \left(v_0^2 - C_0\right) \frac{\partial^2 n_0}{\partial x^2} = 0. \tag{2.228}$$

This equation differs markedly from the classical diffusion equation. For $C_0 > 0$, it is a hyperbolic equation, possessing the corresponding properties. Thus, a complete solution to this equation can be represented as a superposition of two initial distributions $n_0(x, 0)$ moving at different velocities. As is known, the fact that hyperbolic equations have characteristics opens new possibilities for describing nonlocal effects. It should be noted, however, that, from the rigorous point of view, the above passage from a parabolic to a hyperbolic equation is incorrect. The Cauchy problems for these two types of equations are radically different. The well-known example of the transport equation, which has a hyperbolic form, is the telegraph equation:

$$\frac{\partial n}{\partial t} + \tau \frac{\partial^2 n}{\partial t^2} = D \frac{\partial^2 n}{\partial x^2}. \tag{2.229}$$

This equation was one of the first so-called nondiffusion equations to describe turbulent transport [60, 92–95].

2.8.3 The Telegraph Equation

In the theory of random processes [18–20], one of the most widely used correlation functions is an exponential one,

$$C(t) = C_0 \exp\bigl(-|t|/\tau\bigr). \tag{2.230}$$

Here, τ is the characteristic time. This choice is quite natural because it is in this form that the correlation function is used in the Langevin model of random-walk processes. By means of this exponential function, we can transform integral equation (2.220) into a partial differential equation. To do this, we set

$$C(t, t_1) = C(t - t_1). \tag{2.231}$$

Differentiating (2.220) with respect to x gives

$$\frac{\partial^2 n_0}{\partial t \partial x} + v_0 \frac{\partial^2 n_0}{\partial x^2} = \int_0^t C(t - t_1) \frac{\partial^3 n_0(z, t_1)}{\partial x^3}\, dt_1. \tag{2.232}$$

Differentiating (2.220) with respect to t gives

$$\begin{aligned} \frac{\partial^2 n_0}{\partial t^2} + v_0 \frac{\partial^2 n_0}{\partial t \partial x} = C_0 \frac{\partial^2 n_0}{\partial x^2} - \frac{1}{\tau_0} \int_0^t C(t - t_1) \frac{\partial^2 n(z, t_1)}{\partial x^2}\, dt_1 \\ - v_0 \int_0^t C(t - t_1) \frac{\partial^3 n_0(z, t_1)}{\partial x^3}\, dt_1. \end{aligned} \tag{2.233}$$

Eliminating the integral in these two equations yields

$$\frac{\partial n_0}{\partial t} + v_0 \frac{\partial n_0}{\partial x} + \tau_0 \left(\frac{\partial^2 n_0}{\partial t^2} + 2 v_0 \frac{\partial^2 n_0}{\partial x \partial t} + \bigl(v_0^2 - C_0\bigr) \frac{\partial^2 n_0}{\partial x^2} \right) = 0. \tag{2.234}$$

In accordance with the hyperbolic nature of the problem, we introduce the new set of variables

$$\xi = t; \tag{2.235}$$

$$\eta = x - v_0 t \tag{2.236}$$

to obtain the telegraph equation form:

$$\frac{\partial n_0}{\partial \xi} + \tau_0 \frac{\partial^2 n}{\partial \xi^2} = C_0 \tau_0 \frac{\partial^2 n_0}{\partial \eta^2}, \tag{2.237}$$

where $\sqrt{C_0}$ is the propagation velocity of the perturbations. This is actually telegraph equation (2.23) in a frame of reference related to coordinates ξ, η.

One can see that the quasi-linear approach offers the possibility to bring into accord the hydrodynamic equation for the particle density and correlation meaning of the problem.

2.8.4 Magnetic Diffusivity and the Kubo Number

Quasi-linear ideas [23, 24] were used in the first papers [70, 126] devoted to the description of the influence of the stochastic magnetic field on transport processes in a plasma. This allows consideration of the magnetic diffusion coefficient D_m (2.111) from the correlation point of view. The analysis of diffusion in the quasi-linear limit is based on the stochastic equation for force lines

$$\frac{d\vec{r}_\perp}{dz} = \vec{b}(z, \vec{r}_\perp), \quad \vec{b} = \frac{\vec{B}'}{B_0} \approx b_0. \tag{2.238}$$

Here, a weak random field $\vec{B}'(B_x, B_Y, 0)$ is superimposed on a strong constant field $\vec{B}(0, 0, B_0)$ aligned with the z-axis and b_0 is the characteristic relative scale of perturbations. This representation is analogous to the continuity equation of a test particle motion in a flow (2.211). Jokipii and Parker [70] suggested a quasi-linear expression for the transverse diffusion coefficient of the force lines of a magnetic field

$$D_m = \frac{1}{4} \int_{-\infty}^{\infty} dz \left\langle \vec{b}(z, 0)\vec{b}(0, 0) \right\rangle \propto b_0^2 L_Z. \tag{2.239}$$

Here, L_Z is the longitudinal correlation length $L_Z = (1/b_0^2) \int_{-\infty}^{\infty} dz \, \langle \vec{b}(z, 0)\vec{b}(0, 0) \rangle$. The determination of the interrelation between the magnetic diffusion coefficient D_m and the diffusion coefficient of particles in the braided magnetic field is a complex problem. However, there exists a simple model of "double" diffusion (2.116) suggested in [69].

The simple quasi-linear estimate (2.238) that we considered earlier demonstrates the necessity of a careful analysis of longitudinal and transverse correlation effects. Therefore, the neglect of the transverse displacement $\Delta_\perp$ in expression (2.238) $\vec{b}(z, \Delta_\perp) \approx \vec{b}(z, 0)$ is a serious drawback. A similar situation also arises in the theory of the turbulent diffusion of a passive scalar.

The quasi-linear representation of the magnetic diffusion coefficient permits us to obtain an estimate of particle diffusion in the stochastic magnetic field, which differs significantly from the double diffusion. Thus, from the standpoint of the dimensional analysis we can consider the expression

$$D_\perp \approx D_m \frac{L_{\text{cor}}}{\tau} \approx b_0^2 L_z \frac{L_{\text{cor}}}{\tau}. \tag{2.240}$$

Here, L_{cor} and is the particle correlation length and τ is the time that characterizes the particle transport. However, if the longitudinal correlation length L_z that characterizes the stochastic magnetic field is comparable with the longitudinal correlation length L_{cor}, then using the expression for the longitudinal diffusion coefficient $D_\| \approx L_{\text{cor}}^2/\tau$ we obtain

$$D_\perp \approx b_0^2 D_\|. \tag{2.241}$$

Such a representation for the effective diffusion coefficient of particles in the stochastic magnetic field is called a "fluid limit" and appears to be one of the widely encountered estimates of transport related to the stochastic magnetic field. It is important that the dependence on the amplitude of the magnetic field fluctuation b_0 be the same as in formula (2.238).

Many authors have tried to improve the methods of the quasi-linear approximation, since it has a very limited region of applicability. The Dupree papers [64–66] are well known in this domain. Thus, the representation of the diffusion coefficient in the form (2.238) will be valid only for the case when the diffusion displacement in the transverse direction is much less than the transverse correlation scale length $b_0 L_Z \ll \Delta_\perp$.

The case of greatest interest arises when transverse correlation effects play a central role:

$$b_0 L_Z \geq \Delta_\perp. \tag{2.242}$$

Kadomtsev and Pogutse [67] suggested the use of a new approach and formulated a criterion of its applicability in terms of the dimensionless parameter that characterizes the ratio of longitudinal and transverse correlation effects:

$$R_m = \frac{b_0 L_Z}{\Delta_\perp} > 1. \tag{2.243}$$

They related the regimes with $R_m > 1$ to the percolation character of the behavior of streamlines [17]. Undoubtedly, it was a step forward, because the percolation methods are based upon the ideas of long-range correlations and fractality, which could be relevant for "braided" magnetic field problems.

2.9 The Diffusive Renormalization

In the previous sections, different approximations of correlation effects were considered. One of the most effective is a diffusive approximation. Its effectiveness is related to the universality of the Gaussian distribution. Here, we will discuss the diffusive representation of correlation effects by means of direct calculations of the correlation function and by treating renormalized quasi-linear equations.

2.9.1 The Dupree Approximation

In the previous sections, we considered the quasi-linear approximation in the framework of the hydrodynamic approach. However, the quasi-linear equations (which are based on keeping a nonlinear term in the equation for mean density and using a nonlinear equation for perturbations) were first obtained in kinetics for considering the problem of waves and particles interacting on the basis of Vlasov's equation

$$\frac{\partial f}{\partial t} + \vec{V}\frac{\partial f}{\partial x} + \vec{E}\frac{\partial f}{\partial V} = 0, \tag{2.244}$$

$$\operatorname{div}\vec{E} = 4\pi ne\int f\,d\vec{V}. \tag{2.245}$$

Here, f is the velocity distribution function, $\vec{E}$ is the electric field and n is the plasma density. The quasi-linear formulation of this problem has been repeatedly discussed in detail [123–125]. Therefore, we will consider only those aspects that play an important role for subsequent considerations. A kinetic problem is naturally much more complex. Thus, in the one-dimensional case the equations for the mean part of the distribution function f_0 and perturbation f_1 have the form, which is analogous to passive scalar equations (2.213), (2.214)

$$\frac{\partial f_0}{\partial t} + \frac{e}{m}\left\langle E\frac{\partial f_0}{\partial V}\right\rangle = 0, \tag{2.246}$$

$$\frac{\partial f_1}{\partial t} + V\frac{\partial f_1}{\partial x} + \frac{e}{m}\frac{\partial f_0}{\partial V} = 0. \tag{2.247}$$

However, the diffusion equation in the velocity space, which was obtained as the result of transformations

$$\frac{\partial f_0}{\partial t} = \frac{\partial}{\partial V}\left[D_V\frac{\partial f_0}{\partial V}\right], \tag{2.248}$$

with the quasi-linear diffusion coefficient

$$D_V = \left(\frac{e}{m}\right)^2\int\frac{|E_k|^2}{\omega(k) - kV}\,dk, \tag{2.249}$$

is added by the equation describing the energy dissipation of the electric field due to the Landau damping

$$\frac{d}{dt}|E_k|^2 = -2\gamma_k|E_k|^2, \tag{2.250}$$

where the characteristic frequency γ_k is defined by

$$\gamma_k = 2\pi e^2\omega\int\frac{\partial f_0}{\partial V}\delta(\omega - kV)\,dV. \tag{2.251}$$

Here, $\omega(k)$ describes the frequency dependence on the wave number k, and $|E_k|^2$ is the spectral function of the electric field. It is natural that the expression for the quasi-linear diffusion coefficient (2.249) in a velocity space can be interpreted in terms of the auto-correlation function of accelerations C_a,

$$D \approx \int_0^\infty C_a(t)\,dt \approx \left(\frac{e}{m}\right)^2 \int_0^\infty \big\langle E(0)E(t)\big\rangle\,dt. \tag{2.252}$$

One can see the analogy with the Taylor representation for the coefficient of turbulent diffusion (2.6). However, in the case of phase space we deal with a more complex problem. It is well known that the quasi-linear description of weak-turbulent plasma is based on the notion of stochastic instability and randomness of phases. Indeed, many theoretical and numerical investigations confirm the appearance of diffusion in a space of velocities in the stochastic limit. In spite of the effectiveness of the quasi-linear approximation, some correlation effects have not been considered. Thus, the mixing process of stochastically instable trajectories leads to the nonlinear irreversible decay of correlations with the characteristic time

$$\tau_k \propto \frac{1}{(k^2 D_V)^{1/3}}. \tag{2.253}$$

Here, D_V is the diffusion coefficient in velocity space and k is the wave number.

In the Dupree papers it was suggested considering the correlations decay by analogy with the Landau damping [64–66] using the frequency "renormalization" in the form

$$\omega(k) \to \omega(k) + \frac{i}{\tau_k}. \tag{2.254}$$

Such an approach can be interpreted as the renormalization (modification) of the equation for the perturbation of the distribution function f_1

$$\frac{\partial f_1}{\partial t} + \vec{V}\frac{\partial f_1}{\partial x} + \vec{E}\frac{\partial f_0}{\partial V} = \frac{f_1}{\tau_k}. \tag{2.255}$$

Here, the term f_1/τ_k approximates the terms omitted in the quasi-linear approximation.

It is natural to consider the renormalization of the quasi-linear diffusion coefficient in terms of the autocorrelation function of accelerations,

$$C(t) = \left(\frac{e}{m}\right)^2 \big\langle E\big(x(t), t\big)E\big(x(0), 0\big)\big\rangle. \tag{2.256}$$

Then, the particle velocity in the framework of one-dimensional electrostatic turbulence is given by

$$V(t) = V_0 + \frac{e}{m}\int_0^t E\big[x(t'), t'\big]\,dt'. \tag{2.257}$$

Representing the electric field as the totality of many independent Fourier components, one obtains

$$E(x,t)=\sum_k E_k \exp\bigl[i(kx-\omega_k t)\bigr]. \tag{2.258}$$

The formal substitution of this expression into the formula for the correlation function yields

$$C(t)=\left(\frac{e}{m}\right)^2\sum_{kk'}\bigl\langle E_k \exp\bigl[i\bigl(kx(t)-\omega_k t\bigr)\bigr]E_{k'}\exp\bigl[i\bigl(k'x(0)\bigr)\bigr]\bigr\rangle. \tag{2.259}$$

Then, by analogy with Corrsin, Dupree used the independence hypothesis:

$$C(t)=\left(\frac{e}{m}\right)^2\sum_k |E_k|^2\bigl\langle \exp\bigl[i\bigl(kx(t)-\omega_k t\bigr)+i\bigl(k\Delta x(t)\bigr)\bigr]\bigr\rangle. \tag{2.260}$$

For the Gaussian statistics one obtains $\langle \exp A\rangle=\exp\frac{\langle A^2\rangle}{2}$ and hence the formula for the correlation function takes the form

$$C(t)=\left(\frac{e}{m}\right)^2\sum_k |E_k|^2 \exp\left[i(kx-\omega_k t)-\frac{k^2\langle\Delta x^2(t)\rangle}{2}\right]. \tag{2.261}$$

Using the dimensional estimate $\frac{d}{dt}\langle\Delta V^2(t)\rangle \approx 4D_V$, it is easy to find the scaling for $\langle\Delta x^2(t)\rangle \approx 2D_V t^3/3$. The expression for the diffusion coefficient for one-dimensional electrostatic turbulence for $t\to\infty$ then takes the Dupree form [64–66]

$$\begin{aligned} D &= \int_0^t C(\tau)\,d\tau \\ &= \left(\frac{e}{m}\right)^2\sum_k \int_0^\infty |E_k|^2 \exp\left[i(kV-\omega_k\tau)-\frac{1}{3}k^2 D_V\tau^3\right]d\tau. \end{aligned} \tag{2.262}$$

It is easy to note that this expression differs essentially from the quasi-linear one,

$$D_{\mathrm{QL}}=\pi\left(\frac{e}{m}\right)^2\sum_k |E_k|^2\delta(\omega_k-kV), \tag{2.263}$$

where δ is the symbol of the Dirac function. Thus, the Dupree diffusivity scales with E_k as $D\propto |E_k|^{3/2}$, whereas the quasi-linear prediction is $D_{\mathrm{QL}}\propto |E_k|^2$. Naturally, the correlation effects approximation suggested by Dupree and based on the independence hypothesis and dimensional estimates is fairly rough. Moreover, the quasi-linear approximation is very effective for the overwhelming majority of models. However, it allows one to visualize correlation effects omitted in the quasi-linear approach and opens new possibilities to obtain transport estimates [67, 71].

2.9.2 The Dupree Theory Revisited

The Dupree renormalized scaling $D_V \propto |E_k|^{3/2}$ was tested in numerical test particle simulations in [127] and later in [128]. The results were mixed, and no definitive conclusions drawn. The authors of [129] observed that the diffusivity numerically found is significantly smaller than that predicted by the Dupree theory. Ishihara and Hirose [130] confirmed their finding. Moreover, adopting the method proposed by Salat [131], they recalculated the diffusivity without assuming Markovian process and concluded that D_V should be time-dependent [132]. An explicit analytical expression for the diffusivity has been represented by Salat [133] and Ishihara et al. [134]. It has been shown that in the asymptotic limit, D_V scales with the turbulent field and time as

$$D_V \propto |E_k|^{4/3}/t^{1/3}. \tag{2.264}$$

The predicted velocity variance $\langle[\Delta V]^2\rangle \propto t^{2/3}$ in one-dimensional electrostatic turbulence increases with time more slowly than the usual Brownian motion, $\langle[\Delta V]^2\rangle \propto t$. This indicates a diffusion process, which is not free but restricted and dependent on the past history of particle trajectory.

The time integration is to be carried out along the perturbed particle trajectory $x(t)$ given by

$$x(t) = x_0 + V_0 t + \Delta x(t), \tag{2.265}$$

where

$$\Delta x(t) = \frac{e}{m}\int_0^t dt' \int_0^{t'} E\big[x(t''), t''\big]\, dt'' \tag{2.266}$$

is the derivation from the free streaming trajectory $x_0 + V_0 t$.

Then, the velocity variance is formally given, with $V = V_0$, by

$$\begin{aligned}\big\langle\big[\Delta V(t)\big]^2\big\rangle = \left(\frac{e}{m}\right)^2 \sum_k |E_k|^2 \int_0^t dt' \int_{t'-t}^{t'} ds' \exp\big[i(kV-\omega_k)s'\big] \\ \times \big\langle \exp\big[ik\big[\Delta x(t') - \Delta x(t'-s')\big]\big]\big\rangle. \end{aligned} \tag{2.267}$$

For Gaussian statistics, the average in expression (2.267) can be approximated by

$$\big\langle \exp\big[ik\big[\Delta x(t') - \Delta x(t'-s')\big]\big]\big\rangle \approx \exp\left[-\frac{k^2}{2}\big\langle\big[\Delta x(t') - \Delta x(t'-s')\big]^2\big\rangle\right]. \tag{2.268}$$

In the quasi-linear theory, $\Delta x = 0$. This is equivalent to the assumption that the particles continue to experience the Eulerian field. In the original resonance broadening theory by Dupree, the variance of particle trajectories is assumed to be independent of the memory effects, which lead to the following approximation:

$$\big\langle\big[\Delta x(t') - \Delta x(t'-s')\big]^2\big\rangle \approx \big\langle\big[\Delta x(s')\big]^2\big\rangle. \tag{2.269}$$

The correlation function $\langle[\Delta x(t) - \Delta x(t-s)]^2\rangle$ was calculated more rigorously as follows. Each term in the expansion

$$\left\langle\left[\Delta x(t)-\Delta x(t-s)\right]^2\right\rangle=\left\langle\left[\Delta x(t)\right]^2\right\rangle-2\left\langle\Delta x(t)\Delta x(t-s)\right\rangle+\left\langle\left[\Delta x(t-s)\right]^2\right\rangle, \tag{2.270}$$

is in the form of

$$\begin{aligned}&\left\langle\Delta x(t_1)x(t_2)\right\rangle\\&=\left(\frac{e}{m}\right)^2\int_0^{t_1}dt_1'\int_0^{t_1'}dt_1''\int_0^{t_2}dt_2''\int_0^{t_2'}dt_2''\left\langle E\left[x(t_1''),t_1''\right]E\left[x(t_2''),t_2''\right]\right\rangle. \end{aligned}\tag{2.271}$$

If the velocity variance is the result of diffusive process, we can make the following approximation [132–134]:

$$\left(\frac{e}{m}\right)^2\int_0^{t_1'}dt_1''\int_0^{t_2'}dt_2''\left\langle E\left[x(t_1''),t_1''\right]E\left[x(t_2''),t_2''\right]\right\rangle\approx 2D_V\min(t_1',t_2'), \tag{2.272}$$

provided the time-dependence, if any, of D_V is sufficiently weak. The substitution of expression (2.272) into (2.271) yields

$$\left\langle\Delta x(t_1)x(t_2)\right\rangle=2D_V\int_0^{t_1}dt_1'\int_0^{t_2}dt_2'\min(t_1',t_2'). \tag{2.273}$$

For $t_1>t_2$, the double integral reduces to $(3t_1-t_2)t_2^2/6$, and thus for $t>s>0$, the variance $\langle[\Delta x(t)-\Delta x(t-s)]^2\rangle$ becomes

$$\left\langle\left[\Delta x(t)-\Delta x(t-s)\right]^2\right\rangle=\frac{2}{3}(3t-2s)s^2D_V, \tag{2.274}$$

which does depend on t as well as the relative time s. This non-Markovian nature of the spatial variance will be responsible for the time-dependence of the velocity diffusivity. Substituting this expression into the cumulant in the velocity variance in expression (2.267), we finally obtain the following closed form for the diffusivity D_V:

$$\begin{aligned}D_V(t)=&\left(\frac{e}{m}\right)^2\sum_k\int_0^t|E_k|^2\\&\times\exp\left[i(kV-\omega_k)\tau-\frac{1}{3}k^2D_V\tau^2(3t-2\tau)\right]d\tau.\end{aligned} \tag{2.275}$$

For resonant particles with $V\approx\omega_k/k$, the upper limit of D_V is given by

$$D_V=\left(\frac{e}{m}\right)^2\sum_k|E_k|^2\int_0^t\exp\left[-\frac{1}{3}k^2D_Vt\tau^2\right]d\tau. \tag{2.276}$$

In the asymptotic limit $t\to\infty$, the integral approaches $\sqrt{3\pi}/2k\sqrt{Dt}$. Therefore, the upper limit of the diffusivity is

$$D_{V\,\max} = \left(\frac{\sqrt{3\pi}}{2}\right)^{2/3} \left(\frac{e^2}{m^2} \sum_k \frac{1}{k} |E_k|^2\right)^{2/3} \frac{1}{t^{1/3}}. \tag{2.277}$$

Actually, in the approach suggested in [130–134], applying the substitution of a ballistic scaling $\langle \Delta x^2(\tau)\rangle \propto \langle \Delta V^2(t)\rangle \tau^2 \propto (D_V t)\tau^2$, where t is the parameter of the integrand, for a Dupree dimensional approximation $\langle \Delta x^2(\tau)\rangle \propto D_V \tau^3$ yields the coordination of theoretical results and simulations.

2.9.3 The Taylor–McNamara Correlation Function

Taylor and McNamara [71] considered the problem of the direct calculation of the Lagrangian correlation function for the description of strongly magnetized plasma. However, we employ their method regardless of the plasma models. The analysis carried out in [71] was based on the Fourier representation of Lagrangian velocities appearing in the correlation function

$$\begin{aligned} C(t) &= \big\langle V\big(x(t);t\big) V\big(x(0);0\big)\big\rangle \\ &= \sum_{k,k'} \big\langle \tilde{V}_k(t) \exp\big[ikx(t)\big] \tilde{V}'_k(0) \exp\big[ik'x(0)\big]\big\rangle. \end{aligned} \tag{2.278}$$

Here, $\langle \cdots \rangle$ is the averaging symbol and $\tilde{V}_k(t)$ is the Fourier transformation of the velocity $V(x,t)$ over the spatial x-coordinate. The next step in correlation decomposition was called the "independence conjecture" [compare with (2.76)]:

$$C(t) = \sum_k \big\langle \tilde{V}_k(t) \tilde{V}'_k(0)\big\rangle \big\langle \exp\big\{ik\big[x(t) - x(0)\big]\big\}\big\rangle. \tag{2.279}$$

Taylor and McNamara then used the Corrsin and Dupree conjecture [28, 64–66] of "the diffusion behavior of trajectories" $[x(t) - x(0)]^2 \propto Dt$. Here, D is the diffusivity, which depends on the model. This is in fact a "recipe for calculating the average" of the value $\exp[ik\Delta x(t)]$ in accordance with the conventional formula

$$\langle \exp A\rangle = \exp\left[\frac{\langle A^2\rangle}{2}\right]. \tag{2.280}$$

Performing calculations yields $\langle \exp[ik\Delta x(t)]\rangle = \exp[-k^2 Dt]$. The expression for the correlation function was obtained in the form

$$C(t) = \sum_k \big\langle \tilde{V}_k^2\big\rangle \exp\big(-k^2 Dt\big). \tag{2.281}$$

Prior to proceeding with the presentation of the results of [71], we consider formula (2.281) from the "correlation" standpoint. This expression can be interpreted as the sum of the Gaussian exponential correlation functions with "weight factors", which is proportional to the turbulence spectrum $E(k)$:

$$C(t) \propto \sum_k E(k) \exp\left(-\frac{t}{\tau_k}\right). \tag{2.282}$$

Here, $\tau_k = 1/(k^2 D)$ is the characteristic time corresponding to the scale k. It is necessary to take into account that this sum of the larger number of exponents can turn out to be a nonexponential function. Similar expressions are most extensively employed to obtain correlation functions with power tails [17–22]. Another important feature of formula (2.281) is the following formula for the diffusion coefficient:

$$\begin{aligned} D &= \int_0^\infty C(t)\,dt = \frac{1}{D} \sum_k \frac{E(k)}{k^2} \int_0^\infty \exp\left(-k^2 Dt\right) d\left(k^2 Dt\right) \\ &\approx \frac{1}{D} \int \left(E(k)/k^2\right) dk. \end{aligned} \tag{2.283}$$

We note the similarity of the resulting expression to the Howells result:

$$D^2 = \int_k^\infty \frac{E(k)}{k^2}\,dk. \tag{2.284}$$

One can see from the above analysis that the Howells ideas of the interaction of scales and the correlation ideas of "diffusive behavior of trajectory" [28, 64–66] are closely interrelated. Taylor and McNamara introduced a quantity $S(t) = [\Delta x(t)]^2$. Then the expression for the correlation function takes the form

$$C(t) \approx \frac{d}{dt} D \approx \frac{d}{dt} \frac{\Delta x^2}{t} \approx \frac{d^2}{dt^2} S(t). \tag{2.285}$$

On the other hand, from formula (2.283) we obtain

$$C(t) = \int \left\{E(k)\left\{1 - \exp\left[-k^2 S(t)\right]\right\}\right\} dk. \tag{2.286}$$

In fact, one has a "Newtonian"-type differential equation $\frac{d^2}{dt^2} S(t) = F\{S(t)\}$. After a simple transformation we obtain the final solution [71]:

$$D^2 = \int \frac{dk}{k^2} \left\{E(k)\left\{1 - \exp\left[-k^2 S(t)\right]\right\}\right\}. \tag{2.287}$$

To obtain (2.284) it is sufficient to consider the case $k^2 S(t) \gg 1$. Note that [71] does not contain a reference to Howells's paper [73]. Apparently, the Howells result has become widely known more recently due to the Moffat analysis of turbulent transport problems [32, 33].

In the framework of the Taylor and McNamara diffusion approximation the value D is the effective diffusivity; this differs essentially from concepts based on the use of "seed" diffusivity as the "decorrelation mechanism". Thus, Wang and co-workers [135] suggested a modification of the Corrsin conjecture (2.74) by a substitution of the Taylor expression $R_T(t)^2$ for the mean square displacement $2D_0t$:

$$R_D(t)^2 \approx 2\int_0^t (t-t')C(t')\,dt. \tag{2.288}$$

Formal calculations lead to a complex nonlinear integral equation for $C(t)$ [135]. For the purposes of this paper it is sufficient to consider the simplified model of the diffusive evolution of the "correlation cloud" (2.98):

$$C(t) \approx \frac{V_0^2}{nR_D(t)^d} \approx \frac{V_0^2}{n}\left[\int_0^t (t-t')C(t')\,dt'\right]^{-d/2}. \tag{2.289}$$

The simplest case considered by Wang and co-workers [135] corresponds to $d = 2$; therefore, the approximation equation to define the Lagrangian correlation function takes the form

$$C(t)\int_o^t (t-t')C(t')\,dt' = \frac{V_0^2}{n}. \tag{2.290}$$

Unfortunately, even the simplified version of the nonlinear equation cannot be analytically solved. However, numerical simulation that was carried out in [135] permits one to consider complex correlation effects in a stochastic magnetic field.

2.9.4 The Kadomtsev–Pogutse Renormalization and the Stochastic Magnetic Field

The obvious drawback of the quasi-linear theory is that the nonlinear term in the equation for n_0 is retained while the nonlinear terms in the equation for n_1 are omitted. Many authors have tried to refine the quasi-linear approximation. A detailed analysis of such papers was carried out in [125]. In fact, the equation for n_1 (2.215) is linear and hyperbolic and it keeps the Lagrangian character of the correlations. This opens up the possibility of describing the omitted correlation effects by including the additional diffusive term.

In this context, it is expedient to present some of the results obtained by Kadomtsev and Pogutse [67] on anomalous electron transport in a magnetic field. They considered a three-dimensional problem in which a weak random field $\vec{B}'(B_x, B_Y, 0)$ is superimposed on a strong constant field $\vec{B}(0, 0, B_0)$ aligned with the z-axis. The formal quasi-linear representation is valid only when the diffusion-related displacement in the transverse direction is much less than the transverse correlation length (2.239). Kadomtsev and Pogutse considered a more complex case than the quasi-linear one. They introduced a continuity equation for the density of the magnetic field lines,

$$\frac{\partial n_b}{\partial z} + \vec{b}\nabla_\perp n_b(\vec{r}_\perp, z) = 0, \quad \vec{b} = \frac{\vec{B}'}{B_0} \approx b_0, \tag{2.291}$$

and represented n_b as a sum of the mean density $n_0 = \langle n_b \rangle$ and the fluctuation component n_1,

$$n_b = n_0 + n_1. \tag{2.292}$$

Here, b_0 is the relative scale of the fluctuation amplitude and $\langle \cdots \rangle$ is the averaging symbol. The problem as formulated is close to problems (2.213) and (2.214) of the quasi-linear diffusion of a passive scalar. In fact, the authors of [67] wrote the equation for n_0 in the traditional form:

$$\frac{\partial n_0}{\partial z} + \nabla_\perp \langle \vec{b} n_1 \rangle = 0. \tag{2.293}$$

However, in the equation for n_1 (2.214), they replaced the second-order terms

$$v_1 \frac{\partial n_1}{\partial x} - \left\langle v_1 \frac{\partial n_1}{\partial x} \right\rangle \tag{2.294}$$

(which were omitted in earlier studies) by a diffusion term $D_m \nabla_\perp^2 n_1$. In essence, they followed Corrsin's and Dupree's ideas and related the discarded correlation effects to the diffusive spreading of trajectories:

$$\frac{\partial n_1}{\partial z} - D_m \nabla_\perp^2 n_1 = -\vec{b} \nabla_\perp n_0. \tag{2.295}$$

Here, the effective diffusion coefficient was considered as diffusivity. This is similar to the Taylor–McNamara model. The set of renormalized equations (2.293)–(2.294) has retained a convenient form for solution. For passive scalar equations it corresponds to the set of equations

$$\frac{\partial n_0}{\partial t} + \left\langle v_1 \frac{\partial n_1}{\partial x} \right\rangle = 0; \tag{2.296}$$

$$\frac{\partial n_1}{\partial t} + v_1 \frac{\partial n_0}{\partial x} = D \frac{\partial^2 n_1}{\partial x^2}, \tag{2.297}$$

which are similar to (2.213) and (2.215). Thus, they kept (2.297) linear but passed from a hyperbolic equation of form (2.215) to the parabolic equation.

Applying the mathematical apparatus of Green's functions to (2.297), we obtain

$$\frac{\partial G}{\partial z} - D_m \nabla_\perp^2 G = \delta(\vec{r} - \vec{r}\,'). \tag{2.298}$$

Kadomtsev and Pogutse derived the following equation for the mean density n_0:

$$\frac{\partial n_0}{\partial z} = D_m \nabla_\perp^2 n_0, \tag{2.299}$$

where the magnetic diffusion coefficient and the Fourier spectrum of perturbation amplitudes are given by

$$D_m = \frac{1}{2} \int \frac{b^2(\vec{k})}{ik_z + k_\perp^2 D_m}\, d\vec{k}, \tag{2.300}$$

$$b^2(\vec{k}) = \frac{1}{(2\pi)^2} \int \langle b(0)b(r) \rangle \exp(-i\vec{k}\vec{r})\, d\vec{r}. \qquad (2.301)$$

For $\Delta k_z > k_\perp^2 D_m$, they got the quasi-linear expression

$$D_m = \frac{\pi}{2} \int d\vec{k}\, b^2(\vec{k}) \delta(k_z) \propto b_0^2 L_Z, \qquad (2.302)$$

where L_Z is the longitudinal correlation length.

In the case of strong correlations $\Delta k_z < k_\perp^2 D_m$, the authors of [67] arrived at the following result, which is similar to that obtained by Howells [73]:

$$D_m^2 = \frac{1}{2} \int \frac{b^2(\vec{k})}{k_\perp^2}\, d\vec{k}. \qquad (2.303)$$

This result for the magnetic diffusion coefficient

$$D_m \approx b_0 \Delta_\perp \qquad (2.304)$$

corresponds to the Howells estimate $D_H \approx V_0 \Delta$ but for the anisotropic case. It once again shows that, on the one hand, it is important to take into account the additional correlation effects that are neglected in the quasi-linear approach and, on the other hand, these correlations are closely related to interactions between different spatial scales. Note that in contrast to the Dreizin–Dykhne model, here one deals with perpendicular correlations. Moreover, in spite of the simple form of the obtained estimate (2.304), the linear character of the dependence of the effective diffusion coefficient D_{eff} on the "stochastic layer" width $\Delta_\perp$ is used to describe turbulent transport in models with convective cells, percolation transport, etc.

2.10 Anomalous Transport and Convective Cells

The analysis of complex structures plays an important role in the description of turbulent transport in both fluids and plasma. On the one hand, in the presence of structures we deal with essential spatial inhomogeneity (regions of convective transport). On the other hand, many correlation effects can still be approximated by diffusion models. The focus of this section is the derivation of the expression for the effective diffusion coefficient, which is based on the balance of convective and diffusive fluxes, in the convective cells system.

2.10.1 Bohm Scaling and Electric Field Fluctuations

The important peculiarity of the renormalized transport coefficients of Dupree, Taylor–McNamara, and Kadomtsev–Pogutse is the linear dependence of the effective diffusivity on the perturbation amplitude, which differs essentially from the quasi-linear square-law dependence. Thus, in the Dupree approach $D_V \propto |E_k|$; in the Taylor and McNamara model $D_{\text{eff}} \propto E(k)^{1/2}/k \propto V_k$; and in the case of the Kadomtsev–Pogutse renormalization method one deals with the estimate $D_m \propto b_0 \Delta_\perp$. In this relation, it is necessary to note that the question about the character of the dependence of the effective diffusivity on the perturbation amplitude has not only theoretical but also practical importance. For example, the analysis of transport in magnetized plasma leads to the necessity to consider the character of the dependence of turbulent diffusion across a magnetic field $\vec{B}$ on its magnitude. One of the important approaches is the consideration of drift motions of plasma in crossed electric $\vec{E}$ and magnetic $\vec{B}$ fields:

$$\vec{V}_E = c\frac{[\vec{B} \times \vec{E}]}{B^2} \propto \frac{\nabla\varphi}{B}. \tag{2.305}$$

Here, $\vec{V}_E$ is the drift velocity and φ is the potential of the electric field. Then, in terms of the Kubo number $Ku \approx V_0/\lambda\omega \approx k^2\varphi/\omega B$ we can analyze the dependence

$$D_\perp \propto Ku^{\beta_C} \approx \left(\frac{k^2\varphi}{\gamma B}\right)^{\beta_C} \propto V_E^{\beta_C} \approx \left(\frac{k\varphi}{B}\right)^{\beta_C}. \tag{2.306}$$

Here, k is the wave number and $\gamma \approx \omega$ is the characteristic frequency. The conventional representation of the collisional character of transverse diffusion in a strong magnetic field leads to the estimate [5–8]

$$D_\perp \approx \frac{ne^2c^2\sqrt{m_e}}{B^2\sqrt{T}}. \tag{2.307}$$

Here, e is the electron charge, m_e is the electron mass, T is the plasma temperature, and n is the plasma concentration. Actually, this corresponds to $\beta_C = 2$. The prognoses based on this formula provide fairly good confinement of plasma in magnetic traps. However, much experimental data points to the incorrectness of this estimate. The main reason that prevents good confinement is strong plasma turbulence. The simplest Bohm consideration [136] of the effects of turbulent fluctuations of electric fields leads to the linear dependence of the transverse diffusion on the perturbations amplitude with $\beta_C = 1$. The Bohm estimate of plasma diffusivity across a magnetic field is based on the notion of the existence of eddies or nonuniformity in turbulent plasma, which lead to chaotic fluctuations of electric fields. If we introduce a characteristic scale l_B corresponding to the structures under analysis then the simplest correlation estimate of the diffusion coefficient is the expression

$$D_B \approx \frac{l_B^2}{\tau_{\text{cor}}}. \tag{2.308}$$

Here, l_B plays the role of the spatial correlation scale and τ_{cor} is the characteristic correlation time that can be estimated from a dimensional analysis; introducing into consideration the velocity V_E characterizing drift motion in crossed electric $\delta\vec{E}$ and magnetic $\vec{B}$ fields yields

$$\tau_{\text{cor}} \approx \frac{l_B}{V_E} \approx \frac{l_B^2}{c\delta\varphi} B_0. \tag{2.309}$$

Here, use is made of the expression for the drift velocity $V_E \approx (c/B_0)\delta E \approx (c/B_0) \times (\delta\varphi/l_B)$ and the dimensional estimate of electric field fluctuations through the potential perturbation across the structure, $\delta\varphi \approx \delta E l_B$. Upon substitution we obtain the Bohm scaling for transverse diffusion in magnetized turbulent plasma:

$$D_B \approx l_B V_E \approx \frac{c}{B_0}\delta\varphi \approx \frac{cT}{eB_0}\left\langle\left(\frac{e\delta\varphi}{T}\right)^2\right\rangle^{1/2}, \tag{2.310}$$

where T is the plasma temperature. Here, use is made of energetic normalizing of electric field fluctuations, since the dimensional consideration yields

$$e\delta\varphi \approx e\delta E l_B \approx T. \tag{2.311}$$

The absence of the characteristic scale of structures l_B in the final expression is an important particularity of the Bohm scaling, which attaches a "universal" character to this estimate.

The simplest correlation interpretation of the appearance of the linear dependence of $D_{\text{eff}} \propto V_0 \propto Ku$ is the consideration of the decorrelation time τ in the Taylor definition

$$D_T \approx V_0^2 \tau. \tag{2.312}$$

Formally, the estimate $\tau \approx 1/\omega$ could be used as the decorrelation time. However, in the presence of complex structures (like convective cells) trapping could be important and one can estimate $\tau \approx \lambda/V_0$, where λ is the structure spatial scale. If the values V_0 are large then trapping is the main correlation mechanism, since $\lambda/V_0 < 1/\omega$, and hence

$$D_{\text{eff}} \approx V_0^2 \frac{\lambda}{V_0} \approx V_0 \lambda. \tag{2.313}$$

In the next section, we will consider how to obtain the linear dependence of D_{eff} on V_0 in more detail.

2.10.2 The Bohm Regime and Correlations

The scaling suggested by Bohm can be interpreted in terms of the renormalization method that was used by Dupree [64–66] and Taylor and McNamara [71]. In this approach, the Bohm scaling is integrated in terms of the Howells interaction of different scales, which is related to the "diffusion" character of decaying correlations. Thus, the authors of [71] considered an auto-correlation function for the case of strongly magnetized plasma by the guiding centers approximation

$$C(\tau) = \left(\frac{c}{B}\right)^2 \left\langle \delta E_\perp(\tau)\delta E_\perp(0)\right\rangle, \tag{2.314}$$

where $\delta E_\perp$ is the electric field fluctuation in the direction perpendicular to the magnetic field. Using the Fourier representation for electric field fluctuations

$$\delta E_\perp(x,t) = \sum_k \delta E_k(t) \exp\left[i\vec{k}\vec{x}(t)\right] \tag{2.315}$$

and the independence hypothesis [28], the expression for the correlation function can be rewritten in the form

$$C(t) = \left(\frac{c}{B}\right)^2 \sum_{kk'} \left\langle \delta E_k(t) \delta E_{k'}(0) \exp\left\{i\left[\vec{k}\vec{x}(t) + \vec{k}'\vec{x}(0)\right]\right\}\right\rangle$$
$$= \left(\frac{c}{B}\right)^2 \sum_{k} \left\langle \delta E(t) \delta E(0)\right\rangle \left\langle \exp\left[i\vec{k}\Delta\vec{x}(t)\right]\right\rangle. \tag{2.316}$$

Here, $\Delta x(t)$ is the diffusive particle displacement due to the presence of turbulent fluctuations. On the basis of the Gaussian statistics one obtains the expression

$$\left\langle \exp\left[i\vec{k}\Delta\vec{x}(t)\right]\right\rangle = \exp\left[-k^2 D_\perp(t)\right], \tag{2.317}$$

which is analogous to the Corrsin and Dupree representations [28, 64–66]. Then, the formal expression for the turbulent diffusion coefficient in terms of the Taylor definition is given by

$$D_\perp = \int_0^\infty C(t)\, dt = \int_0^\infty \left(\frac{c}{B}\right)^2 \sum_k \left\langle \delta E_\perp(t) \delta E_\perp(0)\right\rangle_k \exp\left[-k^2 D_\perp t\right] dt. \tag{2.318}$$

Taylor and McNamara assumed that the spectrum of statistical fluctuations of electric field $\langle \delta E^2 \rangle_k$ is known and the decaying correlations have the exponential form

$$\left\langle \delta E_\perp(t) \delta E_\perp(0)\right\rangle_k = \left\langle \delta E^2\right\rangle_k \exp\left[-k^2 D_\perp |t|\right] \tag{2.319}$$

with the characteristic correlation time in the diffusive form $\tau \approx 1/k^2 D_\perp$. Integrating the expression for the renormalized correlation function over time yields

$$D_\perp = \int_0^\infty dt \left(\frac{c}{B}\right)^2 \sum_k \left\langle \delta E^2\right\rangle_k \exp\left[-2k^2 D_\perp t\right]$$
$$= \left(\frac{c}{B}\right)^2 \frac{1}{D_\perp} \sum_k \frac{\langle \delta E^2 \rangle_k}{2k^2}. \tag{2.320}$$

Applying the spectrum $\langle \delta E^2 \rangle_k$ in the form [71]

$$\left\langle \delta E^2\right\rangle_k = 4\pi \frac{T}{1 + (k\lambda_D)^2}, \tag{2.321}$$

where $\lambda_D^2 = nT/4\pi e^2$, and integrating over k, it is easy to obtain the formula

$$D_\perp^2 = 4\pi T \left(\frac{c}{B}\right)^2 \int \frac{d\vec{k}}{(2\pi)^2} \frac{1}{2k^2[1 + (k\lambda_D)^2]}. \tag{2.322}$$

Here, T is the temperature and n is the density. This expression can be transformed into the form containing the Bohm factor $D_B \approx cT/eB$

$$D_\perp = \frac{cT}{eB}\sqrt{\frac{e^2}{T}\int_0^\infty \frac{dk}{k[1+(k\lambda_D)^2]}}. \tag{2.323}$$

Here, use was made of the integration over the azimuth angle θ: $d\vec{k} = k\sin\theta\, dk$. The divergence of this integral in the region of the small wave numbers k reflects the slow correlation decay and the necessity for a more detailed consideration of different scale interactions.

2.10.3 Convective Cells and Transport

The system of convective cells is one of the simplest models, permitting one to estimate transport related to self-organized structure. Thus, it is well known that low-frequency drift waves can act as convective cells and cause rapid particle transport if they are excited to a large amplitude [3–8]. The regular character of the location of structure elements simplifies the analysis considerably. However, this model is important and has properties corresponding to a more complex system. The subsequent progress of research on diffusion processes in systems with convective cells (see Fig. 2.4) [80, 81] has led us to the understanding of the importance of the stochastic layer width Δ and the convective fraction of the transport. The simplest estimate of the longitudinal convective transport is as usual the quasi-linear expression

$$D \approx V_0^2 \tau \frac{\Delta}{\lambda}, \tag{2.324}$$

which is corrected by the geometrical factor Δ/λ to account for the fraction of space that is responsible for the convection. Here, λ is the cell size and V_0 is the characteristic velocity of the convective flow. It is natural to use the characteristic time of leaving the particle from the boundary layer as the correlation time

$$\tau \approx \Delta^2/D_0. \tag{2.325}$$

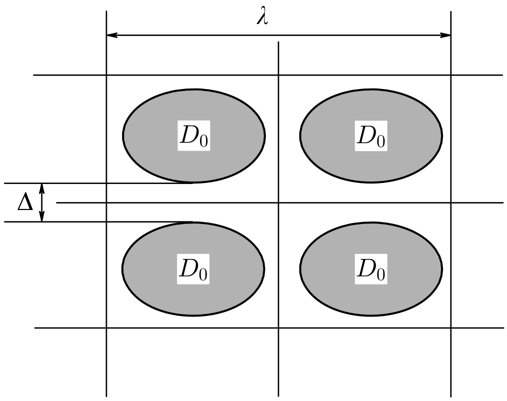

Fig. 2.4. System of convective cells

Here, D_0 is the "seed diffusion" coefficient. Then, the scaling for the convective transport takes the form

$$D_{\text{eff}} \approx V_0^2 \frac{\Delta^3}{\lambda D_0}. \tag{2.326}$$

However, the quasi-linear character of the dependence of D on V_0 does not correspond to the results of numerous simulations in the region

$$Pe \approx \frac{\lambda V_0}{D_0} \geq 1. \tag{2.327}$$

A qualitatively new estimate could be the linear dependence $D_{\text{eff}} \approx V_0 \Delta$. Formally, we must consider the effective diffusivity in the convective form

$$D_{\text{eff}} \approx \lambda V_0 P_\infty, \tag{2.328}$$

where P_∞ is the fraction of space, which is responsible for convective transport. In the case of convective cells, the value of P_∞ can be estimated if we introduce the cell size λ:

$$P_\infty \approx \frac{\lambda \Delta}{\lambda^2} \approx \frac{\Delta}{\lambda}. \tag{2.329}$$

This formula reflects the simple "topology" of the model of convective cells. The diffusive estimate of the stochastic layer width Δ was considered in [80, 81],

$$\Delta = \sqrt{\frac{D_0 \lambda}{V_0}} \approx \sqrt{D_0 \tau}. \tag{2.330}$$

Here, τ is the correlation timescale. This formula clearly defines the physical significance of the particle number balance. The number of particles escaping from a convective cell per unit time is

$$N_D \propto D_0 \frac{n}{\Delta} \lambda. \tag{2.331}$$

The convective flow along the boundary layer carries away a number of particles:

$$N_C \propto n V_0 \Delta. \tag{2.332}$$

Since convective flows exist only in the fraction of space Δ/λ, we obtain

$$D_{\text{eff}} \propto \lambda V_0 \frac{\Delta}{\lambda} = V_0 \Delta. \tag{2.333}$$

Note that the expression obtained is analogous to the nonquasi-linear result of Kadomtsev and Pogutse (2.304). The authors of [80, 81] eventually arrived at the following estimate for the turbulent diffusion coefficient:

$$D_{\text{eff}} = \text{const} \cdot \sqrt{D_0 V_0 \lambda} \approx D_0 Pe^{1/2} \propto V_0^{1/2}. \tag{2.334}$$

This representation of the result in terms of the Peclet number differs significantly from both the quasi-linear and linear estimates $D_{\text{eff}} \propto V_0^2$.

2.10.4 Complex Structures and Convective Transport

In conditions where cells are not regular, the analysis of transport can be based on the statistical properties of the streamline function landscape $\psi(x, y)$. Convective flows of particles along percolation channels contribute most to the effective diffusive coefficient. The topology of these channels is characterized by the second derivative of streamline function $\psi''(r)$. Therefore, introducing a characteristic scale of streamline function ψ_0 and a characteristic spatial scale r_0, we obtain an estimate of the channel width responsible for convection Δ:

$$\psi''(r)\Delta^2 \approx D_0. \tag{2.335}$$

Applying the scaling approach for ψ'', we obtain an expression for the definition of layer width Δ:

$$\Delta^2 \frac{\psi_0}{r_0^2} \approx D_0. \tag{2.336}$$

Simple calculations allow the derivation of the dependence of layer width Δ on the flow parameters ψ_0,D_0, r_0:

$$\Delta = r_0 \left(\frac{D_0}{\psi_0} \right)^{\frac{1}{2}} = r_0 \left(\frac{D_0}{r_0 V_0} \right)^{\frac{1}{2}}, \tag{2.337}$$

or in terms of the Peclet number,

$$\Delta = r_0 \frac{1}{Pe^{1/2}}. \tag{2.338}$$

Here, V_0 is the characteristic velocity scale.

Using the expression obtained above for effective diffusion in a system of random convective flows in the form

$$D_{\mathrm{eff}} \approx V_0 \Delta(\psi_0, D_0, r_0), \tag{2.339}$$

we easily find a scaling describing transport,

$$D_{\mathrm{eff}} \approx D_0 Pe^{\frac{1}{2}}, \tag{2.340}$$

which is in good agreement with the above.

This approach is an attractive one, which could possibly provide an alternative starting point for the analysis of transport effects [40]. However, such an approach is slightly naive and does not use all the possible information concerning flow topology; therefore, it cannot be applied for a rigorous analysis of fractal streamlines. These problems will be considered in the next sections in more detail.

2.11 Stochastic Instability and Transport

The problems of tracer description and the analysis of transport in a stochastic magnetic field have many traits in common. Thus, in the case of magnetized plasma we deal with the anisotropic medium in the presence of several "seed" diffusive mechanisms simultaneously. Moreover, the stochastic instability of trajectories [74] also leads to the appearance of new decorrelation mechanisms. In this section, the Rechester–Rosenbluth transport model [75], in which stochastic instability plays a major role, will be considered.

2.11.1 Stochastic Instability and Correlations

The problem of the divergence of nearby force lines (see Fig. 2.5) has been repeatedly discussed in many books and articles [3–8]. It is obvious that this physical mechanism has a significant influence on the process of particle decorrelation in a stochastic magnetic field. For example, it "destroys" the double diffusion regime, which is based on the repeated returns of magnetized particles under conditions of longitudinal diffusive motion along the magnetic field (2.117). Ptuskin [137] considered this effect in terms of Richardson's relative diffusion [58]. This approach demonstrates the possibilities of a nonquasi-linear method of transport description in the stochastic magnetic field and the importance of using correlation ideas. In the simplest steady case, the equation describing the walks of the separated force line can be expressed in a form that is analogous to (2.1),

$$\frac{d\vec{r}_\perp}{dz} = \frac{\vec{B}}{|B|}. \tag{2.341}$$

Here, z characterizes the distance that was traveled along the force line and $\vec{B}(z)$ is the value of the magnetic field. In the framework of the simplified scenario—the regular component of the magnetic field is absent, $\langle \vec{B} \rangle = 0$, and the absolute value of the magnetic field is constant, $/B/ = \text{const}$—we obtain the following expression, which is analogous to Taylor's formula (2.6)

$$\langle r_i r_j \rangle = \iint dz_1\, dz_2 \left\langle \frac{B_i(z_1) B_j(z_2)}{|\vec{B}|^2} \right\rangle \approx \int^z dz \int_{-\infty}^{\infty} dg\, C_{ij}(g). \tag{2.342}$$

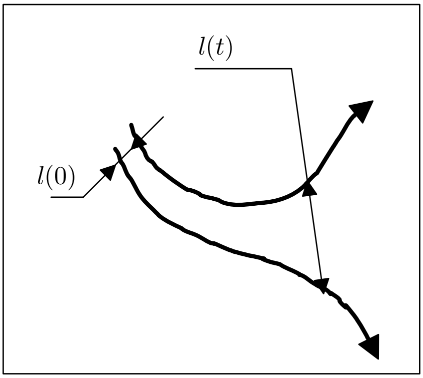

Fig. 2.5. Stochastic instability of trajectories

Here, $C_{ij}(g)$ is the correlation function of the random magnetic field, which characterizes the correlation decay along the chosen force line. Such a consideration is correct only for cases where the force line length is much greater than the correlation length L_z. It is natural that the expression obtained in the framework of Taylor's approximation (2.6),

$$\frac{d}{dz}\langle r_i^2 \rangle \approx \int_{-\infty}^{\infty} dg\, C_{ii}(g), \tag{2.343}$$

can be employed for this case. Obviously, the nonformal analogy of the equations that describe the particle walk and the force line walk allows us to consider the problem of the relative divergence of two force lines [3–8]. The author of [137] considered a relative displacement of two nearby force lines during the process of their random walk:

$$\Delta\vec{r} = \vec{r}^{(1)} - \vec{r}^{(2)} = \int^{z} dz\, \frac{\vec{B}^{(1)}(z) - \vec{B}^{(2)}(z)}{|B|}. \tag{2.344}$$

It is convenient to suppose that $\vec{r}_0^{(1)}$ and $\vec{r}_0^{(2)}$ are the initial points and the force lines pass through these points. The vector $\Delta\vec{r}$ connects two points of two different force lines that have started from the corresponding initial points $\vec{r}_0^{(1)}$, $\vec{r}_0^{(2)}$ and have passed an identical length z. Formal calculations allow us to obtain the expression

$$\begin{aligned}\langle \Delta r_i \Delta r_j \rangle \approx \int^{z} dz \int_{-\infty}^{\infty} dg\, \big[& C_{ii}(g,0) + C_{jj}(g,0) \\ & - C_{ij}(g,\Delta\vec{r}) - C_{ij}(-g,\Delta\vec{r}) \big]. \end{aligned} \tag{2.345}$$

Here, $\langle\,\rangle$ denotes averaging over the ensemble. It is necessary to introduce an additional variable $\Delta\vec{r}$ in the expression for the correlation function $C_{ij}\ (g, \Delta\vec{r})$, since we deal with the correlations of the field on two different force lines. In the case where correlations between the two force lines under consideration are absent, we obtain the result that corresponds to the Taylor representation (2.6),

$$\langle \Delta r_i^2 \rangle \approx 2 \int^{z} dz \int_{-\infty}^{\infty} dg\, C_{ij}(g,0). \tag{2.346}$$

However, taking into account the correlation effects that arise over the small distance Δr and using a decomposition over Δr in (2.345), the following expression was obtained:

$$\langle \Delta r_i^2 \rangle \approx \frac{1}{3} \int^{z} dz \int_{-\infty}^{\infty} dg \left[\frac{\partial^2 C_{ii}(g,0)}{\partial \rho^2} \langle \Delta r_i^2 \rangle \right]. \tag{2.347}$$

Here, ρ characterizes the distance across the tube of the force lines that corresponds to using $C_{ij}(g,\rho)$. Now, it is easy to obtain the exponential estimate that characterizes the process of divergence of nearby correlation force lines:

$$\langle \Delta r_i^2 \rangle \approx \langle \Delta r_i^2 \rangle_0 \exp\left[\frac{z}{3} \int_{-\infty}^{\infty} dg\, \frac{\partial^2 C_{ii}(g,0)}{\partial \rho^2} \right]. \tag{2.348}$$

In spite of the qualitative character of the estimates, this result shows the necessity of the modification of the dimensional subdiffusive expressions for particle transport in the stochastic magnetic field (2.117), taking into account the decorrelation processes of force lines.

2.11.2 The Rechester–Rosenbluth Model

Stochastic instability of trajectories is a nontrivial decorrelation mechanism [74, 75]. On average, two initially close streamlines diverge from one another according to the law

$$\Delta(z) = l_0 \exp\left(\frac{z}{L_K}\right). \tag{2.349}$$

Here, l_0 is the initial separation of the streamlines and z is the distance that was passed along the streamline. The magnitude $h = 1/L_K$ is called the Kolmogorov entropy and defined through

$$h = \lim_{l_0 \to 0, z \to \infty} \left\{ \frac{1}{z} \ln\left(\frac{\Delta(z)}{l_0}\right)\right\}. \tag{2.350}$$

One can see that correlation scales need not be defined by the seed diffusion process alone.

Rechester and Rosenbluth [75] assumed that decorrelation is related to stochastic instability and not to particle collisions. In the problem as formulated the collisional random walks of magnetized particles along and across streamlines of the magnetic field play the role of seed diffusion. The simplest estimate can be obtained by a consideration of the expression for the transverse diffusion coefficient of particles in terms of the magnetic diffusion coefficient (2.112)

$$D_{\text{eff}} \approx \frac{\Delta_{\text{cor}}^2}{2\tau} \approx D_m \frac{L_{\text{cor}}}{\tau}. \tag{2.351}$$

Here, L_{cor} is the longitudinal correlation length related to stochastic instability and τ is the correlation time. This approach implies that the magnetic diffusion coefficient D_m, the collisional longitudinal diffusion coefficient $D_\parallel$, and the collisional transverse diffusion coefficient $D_\perp$ are known. The analysis is often carried out in terms of the heat-conduction coefficient in order not to complicate the problem by taking into account ambipolar effects. However, we will keep using the diffusion symbols in order to retain the uniformity of the terminology. The values L_{cor} and τ are interrelated by the expression for the longitudinal diffusion coefficient:

$$D_\parallel \approx \frac{L_{\text{cor}}^2}{2\tau}. \tag{2.352}$$

We then obtain the following estimate for D_{eff}:

$$D_{\text{eff}} \approx D_m \frac{2D_\parallel}{L_{\text{cor}}}. \tag{2.353}$$

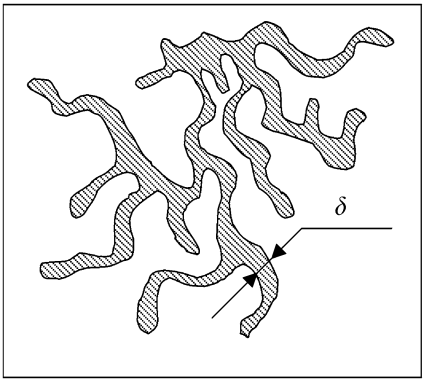

Fig. 2.6. The stochastic instability of phase element

Here, L_{cor} is the parameter of the problem. To define the value L_{cor} we use expression (2.349)

$$L_{cor} \approx L_K \ln\left[\frac{\Delta(L_{cor})}{l_0}\right] \approx L_K \ln\left(\frac{r_0}{l_0}\right). \qquad (2.354)$$

Here, r_0 is the transverse spatial scale. The authors of [75] assumed that the values r_0 and L_K are known and are related to the specific model. Therefore, to determine L_{cor} it is necessary to determine only l_0.

For this purpose, Rechester and Rosenbluth considered a small element of evolving area (see Fig. 2.6), which has a spatial scale l_0. Because of stochastic instability there will be two competing processes at the same time: the distance between streamlines will be exponentially increasing and the width of the area will be exponentially decreasing in order to conserve the total area:

$$\delta(z) = l_0 \exp\left(-\frac{z}{L_K}\right). \qquad (2.355)$$

Here, δ is the width of the area. It is necessary to take into account the influence of perpendicular diffusion processes that increase δ. The authors of [75] considered a balance between these processes:

$$\frac{d\delta}{dz} = -\frac{\delta}{L_K}, \qquad (d\delta)^2 \approx 2D_\perp \, dt. \qquad (2.356)$$

Taking into account the expression that describes the longitudinal diffusive behavior $(dz)^2 \approx 2D_\parallel \, dt$, one obtains the formula

$$l_0 \approx \delta \approx L_K \sqrt{\frac{D_\perp}{D_\parallel}}. \qquad (2.357)$$

The Rechester–Rosenbluth model is based on the assumption of the deterministic role of the stochastic Minstability of trajectories. However, there is also an alternative possibility related to the agreement between the longitudinal and transverse diffusion mechanisms in a strongly anisotropic medium. Thus, in the case of strongly magnetized plasma we deal with $D_\parallel \gg D_\perp$. Kadomtsev and Pogutse used this approach in their paper [67] that is devoted to the anomalous transport mechanisms in a braided magnetic field. In contrast to Rechester and Rosenbluth, the authors of [67] related longitudinal correlation length L_{cor} to the longitudinal diffusive process: $D_\parallel \approx L_{\text{cor}}^2/\tau$, and the decorrelation time τ was related to transverse diffusion: $D_\perp \approx r_0^2/\tau$. Here, r_0 is the characteristic scale in the transverse direction. Calculations then lead to the formula

$$D_{\text{eff}} \approx D_m \frac{\sqrt{D_\parallel D_\perp}}{r_0}, \tag{2.358}$$

which is one of the possibilities for relating the different diffusion mechanisms in the anisotropic medium. There is a new kind of dependence on $D_\parallel$ here.

It is necessary to note that in the case of particle diffusion in the stochastic magnetic field we are dealing with a large variety of regimes: double diffusion (2.116), ballistic behavior (2.113), fluid limit (2.241), the Rechester–Rosenbluth model (2.353), and the Kadomtsev–Pogutse regime (2.358). Moreover, there are several other regimes, which will be considered in the following sections.

2.11.3 Collisional Effects and the Stix Formula

The expression used for the effective diffusion coefficient (2.353) permits us to carry out an interesting parametric analysis. For example, it is possible to estimate the influence of collisions on the effective diffusion coefficient. Following Stix [138], let us introduce the N_{coll} factor accounting for the number of collisions during the correlation time (compare it with the Kubo number $Ku = V_0/\lambda\omega$):

$$N_{\text{coll}} \approx \frac{\tau}{\tau_{\text{coll}}}. \tag{2.359}$$

Here, τ_{coll} is the collisional timescale and τ is the correlation time. The expression for the coefficient of longitudinal diffusion has the form

$$D_\parallel \approx \frac{L_{\text{cor}}^2}{2\tau} \approx \frac{\lambda_{\text{coll}}^2}{2\tau_{\text{coll}}}. \tag{2.360}$$

Here, λ_{coll} is the collisional longitudinal mean free path. Hence, one can obtain

$$L_{\text{cor}} \approx \lambda_{\text{coll}} (N_{\text{coll}})^{1/2}. \tag{2.361}$$

On the other hand, we can represent the longitudinal diffusion coefficient as

$$D_\parallel \approx \lambda_{\text{coll}} V_\parallel. \tag{2.362}$$

Here, $V_\parallel$ is the particle characteristic velocity in the longitudinal direction. Hence, we can rewrite expression (2.353) in the following form:

$$D_{\text{eff}} \approx D_m V_\parallel \frac{1}{\sqrt{N_{\text{coll}}}}. \tag{2.363}$$

We see that collisional effects decrease the effective diffusion coefficient in comparison with the collisionless case $D_{\mathrm{eff}} \approx D_m V_{\|}$. However, in the framework of the approach of [75, 138, 139] it does not lead to the appearance of double diffusion (2.116).

This expression for D_{eff} in the Rechester–Rosenbluth theory is reminiscent of the Dreizin–Dykhne estimate

$$D_{\mathrm{eff}} \approx V_0^2 t \frac{1}{N_I(t)}, \tag{2.364}$$

where $N_I(t) \approx \sqrt{2D_0 t}/a$ is the number of interactions between the particle and transverse flows, which have the "collisional" meaning.

Stix [138] also suggested a somewhat different method to estimate the effective diffusion coefficient for the Rechester–Rosenbluth regime. Considering N_{coll} as the main parameter of the model, the author of [138] used a transcendental equation to define N_{coll}. The basis of this equation is estimate (2.354),

$$r_0 = l_0 \exp\left(\frac{L_{\mathrm{cor}}}{L_K}\right). \tag{2.365}$$

However, the assumption was made that the value l_0 is in agreement with the correlation time τ, $l_0^2 \approx D_\perp \tau$. Then, using the expression describing the relationship between the longitudinal correlation length L_{cor} and the correlation time τ yields the estimate for l_0, which differs from the Rechester–Rosenbluth result

$$r_0 = L_{\mathrm{cor}} \sqrt{\frac{D_\perp}{D_\|}} \ll L_{\mathrm{cor}}. \tag{2.366}$$

The equation for the longitudinal correlation length L_{cor} takes the form

$$r_0 = L_{\mathrm{cor}} \sqrt{\frac{D_\perp}{D_\|}} \exp\left(\frac{L_{\mathrm{cor}}}{L_K}\right). \tag{2.367}$$

Here, as before, the parameters of the problem are $D_\perp$,$D_\|$, r_0, L_K. However, we can re-formulate this equation for L_{cor} in terms of the parameter N_{coll}. Using the expressions for $D_\perp$ and $D_\|$ we obtain

$$D_\perp \approx \frac{\Delta_\perp^2}{\tau}, \qquad D_\| \approx \frac{\lambda_\|^2}{\tau_{\mathrm{coll}}}. \tag{2.368}$$

Here, $\Delta_\perp$ is the transverse correlation scale. Substitution of (2.368) into (2.367) yields

$$r_0 = \Delta_\perp \sqrt{N_{\mathrm{coll}}} \exp\left(\frac{\lambda_\| \sqrt{N_{\mathrm{coll}}}}{L_K}\right). \tag{2.369}$$

This transcendental equation for N_{coll} can be used to calculate D_{eff} in accordance with formula (2.363).

Concluding this section, note that the Kadomtsev–Pogutse result [67] can also be rewritten in a form that uses the collisionless diffusion coefficient with the additional factor. The particle longitudinal velocity enters into the expression for the longitudinal diffusion coefficient:

$$D_{\|} \approx V^2 \tau_{\text{coll}}. \tag{2.370}$$

On the other hand, the transverse diffusion coefficient has the form $D_{\perp} \approx \Delta_{\perp}^2/\tau_{\text{coll}}$. Here, $\Delta_{\perp}$ is the collisional transverse correlation scale. As a result of simple calculations we find the expression for the effective diffusion coefficient for the Kadomtsev–Pogutse regime:

$$D_{\text{eff}} \approx D_m V_e \frac{\Delta_{\perp}}{r_0}. \tag{2.371}$$

A comparison between formulae (2.358) and (2.371) allows us to see the essential difference between these approaches. We have considered the Rechester–Rosenbluth and the Kadomtsev–Pogutse models in terms of the correlation scale $\Delta_{\perp}$ and the collisional time τ_{coll}. But, it is easy to relate these values to the Larmor radius ρ_e of electron and the collisional frequency v_e to describe plasma physics problems [67, 75].

2.11.4 The Quasi-Isotropic Stochastic Magnetic Field and Transport

In the framework of the Rechester–Rosenbluth approach, the expression for longitudinal correlation length

$$L_{\text{COR}} \approx L_K \ln\left(\frac{r_0}{l_0}\right) \tag{2.372}$$

contains the parameters L_K, l_0, and r_0, and their definition depends on a selected model. In the case of magnetized plasma, the effective approximation is given by

$$l_0 \approx L_K \sqrt{\frac{D_{\perp}}{D_{/\!/}}} \quad \text{and} \quad r_0 \approx \rho_e, \tag{2.373}$$

where ρ_e is the Larmor radius of the electron. However, if the tangled magnetic field is described by the only spatial scale l_B, then the estimate used by Rechester and Rosenbluth becomes incorrect. Quasi-isotropic stochastic magnetic fields play an important role in astrophysical problems. Thus, in describing heat-conduction processes in a stochastic magnetic field in clusters of galaxies, there are serious difficulties because the transport observed considerably exceeds theoretical estimates [12]. Chandran and Cowley suggested an interesting modification of the Rechester–Rosenbluth scaling, in which the characteristic spatial scale of nonuniformity of tangled magnetic field l_B is simultaneously the parameter describing electron capture by magnetic traps formed by a significant nonuniformity of a magnetic field in a longitudinal direction. Formally, in the conditions when $l_B \leq \lambda_B$, where λ_B is the mean free path, the correlation characteristics of stochastic magnetic fields can be represented

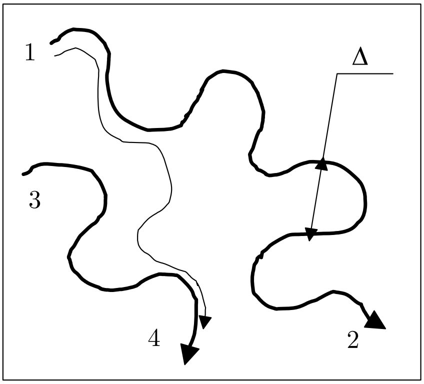

Fig. 2.7. Magnetic force lines 1–2, 3–4, and particle trajectory 1–4

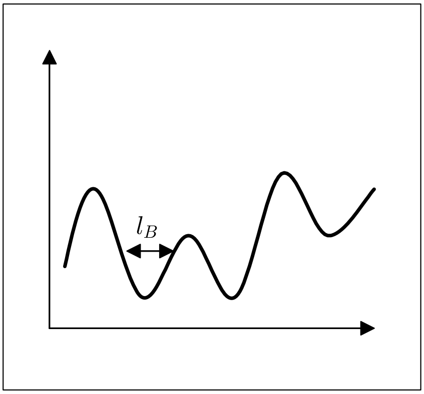

Fig. 2.8. Magnetic traps

in the form

$$L_{\mathrm{COR}} \approx l_B \ln\left(\frac{l_B}{\rho_e}\right), \tag{2.374}$$

$$D_m \approx \frac{l_B^2}{l_B} \approx l_B. \tag{2.375}$$

The authors of [12] assumed that transverse decorrelation in electron motion arises along the whole distance of order l_B and, at the same time, the same scale characterizes the sizes of the magnetic traps, which electrons leave after gaining additional energy in collisions. The situation under analysis is described by the following hierarchy of scales:

$$\rho_e \ll l_B \leq \lambda_B \ll L_{\mathrm{COR}}. \tag{2.376}$$

The expression for the effective diffusivity in a quasi-isotropic stochastic magnetic field takes the form:

$$D_{\mathrm{eff}} \approx D_m \frac{L_{\mathrm{COR}}}{\tau} \approx D_m \frac{D_{/\!/}}{L_{\mathrm{COR}}} \approx D_{/\!/} \frac{l_B}{L_{\mathrm{COR}}} \approx \frac{D_{/\!/}}{\ln(l_B/\rho_e)}. \tag{2.377}$$

The physical problem considered by Chandran and Cowley implies the use of the expression for the electron heat-conduction coefficient of Spitser–Harm χ_{Sp} as $D_{/\!/}$; taking into account the one-dimensional character of electron motion along force lines,

$$D_{/\!/} \approx \frac{L_{/\!/}^2}{2\tau} \approx \frac{\chi_{\mathrm{Sp}}}{3}. \tag{2.378}$$

The estimate of the value ρ_e in the conditions corresponding to clusters of galaxies yields

$$l_B/\rho_e \approx 10^3 \quad \text{or} \quad L_{\mathrm{COR}} \approx 30 l_B; \tag{2.379}$$

therefore, the suggested approach gives the estimate for the effective heat conduction coefficient:

$$\chi_{\mathrm{eff}} \approx D_{\mathrm{eff}} \approx 10^{-2}\chi_{\mathrm{Sp}}. \tag{2.380}$$

From the point of view of the explanation of observed distributions, this estimate is not correct but (as will be discussed below) the Chandran–Cowley approach needs only insignificant modification. The monoscale model in [12] implies that the MHD turbulence has an isotropic character. However, the phenomenological approach, which takes into account the contribution of different turbulence scales in the value l_B, appears to be more adequate for describing galaxy-cluster cooling flows [148].

2.11.5 Quasi-Linear Scaling for the Stochastic Instability Increment

The relative displacement of two nearby force lines during the process of their random walks is given by

$$\Delta\vec{r} = \vec{r}^{(1)} - \vec{r}^{(2)} = \int^z dz\, \frac{\vec{B}^{(1)}(z) - \vec{B}^{(2)}(z)}{|\vec{B}|}. \tag{2.381}$$

It is then easy to obtain the expression describing the divergence of force lines of the stochastic field for small values of $r_2 - r_1$ [67]

$$\frac{\partial}{\partial z}(r_2 - r_1) = b(z, r_2) - b(z, r_1) \approx \frac{\partial b}{\partial r}(r_2 - r_1). \tag{2.382}$$

Formal calculations yield the exponential dependence:

$$r_2(z) - r_1(z) \approx \Delta r(z = 0)\exp\left[\int_0^z \frac{\partial b}{\partial r}\, dz\right]. \tag{2.383}$$

The increment of stochastic instability can be found by averaging this expression with an assumption about the Gaussian character of a random value b, which makes it possible to calculate an average as follows:

$$\langle \exp A\rangle = \exp\{\langle A^2\rangle/2\}, \tag{2.384}$$

and hence:

$$\Delta_{\perp}(z) = \langle r_2(z) - r_1(z)\rangle$$
$$= \Delta r|_{z=0} \exp\left[\frac{1}{2}\int_0^z \int_0^z dz'\, dz'' \left\langle \frac{\partial b(z'', r)}{\partial r}\frac{\partial b(z'', r)}{\partial r}\right\rangle\right]. \quad (2.385)$$

The integral expression in this formula is analogous to the expression for the quasi-linear diffusion coefficient. Simple transformations yield the increment of stochastic instability γ_z in the form

$$\gamma_z = \frac{1}{2}\int_{-\infty}^{\infty} \left\langle \frac{\partial b(0,0)}{\partial r}\frac{\partial b(z,0)}{\partial r}\right\rangle dz. \quad (2.386)$$

In terms of the dimensionless parameter R_m, this result takes the form

$$\gamma_z \approx \frac{b_0^2 L_Z}{\Delta_{\perp}^2} \approx \frac{D_m}{\Delta_{\perp}^2} \approx \frac{1}{L_Z} R_m^2. \quad (2.387)$$

In terms of the Kubo number, $\gamma \propto Ku^2$. Naturally, the limits of applicability of this estimate coincide with the limits of applicability of the quasi-linear approximation,

$$R_m \approx b_0 L_Z/\Delta_{\perp} < 1 \quad \text{or} \quad Ku < 1. \quad (2.388)$$

It is necessary to note that the features of topology play an important role in estimating the increment of stochastic instability. Thus, in the problem of magnetically confined high-temperature plasma, shear effects are of great importance [1–5]. Using simple calculations and introducing an additional characteristic scale

$$L_S = dq/dx \approx \text{const} \quad (2.389)$$

(for the case of constant shear), it is possible to re-define the value γ_Z. Here, q is the shear of the magnetic field. The modified equations take the following form:

$$\vec{B} = B_0\big(\vec{e}_Z + q(x)\vec{e}_Y\big) + \vec{B}'(x, y, z), \quad (2.390)$$

$$\frac{d\vec{r}_{\perp}(x, y)}{dz} = \vec{b}(r_{\perp}, z) + q(x)e_Y. \quad (2.391)$$

In the case of small displacements δx and δy, the analogue of (2.382) is the following set of equations [67]:

$$\frac{d}{dz}\delta x = \frac{\partial b_X}{\partial x}\delta x + \frac{\partial b_X}{\partial y}\delta y, \quad (2.392)$$

$$\frac{d}{dz}\delta y = \left[\frac{\partial b_Y}{\partial x} + \frac{1}{L_S}\right]\delta x + \frac{\partial b_X}{\partial y}\delta y. \quad (2.393)$$

The equation of evolution of the value

$$\Delta\vec{r} = \big(\langle\delta x^2\rangle; \langle\delta y^2\rangle; \langle\delta x\delta y\rangle\big) \quad (2.394)$$

is written in the matrix form:

$$\frac{d\Delta\vec{r}}{dz} = \hat{W}\Delta\vec{r}, \tag{2.395}$$

where the eigenvalues of the matrix $\hat{W}$ define the increment of stochastic instability for the case of constant shear:

$$\gamma_Z = \frac{1}{(L_Z L_S^2)^{1/3}}, \quad \text{where } L_S < L_Z. \tag{2.396}$$

Unfortunately, this important result obtained by Krommes in [38, 39] does not establish the direct relationship between γ_Z and R_m which characterizes the dependence on the magnetic perturbation amplitude.

2.12 Fractal Conceptions and Turbulence

The use of the fractal conceptions to obtain scaling laws is widely practiced. Mandelbrot's papers [56, 140] have played a very important role in this field. Richardson [58] suggested the first nontrivial scaling for turbulent diffusion. But many years after the publication of this paper Richardson proposed another nonconventional expression to describe the length of very "tortuous" curves [141]. This very formula stimulated the very interesting Mandelbrot papers. Mandelbrot introduced the notion of the fractal dimensionality that essentially extends the region of applicability of scaling methods in the turbulence theory and anomalous transport models. In this section, we will consider several problems of turbulence theory in terms of the fractal dimensionality. This allows us to move to the consideration of percolation mechanisms of anomalous transport.

2.12.1 Fractality and Transport

A large variety of nondiffusive transport mechanisms lead to the necessity of using different scaling laws. The scaling method appears to be very fruitful obtaining the relationships between the parameters, which characterize the transport, correlation, and geometric properties of the model under consideration. One of the reasons for such efficiency is the possibility to describe the geometric properties of different objects by using scaling terminology.

Such an approach was developed by Mandelbrot [56, 140] and obtained wide use due to its exceptional universality. The scaling representation for the basic geometric properties of models was suggested. In this approach the expression for the curve length is both the simplest and a very important result. From the formal standpoint [56, 57] the length of the "very tortuous curve" (the fractal curve) $L(\delta)$ can be rewritten in the form

$$L \approx \delta N(\delta), \quad N(\delta) \propto \frac{1}{\delta^{d_F}}. \tag{2.397}$$

In this fractal approach the full length L is approximated by small segments of size δ, $N(\delta)$ is the number of these segments, which are necessary for such an approximation, and d_F is the fractal dimensionality of the curve [56, 57]. In the framework of the conventional representation of the geometry of curves, we have to use the value $d_F = d = 1$. However, in this case the drawbacks of the conventional method of length measurement by a "yardstick" (ruler) remain.

Mandelbrot considered the problem of the measurement of a tortuous seacoast length in which the increase in measurement accuracy (the decrease in the value δ) leads to a growth in the value $N(\delta)$ ($d_F > 1$). From the formal standpoint this approach yields

$$L(\delta) \approx \delta N(\delta)|_{\delta \to 0} \to \infty. \tag{2.398}$$

This means that such a fractal line embraces "almost" the full plane. There are advantages and disadvantages of such a representation. One of the advantages is the possibility to describe the longest and most complex lines. Mandelbrot called them the fractal lines.

A similar situation is for the fractal surface area A:

$$A \approx \delta^2 N(\delta) \approx \frac{\delta^2}{\delta^{d_F}}. \tag{2.399}$$

Here, δ^2 is the small area of size of A for measurement and $d_F > 2$ corresponds to the fractal nature of the surface.

In general, we can obtain the expression for the fractal region in the form

$$W_d \approx \delta^d N(\delta) \approx \delta^{d-d_F}. \tag{2.400}$$

Here, we are dealing with the fractal cases $d_F > d$. It is possible to consider opposite cases when $d_F < d$. This situation can characterize the presence of a large number of voids in the cluster. More detailed information can be found in many books and review articles on fractal geometry and fractal models [56, 57, 140].

The simplest model, which permits us to analyze the fractal properties of transport processes, is d-dimensional random walks:

$$R \approx \sqrt{2dDt}, \quad D \approx \frac{\Delta_{\text{cor}}^2}{2d\tau}. \tag{2.401}$$

Here, Δ_{cor} is the correlation length and τ is the correlation time. For this case, it is easy to obtain an expression that includes the fractal dimensionality of the Brownian trajectory:

$$L \approx N\Delta_{\text{cor}} \approx \frac{t}{\tau}\Delta_{\text{cor}} \approx \frac{2dDt}{\Delta_{\text{cor}}^2}\Delta_{\text{cor}}. \tag{2.402}$$

Hence, one can obtain a number of "steps" in the scaling form

$$N \propto \frac{1}{\Delta_{\text{cor}}^2}, \quad \text{where } d_F = 2. \tag{2.403}$$

Note that the value d_F is not dependent on d. Here, we assume that Δ_{cor} is the small quantity $\Delta_{\text{cor}} \approx \delta$. This corresponds to the definition of the fractal curve (2.397). However, it is possible to describe the fractal properties on the basis of using "large" parameters $R \propto 1/\delta$, which corresponds to the "cluster" terminology. For example the expression

$$N \propto R^{d_F} \tag{2.404}$$

is the equivalent definition of the number of molecules which form the fractal cluster. Here, R is the radius of the region occupied with the cluster. In this case, we can rewrite the Brownian scaling law in the following form:

$$N \approx \frac{t}{\tau} \approx \frac{R^2}{2dD\tau} \propto R^2. \tag{2.405}$$

Hence, $d_F = 2$ and this result exactly corresponds to (2.405).

From the "fractal" point of view, the scaling laws describing anomalous transport in terms of the Hurst exponent $R \propto t^H$ can be interpreted analogously. Another definition of the transport exponent, which is usually called the internal dimensionality [17, 57],

$$t \propto N \propto R^{d_W}, \quad d_W = \frac{1}{H}, \tag{2.406}$$

is often used.

We can relate the Hurst exponent H and the internal dimensionality of the exponent d_W to the properties of the fractal cluster, where transport occurs. A simple estimate, which implies that fractal diffusion is a slower process than the conventional Brownian diffusion, is widely encountered:

$$\frac{R^2}{t} \approx D \approx \frac{1}{R^\theta}. \tag{2.407}$$

Then, simple calculations yield

$$R \propto t^{1/(2+\theta)}, \quad d_W = 2 + \theta. \tag{2.408}$$

This example demonstrates the method for obtaining the relationships between the exponents that describe different physical properties of the system. In the case of (2.407) the value d_W reflects the character of transport processes and θ characterizes the degree of complexity of the fractal structure.

The region of applicability of the fractal ideas for transport models is very wide. Not only the walking particle trajectory, but also the great number of return moments at the initial point, the diffusive front, etc. appear to be fractal values.

2.12.2 The Richardson Law and Fractality

There is a good example of the relation between fractal concepts and turbulence. Even simple observation shows the fractal nature of the cloud boundary. In this connection, great interest has arisen in the experimental measurement of a perimeter of a rainfall P and a cloud area A, determined from radar and satellite data.

Lovejoy obtained the simple scaling that relates the fractal perimeter P of the two-dimensional projections of the cloud region to its area A:

$$P^{1/d_F} \propto A^{1/2}. \tag{2.409}$$

From the fractal point of view, this expression is not surprising. Thus, Mandelbrot considered the formula for the length of the fractal curve that bounds the nonfractal area:

$$L \approx \delta N(\delta) \approx \delta \left(\frac{\lambda}{\delta}\right)^{d_F} \approx \lambda \left(\frac{\delta}{\lambda}\right)^{1-d_F}. \tag{2.410}$$

Here, λ is the characteristic spatial scale. If we suppose $\lambda \propto \sqrt{A}$, then the expression for L takes the form

$$L \approx \delta^{1-d_F} A^{d_F/2}. \tag{2.411}$$

Now it is easy to obtain the Mandelbrot relationship between the perimeter and the area

$$P^{1/d_F} \approx L^{1/d_F} \approx \delta^{1-d_F} A^{1/2}, \tag{2.412}$$

where the value δ is the parameter. This exactly corresponds to the Lovejoy result (2.409).

The correctness of this result in a wide spectrum of parameters has led Hentschel and Procaccia [78] to the idea of the relation between the fractal dimensionality of the cloud perimeter and the universal properties of the Kolmogorov model of isotropic turbulence. There is a simple method to obtain the relationship between the fractal dimensionality of the perimeter and the exponent that describes the turbulence spectrum. It based on the calculation of the effective rate of increase of the area of the cloud cross section due to the turbulent pulsation of velocity:

$$\frac{dA}{dt} \approx l_k V(l_k) N(l_k). \tag{2.413}$$

Here, $l_k \approx 1/k$ is the characteristic spatial scale, $V(l_k)$ is the characteristic velocity scale, and $N(l_k)$ is the number of sections that approximate the fractal perimeter of the cloud. If we use the scaling expressions for the spectrum of energy with an arbitrary exponent ς and for the number of sites,

$$E(k) \propto \frac{V_k^2}{k} \propto k^{-\varsigma}, \qquad N(l_k) \propto l_k^{d_F}, \tag{2.414}$$

then the substitution of (2.414) into (2.413) yields

$$\frac{dA}{dt} \approx l_k^{1-d_F-(1-\varsigma)/2}. \tag{2.415}$$

However, it is obvious that the rate of increase of the area of the cloud cross-section is independent of l_k. Therefore, we obtain the following relationship:

$$d_F = \frac{1+\varsigma}{2}. \tag{2.416}$$

Then in the Kolmogorov case with $\varsigma = 5/3$, we obtain $d_F = 4/3$. This result is in a good agreement with the value defined by Lovejoy, $d_F = 1.35$.

Even this simple estimate demonstrates the efficiency of using fractal ideas. A more rigorous analysis [78] has led to the modification of the Richardson scaling:

$$\langle Y(t)^2 \rangle \approx t^{3+q}, \tag{2.417}$$

where the range for the exponent q is $0.45 > q > 0.15$. Analogous results were later obtained in the framework of using the Levy–Khintchine approximations [140].

Note that the problem of calculating the fractal object perimeter is, in general, a rather complex problem. Moreover, in the problems of the description of turbulent diffusion based on the percolation model, the exponent that characterizes the hull of a fractal cluster (external perimeter) is a key parameter of the theory.

2.12.3 Intermittency and the Kolmogorov Law

The conception of the fractal character of geometrical values yields the possibility of the essential modification of many results. Moreover, often the fractal representation more adequately mirrors the essence of the problem under consideration. A good example is the correction of the universal Kolmogorov spectrum of energy [63]. It was clear at an early stage of development of Kolmogorov and Obuchov's scaling ideas that it is impossible to explain effects connected with intermittency [27, 30, 143] in the framework of the mono-parametric model. Many researches tried to correct "the law of 5/3" [63]. One of the most elegant models is the model of fractal representation of regions of turbulence energy dissipation. Thus, in the classical formulation the Kolmogorov idea can be represented by the dimensional estimates for the dissipation rate ε_k,

$$\text{const} = \varepsilon_k \approx \frac{V_k^2}{\tau} \approx V_k^3 k \approx \frac{V_l^3}{l}, \tag{2.418}$$

and the estimate of the energy spectrum in the space of the wave numbers $k \approx 1/l_k$,

$$E(k) \propto \frac{V_k^2}{k} \approx \left(\frac{\varepsilon_k}{k}\right)^{2/3} \frac{1}{k}. \tag{2.419}$$

Mandelbrot [76] and then Fricsh, Sulem and Nelkin [77] have renormalized these expressions using the fractal representation of energy dissipation regions. The fraction of the volume corresponding to "one dissipation center" can be represented in the form

$$Q \approx \frac{V_0}{N(l_k)} \approx \frac{l_k^d}{l_k^{d_F}} \approx l_k^{d-d_F}. \tag{2.420}$$

Here, $N(l_k)$ is the number of "dissipation centers" in the region of the size l_k and $V_l \approx l_k^d$ is the volume of this region; d is the dimensionality of Euclidean space; and d_F is the fractal dimensionality of the "cluster" consisting of "dissipation centers".

The expression for ε_k and $E(k)$ can then be rewritten in the renormalized form:

$$\text{const} = \varepsilon \approx V_k^3 k Q \approx \frac{V_l^3}{l} Q(l), \tag{2.421}$$

$$E_F(k) \propto \frac{V_k^2}{k}. \tag{2.422}$$

Then, upon performing calculations we arrive at the expression

$$E_F(k) \propto E_K(k) k^{-(d-d_F)/3} \approx \frac{1}{k^{5/3}} \frac{1}{k^{(d-d_F)/3}}. \tag{2.423}$$

Experiments are satisfactorily described by the value $d_F \approx 2.8$ [30]. However, there are many papers that discuss dissipation on an eddy surfaces with $d_F = 2$ or dissipation on eddy filament, which can be considered in terms of self-avoiding random walks (2.110) with $d_F = (2 + d)/3$.

Thus, for example, in the case $d_F = 2$ one obtains the energy spectrum

$$E(k) \approx \frac{1}{k^2} \tag{2.424}$$

that corresponds to the Taunsend suggestions [27], which can be interpreted in terms of the constant spectrum of enstrophy $(\text{rot } V)^2$. Then the condition for the enstrophy spectrum

$$E_w(k) \propto \frac{(V_k k)^2}{k} \approx \text{const}, \tag{2.425}$$

in combination with the spectrum energy from definition (2.419), leads to the spectrum (2.424).

It is obvious that the Kolmogorov idea partially loses its initial universality after we introduce the new parameter d_F. However, at the same time, such a correction essentially increases the possibilities of agreement between theory and experiment.

2.13 Percolation and Scalings

In this section, we discuss the possibility of explaining the anomalous superdiffusion transport in the framework of the percolation threshold. The percolation approach looks very attractive because it gives a simple and, at the same time, universal model of behavior related to both the strong correlation effects and convective transport. On the other hand, for two-dimensional systems it is possible to use computer simulation to check theoretical results. The scaling arguments for both steady and time-dependent flows are presented.

2.13.1 Continuum Percolation and Transport

Kadomtsev and Pogutse [67] suggested a new method of analysis of the magnetic transport effects under conditions where transverse correlation effects play a signif-

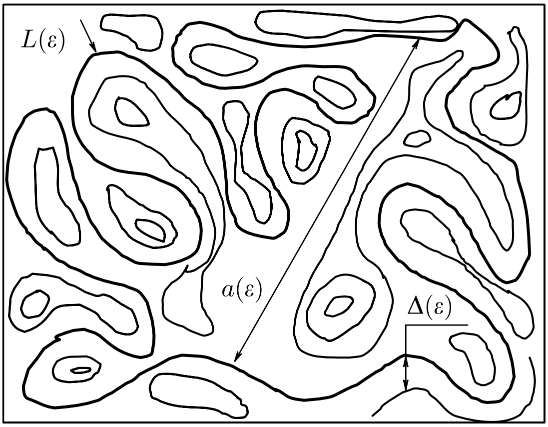

Fig. 2.9. Random steady flow and fractal streamline

icant role, $b_0 L_Z \geq \Delta_\perp$ (2.243). They used the percolation approach [49, 57] and formulated the criterion for its applicability in terms of the dimensionless parameter that characterizes the ratio of longitudinal and transverse correlation effects $R_m \gg 1$.

The percolation methods are based on the ideas of "long-range" correlations and could correspond to the two-dimensional anomalous transport pattern in turbulent plasmas in the presence of a strong magnetic field. A physically clear presentation of fundamental ideas in the percolation theory and the fractal concept can be found in [49, 57]. In the subsequent discussion, we assume that the reader is familiar with the basic definitions in these papers and consider the problems related to anomalous transport. In the context of this approach, the streamlines $\Psi = \Psi(x, y)$ are considered as coastlines in a hilly landscape flooded by water. It is expected that there is a sharp transition from separated lakes on a boundless land to individual islands in an infinite ocean. The percolation theory requires the existence of at least one coastline of infinite length.

Kadomtsev and Pogutse [67] related the anomalous character of diffusion for $R_m \gg 1$ to the fractal character of the behavior of the streamlines of the two-dimensional flow near the percolation threshold (see Fig. 2.9). They used the scaling law for the length of a percolation line of flow:

$$L(\varepsilon) \propto \frac{1}{\varepsilon^{2.4}}. \tag{2.426}$$

Here, ε is a small dimensionless quantity which characterizes the degree of deviation of the system from the critical state (the percolation threshold), $\varepsilon \approx h/\lambda V_0$, where h is the value of the streamline function $\Psi = \Psi(x, y)$ near the percolation threshold, λ is the characteristic scale, and V_0 is the characteristic velocity of the flow. The expression for $L(\varepsilon)$ corresponds exactly to the fractal representation of the curve length. There are advantages and disadvantages to such a representation. One of the advantages is the possibility of describing the longest and most tortuous curves and long range correlations [17, 20, 49, 57].

To describe effects related to the considerable increase in transport coefficients, it is not sufficient to consider the fractal presentation of a streamline alone. Moreover, the fractal character of the curve sometime leads to slower diffusion (subdiffusion). Therefore, it is necessary to introduce another important value. In percolation theory the correlation length $a(\varepsilon)$ is the main magnitude characterizing spatial scales of the system, which is located near the percolation threshold $\varepsilon \to 0$:

$$a(\varepsilon) = \frac{\lambda}{|\varepsilon|^{\nu}}. \tag{2.427}$$

Here, λ is the geometric characteristic scale. Thus, the idea of long-range correlations was realized in the framework of the percolation approach. However, there is a problem, since the diffusion coefficient is directly related to the expression for the correlation length: $D \approx \Delta_{\text{cor}}^2/\tau$. Here, τ is the correlation time. In the case under consideration, estimates yield $\Delta_{\text{cor}} \approx a(\varepsilon)_{\varepsilon \to 0} \to \infty$. For this reason, perhaps, Kadomtsev and Pogutse [67] based their consideration on the "diffusion renormalization" of the quasi-linear equations. However, in this approach the percolation character of correlation effects was lost. It is not surprising that in the framework of the classical diffusion equations we cannot use the percolation exponents ν, d_F.

To develop the percolation approach, it is necessary to take into account the fact that the percolation cluster occupies only a small fraction of the space. Therefore, the value

$$D_{\text{eff}}(\varepsilon) \approx D_C P_{\infty}(\varepsilon) \tag{2.428}$$

can be the estimate of the effective diffusion coefficient. Here, D_C is the diffusion coefficient which corresponds to transport on the percolation cluster and the value $P_{\infty}(\varepsilon)$ defines the fraction of the space that is occupied by the percolation cluster. In percolation theory, the scaling representations for $D_{\text{eff}}(\varepsilon)$ and $P_{\infty}(\varepsilon)$ are used:

$$D_C(a) \propto a^{-\theta}, \qquad D_{\text{eff}}(\varepsilon) \propto \varepsilon^{\mu}, \qquad P_{\infty}(\varepsilon) \propto \varepsilon^{\beta}. \tag{2.429}$$

On substituting (2.429) and (2.427) into expression (2.428) we obtain the relationship between the different percolation exponents: $\mu = \beta - \nu\theta$. In the subsequent consideration, we will use these results to analyze two-dimensional random flows. Therefore, it is important to note that there is an exactly calculated value ν for two-dimensional percolation problems: $\nu = 4/3$ [17, 144–146]. To determine the transport characteristics it is necessary to find the values θ and β, which depend on the physical model.

2.13.2 Renormalization and Percolation

To solve real physical problems, the expression $\varepsilon \to 0$ looks too abstract. Here, we consider a simple method which permits us to obtain effective estimates of values described by scaling laws (2.427), (2.428) by using the finite value of the percolation parameter ε_* instead of $\varepsilon \to 0$. The correlation length is one of the most important values describing transport. However, in a system of finite size L_0 we cannot consider

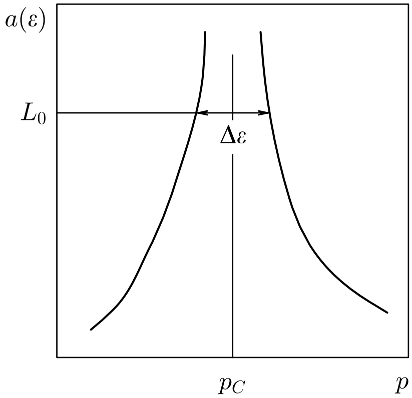

Fig. 2.10. Renormalization of the small parameter $\varepsilon = p - p_C$ for finite size samples

the infinite value

$$a(\varepsilon)|_{\varepsilon \to 0} \to \infty. \tag{2.430}$$

Here, it is relevant to introduce a new small "renormalization" parameter ε_* [79] as the value that gives the condition

$$a(\varepsilon_*) \approx L_0. \tag{2.431}$$

The simplest calculations yield

$$\varepsilon_* \approx \left(\frac{\lambda}{L_0}\right)^{1/\nu}. \tag{2.432}$$

This result can be interpreted in the framework of percolation experiments with finite size samples. Under these conditions, the percolation threshold arises when the value of ε_* slightly differs from zero and is situated in some $\Delta\varepsilon$ interval. The estimate obtained for ε_* can be considered as the characteristic width of this diapason (see Fig. 2.10)

$$\Delta\varepsilon \approx \varepsilon_*. \tag{2.433}$$

Actually, we are dealing with the small parameter

$$\varepsilon_0 \approx \frac{\lambda}{L_0} \ll 1, \tag{2.434}$$

which describes the real physical system with the characteristic scales L_0 and λ. On "renormalization", we obtain a new percolation parameter

$$\Delta\varepsilon \approx \varepsilon_* \approx \varepsilon_0^{1/\nu}. \tag{2.435}$$

It is natural that the value $\Delta\varepsilon$ decreases if the system size L_0 increases. Here, the value of $\Delta\varepsilon$ decreases if the system size L_0 increases. Now we can calculate the diffusion coefficient that is based on the estimate of the finite correlation length a:

$$D_{\text{eff}} \propto \frac{a^2(\varepsilon)}{\tau}. \tag{2.436}$$

Usually, the main problem of the percolation theory is to obtain interrelations between the percolation exponents. However, in the percolation models of turbulent diffusion the key problem is to determine a small parameter ε_0 and to find an adequate renormalization condition for ε_*. The next sections of this paper will consider in detail several specific models of turbulent diffusion from this standpoint.

2.13.3 Graded Percolation

An important typical example of the small renormalization parameter is the consideration of percolation in graded type systems. Trugman was the first to analyze this situation [147]. The graded character of the model corresponds to the assumption that the system is subject to a small external influence, which does not in general destroy the percolation character of the system's behavior, but can essentially change its properties.

First, we will consider this method from the formal point of view. Let us introduce a parameter ε_0 characterizing the smallness of an influence. In contrast to the renormalization, which uses the dependence of the percolation parameter on the system size $\Delta\varepsilon \approx \Delta\varepsilon(L_0) \approx \varepsilon_*$, here we will deal with the spatial dependence, which is related to the graded character of the problem $\varepsilon \approx \varepsilon(x)$. From the dimensional consideration we can obtain the expression that characterizes the uncertainty of the choice of the small parameter for these conditions, $\varepsilon_* \approx \Delta\varepsilon \approx \varepsilon'(x)a(\varepsilon_*)$. Then, simple calculations yield

$$a(\varepsilon_*) \approx \lambda \frac{1}{\varepsilon_*^{v}} \approx \frac{\lambda}{[\varepsilon'(x)a(\varepsilon_*)]^{v}}. \tag{2.437}$$

After the dimensional estimate in the form $\varepsilon'(x) \approx \varepsilon_0/\lambda$, we obtain the Trugman renormalization condition for the correlation scale:

$$a(\varepsilon_*) \approx \lambda \frac{1}{\varepsilon_*^{v}} \approx \frac{\lambda}{\varepsilon_0^{v/(1+v)}}. \tag{2.438}$$

Here, the value

$$\varepsilon_* = \varepsilon_0^{1/(1+v)} \gg \varepsilon_0 \tag{2.439}$$

is the new renormalized small parameter. Note that the direct use of the value ε_0 as the parameter in the percolation dependences is not correct, since it characterizes the destructive influence of a superimposed perturbation and not the degree of departure of the system from the percolation threshold.

This method looks quite formal, but renormalization (2.439) was repeatedly used to obtain information about the critical exponents that describe the hull of a percolation cluster, to analyze transport in a system with shear flows, and to consider the models of multiscale percolation. In specific problems, which will be considered below, a more detailed interpretation of a similar transformation will be given on the basis of taking into account the physical parameters that influence the topology of the flow under analysis. However, the first step is to obtain these physical values and introduce the small parameter that characterizes a percolation threshold.

Using the graded percolation method allows one to describe the structure of the diffusion front, which has a fractal nature [49, 57]. Another aspect of this problem also exists. We can describe the external perimeter of the fractal cluster (the hull) in terms of the diffusion front. From the diffusion standpoint the important value is the average distance between the source and the "front" $l_F \propto \sqrt{Dt}$. In the context of the problem the value l_F is the characteristic spatial scale. Such a probabilistic formulation of the problem of the particle reaching the diffusion front is very fruitful, since it is possible to interpret the problem in terms of the graded percolation (2.437), where $\varepsilon = \varepsilon(x)$. Then we can choose the value $\varepsilon_0 \approx \lambda / l_F$ as the initial parameter of the problem. In accordance with expression (2.439) we obtain

$$l_F(a) \approx \lambda \left(\frac{a}{\lambda} \right)^{(v+1)/v}. \tag{2.440}$$

Here, a is the correlation size that characterizes the structure of the diffusive front. Numerical and theoretical research on the external perimeter of the percolation cluster has arrived at the conclusion that in the two-dimensional case the hull $L(a)$ is equivalent to the value $l_F(a)$ [17, 49, 57]. Hence, the fractal dimensionality of the hull D_h is defined by the formula

$$D_h = 1 + \frac{1}{\nu} = 7/4. \tag{2.441}$$

Indeed, rigorous mathematical consideration confirms this result [144–146].

Note that in the two-dimensional percolation models of turbulent diffusion [17, 148], the hull is considered as a percolation streamline. The characteristic scale of the flow velocity V_0 is usually a known parameter; then, the dimensional estimates of many values can be obtained by way of combinations of the values V_0 and L. From this standpoint the relationship between D_h and ν allows all characteristics of the system to be described in terms of the universal exponent ν that reflects the correlation character of the percolation models.

2.14 Percolation and Turbulent Transport Scalings

The use of the "renormalization" method makes it possible to apply the percolation approach to the description of turbulent transport in two-dimensional random flows. The percolation scalings obtained by this method of the turbulent diffusion coefficient differ significantly from the quasi-linear one. This considerably increases the range of problems that can be considered in the framework of the scaling approach.

2.14.1 Random Steady Flows and Seed Diffusivity

Isichenko et al. [82] realized the potentiality of the percolation approach. They considered a two-dimensional zero-average-velocity steady flow specified by the bounded "common position" stream function $\Psi(x, y)$. They implied an isotropic-on-average oscillating function with a quasi-random location of saddle points along its height. The following scales were selected:

$$\Psi_0 \approx \lambda V_0, \quad \lambda \approx \left| \frac{\Psi}{\nabla \Psi} \right|. \tag{2.442}$$

The authors of [82] used formula (2.428) for effective diffusion and ideas of the convective nature of the flow along the percolation streamline,

$$D_{\text{eff}}(\varepsilon) \approx D_C \frac{L(\varepsilon)\Delta(\varepsilon)}{a^2}, \tag{2.443}$$

$$D_C(\varepsilon) \approx \frac{a^2}{\tau}. \tag{2.444}$$

Here, $L(\varepsilon)$ is the length of the percolation streamline, a is the spatial correlation scale [17], τ is the correlation time, and D_C is the correlation contribution to the effective diffusion coefficient. The value $h = \varepsilon \lambda V_0$ is the percolation scale of the stream function near a threshold. Effects of "long range correlations" enter into the expression for the diffusion coefficient precisely through $a(\varepsilon)$. Expression (2.443) is similar to the formula for effective diffusivity in the convective cell system from [80, 81], but here we are dealing with the dependence $\Delta = \Delta(\varepsilon)$. Moreover, in line with ideas in the literature on percolation theory, the authors of [82] suggested "a renormalization", i.e., a method of calculating the universal value of the small parameter ε in their percolation diffusion theory. They identified the small "width" of a percolation streamline with the small parameter of the percolation theory (see Fig. 2.9):

$$\Delta(\varepsilon) = \lambda \varepsilon. \tag{2.445}$$

This renormalization has become the main step in [82] and has begun to be actively used to solve other problems [17]. Representation (2.330) for the value Δ will be used in this formula. However, in the percolation case, the correlation effects should be taken into account by using $L(\varepsilon)$ instead of the geometric scale λ,

$$\Delta(\varepsilon) \approx \sqrt{\frac{D_0 L(\varepsilon)}{V_0}}. \tag{2.446}$$

This approach creates a dependence of Δ on the parameter ε. Now, we obtain the equation for the determination of the "universal" value of $\varepsilon_* = h_*/\lambda V_0$ as a function of the flow parameters D_0, V_0, λ,

$$\sqrt{\frac{D_0 L(\varepsilon)}{V_0}} = \varepsilon \lambda. \tag{2.447}$$

The specific calculations can be completed by using the rigorous scaling results of percolation theory [17, 49, 57] obtained for the correlation scale a and the length of the fractal streamline L as functions of ε for the two-dimensional case,

$$a(\varepsilon) = \lambda|\varepsilon|^{-\nu}, \qquad L(\varepsilon) = \lambda\left(\frac{a}{\lambda}\right)^{D_h}, \qquad \nu = 4/3, \qquad D_h = 1 + \frac{1}{\nu}. \quad (2.448)$$

The functional form of these dependences reflects the fractal and percolation behavior of the streamlines introduced in [67]. The solution of (2.447) in terms of the Peclet number leads to the expressions

$$h_* = \lambda V_0 \varepsilon_* = \lambda V_0 Pe^{-3/13} \propto V_0^{10/13}, \quad (2.449)$$

$$D_{\text{eff}} \approx V_0 \Delta(\varepsilon_*) \approx V_0 \lambda \left(\frac{1}{Pe}\right)^{1/(3+\nu)} = D_0 Pe^{10/13}. \quad (2.450)$$

This corresponds to the value $\mu = 1$ [see (2.429)]. From the point of view of the renormalization of the initial small parameter $\varepsilon_0 = 1/Pe$, the expression for the percolation small parameter can be obtained:

$$\varepsilon_* = (\varepsilon_0)^{1/(3+\nu)} \gg \varepsilon_0. \quad (2.451)$$

Some "arbitrariness" in expression (2.445) in the selection of the value $\lambda\varepsilon$, rather than $\lambda\varepsilon^2$ or $\lambda\varepsilon^3$, can be interpreted as a desire to have a universal small parameter, which is analogous to a single characteristic scale—the correlation length in the theory of phase transitions. Here, it should be particularly emphasized that the length of the fractal percolation line is not infinitely large because the small parameter ε_* does not tend to zero but has a finite value $\varepsilon_* = h_*/\lambda V_0$ for all types of flows with the characteristics D_0, V_0, λ. Therein lies the universality of formula (2.445).

2.14.2 The Spatial Hierarchy of Scales and Stochastic Instability

Note that the simplicity of the percolation estimate of turbulent transport is elusive. It will suffice to recall in this connection the "hierarchy" of scales used by the authors of [82] for their analysis,

$$\lambda\left(\frac{a}{\lambda}\right)^{D_h} \approx L \approx \frac{a}{\varepsilon_*} \gg a \approx \frac{\lambda}{\varepsilon_*^{\nu}} \gg \lambda \gg \frac{h_*}{V_0} \approx \Delta \approx \lambda\varepsilon_*. \quad (2.452)$$

Here, the values $L(\varepsilon_*) \approx \lambda/\varepsilon_*^{7/3}$ and $a(\varepsilon_*) = \lambda/\varepsilon_*^{4/3}$, which are responsible for the percolation behavior, are not infinitely large, since ε_* has a precise value. The fraction of the volume occupied by the percolation streamlines is now estimated as

$$P_\infty = \frac{L(\varepsilon)\Delta(\varepsilon)}{a(\varepsilon)^2} \approx \varepsilon_*^{4/3} \propto \frac{1}{a}. \quad (2.453)$$

This corresponds to the exponent $\beta = \nu$ [see (2.429)].

Besides the scaling laws (2.450), we can also obtain some additional information that is useful for the subsequent analysis. Let us note that in terms of the Peclet number the percolation regime is intermediate between the regime of convective cells from [80, 81] and the purely convective regime, where $D_{\text{eff}} \approx \lambda V_0$. We can estimate the range of the percolation scaling applicability in term of spatial scales. It is necessary to take into account the finite size L_0 of a real system. By analogy with (2.431) we can consider the estimate

$$a(\varepsilon_*) = \lambda Pe^{\nu/(\nu+3)} \leq L_0. \tag{2.454}$$

Then, calculations yield the inequality for the Peclet number in the form

$$1 < Pe < \left(\frac{L}{\lambda}\right)^{(\nu+3)/\nu}. \tag{2.455}$$

There is also a correlation meaning of percolation scaling. In the steady case the correlation time τ is described by the scaling law

$$\tau \approx \frac{L(\varepsilon)}{V_0} \approx \frac{\lambda}{V_0}\frac{1}{\varepsilon_*^{7/3}} \gg \frac{\lambda}{V_0}. \tag{2.456}$$

On the other hand, the correlation scale a can be represented in the form

$$a \approx \varepsilon_* L \approx \varepsilon_* V_0 \frac{\Delta^2}{D} \approx \varepsilon_* V_0 \tau_D \ll V_0 \tau_D. \tag{2.457}$$

From the formal point of view one can expect that there exists an additional spatial scale l_S,

$$\frac{L(\varepsilon) l_S}{\lambda^2} \approx 1. \tag{2.458}$$

Indeed, the scale

$$l_S(\varepsilon_*) \approx \frac{\lambda^2 \varepsilon_*}{a(\varepsilon_*)} \approx \lambda \varepsilon_*^{\nu+1} \approx \varepsilon_*^{\nu} \Delta(\varepsilon_*) \tag{2.459}$$

plays an important role in the analysis of the reconnection process [83]. This problem will be discussed in the next section. Now the entire spatial hierarchy of scales is given by

$$\lambda\left(\frac{a}{\lambda}\right)^{D_h} \approx L \approx \frac{a}{\varepsilon_*} \gg a \approx \frac{\lambda}{\varepsilon_*^{\nu}} \gg \lambda \gg \Delta \approx \lambda \varepsilon_* \gg l_S \approx \lambda \varepsilon_*^{\nu+1} \approx \varepsilon_*^{\nu} \Delta. \tag{2.460}$$

This gives wide possibilities to obtain new scalings in the framework of the percolation method.

2.14.3 Low Frequency Regimes

It is well known than the temporal reconstruction of a flow "topology" leads to considerable change in the transport in comparison with the quasi-linear one. The best illustration of this fact is the dependence of the effective diffusion coefficient on the Kubo number [3, 7, 8]. Following the ideas of [82], Grusinov, Isichenko, and Kalda [83] considered the percolation limit of the turbulent diffusion of a passive scalar in a time-dependent, incompressible, two-dimensional flow. In estimating the time it takes the flow pattern to change completely as $T_0 \approx 1/\omega$, the authors of [83] considered the low frequency case:

$$\omega \ll \frac{V_0}{\lambda} \quad \text{or} \quad \lambda \ll V_0 T_0. \tag{2.461}$$

In this formulation of the problem, the lifetime of the individual percolation streamline τ is the main parameter. The standard expression can be used for the diffusion coefficient,

$$D_C(\varepsilon) \approx \frac{a^2}{\tau}. \tag{2.462}$$

In the context of this problem the expression

$$\tau \approx \varepsilon \frac{1}{\omega} \approx \varepsilon T_0 \tag{2.463}$$

was used, where ε is the small parameter of the problem, which is analogous to that of [82]. In the time-dependent flow under consideration, one would expect a universal result, provided it is possible to calculate a specific "universal" value ε_*. For this purpose, the authors of [83] suggested a simple expression accounting for the convective nature of motion along the percolation streamline during the lifetime of this streamline:

$$\tau \approx \varepsilon \frac{1}{\omega} = \frac{L(\varepsilon)}{V_0}. \tag{2.464}$$

We see the analogy between this formula and formula (2.445). Using the scaling laws from percolation theory yields $a(\varepsilon) = \lambda \varepsilon^{-\nu}$, $L(\varepsilon) = \lambda (a/\lambda)^{D_h}$, $\nu = 4/3$, and $D_h = 1 + 1/\nu$. Now, we easily obtain $\varepsilon_* = h_*/\lambda V_0$ as a function of the flow parameters ω, V_0, λ,

$$\varepsilon_* = \left(\frac{\lambda\omega}{V_0}\right)^{1/(2+\nu)} = Ku^{-3/10} \propto \omega^{3/10}. \tag{2.465}$$

Here, it is relevant to introduce the Kubo number $Ku = V_0/\lambda\omega$ instead of the Peclet number, which was used for the analysis of a steady flow. From the standpoint of the renormalization of the initial small parameter $\varepsilon_0 \approx 1/Ku$ we obtain the expression

$$\varepsilon_* = (\varepsilon_0)^{1/(2+\nu)} \gg \varepsilon_0. \tag{2.466}$$

Upon direct substitution of the expression for ε_* into (2.462) we arrive at the formula

$$D_C(\varepsilon_*) \approx \frac{a(\varepsilon_*)^2}{\tau(\varepsilon_*)}. \tag{2.467}$$

Note that the dependence on T_0 appears quite odd:

$$D_C \propto T_0^{1/10} \approx \frac{1}{\omega^{1/10}}. \tag{2.468}$$

The slow "restructuring" of the flow is unlikely to result in a significant growth in turbulent diffusion. The reason lies in the fact that we have not taken into account the fraction P_∞ of percolation streamlines in the total flow,

$$P_\infty = \frac{L(\varepsilon)\Delta(\varepsilon)}{a(\varepsilon)^2}. \tag{2.469}$$

It is now evident that we need additional information on the value of $\Delta(\varepsilon)$, despite the fact that we have calculated ε_*. Unlike [82], we are forced to make an additional assumption here other than expression (2.464). The authors of [83] assumed $\Delta(\varepsilon)$, similarly to [82]. In fact, use is made of formulae (2.445) and (2.453):

$$\Delta \approx \varepsilon_* \lambda, \qquad P_\infty \approx \varepsilon_*^{4/3} \approx \frac{\lambda}{a(\varepsilon_*)}. \tag{2.470}$$

Calculations now lead to the final expression for D_{eff},

$$D_{\mathrm{eff}} = D_C(\varepsilon_*)P_\infty(\varepsilon_*) = \lambda V_0 \left(\frac{1}{Ku}\right)^{1/(\nu+2)} \propto V_0^{7/10}\omega^{3/10}. \tag{2.471}$$

The formula obtained reflects the universal character of percolation diffusion in the time-dependent flows, since the value ε_* depends only on the flow parameters ω, V_0, λ.

2.15 The Temporal Hierarchy of Scales and Correlations

The consideration of the temporal hierarchy of scales of a percolation model allows one to establish the bounds of applicability of the results obtained in the previous section. Besides that, we will consider the method to obtain percolation transport estimates that is based on the correlation scales balance, which makes it possible both to reproduce known results and to obtain new scalings.

2.15.1 The Spatial and Temporal Hierarchy of Scales

Assuming small percolation parameters implies that $\varepsilon_* < 1$ and, at the same time, it is important to take into account the finite size of the system $a(\varepsilon_*) \le L_0$. From this point of view we can find the inequality for the Kubo number, which describes the time-dependent percolation,

$$1 < Ku < \left(\frac{L}{\lambda}\right)^{(\nu+2)/\nu}. \tag{2.472}$$

In the context of the definition of the Kubo number we noted that in low-frequency regimes the real correlation scale Δ_{cor} is less than the frequency path $l_\omega = V_0/\omega$. Indeed, the scaling (2.464) reflects the correlation meaning of the problem since

$$\Delta_{\text{cor}} \approx a \approx \varepsilon_* L \approx \varepsilon_*^2 l_\omega \ll l_\omega. \tag{2.473}$$

Note that the condition $a \approx \varepsilon_* l_\omega$ leads to the renormalization $\tau_B \approx T_0 \approx 1/\omega$.

On the other hand, additional estimates should be made of the effect of the diffusion escape of particles from the streamlines. In fact, it is necessary to calculate the time of the escape of particles from the streamlines τ_D. The formulae of [83] were obtained in the framework of the condition $\tau < \tau_D$. To receive estimates, we make use of the diffusion coefficient of streamlines D_ψ and relate it to the coefficient of "seed" diffusion D_0,

$$\tau_D \approx \frac{h^2}{D_\psi}, \quad D_\psi = V_0^2 D_0. \tag{2.474}$$

The applicability condition for the results [83] takes the form

$$\frac{h}{\lambda V_0 \omega} < \frac{h^2}{V_0^2 D_0}. \tag{2.475}$$

This is in fact a limitation on the value of the "seed" diffusion coefficient D_0,

$$D_0 < h\omega(h)\frac{\lambda}{V_0} < h^{\nu+3}. \tag{2.476}$$

To conclude the discussion of this issue, we give the hierarchy of characteristic times in the problem on percolation in a time-dependent flow,

$$\frac{1}{\omega}\left(\frac{h}{\lambda V_0}\right)^{1+\nu} = \tau_S \ll \tau \approx \frac{h}{\omega\lambda V_0} \ll \frac{h^2}{D_0 V_0^2} \approx \tau_D \ll \frac{1}{\omega} \approx T_0. \tag{2.477}$$

Here, $\tau_S = l_S/V_0$ is the characteristic time that describes the stochastic instability of streamlines [83]. This means that one deals with the temporal interval $\tau_S \ll \tau < \tau_D$. In a similar manner to the above-considered hierarchy of scales in steady percolation (2.460), this set of characteristic times (2.477) allows us to distinguish the regimes of flow, where the "long-range" correlation effects become the principal ones. The interpretation of renormalization conditions in terms of the characteristic time is a very important aspect of the problem. For example, the condition for the steady case (2.445) can be represented in the form of an equilibrium of the ballistic and diffusive times:

$$\tau \approx \frac{L(\varepsilon_*)}{V_0} \approx \frac{\Delta^2(\varepsilon_*)}{D_0}. \tag{2.478}$$

It is easy to note that there are several characteristic times that do not play essential roles at this stage:

$$\frac{h}{\omega L(h) V_0} \ll \frac{h}{\omega a(h) V_0} \ll \tau. \tag{2.479}$$

2.15.2 The Isichenko Intermediate Regime

Isichenko [17] considered the intermediate regime with the motion of particles along the percolation streamline during the times $t < \tau_B \approx L/V_0$, which is analogous to the fractal diffusion (this case differs significantly from the percolation model of turbulent diffusion with $t \geq \tau_B$). The author of [17] used the estimate of the correlation scale in the form

$$a_I(t) \approx \lambda \left(\frac{L(t)}{\lambda} \right)^{1/D_h} \approx \lambda \left(\frac{V_0 t}{\lambda} \right)^{1/D_h}. \tag{2.480}$$

Here, the supposition was made that the test particle path at this stage is approximately ballistic, $L(t) \approx V_0 t$. To describe the initial stage of percolation $t < \tau_B \approx L/V_0$ in the two-dimensional random flow the authors of [17] offered the expression

$$R^2 \approx D_{\text{eff}} t \approx a^2 P_\infty \approx \lambda a \approx \lambda^2 \left(\frac{L}{\lambda} \right)^{1/D_h} \approx \lambda^2 \left(\frac{V_0 t}{\lambda} \right)^{1/D_h}. \tag{2.481}$$

Here $D_h = 1 + \frac{1}{\nu}$ and $\nu = 4/3$, and R is the mean free path of the particle. This leads to the new subdiffusive regime

$$R \propto t^{1/2D_h} = t^{2/7} \tag{2.482}$$

with the Hurst exponent

$$H = \frac{1}{2D_h} = 2/7. \tag{2.483}$$

This corresponds to the subdiffusion character and reflects the initial period when the particle moved along the fractal streamline.

The model of the evolution of correlation scale $a_I(t)$ suggested by Isichenko can be used to interpret and to analyze other percolation regimes [149]. Thus, simultaneously with the increase in the correlation scale $a_I(t) \approx (L(t)/\lambda)^{1/D_h}$, it is necessary to take into account the increase in the stochastic layer width $\Delta = \Delta(t)$ which, in the framework of percolation models of turbulent diffusion, is closely related to the value of the small parameter $\varepsilon_* \approx \Delta/\lambda$, and hence to the definition of the correlation scale $a \approx \lambda/\varepsilon^\nu$. Easy calculations allow one to obtain the expression describing the increase in the correlation scale $a_D(t)$ due to the increase in the stochastic layer width

$$a_D(t) \approx \frac{\lambda}{(\Delta(t)/\lambda)^\nu}. \tag{2.484}$$

In the framework of mean field theory the consideration of the balance between $a_D(t)$ and $a_I(t)$ makes it possible to find the estimate of the characteristic time t_0, which has to be used to define the effective diffusion coefficient D_{eff}. Thus, in the case of the diffusive character of increasing the stochastic layer width $\Delta^2 \approx D_0 t$, one obtains

$$\lambda \left(\frac{V_0 t_0}{\lambda} \right)^{1/D_h} \approx \frac{\lambda}{(\sqrt{D_0 t_0}/\lambda)^\nu}. \tag{2.485}$$

Calculations lead to the estimate

$$t_0 \approx \frac{\lambda^2}{D_0}\left(\frac{1}{Pe}\right)^{1/(\gamma+3)} = \frac{\lambda^2}{D_0}\left(\frac{D_0}{\lambda V_0}\right)^{1/(\gamma+3)}, \tag{2.486}$$

which after substitution into the formula for the stochastic layer width yields

$$\Delta \approx (D_0 t_0)^{\frac{1}{2}} \approx \lambda\left(\frac{1}{Pe}\right)^{1/(\gamma+3)}. \tag{2.487}$$

It is easy to see that this expression coincides exactly with the expression for the steady case (2.449) and the corresponding estimate of the effective diffusion coefficient is given by the formula $D_{\text{eff}} \approx V_0\Delta$. Naturally, other estimates can also be used to describe the growth of the stochastic layer width. Thus, in dynamical system theory the linear estimate $\Delta \propto t$ is widely used. In the context of the description of time-dependence effects it is easy to represent this expression in the form

$$\Delta(t) = (\lambda\omega)t, \tag{2.488}$$

where ω is the characteristic frequency. Then the consideration of the correlation scales balance in the form

$$\lambda\left(\frac{V_0 t_0}{\lambda}\right)^{1/D_h} \approx \frac{\lambda}{(\omega t_0)^{\nu}} \tag{2.489}$$

allows the estimate of the characteristic time t_0 to be obtained:

$$t_0 \approx \frac{1}{\omega}\left(\frac{\lambda\omega}{V_0}\right)^{1/(\nu+2)} \approx \frac{1}{\omega}\left(\frac{1}{Ku}\right)^{1/(\nu+2)}. \tag{2.490}$$

The expression for the stochastic layer width then takes the form corresponding to the percolation model (2.465)

$$\Delta = \lambda\varepsilon_* = \lambda\left(\frac{1}{Ku}\right)^{1/(\nu+2)}, \tag{2.491}$$

and hence the estimate of the turbulent diffusion coefficient is given by expression (2.471). Note that the approach under consideration makes it possible to use the correlation scales balance as the basis for constructing new percolation transport models based on approximations $\Delta(t)$.

2.15.3 Dissipation and Percolation Transport

In this section, we consider the influence of weak dissipative effects on the percolation layer width. The presence of even small dissipation can considerably change the character of streamlines behavior [17, 149]. It is possible to introduce the rate of energy dissipation ε_K by analogy with isotropic turbulence theory [27, 30], $\varepsilon_K =$

$[m^2/c^3] = \text{const}$. Note that in the framework of such an approach even a simple dimensional estimate of the characteristic time $\tau_K \approx (\varepsilon_K k^2)^{-1/3}$ together with the Fourier representation of the Einstein–Smolukhowski nonlocal functional yields the classical Richardson law [62] for the relative diffusivity: $R^2 \propto t^3$. Here, k is the wave number.

In the percolation case under consideration, the weak dissipation leads to an increase in the stochastic layer width. We can estimate this at the initial stage of the percolation process by the linear dimensional expression

$$\Delta \approx V_* t \approx \lambda \left(\frac{\varepsilon_K}{\lambda^2} \right)^{1/3} t. \tag{2.492}$$

Here, $V_* \approx \delta/\tau_K$ characterizes the rate of growth of the stochastic layer width and δ is the spatial dissipative scale. Formally, the value δ can be considered as an independent parameter. However, in the framework of the hierarchy of spatial scales, which corresponds to the percolation model

$$\Delta \approx \lambda\varepsilon \ll \lambda \ll a \approx \frac{\lambda}{\varepsilon^{\nu}} \ll L \approx \frac{a}{\varepsilon}, \tag{2.493}$$

the estimate $\delta \approx \Delta$ is fairly adequate for the weak dissipation since Δ is the least among spatial scales. Then simple calculations yield

$$\Delta \approx \lambda \left(\frac{\varepsilon_K}{\lambda^2} \right)^{1/5} t^{3/5}. \tag{2.494}$$

At the initial stage we deal with two competing processes: an increase in the correlation scale a due to growth of the distance passed by the test particle, and a decrease in the correlation scale due to dissipative effects. Indeed, in the case under consideration the dissipation leads to an increase in the stochastic (percolation) layer width $\Delta(t)$ and hence to the decrease of the correlation scale:

$$a_D(t) \approx \lambda \left(\frac{\Delta(t)}{\lambda} \right)^{-\nu} \approx \lambda \left(\frac{\lambda}{\lambda(\varepsilon_K/\lambda^2)^{1/5} t^{3/5}} \right)^{\nu}. \tag{2.495}$$

On the other hand, it is also necessary to take into account the increasing correlation scale a due to the percolation character of streamlines

$$a_I(t) \approx \lambda \left(\frac{L(t)}{\lambda} \right)^{1/D_h} \approx \lambda \left(\frac{V_0 t}{\lambda} \right)^{1/D_h}. \tag{2.496}$$

Here, the supposition was made that the test particle path at this stage is approximately ballistic, $L(t) \approx V_0 t$.

In the framework of scaling arguments we consider the balance between these processes as the balance of the correlation scales $a_I(t_0) \approx a_D(t_0) \approx a$,

$$\left(\frac{\lambda}{\lambda(\varepsilon_K/\lambda^2)^{1/5} t_0^{3/5}} \right)^{\nu} \approx \left(\frac{V_0 t_0}{\lambda} \right)^{1/D_h}. \tag{2.497}$$

Here, t_0 is the mean field estimate of the characteristic time that corresponds to the correlation scale balance. The solution of this equation yields

$$t_0 \approx \left(\frac{\lambda}{V_0}\right)^{5/12} \left(\frac{\lambda^2}{\varepsilon_K}\right)^{7/36}. \tag{2.498}$$

This expression allows us to define the small percolation parameter that characterizes the analyzed model based on approximation (2.445) of the stochastic layer width,

$$\varepsilon = \frac{\Delta}{\lambda} \approx \left(\frac{(\varepsilon_K^{\lambda})^{1/3}}{V_0}\right)^{1/4}. \tag{2.499}$$

Now, one can obtain the scaling for the percolation layer width:

$$\Delta(t) \approx \left(\frac{\varepsilon_K}{\lambda^2}\right)^{1/5} t_0^{3/5} \approx \lambda \left(\frac{U}{V_0}\right)^{1/4}. \tag{2.500}$$

Here, $U = (\varepsilon_K \lambda)^{1/3}$ is the dimensional estimate of the characteristic velocity that is related to dissipative effects. Note that the very small percolation parameter $\varepsilon = \varepsilon_0^{1/4} = ((\varepsilon_K \lambda)^{1/3}/V_0)^{1/4}$ differs from the initial dimensionless parameter $\varepsilon_0 = U/V_0 = (\varepsilon_K \lambda)^{1/3}/V_0$.

In the framework of the percolation approach, the expression for effective diffusivity has the form (2.450) $D_{\text{eff}} \approx V_0 \Delta(\varepsilon)$, which mirrors the key role of the stochastic layer width Δ. The expression for the effective diffusivity takes the form

$$D_{\text{eff}} \approx V_0 \Delta(\varepsilon) \approx V_0 \lambda \left(\frac{(\varepsilon_K \lambda)^{1/3}}{V_0}\right)^{1/4} \propto V_0^{3/4} \varepsilon_K^{1/12}. \tag{2.501}$$

Note that such a form is true only for the small values of the parameter $\varepsilon_0 = U/V_0 = (\varepsilon_K \lambda)^{1/3}/V_0$. On the other hand, it is necessary to take into account that correlation size is limited by the sample size

$$a(\varepsilon) < L_0. \tag{2.502}$$

Here, L_0 is the characteristic external size of the system. We, in fact, obtain the condition

$$\left(\frac{\lambda}{L_0}\right)^{1/\nu} < \varepsilon = \left(\frac{(\varepsilon_K \lambda)^{1/3}}{V_0}\right)^{1/4} \ll 1. \tag{2.503}$$

In relation to the consideration of the correlation scales balance method, it is interesting to observe the dynamics of growth of two-dimensional small-scale structures $\lambda(t)$ near the percolation threshold. Computer simulations of turbulent flows often need in obtaining a scaling describing small-scale structure evolution. Formally, we can write the following expressions:

$$\lambda(t) \approx \varepsilon^{\nu} a(t), \tag{2.504}$$

$$L(t) \approx \lambda \left(\frac{a(t)}{\lambda} \right)^{D_h} \approx V_0 t. \tag{2.505}$$

Then, simple calculations yield

$$\lambda(t) \approx \varepsilon_*^{\nu} a(t) \approx \varepsilon_*(\lambda)^{\nu} (V_0 t)^{1/D_h}, \tag{2.506}$$

where ε_* is the renormalized percolation parameter, which could be taken from known percolation models. For instance, in the presence of seed diffusivity,

$$\varepsilon \approx \left(\frac{1}{Pe} \right)^{\frac{1}{\nu+3}} \propto \left(\frac{1}{\lambda} \right)^{\frac{1}{\nu+3}}. \tag{2.507}$$

After substitution one obtains

$$\lambda \approx \left(V_0^2 D_0^{\nu+1} \right)^{\frac{1}{2\nu+4}} t^{\frac{\nu+3}{2\nu+4}} \propto t^{13/20} \approx t^{0.65}, \tag{2.508}$$

where $\nu = 4/3$ was used, and the correlation scale $a(\varepsilon)$ is much less than the particle diffusive path

$$a \approx \varepsilon^3 V_0 \tau_D. \tag{2.509}$$

Formula (2.508) leads to the simplest percolation estimate of the growth of the characteristic scale of small structures in the system under analysis. Similar regimes were obtained by simulations of astrophysical turbulence, where the value of the exponent describing structure evolution was found to be 0.7 [103].

2.16 The Stochastic Magnetic Field and Percolation Transport

The results obtained in the framework of the time-dependent percolation model are expressed in terms of the Kubo number. This makes it possible to use percolation scalings to describe stochastic magnetic fields, since there exists a direct analogy between the Kubo number and the magnetic Kubo number that is responsible for correlation effects in a "braided" magnetic field.

2.16.1 The Stochastic Magnetic Field and Percolation Transport

We have considered the percolation approach from the simplest models that allow us to obtain the diffusion coefficient of magnetic streamlines D_m. The percolation model was suggested in order to describe cases with

$$R_m \approx \frac{b_0 L_Z}{\Delta_\perp} > 1. \tag{2.510}$$

Here, the value R_m is analogous to the Kubo number $Ku = V_0 T_0 / \lambda$. Therefore, we can use the result of the time-dependent percolation case to analyze a "braided" magnetic field. Isichenko [150, 151] applied this analogy directly. He rewrote the expression for D_m in the form (2.471)

$$D_m = b_0 \Delta_\perp R_m^{-1/(\nu+2)}. \tag{2.511}$$

Here, the value of the relative amplitude of the stochastic magnetic field b_0 is used instead of the velocity V_0, $\Delta_\perp$ corresponds to the spatial scale λ, and the value L_Z that enters into quasi-linear expression (2.239) corresponds to T_0 that was used in defining the Kubo number $Ku = V_0 T_0/\lambda$. Many authors have carried out numerical simulations [152–154] which allow us to consider that the analytical result (for the monoscale model with the exponent 7/10) $D_m \propto b_0^{7/10}$ is in qualitative agreement with the simulation results 0.6–0.8.

Isichenko [150, 151] also suggested using the percolation method to describe the particle transverse transport in a stochastic magnetic field. Earlier, we considered the interpretation of the flow parameters V_0, λ, T_0. In order to obtain the complete pattern it is necessary to interpret the values

$$a(\varepsilon) = \lambda|\varepsilon|^{-\nu}, \qquad L(\varepsilon) = \lambda\left(\frac{a}{\lambda}\right)^{D_h}, \qquad \Delta \approx \lambda\varepsilon. \tag{2.512}$$

To retain the physical meaning of these values we assume that the length of the percolation streamline on the plane, which is perpendicular to the magnetic field, can be estimated in the form $L \approx b_0 z$. Here, z is the distance traversed along the force line. We will consider the value $\Delta_b \approx \varepsilon\Delta_\perp$ as a width of the stochastic layer Δ, which is responsible for the particle percolation transport. The correlation (percolation) scale $a(\varepsilon)$ characterizes the transport properties of the system in the transverse direction in accordance with the expressions considered above. Then, in terms of magnetic diffusion we can obtain the expression for the particle transverse transport:

$$D_{\text{eff}} \approx D_m \frac{z(\tau)}{\tau} \approx b_0 \Delta_\perp R_m^{-1/(\nu+2)} \frac{z(\tau)}{\tau}. \tag{2.513}$$

Here, τ is the correlation time. This expression implies that $b_0 z(\tau) > a$.

Another important case is "ballistic" transport under the conditions when $b_0 z(\tau) < \Delta_\perp$. For the same conditions the author of [150, 151] considered the estimate [see the "fluid limit" (2.241)]

$$D_{\text{eff}} \approx b_0^2 \frac{z(\tau)^2}{\tau}. \tag{2.514}$$

There also exists an intermediate regime that corresponds to the "initial" stage of the motion along the percolation streamline (2.480) when $a > L \approx b_0 z > \Delta_\perp$. Here, it is convenient to use the running correlation scale $a_0(\tau)$,

$$a_0 \approx \Delta_\perp \left(\frac{L}{\Delta_\perp}\right)^{1/D_h} \approx \Delta_\perp \left(\frac{b_0 z(\tau)}{\Delta_\perp}\right)^{1/D_h}, \tag{2.515}$$

as a parameter of the problem. This corresponds to the intermediate regime (2.482) in the time-dependent model. This estimate is correct if $a_0(t) < a(\varepsilon_*) \approx \Delta_\perp R_m^{\nu/(\nu+2)}$.

We can easily calculate the boundary value to be

$$z_m \approx \frac{\Delta_\perp}{b_0} R_m^{D_h \nu/(\nu+2)}. \tag{2.516}$$

Then, applying the results obtained earlier one can obtain

$$D_{\text{eff}} \approx \frac{a_0^2}{\tau} P_\infty(a_0). \tag{2.517}$$

In the case under consideration the full hierarchy of spatial scales can be presented in the form

$$\begin{aligned} \Delta_b(\varepsilon) &\approx \Delta_\perp R_m^{-1/(\nu+2)} < b_0 z \le \Delta_\perp < \Delta_\perp \left(\frac{b_0 z_m}{\Delta_\perp}\right)^{1/D_h} \\ &\le \Delta_\perp R_m^{\nu/(\nu+2)} \approx a(\varepsilon_*). \end{aligned} \tag{2.518}$$

Here, the appearance of "intermediate" scales is related to the ballistic character of the estimate of the transverse displacement $L \approx b_0 z$.

Isichenko [150, 151] suggested the consideration of two mechanisms of motions along the z-axis related to a magnetic force line. The diffusion mechanism is

$$z \approx \sqrt{D_\parallel t} \quad \text{for } t > \tau_{\text{coll}}. \tag{2.519}$$

The ballistic (kinetic) mechanism corresponds to the expression

$$z = V_0 t \quad \text{for } t < \tau_{\text{coll}}. \tag{2.520}$$

To define the correlation times τ the author of [150, 151] used several models considered earlier: the percolation estimate $\tau \approx \varepsilon T_0$; the Kadomtsev–Pogutse estimate $\tau \approx \Delta_b^2/D_\perp$; and the correlation time that corresponds to the Rechester–Rosenbluth model with $L_{\text{cor}} \approx \sqrt{D_\parallel \tau}$.

A good example of the efficiency of the suggested approach is the possibility of obtaining characteristic transport regimes. Thus, the use of diffusive and ballistic expressions in the formula for D_{eff} (2.514) leads to the fluid limit $D_{\text{eff}} \approx b_0^2 D_\parallel$. On the other hand, the collisionless result $D_m V_0$ can be obtained by the substitution of the ballistic expression into the formula for D_{eff} (2.513). It is obvious that many possible combinations lead to a large variety of regimes. The author of [150, 151] considered in detail all the possible situations and the corresponding graphs are shown.

2.16.2 Percolation and the Kadomtsev–Pogutse Scaling

It is possible to consider percolation effects in the stochastic magnetic field in the context of the well-known Kadomtsev–Pogutse scaling (2.358). The model suggested in [67] is based on the assumption of the presence of a strong longitudinal magnetic field. For these conditions the longitudinal diffusion coefficient is much greater than the transverse diffusion coefficient $D_{\|} > D_{\perp}$ and the choice of the value $\varepsilon_0 = D_{\perp}/D_{\|}$ as an initial small parameter is fairly natural. The renormalization condition, which allows the true small parameter to be obtained, has to mirror the competition between the longitudinal and transverse decorrelation mechanisms.

Isichenko [150, 151] suggested reformulating the particle balance condition in the stochastic layer (2.331), (2.332) with allowance for the diffusion character of longitudinal motions:

$$D_{\perp} \frac{n}{\Delta} L \approx D_{\|} \frac{n}{L} \Delta. \tag{2.521}$$

Here, n is the particle number density, $L = L(\varepsilon)$ is the length of the fractal streamline, and $\Delta = \Delta(\varepsilon)$ is the width of the stochastic layer. We can rewrite this condition in terms of the equivalence of decorrelation times, by analogy with the convective cells case:

$$\tau \approx \frac{L(\varepsilon)^2}{D_{\|}} \approx \frac{\Delta(\varepsilon)^2}{D_{\perp}}. \tag{2.522}$$

Equations (2.521) and (2.522) are the conditions to determine the small parameter of the percolation problem:

$$\varepsilon_* = \varepsilon_*(\varepsilon_0) = \varepsilon_*\left(\frac{D_{\perp}}{D_{\|}}\right). \tag{2.523}$$

To solve these equations we have to find the value $\Delta(\varepsilon)$. However, the result of interest to us can be obtained from the formal definition of the value D_{eff} (2.443):

$$D_{\mathrm{eff}} \approx \frac{a^2}{\tau} \frac{L\Delta}{a^2} \approx \frac{L\Delta}{\tau}. \tag{2.524}$$

It is easy to see that in our case

$$D_{\mathrm{eff}} \approx \frac{\Delta}{L} D_{\|} \approx \frac{L}{\Delta} D_{\perp} \approx \sqrt{D_{\|} D_{\perp}}, \tag{2.525}$$

where $\Delta/L \approx \sqrt{D_{\perp}/D_{\|}}$. Using the percolation expression for $L(\varepsilon)$ and conjecture $\Delta = \varepsilon\lambda$, one can obtain the expression for the correlation scale:

$$a = \lambda \left(\frac{D_{\|}}{D_{\perp}}\right)^{\nu/(2\nu+4)}. \tag{2.526}$$

Hence, the percolation interpretation of the Kadomtsev–Pogutse scaling is related to the renormalization of the initial small parameter in the following form:

$$\varepsilon_* = \varepsilon_0^{1/(2\nu+4)}. \tag{2.527}$$

Now it is possible to express all the values by means of the small parameter ε_0 and the percolation exponent ν.

Obviously, the percolation interpretation for scaling (2.358) is not necessary. However, the calculations point out the possibilities that exist for the generalization of both the renormalization condition and the alteration of the small parameter ε_0.

2.16.3 Percolation Renormalization and the Stochastic Instability Increment

The consideration of time-dependent two-dimensional random flow is of particular interest because there is no exponential separation of initially nearby streamlines in the steady case in a bounded two-dimensional area. Actually, in the steady case we deal with the Hamiltonian one-dimensional problem, and only in the case $\omega \neq 0$ is there the possibility to investigate stochastic behavior, since the time-dependence adds a degree of freedom. The percolation approach to the consideration of the hierarchy of spatial and temporal scales allows us to treat long-range correlation effects in terms of simple scalings. One of the important problems here is to obtain estimates of the stochastic instability increment. In the framework of the mono-scale approach, the scaling for the stochastic instability increment was obtained in the paper by Grusinov, Isichenko, and Kalda [83]. Analyzing the spatial scales hierarchy in a two-dimensional random time-dependent velocity field, the authors of [83] estimated the square corresponding to the stochastic layer Δ as

$$L(\varepsilon_*)\Delta(\varepsilon_*) \approx a(\varepsilon_*)\lambda\varepsilon_*/\varepsilon_* \approx a\lambda \gg \lambda^2. \tag{2.528}$$

Naturally, this is because there are many streamlines in the stochastic layer. At the same time, this means that there exists a spatial scale l_S that characterizes a single streamline. Indeed, a possible estimate of l_S is the expression [40]

$$l_S(\varepsilon) \approx \frac{\lambda^2}{L(\varepsilon)} \approx \lambda\varepsilon^{\nu+1} \approx \varepsilon\Delta \ll \Delta \approx \lambda\varepsilon. \tag{2.529}$$

The characteristic reconnection time of a pair of nearby separatrixes can be estimated as

$$\gamma_S \approx \frac{1}{\tau_S(\varepsilon)} \approx \frac{V_S}{l_S(\varepsilon)} \approx \frac{\lambda\omega}{l_S(\varepsilon)} \approx \frac{L(\varepsilon)\omega}{\lambda}, \tag{2.530}$$

where $V_S = \lambda\omega$ is the dimensional estimate of velocity of separatrix motion. On the other hand, the balance of characteristic times $\tau_S \approx \tau_B$, which has the form

$$\tau_S = \frac{\lambda}{L(\varepsilon_*)\omega} \approx \frac{L(\varepsilon_*)}{V_0} = \tau_B, \tag{2.531}$$

allows the small percolation parameter ε_* to be defined:

$$\varepsilon_* \approx \left(\frac{\lambda\omega}{V_0}\right)^{\frac{1}{2(\nu+1)}} \approx \left(\frac{1}{Ku}\right)^{\frac{1}{2(\nu+1)}} \approx \left(\frac{1}{Ku}\right)^{\frac{3}{14}}, \quad \text{where } \nu = 4/3. \tag{2.532}$$

The final expression for the stochastic instability increment γ_S then takes the following form:

$$\gamma_S \approx \frac{1}{\tau_S} \approx \omega\frac{L(\varepsilon_*)}{\lambda} \approx \omega\sqrt{Ku}. \tag{2.533}$$

It is easy to take into consideration here the logarithmic factor, which leads to the result

$$\gamma_S \approx \omega\sqrt{Ku}/\ln Ku \quad \text{for } Ku > 1. \tag{2.534}$$

Since the Kubo number Ku can be easily interpreted in terms of the magnetic Kubo number $R_m \approx b_0 L_0/\Delta_\perp$, it is interesting to compare the obtained expression with the Kadomtsev–Pogutse result [67], $\gamma_Z \approx R_m^2/L_Z$ for the quasi-linear case. We see that the stochastic instability increment in the percolation case (long-range correlations) is characterized by smooth scaling, which is analogous to the dependence of the effective diffusion coefficient on the Kubo number.

2.17 Percolation in Drift Flows

Drift effects play an important role in turbulence. Even a small drift velocity can significantly change the character of turbulent transport. In this section, we consider both the steady and time-dependent models of drift effects in terms of the renormalization of the small percolation parameter.

2.17.1 Graded Percolation and Drift Flows

The problem of the influence of the small external perturbation on the percolation system has been considered in terms of the graded approach [147]. Yushmanov [84] analyzed the influence of a small drift velocity U_d on the fractal topology of streamlines (see Fig. 2.11) in the framework of the Trugman theory:

$$V = V_0 + U_d, \quad U_d \ll V_0. \tag{2.535}$$

Here, V_0 is the mean flow velocity. Zeldovich [155] has already formulated this problem, but at that time the renormalization methods had not yet been developed. The simplest way to alter the small parameter is by using the value

$$\varepsilon_0 = \frac{U_d}{V_0}. \tag{2.536}$$

However, in this approach the fractal character of percolation streamlines is completely lost. Yushmanov suggested the use of the following dimensional estimate of

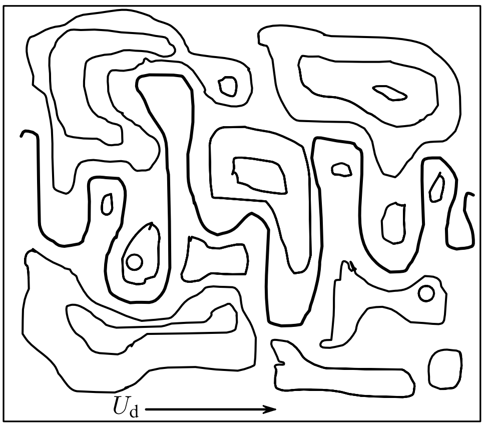

Fig. 2.11. Disconnected streamline and drift flow

the drift velocity:

$$U_d = \frac{a(\varepsilon)}{\tau(\varepsilon)} P_\infty(a), \quad a(\varepsilon) \approx \lambda|\varepsilon|^{-\nu}, \; \tau(\varepsilon) \approx \frac{L(\varepsilon)}{V_0}. \tag{2.537}$$

For P_∞ he used an additional expression, which was suggested in the steady case, $P_\infty \approx \lambda/a$. Simple calculations allow us to obtain the parametric dependence for the renormalized small parameter ε_* on the flow parameters V_0 and U_d,

$$\varepsilon_* = \left(\frac{U_d}{V_0}\right)^{1/(1+\nu)}, \tag{2.538}$$

where $\nu = 4/3$. It is easy to see that this expression completely coincides with the Trugman result (2.439) and can be interpreted in terms of the streamline function,

$$U_d \approx \frac{\Psi_1}{a(\varepsilon)} \approx \frac{\varepsilon \Psi_0}{a(\varepsilon)}. \tag{2.539}$$

Here, we are dealing with the conditions

$$\Psi_1 \ll \Psi_0 \approx \lambda V_0 \quad \text{and} \quad a(\varepsilon) \gg \lambda. \tag{2.540}$$

One obtains an estimate that is related to the finite size of a system $a(\varepsilon_*) \leq L_0$: $V_0(\lambda/L_0)^{(\nu+1)/\nu} < U_d < V_0$. Moreover, we can note how the spatial hierarchy of scales is included in the description of perturbations [156]:

$$U_d \approx \varepsilon \frac{\lambda}{a(\varepsilon)} V_0 \approx \frac{\lambda}{L(\varepsilon)} V_0 \approx \frac{\Delta}{a(\varepsilon)} V_0. \tag{2.541}$$

We see that parameter λ does not enter into the expression for the renormalized value ε_*. It is possible to determine some velocity U, which will be much less than U_d:

$$U \approx \frac{\Delta}{L(\varepsilon)} V_0 \ll U_d \ll V_0. \tag{2.542}$$

This problem will be considered below in connection with the study of compressibility effects.

There are also alternative possibilities for the renormalization. For example, we can consider the following expression:

$$U_d = \varepsilon \frac{a(\varepsilon)}{\tau(\varepsilon)} = \frac{\varepsilon a(\varepsilon)}{L(\varepsilon)} V_0. \tag{2.543}$$

This case corresponds to setting $P_\infty(\varepsilon) \approx \varepsilon$ [compare with (2.453)]. However, in contrast to the Yushmanov case, these estimates lead to the expression $U_d \approx \varepsilon^2 V_0$, which does not contain the percolation exponent ν. Undoubtedly, this is an important drawback. Therefore, taking into account the transport effects, we will follow the Trugman renormalization (2.439).

Formally applying the results of the previous sections we can obtain the estimate of the diffusion coefficient in terms of the stochastic layer width $\Delta \approx \lambda\varepsilon_*$:

$$D_{\text{eff}} \approx V_0 \Delta(\varepsilon_*) \approx \lambda V_0 (\varepsilon_0)^{1/(1+\nu)} \approx \lambda V_0 \left(\frac{U_d}{V_0}\right)^{3/7} \propto V_0^{4/7}. \tag{2.544}$$

A more complex situation arises when both the drift effects and the time-dependence characterized by the time $T_0 \approx 1/\omega$ exist simultaneously in a system.

2.17.2 Low Frequency Regimes and Drift Effects

The analysis of drift effects on the basis of Trugman's renormalization does not take into account processes related to the temporal fluctuations of the velocity field. Moreover, in the framework of the "graded" approach (2.539) the correlation time τ plays a formal role because to define the effective diffusion coefficient $D_{\text{eff}} = V_0\Delta$, the conjecture $\Delta = \lambda\varepsilon_*$ is usually used. Nevertheless, the scaling approach allows us to consider percolation transport in the presence of both drift effects and fluctuations. The main parameter that characterizes the temporal dependence of the stream function is the characteristic time:

$$\tau_D \approx \frac{\Psi}{\partial\Psi/\partial t}. \tag{2.545}$$

The percolation character of transport is manifested in the estimate $\Psi \approx \varepsilon_*\Psi_0 \approx \varepsilon_* V_0 \lambda$. Here, ε_* is the small parameter of the percolation model. On the other hand, it is necessary to take into account the "graded" character of perturbations (2.539),

$$\Delta\Psi \approx U_d a(\varepsilon_*), \quad \varepsilon_* = \varepsilon_0^{1/(1+\nu)}. \tag{2.546}$$

Then, estimates yield:

$$\frac{\partial\Psi}{\partial t} \approx U_d a(\varepsilon_*)\omega. \tag{2.547}$$

Here, U_d is the drift velocity, a is the correlation scale, and ω is the characteristic frequency of the stream function alteration. Calculations yield

$$\tau = \frac{1}{\omega}\varepsilon_0^{\nu/(1+\nu)}. \tag{2.548}$$

Yushmanov [84] suggested using the simplest quasi-linear dependence $\tau(\omega) \approx 1/\omega$ to represent the effective diffusion coefficient (2.428):

$$D_{\text{eff}} \approx P_\infty \frac{a^2}{\tau} \approx U_d^2 \tau \frac{a(\varepsilon_*)}{\lambda}. \tag{2.549}$$

Here, $P_\infty \approx \lambda/a(\varepsilon_*) \ll 1$, which corresponds to the drift model [84] and $\varepsilon_* = (U_d/V_0)^{1/(1+\nu)}$, which corresponds to the Trugman approach. Upon substituting the expression for $\tau = 1/\omega$ into (2.549), we obtain the scaling

$$D_{\text{eff}} \approx \frac{U_d^2}{\omega}\left(\frac{1}{\varepsilon_0}\right)^{\nu/(1+\nu)} \approx \frac{U_d^2}{\omega}\left(\frac{V_0}{U_d}\right)^{4/7} \propto U_d^{10/7}. \tag{2.550}$$

This dependence shows that there is an essential difference between transport in the presence of velocity field fluctuations and the steady case (2.544). However, the method of calculating the effective diffusion coefficient D_{eff}, which was suggested by Yushmanov, only corrects the percolation expression (2.549), whereas the correct method would be to include the frequency ω into the renormalization condition that characterizes transport in the drift flow in the presence of the time-dependent perturbation of the stream function. Thus, in the steady case [82] the balance of characteristic times was the main condition for the renormalization

$$\tau \approx \frac{\Delta(\varepsilon)^2}{D_0} \approx \frac{L(\varepsilon)}{V_0}. \tag{2.551}$$

In considering the fluctuations of the stream function, the diffusion estimate of the characteristic time is given by (2.474)

$$\tau_D \approx \frac{h^2}{D_\Psi} \approx \frac{(\varepsilon\lambda V_0)^2}{D_\Psi}, \quad \text{where } D_\Psi \approx V_0^2 D_0. \tag{2.552}$$

However, in considering the drift effects we will use the correlation estimate [84] $\Delta\Psi \approx U_d a(\varepsilon_*)$. The important aspect is that the streamline diffusivity D_Ψ is responsible for the physical mechanism of the distortion of streamlines. Let us approximate the value D_Ψ in the form that mirrors the certain character of the external influences (drift flow and time dependent perturbation):

$$D_\Psi \approx (\Delta\Psi)^2\omega \approx U_d^2 a(\varepsilon)^2\omega. \tag{2.553}$$

The new equation for the small percolation parameter ε_* takes the form [157]

$$\frac{(\varepsilon\lambda V_0)^2}{U_d^2 a(\varepsilon)^2\omega} = \frac{L(\varepsilon)}{V_0}. \tag{2.554}$$

In fact, we have renormalized the value $D_\Psi \approx V_0^2 D_0$ in expression (2.191) in accordance with mechanisms distorting streamlines (the drift flow with the characteristic velocity U_d and temporal fluctuations with the frequency ω):

$$D_0 \to \left(\frac{U_d}{V_0}\right)^2 a(\varepsilon)^2\omega. \tag{2.555}$$

Solving (2.554), we obtain a new small parameter for the problem of percolation transport in the presence of both the drift flow U_d and fluctuations with the characteristic frequency

$$\varepsilon_* \approx \left(\frac{U_d}{V_0}\right)^{\frac{2}{3(1+\nu)}}\left(\frac{1}{Ku}\right)^{\frac{1}{3(\nu+1)}} \propto U_d^{\frac{2}{7}} V_0^{-\frac{3}{7}}\omega^{\frac{1}{7}}. \tag{2.556}$$

Note that the characteristic size λ is included in the definition of the small parameter in contrast to the Yushmanov model. The expression for the effective diffusion coefficient takes the form

$$D_{\text{eff}} \approx V_0 \lambda \varepsilon_* \approx \left(\frac{U_d}{V_0}\right)^{\frac{2}{3(\nu+1)}} \left(\frac{\lambda\omega}{V_0}\right)^{\frac{1}{3(\nu+1)}} \propto U_d^{\frac{2}{7}} \omega^{\frac{1}{7}}. \tag{2.557}$$

This result differs significantly from the quasi-linear representation (2.550).

The increase in the number of parameters allows us to consider different transport regimes. For example, in the case $U_d = \lambda\omega$ we obtain

$$\varepsilon_* \approx \left(\frac{U_d}{V_0}\right)^{\frac{2}{3(1+\nu)}} \left(\frac{1}{Ku}\right)^{\frac{1}{3(\nu+1)}}. \tag{2.558}$$

The physical meaning of this regime becomes clear when we consider the renormalization condition $L(\varepsilon)/V_0 = 1/\omega$ and compare it with (2.464). This shows the absence of the intermediate characteristic time τ_D in this case. It is possible to obtain other estimates also based on the conditions $U_d \ll \lambda\omega$ or $U_d \gg \lambda\omega$.

2.17.3 Compressibility and Percolation

In the models of turbulent diffusion, the subdiffusion character of transport can be related to the presence of compressibility effects and the "trapping" character of the interaction between a passive tracer and vortex structures. The analysis of the compressibility effects is important for two-dimensional flows since in two-dimensional incompressible flows the subdiffusion mechanism cannot be realized [114].

The author of [17] mentioned the computer simulation of the influence of small compressibility effects on a percolation flow. The monoscale approach based on

$$\vec{V} \approx [\nabla\Psi \times e_z] + \varepsilon\nabla\Psi \tag{2.559}$$

was suggested. In this equation, the second term describes the deviation effect of the real velocity from the streamline. The results of the computer simulation are given in [17] and clearly show the appearance of "trapping" in the flow. We see that the dimensional estimate of the flow pattern "distortion" by the compressibility effects is similar to the "graded" estimate. However, we can obtain a new type of "renormalization" for this case if we note that in the framework of the graded method the following relationship was used:

$$U_d \approx V_0 \frac{\lambda}{L(\varepsilon_*)} \approx V_0 \frac{\Delta(\varepsilon_*)}{a(\varepsilon_*)} \approx V_0 \varepsilon_*^{\nu+1}. \tag{2.560}$$

Applying the assumption of the "weakness" of compressibility effects we can obtain another condition of renormalization to describe the velocity deviations:

$$U_c \approx V_0 \frac{\Delta(\varepsilon_*)}{L(\varepsilon_*)} \approx V_0 \varepsilon_*^{\nu+2}. \tag{2.561}$$

It can also be interpreted by taking into account the particle balance (compare with the convective cells case)

$$nU_c L(\varepsilon_*) \approx nV_0 \Delta(\varepsilon_*). \tag{2.562}$$

Hence, in the problems accounting for a weak compressibility, the new parameter of smallness is given by

$$\varepsilon_* = \left(\frac{U_c}{V_0}\right)^{\frac{1}{2+\nu}} = (\varepsilon_0)^{\frac{1}{2+\nu}} \gg \varepsilon, \tag{2.563}$$

where $\nu = 4/3$. In the framework of the monoscale approach it is easy to obtain the dependence for the effective diffusion coefficient:

$$D_{\text{eff}} \approx V_0 \Delta(\varepsilon) = V_0 \lambda \varepsilon_* \propto U_c^{3/10} V_0^{7/10}. \tag{2.564}$$

Considering the compressibility effects on the basis of using the small parameter $\varepsilon_0 \approx U_c / V_0$, we are in fact dealing with the Kubo number. Thus, if we introduce the characteristic time $\tau_c \approx \lambda / U_c$ then the expression for the small percolation parameter takes the form

$$\varepsilon_* \approx \left(\frac{\lambda}{V_0 \tau_c}\right)^{\frac{1}{\nu+2}} \approx \left(\frac{1}{Ku}\right)^{\frac{1}{\nu+2}}. \tag{2.565}$$

As was mentioned earlier, there is a close interrelation between the compressibility effects and trapping; [158] was devoted to the analysis of the trapping based on the analysis of the correlation mechanisms. Even simple estimates of the correlation time

$$\tau \approx \lambda / V_0 + \tau_T \tag{2.566}$$

using the characteristic time of finding the particles in traps $\tau_T = \tau_T(Ku)$ show the essential alteration of the transport character with $Ku \gg 1$:

$$D_{\text{eff}} \approx \frac{\lambda^2}{\tau} \approx D_0 \frac{Ku}{1 + \frac{\tau_T(Ku)}{\tau} Ku} \approx \frac{\lambda^2}{\tau_T(Ku)}. \tag{2.567}$$

The analysis of the regimes in [158] was also carried out using the power form of correlation functions. Moreover, the model approximation of the streamline function was applied. However, the method suggested in [158] differs significantly from the percolation method, since the analysis was carried out on the basis of the special trajectory ensemble. This approach will be discussed.

2.18 Multiscale Flows

The above-considered percolation approach to turbulent transport problems was based on the monoscale representation of a flow with the parameters V_0, λ. The natural generalization of this model is the analysis of multiscale flows where the hierarchy of spatial scales is related to the velocity hierarchy. This makes it possible to treat the anomalous transport in terms of the correlation function exponent and the Hurst exponent.

2.18.1 The Nested Hierarchy of Scales and Drift Effects

Here, we consider the generalization of the monoscale percolation model by the analysis of multiscale flows with the hierarchy of spatial scales, which is related to the velocity hierarchy. The main difference of this multiscale approach from the Kolmogorov hierarchical model of turbulence is the assumption of the percolation character of the streamline behavior. Such a model has been considered by Isichenko and Kalda in [85, 86]. The expression for the streamline function Ψ_λ as a function of the parameter λ was presented in the scaling form with the stream function exponent M:

$$\Psi_\lambda \approx \Psi_0 \left(\frac{\lambda}{\lambda_0} \right)^M . \tag{2.568}$$

Here, Ψ_0 is the scale of the streamline function that corresponds to the characteristic spatial scale λ_0 and the characteristic velocity V_0. In agreement with the dimensional estimates, we can obtain the expression for the velocity V_λ that corresponds to the scale λ:

$$V_\lambda \approx \frac{\Psi_\lambda}{\lambda} \approx V_0 \left(\frac{\lambda}{\lambda_0} \right)^{M-1} . \tag{2.569}$$

In the framework of the percolation approach, the most intensive streamlines will contribute most to the transport. Two different situations occur with respect to the value of M.

Let us consider the first case, $M > 1$. Here, the characteristic flow pattern is determined by the maximum value of $\lambda \approx \lambda_m$ for such a system.

The second case of interest arises when $M < 1$ and appears to be more complex. The authors of [85, 86] considered the hierarchy of spatial scales,

$$\lambda_0 \ll \lambda_1 \ll \lambda_2 \ll \cdots , \tag{2.570}$$

and the corresponding hierarchy of velocities,

$$V_0 \gg V_1 \gg V_2 \gg \cdots . \tag{2.571}$$

Here, the total velocity $V = V_0 + V_1 + V_2 + \cdots$ is the superposition of flows entering in the hierarchy. Formally, this flow pattern is similar to the hierarchy used by Kolmogorov to describe isotropic turbulence [27, 29, 30, 63]. In that case, the Kolmogorov scaling law for the spectrum of energy $E(k)$ is one of the important characteristics, $E(k) \propto V_k^2/k \propto 1/k^{5/3}$. Here, k is the wave number. The estimate of the velocity gives $V_k \propto 1/k^{1/3} \approx \lambda^{1/3}$. A comparison with the multiscale expression yields $M = 4/3 > 1$. An analogous situation arises when considering the spectrum for the two-dimensional model $E(k) \approx 1/k^3$, which is more relevant for the two-dimensional percolation case under consideration. We see that the Kolmogorov approach differs significantly from the case considered in [85, 86] where $M < 1$. Isichenko and Kalda based their analysis of the hierarchy on Trugman's ideas of "graded" percolation. In the previous section, we noted that this approach [147] is equivalent to the Yushmanov relationship [84]. These approaches are based

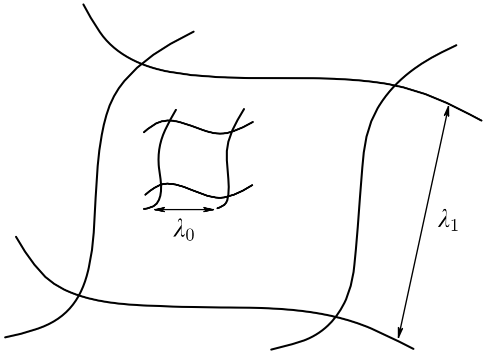

Fig. 2.12. Hierarchy of scales

upon the concept of the distortion of a small scale related flow, by way of superimposition of a weaker drift flow related to a large scale over $V = V_0 + V_1$. In the case of the scale hierarchy the Trugman renormalization [84] can be represented in the form

$$\varepsilon_*(i) = \varepsilon_0(i)^{\frac{1}{1+\nu}} \gg \varepsilon_0(i) \approx \frac{V_{i+1}}{V_i}. \qquad (2.572)$$

Following the ideas of the monoscale percolation approach, the authors of [85, 86] suggested

$$a_i(\varepsilon_*) = \lambda_i \varepsilon_*^{-\nu}, \qquad L_i(\varepsilon_*) = \lambda_i \left(\frac{a_i}{\lambda_i}\right)^{D_h}, \qquad P_\infty(i) \propto \frac{1}{a_i}. \qquad (2.573)$$

Here, the values a_0, Δ_0, L_0 correspond to the scale λ_0. The values $P_\infty(i)$ and Δ_i are interdependent,

$$P_\infty(i) = \frac{L_i \Delta_i}{a_i^2}. \qquad (2.574)$$

Therefore, we obtain a relationship that is similar to the case of monoscale percolation $\Delta_i(\varepsilon_*) \approx \varepsilon_* \lambda_i$. An assumption was made about the hierarchical flow pattern based on the system of nested scales (see Fig. 2.12),

$$a_i(\varepsilon_*) \leq \lambda_{i+1}. \qquad (2.575)$$

This condition plays an important role in the multiscale approach, since the value ε_* can be expressed as a function of λ_{i+1} and λ_{1i}:

$$\varepsilon_0(i) \approx \frac{V_{i+1}}{V_i} \approx \left(\frac{\lambda_{i+1}}{\lambda_i}\right)^{M-1}. \qquad (2.576)$$

Then, simple calculations yield

$$\frac{\lambda_i}{\lambda_{i+1}} \left(\frac{\lambda_{i+1}}{\lambda_i}\right)^{\frac{\nu(1-M)}{1+\nu}} < 1. \qquad (2.577)$$

This condition means that the assumption of nested scales is correct only for

$$-\frac{1}{\nu} < M < 1. \tag{2.578}$$

In fact, we have a double inequality for the value M that describes the case of interest.

2.18.2 The Brownian Landscape and Percolation

The scaling representation of properties within closed fractal loops plays an important role in the problem of the description of turbulent diffusion in two-dimensional geometry. In this paper we have considered the possibility of using the exact scaling dependences for a "cluster hull" to describe the percolation transport. There is one more interesting problem related to the fractal dimensionality of single loops in the framework of the modeling of the "rough surface" problem. Moreover, the multiscale approach [85, 86] is the "percolation version" of the rough surface problem.

The simplest interpretation of this problem [56, 57] is based on the representation of a "rough" $1D + 1D$ landscape as a graph of one-dimensional random walks in x–t axes, where the t-axis can be interpreted as a horizontal coordinate and the x-axis can be a vertical one. Then, different values of the Hurst number correspond to different types of landscape "roughness" $\langle(\Delta x)^2\rangle \propto t^{2H}$. This implies that the "rough landscape" is a statistically self-affine fractal over a corresponding range of length scales with the characteristic Hurst exponent equal to the roughness exponent H (see Fig. 2.13). For such landscapes the mean height difference $\sqrt{(\Delta h)^2}$ between the pairs of points separated by a "horizontal" distance Δr is given by

$$\sqrt{(\Delta h)^2} \propto (\Delta r)^H. \tag{2.579}$$

It is easy to generalize this representation for the case of a rough surface with another dimensionality. Note that Isichenko and Kalda [85, 86] considered a similar

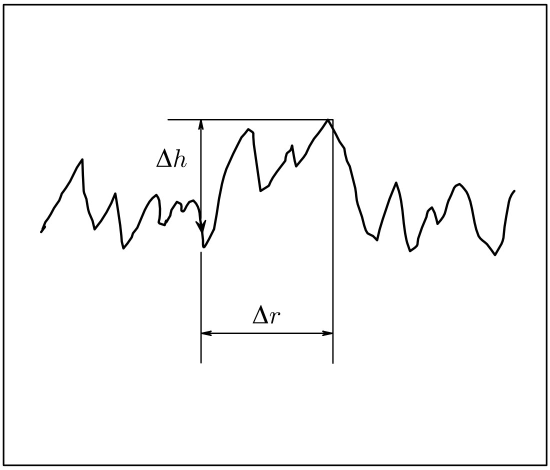

Fig. 2.13. The Brownian landscape

model where the streamline function Ψ_λ is used as the "height" characteristic of the two-dimensional random field $\Psi_\lambda \approx \Psi_0(\lambda/\lambda_0)^M$. This is analogous to the model of continuum percolation; the loops arise when considering a coastline that was formed under the conditions of a "landscape flooded by water". In this connection, there is a problem in obtaining the relationship between the fractal dimensionality characterizing a single loop $\tilde{D}_h$ and the Hurst exponent H (or the stream function exponent M). Here, we will use another symbol $\tilde{D}_h$ instead of the hull percolation exponent D_h, since in order to describe the Brownian surface the percolation ideas were used as approximations only.

The theoretical probabilistic approximation is, as usual, the simplest method. The authors of [159] suggested the use of the model of self-avoiding random walks to describe the single loop character. The functional suggested by Flory (2.110) could be an adequate model. However to describe cases with different Hurst exponents it is necessary to use the probability density function with the arbitrary values $H : R \propto N^H$, instead of the Brownian case, where $H = 1/2$. Then, the expression for the probability of self-avoiding Brownian motion takes the form

$$P_S(t) = \int_{-\infty}^{\infty} \exp\left(-\frac{1}{R^d}(N)^2\right)\frac{1}{(N^H)^d}\exp\left(-\frac{R^2}{N^{2H}}\right)(dR)^d. \tag{2.580}$$

We assume that the main contribution to the integral comes from the extremum of the integrand,

$$\min\left(\frac{1}{R^d}(N)^2 + \frac{R^2}{N^{2H}}\right). \tag{2.581}$$

Performing calculations we can obtain the scaling

$$N \propto R^{(d+2)/2(1+H)}. \tag{2.582}$$

The authors of [166] suggested considering the fractal dimensionality

$$d_F = \frac{d+2}{1+H} \tag{2.583}$$

for the two-dimensional case ($d = 2$) as a fractal dimensionality of the single contour loop (coastline) of a self-affine surface with the Hurst exponent H:

$$\tilde{D}_h = \frac{2}{1+H}. \tag{2.584}$$

Now it is possible to make several simple estimates. The value of $H = 1$ yields result which corresponds to the linear type of behavior with $\tilde{D}_h = 1$. The random walk with $H = 1/2$ corresponds to $\tilde{D}_h = 4/3$.

However, approximation (2.584) is not correct in the region of small H since the following condition must be realized:

$$\tilde{D}_h \le D_h = 1 + \frac{1}{\nu} = \frac{7}{4}. \tag{2.585}$$

This condition has a clear physical meaning. The fractal dimensionality of the hull that has a percolation nature has to be larger than the fractal dimensionality of the coastline of the self-affine surface.

Isichenko and Kalda [85, 86] suggested another version of the approximation $\tilde{D}_h$ based on the hierarchy of nested scales (2.570). In the framework of this approach the correct description of the regimes, where $\tilde{D}_h$ tends to the hull exponent D_h, is possible, since the multiscale approach is based on "graded" percolation. Under these new conditions the expression for the value D_h, with $a_0 \to \lambda_1$, should be reconsidered from the standpoint of the interaction of nearby scales of the hierarchy. Recall that $D_h = 1 + 1/\nu$; therefore, in the monoscale approach we have $L(a) \approx a/\varepsilon_*$. Then, using the assumption $a_0 \to \lambda_1$, the authors of [85, 86] suggested the simple approximation

$$L(\lambda_i) \propto \frac{\lambda_i}{\varepsilon_*(\lambda_i)}. \tag{2.586}$$

In the framework of this approach, the calculations yield the renormalized value $\tilde{D}_h$,

$$\tilde{D}_h = D_h \frac{\nu}{1+\nu}(1-M) + \frac{1+\nu M}{1+\nu}. \tag{2.587}$$

For the two-dimensional case, the following simple expression was obtained:

$$\tilde{D}_h = \frac{10-3M}{7}, \tag{2.588}$$

where $\tilde{D}_h(-1/\nu) = D_h$ and $\tilde{D}_h(1) = 1$. However, this result has not passed recent tests [165] because there is a rigorous result, which gives the value $\tilde{D}_h(0) = 3/2$. A new approximation for $0 < M < 1$ was suggested, namely $\tilde{D}_h = (3-M)/2$, which is in agreement with the rigorous result for $\tilde{D}_h(0)$ [163, 164].

Unfortunately, this new approximation does not give any information about the behavior of $\tilde{D}_h$ in the region of negative M. This is not surprising, since in the framework of the Brownian theory of "rough" surfaces we cannot interpret the values $H < 0$. However, the "graded" percolation method used in [85, 86] allows these values to be analyzed. In the next section, we will consider the physical interpretation of the exponent M from the correlation point of view.

2.18.3 Correlations and Transport Scalings

Completing the consideration of the basic assumptions of the multiscale approach, let us focus on the physical meaning of the parameter M. Obviously, this parameter governs the character of a flow. We can relate it to the correlation properties of a flow. The simple estimate for the spatial correlation function in the scaling law form is given by

$$C(\lambda) \propto V(\lambda)^2 \propto \lambda^{2(M-1)} \propto \frac{1}{\lambda^{\alpha_C}}. \tag{2.589}$$

Here, α_C is the correlation exponent that describes the rate of decay of the correlation function

$$\alpha_C = 2(M - 1). \tag{2.590}$$

Cases where $M \approx 1$ correspond to the scaling law $C(\lambda) \approx$ const. In the cases $M \geq -1/\nu$ the correlation function is "steepest". The condition of applicability of the Isichenko–Kalda hierarchical model takes the following form [111]:

$$0 < \alpha_C < 7/2. \tag{2.591}$$

In subsequent considerations, in order to describe transport properties we will use the exponent α_C together with the exponent M. The above analysis permits us to interpret the scaling estimate of transport, because the rigorous methods often show the relationships between the Hurst exponent and the correlation exponent.

Following the ballistic character of the estimates of the percolation effects, Isichenko and Kalda [85, 86] suggested a scaling law for the calculation of the Hurst exponent H in the multiscale case:

$$\lambda(t) \propto V(\lambda)t \approx V_0\left(\frac{\lambda(t)}{\lambda_0}\right)^{M-1} t. \tag{2.592}$$

Then, simple calculations make it possible to obtain the expression

$$\lambda(t) \approx \lambda_0\left(\frac{V_0 t}{\lambda_0}\right)^{1/(M-2)} \propto t^H. \tag{2.593}$$

Hence, the Hurst exponent is

$$H = \frac{1}{2 - M} = \frac{2}{2 + \alpha_C}. \tag{2.594}$$

This ballistic estimate (2.592) looks too rough [compared with (2.177)]. However, in terms of the correlation exponent α_C, one obtains the rigorous result for incompressible flows with the power correlation function [51] where $a_C < 2$. We see that the steeper correlation functions correspond to the lower values of the Hurst exponent. The correlation function $C(\lambda) \propto 1/\lambda^2$corresponds to the case of classical diffusion with $H = 1/2$.

The efficiency of similar estimates allows us to consider more complex flows, where the effects of the anisotropy of the medium play an important role, together with the multiscale effects $\lambda_\perp(t) \propto V_\perp(\lambda_\perp, \lambda_\parallel)t$. Formula (2.592) does not take into account the anisotropy effects; however, one can consider an analogous approach for the simplest anisotropic case with separated spatial scales [17, 72]:

$$\lambda_\perp(t) \propto V_\perp(\lambda_\parallel)t. \tag{2.595}$$

Here, $\lambda_\perp$ is the perpendicular displacement and $\lambda_\parallel$ is the longitudinal displacement. If the case under consideration shows a diffusion character in the longitudinal motion (the double diffusion, the Dreizin–Dykhne model, etc.), then we obtain $\lambda_\parallel \approx \sqrt{2D_0 t}$.

Upon substitution of this estimate into (2.595) we find the scaling

$$\lambda_\perp(t) \propto V_0\left(\frac{\lambda_0^2}{D_0}\right)^{(1-M)/2} t^{(1+M)/2}. \tag{2.596}$$

The expression for the Hurst exponent takes the form [167, 168]

$$H = \frac{1+M}{2} = 1 - \frac{\alpha_C}{4}, \tag{2.597}$$

where $0 < \alpha_C < 7/2$. The comparison between (2.597) and (2.594) shows the coincidence of both these dependences at two points, $\alpha_C = 0$ ($H = 1$ is the ballistic case) and $\alpha_C = 2$ ($H = 1/2$ is the classical diffusion equation). The characters of both these dependences $H(\alpha_C)$ are similar. Moreover, the exponent M really characterizes not only scaling but also the physical properties of the flow. Thus, for $M = 1/2$ we obtain the Dreizin–Dykhne result $H = 3/4$, which is in agreement with the isotropic case (2.594), where for $M = 1/2$ one can obtain $H = 3/2$, which corresponds to the "Manhattan grid" flow [17] (the generalization of the shear flows model [72]). Note that for $\alpha_C > 2$ scaling (2.597) yields the subdiffusive regime, which contradicts the initial assumptions about the incompressibility of the flow and using the streamline concept.

2.18.4 The Diffusive Approximation and the Multiscale Model

Besides the ballistic approach (2.592), it is possible to consider the diffusion approximations

$$\lambda^2 \approx D(\lambda)t. \tag{2.598}$$

Here, $D(\lambda)$ is the coefficient corresponding to the scale λ. However, the expressions for $D(\lambda)$, which were suggested by Isichenko and Kalda, are based on the approximation (2.588) of the exponent $\tilde{D}_h$. This is not surprising, since in the monoscale approach the expression for $D_h = 1 + 1/\nu$ also plays a key role. The diffusion coefficient $D(\lambda)$ can be expressed in the form that is analogous to the monoscale case:

$$D(\lambda) \approx \frac{\lambda^2}{\tau} P_\infty(\lambda), \tag{2.599}$$

where $P_\infty(\lambda) \approx L(\lambda)\Delta(\lambda)/\lambda^2$. The authors of [85, 86] suggested an approximation of $P_\infty(\lambda)$ in the form corresponding to the monoscale approach (2.453):

$$P_\infty(i) \approx \frac{\lambda_i}{a_i(\lambda_i)}. \tag{2.600}$$

Then, calculations yield the expression

$$P_\infty(\lambda) \approx \left(\frac{\lambda_0}{\lambda}\right)^{4(1-M)/7}. \tag{2.601}$$

This result allows the width of the percolation layer to be defined:

$$\Delta(\lambda) \approx P_{\infty}(\lambda)\frac{\lambda^2}{L(\lambda)} \approx \lambda_0\left(\frac{\lambda}{\lambda_0}\right)^M. \tag{2.602}$$

Introducing the correlation time τ into the ballistic form $\tau \approx L/V_0$ into the expression for $D(\lambda)$ leads to the Koch–Brady result (2.594). In this case, the conditions $M > 0$ ($\alpha_c < 2$) are automatically satisfied, since $D(\lambda)$ has to increase if λ increases:

$$D(\lambda) \approx V_0\Delta(\lambda) \approx V_0\lambda_0\left(\frac{\lambda}{\lambda_0}\right)^M. \tag{2.603}$$

A new regime arises when the correlation time is considered in the diffusive form $\tau = \Delta^2(x)/D_0$:

$$\lambda^2 \approx D_0\frac{L(\lambda)}{\Delta(\lambda)}t. \tag{2.604}$$

Simple calculations [85, 86] lead to the scaling for the Hurst exponent

$$H = \frac{7}{10M+4}. \tag{2.605}$$

Here, $-2/5 < M < 1$. It easy to see that the scaling obtained by Isichenko and Kalda depends essentially on the choice of the expression for $L(\lambda)$. Thus, for the approximation of $L(\lambda)$, the substitution of a_i for λ_i was used, whereas for the approximation of $F(\lambda)$ the conventional form of a_i was retained. It is easy to explain the choice made in [85, 86], since the expression in the form $L(\lambda_i) \approx a_i/\varepsilon$ leads to the value $\tilde{D}_h(1) = 0$, which is absolutely unacceptable. On the other hand, approximation (2.321) provides the correct limit for negative values of M: $\tilde{D}_h(-1/\nu) = D_h$ and the realization of Mandelbrot's condition $\tilde{D}_h < 2 - M$ with $M < 1$. From the modern standpoint correct calculations could be based on the recent results of Kondev et al. [162, 163] and Kalda [164, 165]:

$$\tilde{D}_h = \frac{3-M}{2}. \tag{2.606}$$

Then, upon carrying out calculations we obtain

$$D \approx D_0\frac{L(\lambda)}{\Delta(\lambda)} \approx D_0\frac{L^2(\lambda)}{\lambda^2 P_{\infty}} \approx D_0\left(\frac{\lambda}{\lambda_0}\right)^{11(1-M)/7}. \tag{2.607}$$

The diffusion coefficient $D(\lambda)$ increases with λ for the case when $M < 1$, yielding the superdiffusion character of the behavior in the region $0 < M < 1$:

$$H = \frac{7}{3+11M}. \tag{2.608}$$

Note that the use of new approximation (2.606) leads to alteration in the formula for the diffusion coefficient $D(\lambda)$that is based on the ballistic expression for τ, since

$$D(\lambda) \approx V_0 \Delta(\lambda) \propto \frac{1}{L(\lambda)}. \tag{2.609}$$

In this case the new scaling for the Hurst number does not coincide with the expressions by Koch and Brady (2.594).

However there are also other possibilities, since the approximation of $P_\infty(\lambda)$ in the form (2.600) is not universal. Thus, the estimate $P_\infty \approx \varepsilon_0 \approx (\lambda/\lambda_0)^{M-1}$ can be used in the region of values $M \leq 1$. Another way is based on using the united approximation formula on the basis of three characteristic values of $\tilde{D}_h(M)$ at the points $M = 1$, $M = 0$, and $M = -1/\nu$ for the whole diapason of parameters $-1/\nu < M < 1$. The estimates considered show that diffusive approximation (2.598) has several degrees of freedom, which leads to considerable uncertainties in the results. Nevertheless, the multiscale approach essentially increases the possibilities of applying percolation ideas for the description of turbulent diffusion.

2.18.5 Stochastic Instability and Time Scales

To consider stochastic instability in the framework of the multiscale approach it is convenient to introduce the hierarchy of characteristic times (frequency scales)

$$t_\lambda \approx \frac{1}{\omega_\lambda} \approx \left(\frac{\lambda}{\lambda_0}\right)^G \frac{\lambda_0}{V_0}, \tag{2.610}$$

where G is the frequency exponent, which permits modeling both ballistic $G = 1$ and diffusive regimes $G = 2$. Based on the multiscale results obtained by way of multiscale approximation, we can consider the stochastic instability increment in terms of the monoscale definition

$$\tilde{\gamma}_S(\lambda) \approx \frac{V_S}{l_S} \approx \frac{L(\lambda)\lambda\omega_\lambda}{\lambda^2} \propto \lambda^{\tilde{D}_h - G - 1}. \tag{2.611}$$

Introducing the local Kubo number Ku_λ corresponding to the selected scale λ yields

$$Ku_\lambda \approx \frac{V_\lambda}{\lambda\omega_\lambda} \propto \lambda^{G+M-2}. \tag{2.612}$$

Then, in terms of the Kubo number the expression for the stochastic instability increment takes the form

$$\tilde{\gamma}_S(\lambda) \propto Ku_\lambda^{\frac{1+G-\tilde{D}_h(M)}{2-G-M}}. \tag{2.613}$$

As already mentioned, there is still no correct approximation for $\tilde{D}_h(M)$ in the whole interval

$$-1/\nu < M < 1. \tag{2.614}$$

However, the exact value of $\tilde{D}_h$ is calculated for $M = 0$:

$$\tilde{D}_h(0) = 3/2; \tag{2.615}$$

in combination with the assumption of the ballistic character of particle motion along percolation streamlines it could yield a scaling similar to the monoscale estimate. Indeed, if

$$M = 0, \quad \tilde{D}_h = 3/2, \quad \text{and} \quad G = 1, \tag{2.616}$$

we obtain [40, 148]

$$\tilde{\gamma}_S(\lambda) \propto \sqrt{\frac{V_\lambda}{\lambda \omega_\lambda}} \propto \sqrt{Ku_\lambda}. \tag{2.617}$$

Note that the passage from the monoscale percolation model to the multiscale one makes it possible to describe essentially nondiffusive transport regimes in both isotropic and anisotropic models. Therefore, it is only natural to apply the multiscale description for other problems, where long-range correlation effects play a significant role.

2.18.6 Isotropic and Anisotropic Turbulent Energy Spectra

The important aspect of turbulent transport is to establish a relation to spectral turbulence characteristics. Thus, in the framework of the scaling approach, the most universal is the Kolmogorov model with a constant energy flux over a spectrum [27]. In the case of isotropic hydrodynamical turbulence, the expression for the energetic spectrum $E(k) \approx V_k^2/k$ can be obtained from the condition that the dissipation rate is constant:

$$\varepsilon_K = \frac{V_k^2}{\tau_{\text{CASC}}} = \text{const}. \tag{2.618}$$

Here, V_k is the rate of turbulent pulsations corresponding to the wave number $k \approx 1/\lambda_k$ and the characteristic time of nonlinear interaction $\tau_{\text{CASC}} \approx (V_k k\}^{-1}$. Simple calculations lead to the Kolmogorov spectrum $E(k) \propto 1/k^{5/3}$ for three-dimensional isotropic hydrodynamical turbulence. The multiscale model of percolation transport considered in the previous sections is also based on the scaling representation for velocity. However, the consideration of percolation transport channels system requires the separation of characteristic scales in the framework of the hierarchy

$$\lambda_0; \qquad \lambda_1 = \mu\lambda_0; \qquad \lambda_2 = \mu^2\lambda_0; \qquad \cdots \qquad \lambda_m; \quad \mu \gg 1. \tag{2.619}$$

Analysis shows that the limit of applicability of the multiscale model is $\mu \approx 2$. On the other hand, the multiscale percolation model is closely related to drift effects, which, naturally, lead to a considerable difference between the percolation scaling for velocity $V_k \propto (1/k)^{M-1}$, where $-1/\nu < M < 1$, and the expression for two-dimensional isotropic turbulence [148]

$$V_k \approx \sqrt{E(k)k} \approx 1/k, \quad \text{where } E(k) \propto 1/k^3. \tag{2.620}$$

The consideration of the multiscale transport model in the framework of MHD turbulence is also closely related to the energetic spectrum form. Formally, the time of nonlinear interaction of waves is defined as

$$\tau_{\text{CASC}} \approx \left(\frac{V_p}{V_k}\right)^{m-1} \frac{1}{\omega_p}, \tag{2.621}$$

where $\omega_p = V_p k$, V_p is the phase velocity and m characterizes the type of nonlinear interaction ($m = 3$ for a three-wave interaction, $m = 4$ for a four-wave interaction, etc.) The MHD turbulence model of Iroshnikov and Kraichnan [172, 173] for Alfven's waves is widely practiced now:

$$\begin{aligned} &\tau_{\text{CASC}} \approx \left(\frac{V_A}{V_k}\right)^2 \frac{1}{V_A k}, \quad V_p \equiv V_A = \frac{B_0}{\sqrt{4\pi n}} \gg V_k, \quad m = 3, \\ &\tau_A \ll \tau_{\text{CASC}}. \end{aligned} \tag{2.622}$$

Here, V_A is the Alfven velocity and n is the plasma density. Calculations based on the constancy of the dissipation rate $\varepsilon_K \approx V_k^2/\tau_{\text{CASC}}$ yield $E(k) \propto 1/k^{3/2}$ for the turbulence spectrum. In terms of energy dissipation,

$$\delta E \approx \varepsilon_K \tau_A \approx V_k^3/V_A, \tag{2.623}$$

the model from [172, 173] describes the diffusive character of energy transfer in nonlinear wave interaction $V_k^2 \propto \tau_{\text{CASC}}^{1/2}$:

$$\frac{V_k^2}{\delta E} \approx \left(\frac{V_A}{V_k}\right)^2 \approx \sqrt{\frac{\tau_{\text{CASC}}}{\tau_A}}. \tag{2.624}$$

Moreover, Kraichnan noted [40] that in the framework of the isotropic model of MHD turbulence there is a linear dependence of the dissipation rate on the characteristic time $\varepsilon_K \propto \tau_A$, whereas in the classical Kolmogorov approach $\varepsilon_K \propto 1/\tau_{\text{CASC}}$.

Naturally, the isotropic model is inadequate for describing turbulent transport processes in a strong magnetic field. Indeed, in the case of strong MHD turbulence, the separation of longitudinal and transverse scales plays an important role. The scaling approach to the description of essentially nonisotropic MHD turbulence was suggested by Goldreich and Sridhar [176]. It was based on the balance of characteristic times in Alfven's MHD turbulence

$$\frac{1}{\tau_A} \approx k_{/\!/} V_A \approx k_\perp V_\perp(k_\perp) \approx \frac{1}{\tau_\perp}, \tag{2.625}$$

where $\omega_A = 1/\tau_A$ is Alfven's frequency, V_A is Alfven's velocity, $k_{/\!/} \approx 1/l_{/\!/}$ is the longitudinal wave number, $k_{\perp/} \approx 1/l_\perp$ is the transverse wave number, $V_\perp(k_\perp)$ is the scale of transverse velocity related to the spatial scale $k_\perp$, and $\tau_\perp$ is the dimensional estimate of the time of nonlinear interaction that characterizes the turbulent cascade in the transverse direction to the magnetic field with the constant dissipation rate

$$\varepsilon_\perp = \frac{V_\perp^3}{l_\perp} = \text{const.} \tag{2.626}$$

This considerably differs from isotropic representations, which were used by Iroshnikov and Kreichnan [172, 173]. Expression (2.625) is, naturally, only an approximation analogous to the percolation renormalizations (2.531), but its efficiency has been confirmed repeatedly by simulations, which demonstrate the correctness of the scaling

$$l_{/\!/} \approx \frac{1}{k_{/\!/}} \approx \frac{V_A l_\perp}{V_\perp} \approx \frac{V_A l_\perp}{(\varepsilon_\perp l_\perp)^{1/3}} \approx \frac{V_A}{\varepsilon_\perp^{1/3}} l_\perp^{2/3}. \tag{2.627}$$

The relationship between the longitudinal and transverse scales in the form $l_{/\!/} \propto l_\perp^\alpha$, where $\alpha = 2/3$, corresponds to strong MHD turbulence [176]. Note that the method of separation of longitudinal and transverse spatial scales is also fairly effective in analyzing multiscale percolation flows.

2.18.7 The Multiscale Model of Transport in a Tangled Magnetic Field

The incorporation of the complete hierarchy of spatial scales considerably improves the agreement of theoretical predictions and observation results. Thus, the authors of [54] obtained a correct estimate of electron heat-conductivity in galaxy clusters; the assumption was made that the characteristic spatial scale l_B in model [12] must be calculated taking into account the anisotropic MHD turbulence spectrum. They used the phenomenological model of Goldreich and Sridhar [176], where the longitudinal and transverse scales are related by $l_{/\!/} \propto l_\perp^\alpha$, where $\alpha = 2/3$ corresponds to strong MHD turbulence, and $\alpha = 4/3$ corresponds to the intermediate turbulence regime. This allows us to assume that the correlation scales characterizing transport in a stochastic magnetic field have the form

$$\frac{L_{\mathrm{COR}}}{l_B} \approx \left(\frac{\Delta_\perp}{l_B}\right)^\alpha. \tag{2.628}$$

This estimate differs significantly from the Chandran and Cowley estimate $L_{\mathrm{COR}} \approx 30 l_B$ and for transverse displacements $\Delta_\perp \approx l_B$ it leads to the value of longitudinal correlation length

$$L_{\mathrm{COR}} \approx \Delta_\perp \approx l_B \ll 30 l_B. \tag{2.629}$$

Then, the electron heat-conductivity estimate has the form

$$\chi_{\mathrm{eff}} \approx D_{/\!/} \frac{l_B}{L_{\mathrm{COR}}} \approx \frac{\chi_{\mathrm{Sp}}}{3}, \tag{2.630}$$

which agrees well with the data of astrophysical observations. To substantiate obtained scalings, let us consider the model equation describing the separation of initially close force lines. The approximation equation describing the exponential divergence of force lines Δ_m could take the form

$$\frac{d}{dl} \Delta_m^2 \propto \frac{\Delta_m^2}{l_B}. \tag{2.631}$$

However, the exponential regime for $\Delta_m^2 > l_B^2$ has to move into the diffusive one,

$$\frac{d\Delta_m^2}{dl} \approx D_m \approx \frac{l_\perp^2}{l_B}. \tag{2.632}$$

From this standpoint, it is natural to describe intermediate regimes by the modification of the factor $1/l_B$ in (2.631), taking into account the increasing role of large scales.

Considering the scale hierarchy corresponding to the model of a quasi-isotropic stochastic magnetic field, the authors of [54] used the scaling from the model of strong Alfven's turbulence [176]

$$\frac{l_{/\!/}}{l_B} \approx \left(\frac{l_\perp}{l_B}\right)^\alpha, \tag{2.633}$$

with the hierarchy of scales

$$l_{\min} < l_\perp < l_B \le L_{\mathrm{COR}}. \tag{2.634}$$

Then, in terms of the wave numbers $k_\perp \approx \frac{1}{l_\perp}$ and $k_{/\!/} \approx \frac{1}{l_{/\!/}}$, it is convenient to rewrite model equation (2.631) in a form that takes into account the contribution of different scales of hierarchy in the representation of $L_K \approx l_B$:

$$\frac{d\langle\Delta_m^2\rangle}{dl} \approx \left\langle\Delta_m^2\right\rangle \int_{1/l_B}^{1/\Delta_\perp} k_{/\!/}(k_\perp)\, d\ln k_\perp + \int_{1/\Delta_\perp}^{1/l_{\min}} \frac{k_{/\!/}(k_\perp)}{k_\perp^2}\, d\ln k_\perp, \tag{2.635}$$

where $k_{/\!/} \propto k_\perp^{1/\alpha}$; hence, this equation describes transition to regimes with

$$\Delta_\perp^\alpha \approx l_\perp^\alpha \approx l_{/\!/}. \tag{2.636}$$

It is important to note that in spite of using the multiscale approach relating longitudinal and transverse scales in the strong Alfven's turbulence, the characteristic spatial scale l_B of a tangled magnetic field appears to be the universal parameter of model

$$l_B \approx L_{\mathrm{COR}} \approx L_K \approx \Delta_\perp, \tag{2.637}$$

and the characteristic correlation scale does not enter the final expression for χ_{eff}.

2.19 Subdiffusion and Traps

In the presence of structures, it is possible that increasing effective transport owing to convective flows and trapping lead to subdiffusion. In this section we consider some simple approximations of trapping effects that allow us to obtain estimates of the effective diffusion coefficient in the presence of spatially distributed traps, and on comb structures. In the models of turbulent diffusion, the subdiffusion character of transport can be related to the presence of compressibility effects and the "trap" character of interaction of a passive tracer with vortex structures. Note that without compressibility in two-dimensional flows the subdiffusion mechanism cannot be realized.

2.19.1 The Balagurov and Vaks Model of Diffusion with Traps

One of the simplest methods of approximation of compressibility effects in the anomalous transport models relates to using different "trap" mechanisms. We will analyze a particular physical model of diffusion in a medium with traps on the basis of the well-known paper by Balagurov and Vaks [46]. Using theoretical probabilistic estimates, we can derive scaling relations, which can be interpreted on the basis of relaxation functions. On long time scales, the diffusion of particles in a medium with traps is governed by the fluctuating character of the appearance and disappearance of regions free of traps. We introduce the trapping probability (i.e., the probability of a particle being captured in a trap) in terms of the Poisson distribution:

$$P_c \propto \exp\left(-\frac{t}{\tau_D}\right). \tag{2.638}$$

Here, $\tau_D \approx R^2/D$ is the characteristic time scale on which the particle diffuses through the medium until it reaches the boundary of the trap-free region of the radius R and D is the local diffusion coefficient. We assume that trap-free regions obey the Poisson distribution,

$$P_T \propto \exp\left(-\left(\frac{R}{R_0}\right)^d\right), \tag{2.639}$$

where R_0 is the mean radius of the trap-free regions in the space of dimensionality d. Now, we can estimate how the radius $R(t)$of the trap-free region should change in time in order for the survival probability to be the highest:

$$P = P_c P_T \propto \exp\left(-\left(\frac{R}{R_0}\right)^{d-1} - \frac{t}{\tau_D}\right). \tag{2.640}$$

Calculating the time derivative of the argument of the exponential functions in this expression, we obtain

$$R(t) \propto t^{1/(2+d)}. \tag{2.641}$$

For $d > 0$, the diffusion described by this scaling is obviously slower than that described by the classical diffusion scaling [170]

$$R^2(t) \propto t^{2/(2+d)} \ll t. \tag{2.642}$$

In the language of fractional derivatives, this indicates that a fractional derivative with respect to time can serve as a model equation for describing diffusion in the situation at hand:

$$\frac{\partial^\gamma \tilde{n}(k,t)}{\partial t^\gamma} = \frac{\partial}{\partial t}\int_0^t \frac{\tilde{n}(k,\tau)}{(t-\tau)^\gamma}\, d\tau, \quad \gamma = \frac{2}{2+d}. \tag{2.643}$$

Note that the problem of diffusion in a medium with traps is not necessarily related to such issues as condensed states or chemical reactions. The ideas associated with traps are also used in the study of particle trapping by vortices in order to describe the behavior of a passive scalar in a turbulent field [17, 18, 158, 169] or in the analysis of the correlation functions of a turbulent field. In what follows, we will consider the problem in which traps in a medium manifest themselves in particle diffusion in a magnetic field with "braided" force lines.

2.19.2 Subdiffusion and Fractality

The diffusion approximation $\lambda_{\parallel} \propto \sqrt{2Dt}$ of longitudinal motion in double diffusion and the Dreizin–Dykhne models lead us to expect that the subdiffusive character of transport can also be interpreted by means of the "renormalization" that is analogous to $t \to t\delta N/N$. Indeed, the diffusive character of motion in the one-dimensional case leads to numerous "returns", hence the particle takes part in the transverse diffusion process only a fraction of the total time t. Let us assume the fraction of the time during which the particle takes part in the transverse diffusion has a fractal character with the dimensionality d_F. Actually, we can use the representation

$$\Delta_{\perp}^2 \approx D_{\perp} t \frac{\delta N}{N}, \tag{2.644}$$

where $\delta N \propto (t/\tau_{\parallel})^{d_F}$, $N \propto t/\tau_{\parallel}$. Here, $\tau_{/\!/}$ is the longitudinal correlation time and $D_{\perp}$ is the transverse diffusion coefficient. Simple calculations yield the expression

$$\Delta_{\perp}^2 \approx \left(\frac{D_{\perp}}{(\tau_{\parallel})^{d_F - 1}} \right) t^{d_F}. \tag{2.645}$$

Changing to the symbols $D_{\perp} \approx D_m L_{\parallel}/\tau_{\perp}$, $D_0 \approx L_{\parallel}^2/\tau_{\parallel}$ used above, we find that

$$\Delta_{\perp}^2 \approx D_m \frac{\sqrt{D_0 \tau_{\parallel}}}{\tau_{\perp}} \left(\frac{t}{\tau_{\parallel}} \right)^{d_F}. \tag{2.646}$$

In the case of "double" diffusion $d_F = 1/2$, we obtain the expression for double diffusion (2.117). Note that the cases where $d_F = d/2$ are very frequent. For example, in the percolation models of turbulent diffusion [17], the fraction of the percolation streamlines is

$$P_{\infty} \approx \frac{a^{d_F}}{a^2} \approx \frac{1}{a}, \quad d_F = d/2 = 1. \tag{2.647}$$

The diffusion equation corresponding to the specific fractional value d_F has the form of an equation with fractional derivatives [18–22]. Indeed, based on the definition of the Hurst exponent H, one obtains

$$\Delta_{\perp}(t) \propto t^H, \quad H = d_F/2. \tag{2.648}$$

The rigorous theory for such problems is based on continuum time random walks (CTRW) or on the diffusive models for a medium with "traps" [18–22]. To describe the transport in a stochastic magnetic field, this approach was used in [20] very successfully. The main assumption in that approach is the consideration of the probability $\Phi(t)$ of a particle remaining in a trap during the time t. The following function in

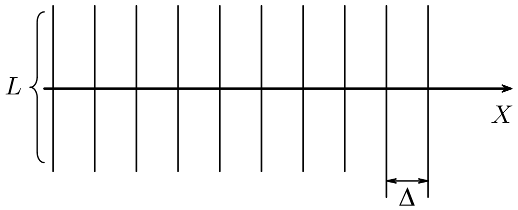

Fig. 2.14. Comb-like structure

the scaling law form was usually used:

$$\Phi(\tau) \propto \frac{1}{\tau^{\gamma}}, \tag{2.649}$$

where $\gamma = d_F$ for $\gamma < 1$. Here, γ is the parameter of the probability function. There exists a simple estimate for $\Phi(t)$ based on the probability of the return (2.104) given as

$$\Phi(t) \propto \rho(0,t)\Delta \propto \frac{\Delta}{\sqrt{4\pi D_0 t}}. \tag{2.650}$$

Here, Δ is the correlation scale. We obtain the relation between the probability of finding the particle in the trap and the "return" probability. We can imagine the "traps" as teeth in the "comb-like structure" (see Fig. 2.14). If the teeth length tends to infinity, then our expression (2.650) is satisfactory. The models with teeth, which have a limited length and number of teeth and which have fractal structures, appear to be the natural generalization of the "comb-like" model [18–20].

2.19.3 Comb Structures and Transport

Anomalous transport on comb structures plays an important role due to the fairly universal kind of trap topology. Therefore, we will consider a more general comb structure model, where the length of the "teeth" is distributed in accordance with power laws. We will consider the structure that consists of a backbone directed along the z-axis and orthogonal teeth connected to this backbone. The distances between the teeth Δ are identical; however the tooth distribution along the length is given by the scaling

$$f(l) = \frac{l_0^{\gamma_S - 1}}{l}. \tag{2.651}$$

Here, $f(l)$ is the probability density of finding a tooth with the length l; l_0 is the tooth characteristic length, and γ_S is the characteristic exponent. In the model under analysis, the minimum tooth length l_0 must be of order the characteristic longitudinal scale Δ,

$$l_0 \approx \Delta. \tag{2.652}$$

On the other hand, it is necessary to take into account the renormalization condition of the distribution function $f(l)$:

$$\int_{l_0}^{\infty} f(l)\, dl = 1, \tag{2.653}$$

$$\int_{l_0}^{\infty} f(l) l^n\, dl = \infty, \tag{2.654}$$

where $n = 1, 2, 3, \ldots$. In such a formulation of the problem, the description of anomalous transport on comb structures was repeatedly discussed in [171–173]. Therefore, here we develop only qualitative estimates.

Following Lubashevskiy and Zemlianov [171], let us define the mean length $\langle l \rangle$ that describes the spatial scale corresponding to diffusive walks along teeth with the diffusion coefficient D_0:

$$\langle l(t) \rangle \int_{l_0}^{\sqrt{D_0 t}} l f(l)\, dl \approx \frac{D_0 t}{l_0} \left(\frac{l_0}{\sqrt{D_0 t}} \right)^{\gamma s} \propto \frac{1}{t^{\gamma s/2}}. \tag{2.655}$$

The mean time $\langle T \rangle$ that the particle diffuses along a tooth can be estimated as

$$\langle T \rangle \propto \frac{\Delta}{\langle l \rangle} t \propto \frac{\Delta l_0}{D_0} \left(\frac{D_0 t}{l_0^2} \right)^{\gamma s/2} \propto t^{\gamma s/2}. \tag{2.656}$$

Then, the mean-squared displacement is estimated by the scaling

$$R^2 = \langle \Delta x^2(t) \rangle \approx D_0 \langle T \rangle \approx \Delta l_0 \left(\frac{D_0 t}{l_0^2} \right)^{\gamma s/2} \propto t^{\gamma s/2}. \tag{2.657}$$

On the other hand, one can obtain the estimate of the probability of avoiding a return to the backbone $\Phi(t)$:

$$\Phi(t) \approx \frac{\langle T \rangle}{t} \propto \frac{1}{t^{\gamma s/2}}. \tag{2.658}$$

Note that in the case of comb structures with the power form of length distribution, the expression for $\Phi(t)$ differs essentially from the diffusive estimate for regular comb structures:

$$\Phi(t) \propto \frac{1}{t^{1/2}}. \tag{2.659}$$

The consideration of the probability $\Phi(t)$ in the framework of the more rigorous approach (continuous time random walk) makes it possible to obtain not only scalings for the mean-squared displacement but also fractional differential equations to describe particle density. This approach will be developed in the next section.

2.20 Continuous Time Random Walks

The nonlocal nature of turbulent diffusion has stimulated the search for equations that differ significantly from the conventional diffusive representation. An elegant integral equation corresponding to this problem was suggested by Einstein and Smoluchowski. However, memory effects were not included in this equation. To describe trapping and subdiffusive regimes, the continuous time random walk model was suggested [174, 175]. It is possible to combine both these approaches to describe the anomalous transport, where memory and nonlocality effects play important roles.

2.20.1 The Montroll and Weiss Approach and Memory Effects

A careful analysis of the problems involving random-walk processes shows that a fundamentally important role is played by the transition probability density. In Markov's approach, the transition probability density is assumed to depend on the spatial variable, $W(\Delta)$, where Δ is a spatial step. Montroll and Weiss [174] used a fundamentally different dependence—they assumed that the transition probability density depends on time, $\psi(t)$. They also introduced a physically clear quantity—the probability of not undergoing a transition from a point y to any other points during a time t:

$$\Phi_Y(t) = 1 - \int_0^t \psi_Y(t)\, dt. \tag{2.660}$$

The subscript Y in the functions Φ and ψ served merely to mark an arbitrarily chosen point. The function $\Phi(t)$ reflects the relaxation properties of the system. In the simplest case, the function $\Phi(t)$ is represented in the form of the Poisson distribution

$$\Phi(t) = \exp(-t/\tau), \tag{2.661}$$

where τ is the mean time between transition events. The function $\Phi(t)$ can also be represented in some other forms capable of reflecting the characteristic behavior of relaxation character of systems:

$$\text{Kohlrausch relaxation function} \quad \Phi(t) = \exp(-\sqrt{\alpha t}), \tag{2.662}$$

$$\text{algebraic relaxation function} \quad \Phi(t) = (\alpha t)^{-\gamma}, \tag{2.663}$$

$$\text{Montroll function} \quad \Phi(t) = \exp\bigl(-\ln^{\beta}[-\alpha t]\bigr). \tag{2.664}$$

Here α, β, and γ are the characteristic parameters of the problem. In the Montroll–Weiss theory, the function $\Phi(t)$ plays a governing role. The authors of [174] succeeded in writing an elegant chain equation for the probability of a randomly walking particle to be at the point x at time t:

$$P(x,t) = \int_0^t R_p(x,\tau)\Phi(t-\tau)\, d\tau. \tag{2.665}$$

Here, $R_p(x,t)$ is the probability of transitions from other points to the point x during the time interval $(t; t+dt)$. The functions on the right-hand side of this equation have an essentially similar physical meaning as the function ψ [see definition (2.660)]. Consider the point x_1 and let the function ψ_{X_1} be represented as a sum of the probability densities for transitions from the point x_1 to all allowed points x. Then, we have $\psi_{X_1}(t) = \sum_{X_1} \psi(x_1 \to x, t)$ and, consequently,

$$R_p(x,t) = \sum_{X_1} \int_0^t R_p(x_1,\tau)\psi(x_1 \to x, t-\tau)\,d\tau + P(x,0)\delta(t), \qquad (2.666)$$

where $\int_0^t \psi(x_1 \to x, t)$ is the probability density for a transition from the point x_1 to the point x at the time t. Note that the function ψ depends not only on the time t but also on the relative spatial positions of the points x_1 and x, in which case we have

$$\int_{-\infty}^{\infty} dx \int_0^t \psi(x_1 \to x, t)\,dt = 1. \qquad (2.667)$$

The probability density $P(x,t)$ is related to the particle density by

$$n(x,t) = \frac{NP(x,t)}{\delta x}, \qquad (2.668)$$

where N is the total number of particles and δx is a volume element. Applying the Laplace transformation in time and the convolution theorem, we obtain from expressions (2.310) and (2.666)

$$s\tilde{P}(x,s) - P(x,0) = \sum_{X_1}\left[\tilde{R}_p(x_1,s) - \tilde{R}_p(x,s)\right]\tilde{\psi}(x_1 \to x, s), \qquad (2.669)$$

where, in accordance with expression (2.310), $\tilde{P}$ and $\tilde{R}_p$ are related by

$$\tilde{R}_p(x,s) = \frac{\tilde{P}(x,s)}{\tilde{\Phi}(s)} = \frac{s\tilde{P}(x,s)}{1 - \sum_{X_1} \tilde{\psi}(x_1 \to x, s)}. \qquad (2.670)$$

Then, returning to the physical variables, we arrive at the Montroll–Weiss equation

$$\frac{\partial}{\partial t}P(x,t) = \sum_{X_1} \int_0^t \left[P(x_1,\tau) - P(x,\tau)\right]F(x_1 \to x, t-\tau)\,d\tau, \qquad (2.671)$$

where the memory function F is defined in terms of its Laplace transform,

$$\tilde{F}(x_1 \to x, s) = \frac{s\tilde{\psi}(x_1 \to x, s)}{1 - \sum_{X_1} \tilde{\psi}(x_1 \to x, s)}. \qquad (2.672)$$

In what follows, we will be interested in the functions that depend only on the difference between x and x_1; this corresponds to the case of a uniform medium $F(x_1 \to x, s) = F(x - x_1, s)$.

Assuming that the variable x takes on continuous values, we can generalize (2.671) to a sort of the Smoluchowski–Chapman–Kolmogorov equation (2.50) with memory effects:

$$\frac{\partial}{\partial t}P(x,t) = \int_{-\infty}^{\infty} dx_1 \int_0^t d\tau\, P(x_1,\tau)F(x - x_1, t-\tau) + Q, \qquad (2.673)$$

where Q is expressed in terms of Laplace transforms as follows:

$$\tilde{Q}(x,s) = P(x,0) - \tilde{P}(x,s)\tilde{F}(x - x_1, s). \quad (2.674)$$

The assumption that the memory function is of a multiplicative nature yields

$$F(x - x_1, t - \tau) = G(x - x_1)M_B(t - \tau). \quad (2.675)$$

Here, G corresponds to the kernel of the Chapman–Kolmogorov functional and M_B is the memory function. Switching now to Fourier transforms in x and Laplace transforms in t, we arrive at the following equation for the particle density:

$$s\tilde{\tilde{n}}(k,s) - \tilde{n}(k,0) = -\frac{s\tilde{\psi}(s)}{1 - \tilde{\psi}(s)}\big(1 - \tilde{G}(k)\big)\tilde{\tilde{n}}(k,s). \quad (2.676)$$

Here, $\tilde{\tilde{n}}(k,s)$ is both the Fourier and Laplace transformation of the density $n(x,t)$. It is easy to draw an analogy between this equation and the Einstein functional equation. Obviously, under the conditions $M_B(t) \propto \delta(t)$, $\tilde{M}_B(s) = \text{const}$ the Montroll–Weiss equation passes over to the Smoluchowski–Chapman–Kolmogorov equation. In fact, choosing the Poisson distribution for the function $\Phi(t)$ ensures the required limiting transition for the equation with memory effects. Telegraph equation (2.229) was derived for an exponential memory function $M_B(t) = \exp(-t/\tau)$ and for a Gaussian memory function with $1 - \tilde{G}(k) = -Dk^2$. It is of interest to note that, although the equation considered above and the memory function $M_B(t)$ both have a simple form, the expression for $\Phi(t)$ is fairly complicated in structure [18, 19]. Hence, we see that it is necessary to choose different model functions for different physical situations.

There are numerous investigations of the continuous time random walk models. Fortunately, several detail reviews [18–22] have been published recently. Therefore, in the next sections we will consider a few examples closely related to the renormalization of quasi-linear equations.

2.20.2 Fractional Differential Equations

An important physical quantity in the description of random walk processes with memory is the mean waiting time $\langle t \rangle$ until an event occurs:

$$\langle t \rangle = \int_0^\infty t\psi(t)\,dt. \quad (2.677)$$

This time is analogous to the mean length of the jump in the theory of Markovian processes. This is not surprising because, in the approach based on memory effects, the transition probability density $\Phi(t)$ is an analogue of the function $W(y)$. For the Poisson distribution (2.661), we have $\langle t \rangle = \tau$.

An important particular case of relaxation functions is represented by those that decrease according to a power law,

$$\Phi(t) \propto \left(\frac{\tau}{t}\right)^{\gamma}, \quad 0 < \gamma < 1. \tag{2.678}$$

In this case, the mean waiting time until an event occurs tends to infinity:

$$\langle t \rangle = \int_0^{\infty} t\psi(t)\,dt \to \infty. \tag{2.679}$$

The power relaxation functions were found to provide an efficient tool for analysis of transport processes [21, 22]. For long times t, simple manipulations yield the following expression for $\tilde{M}_B(s)$:

$$\tilde{M}_B(s) = \frac{s\tilde{\Phi}(s)}{1 - s\tilde{\Phi}(s)} \approx s\tilde{\Phi}(s) = \Gamma(1-\gamma)s^{\gamma}, \tag{2.680}$$

where $\Gamma(z)$ is Euler's gamma function. The equation describing memory effects takes the form

$$s\tilde{\Phi}(s)\tilde{\tilde{n}}(k,s) = \big(1 - \tilde{G}(k)\big)\tilde{\tilde{n}}(k,s) + \tilde{n}(k,0)\tilde{\Phi}(s). \tag{2.681}$$

The expression

$$s\tilde{\Phi}(s)\tilde{\tilde{n}}(k,s) \approx s^{\gamma}\tilde{\tilde{n}}(k,s) \tag{2.682}$$

can be interpreted as a time derivative of order γ [21, 22, 174–176]:

$$s\tilde{\Phi}(s)\tilde{\tilde{n}}(k,s) \approx s^{\gamma}\tilde{\tilde{n}}(k,s) \to \frac{\partial^{\gamma}\tilde{n}(k,t)}{\partial t^{\gamma}} = \frac{\partial}{\partial t}\int_0^t \frac{\tilde{n}(k,\tau)}{(t-\tau)^{\gamma}}\,d\tau. \tag{2.683}$$

Representing the results in such a manner facilitates interpretation of scaling relations of the form

$$R(t) \propto t^{\frac{\gamma}{\alpha_L}}, \tag{2.684}$$

which have found increasingly wider application in the analysis of fractional derivatives:

$$\frac{\partial^{\gamma} n(x,t)}{\partial t^{\gamma}} = \frac{\partial^{\alpha_L} n(x,t)}{\partial x^{\alpha_L}} + Q(n,x,t). \tag{2.685}$$

Here, α_L, γ are the parameters and Q is the additional term related to the initial conditions.

2.20.3 The Taylor Definition and Memory Effects

The approximations of the function $\psi(x_1 \to x; t)$, which were used in the previous sections, allow one to investigate the models in which it is easy to use the decoupling

$$\psi(x,t) = \varphi(x)\psi(t). \tag{2.686}$$

However, many important results can be obtained in the framework of a more general analysis. Thus, consider the system of the Montroll–Weiss equations in the form

$$P(x,t) = \sum_{x_1} \int_0^t P(x_1,\tau)\psi(x-x_1,t-\tau)\,d\tau + \Phi(t)\delta(x), \tag{2.687}$$

$$\psi(t) = \sum_x \psi(x;t) = \psi(k=0;t). \tag{2.688}$$

Then, upon applying both the Laplace and Fourier transformations one obtains

$$\tilde{\tilde{P}}(k,s) = \tilde{\tilde{P}}(k,s)\tilde{\tilde{\psi}}(k,s) + \Phi(s), \tag{2.689}$$

$$\Phi(s) = \frac{1-\tilde{\psi}(s)}{s}. \tag{2.690}$$

Formal calculations yield the expression for $\tilde{\tilde{P}}(k,s)$ in the form

$$\tilde{\tilde{P}}(k,s) = \frac{1-\tilde{\psi}(s)}{s}\frac{1}{1-\tilde{\tilde{\psi}}(k,s)}. \tag{2.691}$$

Following the approach developed in [177] it is easy to obtain a formal expression for the mean squared displacement:

$$R^2 \equiv \langle \Delta x^2(t) \rangle = \int x^2 P(x,t)\,dx = -\frac{\partial^2 \tilde{P}(k,t)}{\partial k^2}\bigg|_{k=0}. \tag{2.692}$$

On the other hand, the expression suggested by Taylor (2.6) relates the mean square displacement to the correlation function

$$\frac{dR^2}{dt} = 2\int_0^t C(\tau)\,d\tau. \tag{2.693}$$

The authors of [176] used the Fourier transformation of

$$s\tilde{R}^2(s) = 2\frac{\tilde{C}(s)}{s} \tag{2.694}$$

in order to establish the relationship between the Lagrangian correlation function and the memory function. The comparison between expressions (2.692) and (2.694) yields this relationship in terms of the Laplace transform

$$\tilde{C}(s) = \zeta^2 s \frac{\tilde{\psi}(s)}{1-\tilde{\psi}(s)}, \tag{2.695}$$

where we used the Gaussian approximation for the step length distribution

$$\tilde{\tilde{\psi}}(k,s) = \tilde{\psi}(s)\exp(-\zeta^2 k^2). \tag{2.696}$$

It is well known that the exponential correlation function corresponds to the conventional Brownian motion. Therefore, the correctness of the formula obtained in [177] must be first proved for $\psi(t) = \delta(t - \tau)$. Then, substituting $\tilde{\psi}(s) = \exp(-s\tau)$ it is easy to find

$$\tilde{C}(s) = \zeta^2 \frac{s}{e^{s\tau} - 1}. \tag{2.697}$$

To compute the Laplace inverse of this expression one keeps the three lowest orders of the exponential as $s\tau \to 0$ (the observation time is much lower than the microscopic waiting time: $t \gg \tau$) and obtains

$$C(t) = \left(\frac{2\zeta^2}{\tau^2}\right) \exp\left(-2\frac{t}{\tau}\right). \tag{2.698}$$

This result corresponds exactly to the Langevin equation

$$\dot{V}(t) = -\frac{2}{\tau} V + \frac{\zeta^2}{\tau} \xi(t), \tag{2.699}$$

where $V(t)$ is the Brownian particle velocity and $\xi(t)$ is the white noise random function.

Now we are able to consider more complex models, where the memory function is represented by the stable law

$$\tilde{\psi}(s) = \exp\left(-(s\tau)^\gamma\right) \tag{2.700}$$

with the parameter σ; $0 < \gamma < 1$. Simple calculations in the framework of continuous time random walks allow the following expression to be obtained:

$$R^2 = 2\frac{\zeta^2}{\tau^\sigma} \frac{t^\gamma}{\Gamma(1 + \gamma)}, \tag{2.701}$$

where Γ is the Gamma function symbol. The expression for the Laplace transform of the velocity correlation function takes the form

$$\tilde{C}(s) = \frac{\zeta^2}{\tau} s^{1-\gamma} \frac{s^{1-\gamma}}{[1 + (\tau^\gamma s^\gamma / 2)]}, \tag{2.702}$$

where the three lowest orders in $s\tau$ were kept to compute $\exp[(s\tau)^\gamma]$. Formal calculations [177] yield the final expression for the correlation function in the form

$$C(t) = \frac{2}{\tau^\gamma} \frac{\zeta^2}{\tau} t^{2\gamma - 2} E_{\gamma, 2\gamma - 1}\left[-2\left(\frac{t}{\tau}\right)^\gamma\right], \tag{2.703}$$

where $1/2 < \gamma < 1$ since we restrict the parameter γ in order to express $C(t)$ in terms of the Mittag–Leffler functions $E_{\gamma, 2\gamma-1}$. This result leads to the power tail asymptotic

$$C(t) \propto \frac{1}{t^{2-\gamma}}. \tag{2.704}$$

This agrees well with the simple estimates based on the transport scaling $R^2 \propto t^\gamma$, since $C(t) \approx R^2/t^2 \approx t^{\gamma - 2}$. Hence, the method suggested in [177] is effective for analyzing the correlation properties of the system in which memory effects play an important role.

2.21 Fractional Differential Equations and Scalings

A fractional differential equation is an especially effective tool for investigating anomalous transport. These equations allow us to obtain scalar probability density functions based on scaling representation of waiting time distributions. On the other hand, the consideration of correlation effects in the framework of renormalized quasi-linear equations can also lead to the appearance of fractional derivatives. In this section, we consider the Richardson law, trapping in vortex structures, transport in a stochastic magnetic field, and shear flow systems in terms of fractional differential equations.

2.21.1 The Klafter, Blumen, and Shlesinger Approximation

Applying the continuous time random approach makes it possible to consider both nonlocality and memory effects by the approximation of model function $\psi(x,t)$. Blumen, Klafter, and Shlesinger [142] suggested using the advantages of this method to describe the Richardson relative diffusion $R^3 \propto t^3$. Recall that in the Monin model [62] use was made only of the dimensional estimate of nonlocality effects by the power approximation of the kernel of the Einstein–Smoluchowski functional (2.52)

$$G(k) \propto \varepsilon_k^{1/3} k^{2/3}. \tag{2.705}$$

The authors of [142, 178] suggested the dynamical interpretation of nonlocality and memory effects by using the model function $\psi(x,t)$ in the form

$$\psi(x,t) = \varphi(x)\psi(t/x) = \varphi(x)\delta\left(t - \frac{x}{V(x)}\right), \tag{2.706}$$

where, through the δ function, x and t are coupled. Here, the functions $\varphi(x)$ and $V(x)$ are represented by the following scalings:

$$\varphi(x) \propto \frac{1}{x^{1+\beta_R}}, \tag{2.707}$$

$$V(x) \propto x^{\gamma_R}. \tag{2.708}$$

Then, the case $\gamma_R = 0$ corresponds to the ballistic model and the case $\gamma_R = 1/3$ corresponds to the Kolmogorov scaling

$$V_k^2 \propto E(k)k \approx \frac{1}{k^{2/3}}. \tag{2.709}$$

Then, for $\gamma_R = 1/3$, using the expression for mean-squared displacement in the form

$$R^2 = -\frac{\partial^2}{\partial k^2}\tilde{P}(k,t)\bigg|_{k=0}, \tag{2.710}$$

where the expression for $\tilde{P}(k, t)$ is given by the formula (2.691), the authors of [142] obtained the following relationships:

$$R^2 \propto t^3 \quad \text{for } \beta_R \le \frac{1}{3}; \tag{2.711}$$

$$R^2 \propto t^{2+\frac{2}{3}(1-\beta_R)} \quad \text{for } \frac{1}{3} \le \beta_R \le \frac{1}{2}; \tag{2.712}$$

$$R^2 \propto t \quad \text{for } \beta_R \ge \frac{1}{2}. \tag{2.713}$$

One can see that for $\beta_R \le 1/3$ the Richardson law $R^2 \propto t^3$ is obtained, as we could anticipate. Moreover, in [142] the modified model was considered, where the intermittency effects are included:

$$V(x) \propto x^{\gamma_R}, \quad \gamma_R = \frac{1}{3} + \frac{d - d_F}{6} = \frac{1}{3}\left(1 + \frac{\mu_F}{2}\right). \tag{2.714}$$

Then, the mean-squared separation of two particles is given by

$$R^2 \propto t^{\frac{12}{4-\mu_F}}, \qquad \beta_R \le \frac{1-\mu_F}{3}; \tag{2.715}$$

$$R^2 \propto t^{2+6\frac{1-\beta_R}{4-\mu_F}}, \qquad \frac{1-\mu_F}{3} \le \beta_R \le \frac{10-\mu_F}{6}; \tag{2.716}$$

$$R^2 \propto t, \qquad \frac{10-\mu_F}{6} \le \beta_R. \tag{2.717}$$

Here, the scaling exponents depend on the index β_R as well as the fractal dimension $d_F = d - \mu_F$. Note that the scaling for

$$\beta_R \le \frac{1-\mu_F}{3} \tag{2.718}$$

was previously obtained by Hentschel and Procaccia [78], who used a much different approach.

2.21.2 The Stochastic Magnetic Field and Balescu Approach

Fractional differential equations are especially relevant for analyzing different anomalous transport mechanisms. Since double diffusion corresponds to the subdiffusion character of transport with $H = 1/4$, the corresponding equation could be in agreement with the continuous time random walk approach. This model was considered by Balescu [179]. The authors of [179–189] investigated the transport effects in the stochastic magnetic field in terms of the correlation function. Here, we represent this approach in the simplified form, which is related to earlier discussions on the renormalization of quasi-linear equations (2.213) and (2.214). Instead of introducing the additional diffusion term $D(\partial^2 n_1/\partial x^2)$ that describes transverse correlation effects, the author of [179] kept one of the usually omitted terms $v_1(\partial n_1/\partial x)$, which allows the memory effects to be described. As a result, the transformations put (2.214) for n_1

into the form

$$\frac{\partial n_1}{\partial t} + v_1 \frac{\partial n_1}{\partial x} = -v_1 \frac{\partial n_0}{\partial x}. \tag{2.719}$$

This equation can be considered as a first-order linear hyperbolic equation with the source term

$$I(x,t) = -v_1 \frac{\partial n_0}{\partial x}, \tag{2.720}$$

where the derivative $\partial n_0/\partial x$ is the parameter of the problem. We also supplement the equation with the uniform initial condition $n_1(x,0) = 0$. This formulation is similar to (2.215) but here we deal with the characteristic

$$z = x - v_1(t - t_1) \tag{2.721}$$

instead of the characteristic of the conventional quasi-linear approach $z = x - v_0(t - t_1)$,

$$n_1(x,t) = -\int_0^t v_1(t_1) \frac{\partial_0^n(z,t)}{\partial z} \, dt_1. \tag{2.722}$$

We substitute this expression for n_1 into (2.213) and perform simple manipulations to obtain

$$\frac{\partial n_0}{\partial t} = \int_0^t \big\langle v_1(t) v_1(t_1) \big\rangle \frac{\partial^2 n_0(z,t_1)}{\partial z \partial x} \, dt_1. \tag{2.723}$$

Now one can see that the use of the correlation function in the power form

$$C(t) = M_B(t) \propto (\tau/t)^{\alpha} \tag{2.724}$$

leads to the continuous time random walk representation for the transport equation

$$\frac{\partial^2 n_0(x,t)}{\partial t^2} = -\frac{D}{\tau} \frac{\partial}{\partial t} \int_0^t \frac{\partial^2}{\partial x^2} n_0(x,\tau) \left(\frac{\tau}{t-\tau} \right)^{\alpha_C} d\tau. \tag{2.725}$$

Here, D_0 is the seed diffusivity, τ is the characteristic time, and α_C is the correlation exponent. Actually, the renormalized quasi-linear equations, together with the approximation of the correlation function, make it possible to obtain the fractional differential equation

$$\frac{\partial^2 n}{\partial t^2} = -\frac{D_0}{\tau} \frac{\partial^{\alpha_C}}{\partial t^{\alpha_C}} \left(\frac{\partial^2 n}{\partial x^2} \right), \tag{2.726}$$

which corresponds to the continuous time random walk with the scaling for the Hurst exponent

$$R^2(t) \propto t^{\gamma} = t^{2-\alpha_C}, \tag{2.727}$$

$$H = \frac{\gamma}{2} = 1 - \frac{\alpha_C}{2}, \quad \alpha_C < 2. \tag{2.728}$$

However, in this simplified approach we do not consider the aniso tropy effects and longitudinal collisional diffusion, which are essential for describing the anomalous transport in the stochastic magnetic field. Balescu et al. [179, 180] considered all these aspects in detail. The final equation for the transverse transport with the modified memory function

$$M_B \approx D_0\delta(t) + \frac{D_0}{\tau}\left(\frac{\tau}{t}\right)^{\alpha_c} \tag{2.729}$$

takes the form

$$\frac{\partial n_0(x,t)}{\partial t^2} = -D_0\frac{\partial^2 n_0}{\partial x^2} - \frac{D_0}{\tau}\int_0^t \frac{\partial^2}{\partial x^2} n_0(x,t')\left(\frac{\tau}{t'-t}\right)^{\alpha_C} dt', \tag{2.730}$$

which allows the investigation of both conventional diffusion and subdiffusive behavior. Note that the authors of [179–189] carried out a thorough analysis of the correlation function. They interpreted different regimes of the anomalous transport in the stochastic magnetic field on the basis of the renormalized quasi-linear equations with

$$H = 1 - \alpha_C/2, \tag{2.731}$$

where the case with $\alpha_C = 3/2$ corresponds to the double diffusion (2.117).

2.21.3 Longitudinal Correlations and the Diffusive Approximation

The Kadomtsev–Pogutse analysis [67] was based on the ballistic representation of longitudinal (z-axis) motion and the diffusion approximation $D_{\text{eff}}\nabla_\perp^2 n_1$ of transverse correlation effects. In fact, the opposite case corresponds to the shear flow model (2.177) and the double diffusion (2.114) where longitudinal motions have the diffusion character $\lambda_\| \approx \sqrt{2D_0 t}$. From this standpoint, it is easy to obtain an equation for the passive tracer density under conditions when longitudinal correlation effects can be approximated by the longitudinal diffusion term $D_0\partial^2 n_1/\partial z^2$ [181]. Thus, in the two-dimensional case the corresponding renormalized equations have the form

$$\frac{\partial n_0}{\partial t} = -\left\langle V_X(z)\frac{\partial n_1}{\partial x}\right\rangle; \tag{2.732}$$

$$\frac{\partial n_1}{\partial t} = D_0\frac{\partial^2 n_1}{\partial z^2} - V_X(z)\frac{\partial n_0}{\partial x}. \tag{2.733}$$

Here, in contrast to [67], the diffusion coefficient D_0 characterizes the seed diffusion. The dependences $n_0 = n_0(x,t)$ and $n_1 = n_1(x,z,t)$ were used to describe the two-dimensional case. Indeed, the author of [182] obtained a similar set of equations by averaging the diffusion equation with the random convective term

$$\frac{\partial n}{\partial t} = D_0\Delta n - V_X(z)\frac{\partial n}{\partial x}. \tag{2.734}$$

Using the Laplace transformation over t and the Fourier transformation over z, one obtains from (2.732) and (2.733)

$$s\tilde{n}_0(s,x) - n_0(x,0) = \tilde{D}(s)\frac{\partial^2 \tilde{n}_0}{\partial x^2}, \tag{2.735}$$

$$\tilde{D}(s) = \lim_{L_0 \to \infty} \frac{1}{2L_0} \int_{-L_0}^{L_0} dz \int_{-\infty}^{\infty} dz' \left\{ \frac{\exp[-\sqrt{s|z-z'|^2/D_0}]}{\sqrt{D_0 s}} V_X(z) V_X(z') \right\}. \tag{2.736}$$

The aim of the author of [182] was to obtain a diffusion equation for the model of random drift flows [72]. This corresponds to the condition $z \to z'$ (the condition of "return" of the particle to the initial point). A fractional differential equation was found,

$$\frac{\partial^{3/2} n_0(t,x)}{\partial t^{3/2}} = \frac{\partial^2}{\partial t^2} \int_0^t \frac{n_0(t',x)\,dt'}{\sqrt{\pi(t-t')}} = \frac{V_0^2 a}{\sqrt{2D_0}} \frac{\partial^2 n_0(t,x)}{\partial x^2} - \frac{n_0(0,x)}{2\sqrt{\pi} t^{3/2}}. \tag{2.737}$$

Indeed, the "renormalization" of the quasi-linear equations allows us to obtain the transport equations, which differ significantly from the classical diffusion equation [20–22]. Now, we will consider using the correlation properties of a system of random flows (see Fig. 2.15). The correlation function can be represented in the power form. We can change the form of the equation for n_0 by means of a more detailed consideration of the function $K(|z-z'|) = V_X(z)V_X(z')$ in (2.736). This function describes the correlation properties. The question of the correlation nature of this function was discussed in detail in [182]. However, the choice of the form of the function K was not important there because Dreizin and Dykhne considered the model taking into account the return effects ($z \to z'$). Let us consider the power approximation of the function $K(w)$,

$$K(w) = K\big(|z-z'|\big) \propto \frac{V_0^2}{1+w^{\alpha_C}}. \tag{2.738}$$

The power approximations of the correlation function are often used for obtaining the scaling law [17–22]. Using the symmetry of integral (2.736) and the known formula of Kampe-de-Feriet [25–27], we can easily simplify integral (2.736). In terms of

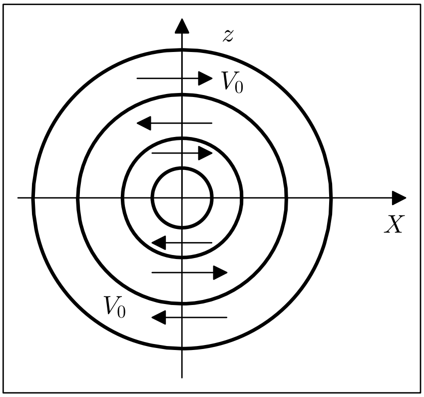

Fig. 2.15. Zonal flows system

the Laplace transformation, the equation that is determined takes the form

$$s\tilde{n}_0(s,x) - n_0(x,0) = \frac{V_0^2}{\sqrt{2D_0}}\left(\frac{s}{2}\right)^{\alpha_C/2-1}\frac{\partial^2\tilde{n}_0}{\partial x^2}. \tag{2.739}$$

Changing to the dependence in time, we obtain the subdiffusion equation [17–22]

$$\frac{\partial^\gamma n_0}{\partial t^\gamma} = D_{\text{eff}}\frac{\partial^2 n_0}{\partial x^2} - Q(t,x), \tag{2.740}$$

$$D_{\text{eff}} = \frac{V_0^2 a^{\alpha_C}}{(2D_0)^{\alpha_C/2}}, \qquad Q = \frac{n_0(0,x)}{2\sqrt{\pi}t^\gamma}. \tag{2.741}$$

Here, the order of the derivative with respect to time γ depends on the parameter α_C (2.740),

$$\gamma = 2H = 2 - \frac{\alpha_C}{2}, \quad 0 < \alpha_C < 4, \tag{2.742}$$

which describes correlation properties in the longitudinal direction.

In the case of an anisotropic medium this relationship can be related to the Corrsin functional in the form (2.179)

$$C(t) \approx \frac{\lambda_\perp^2}{t^2} \approx \int_{-\infty}^{\infty}\frac{V_0^2}{1+(z/z_0)^{\alpha_C}}\exp\left(-\frac{z^2}{4D_0 t}\right)\frac{dz}{\sqrt{4\pi D_0 t}}. \tag{2.743}$$

Here, V_0 and z_0 are the dimensional parameters of the correlation function. Moreover, it is possible to recognize the Corrsin integral in the expression for the Laplace transformation (2.736). Using the dimensionless variable $z^2/4D_0 t$ in order to calculate the integral, we obtain the simple estimate in the scaling form

$$C(t) \approx \frac{\lambda_\perp^2}{t^2} \approx \frac{\text{const}}{t^{\alpha_C/2}} \quad \text{and} \quad \lambda_\perp \propto t^{1-\alpha_C/4}. \tag{2.744}$$

Actually, this is scaling law (2.742). Note that the regime with $\alpha_C = 1$ ($H = 3/4$), which was considered in [72, 120], has a clear physical interpretation in terms of the spectrum $S_c(k)$ [120]:

$$\left\langle \tilde{V}_x(k)\tilde{V}_x(k')\right\rangle = S_c(k)\delta(k-k'). \tag{2.745}$$

Here, $\tilde{V}_x(k)$ is the Fourier representation of $V_x(z)$ and $\delta(k-k')$ is the Dirac function. For $k \ll 1$ and the power form of $S_c(k) \approx k^{\alpha_C - 1}$ the regime with $H = 3/4$ corresponds to a shear velocity field, which is white noise.

2.21.4 Vortex Structures and Trapping

Cardoso et al. [183, 184] carried out experimental research on anomalous diffusion of scalars in the field of several vortices. Actually, the authors of [183, 184] studied trapping effects related to the capture of test particles by vortices (see Fig. 2.16), which plays an important role. Naturally, in such a formulation of the problem continuous time random walks are an adequate theoretical model.

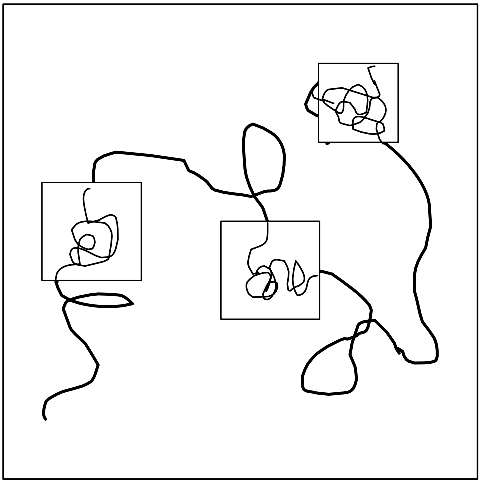

Fig. 2.16. Vortex trapping regions

From the formal standpoint we must introduce a scaling to describe the waiting time distribution

$$\psi(t) \propto \frac{1}{t^{\gamma-1}}. \tag{2.746}$$

Then, the mean waiting time between two "jumps" is estimated by the expression

$$\tau_T \approx \int_0^{t_{\max}} t\psi(t)\,dt \propto t_{\max}^{3-\gamma} \approx t^{3-\gamma}. \tag{2.747}$$

On the other hand, the full walking time can be estimated through τ_T and the number of pauses N,

$$t \approx N\tau_T \approx t^{3-\gamma}N. \tag{2.748}$$

Hence, one obtains the scaling for N in the form:

$$N \propto t^{\gamma-2}. \tag{2.749}$$

Since the mean squared displacement is related to N by the scaling $R^2 \propto N$, one arrives at the relationship

$$R \propto \sqrt{N} \approx t^{\gamma/2-1}. \tag{2.750}$$

The experimental results obtained by Cardose et al. allow one to define scaling for the mean squared displacement in the following form

$$R \propto t^{1/3}, \tag{2.751}$$

where the Hurst exponent $H = 1/3$ and the exponent $\gamma = 8/3$. On the other hand, the probability density function $\psi(t)$ corresponding to these scalings was successfully measured [183, 184], which permits us to consider the continuous time random walk prediction as correct.

Naturally, the subdiffusive regime that was experimentally found is not the only one possible. In the presence of vortex structures, there are both trapping effects and flights. Thus, the authors of [185, 186] experimentally investigated test particle transport in an almost two-dimensional flow in an annular tank ("Texas experiments"). The tank was rotating at about 1 or 2 Hz and the bottom was sloped to simulate β-effects. Because of the rapid rotation, the flow was quasi-two-dimensional. Two types of particle trajectories were found. Particles within a vortex remain trapped for very long time (stick). Particles in the azimuthal jet experience prolonged flights around the circumference of the tank. Because the vortex pattern is not perfectly stationary particles alternate, apparently randomly, between flying in jets and sticking in vortices. The authors of [185, 186] obtained superdiffusive scaling for the angular displacement

$$\left\langle \Delta\theta^2 \right\rangle \propto t^{\gamma}, \tag{2.752}$$

where $\gamma \approx 1.4$–1.7. It was also possible to observe conventional diffusion with $\gamma = 1$ by breaking the azimuthal symmetry of the forcing the flow.

2.21.5 Correlations and Trapping

Fractional differential equations appear to be the relevant tool to visualize nondiffusive scalings. Instead of the classical scaling $r^2 \propto Dt$, which corresponds to the conventional diffusive equation for the description of the double diffusion regime, use was made of

$$\frac{\partial^{1/2} n}{\partial t^{1/2}} = D_{\text{eff}} \frac{\partial^2 n}{\partial r^2}, \tag{2.753}$$

where the expression $\frac{\partial^{1/2} n}{\partial t^{1/2}}$ is the nonlocal fractional differential operator describing temporal alteration of density accounting for long-range correlation effects [22, 42]. This operator can be interpreted as a fractional time derivative of order α [121, 181]:

$$\frac{\partial^{\gamma} n(r,t)}{\partial t^{\gamma}} = \frac{\partial}{\partial t} \int_0^t \frac{n(r,\tau)}{(t-\tau)^{\gamma}}\, d\tau. \tag{2.754}$$

Representing the results in such a manner facilitates interpretation of the nondiffusive scaling relations. Such an approach is rather unusual but it is based on simple ideas. Thus, arising nondiffusive effects are related to particles staying in "traps". If the probability of the particle staying in a trap during the time t is described by the scaling

$$\Phi(t) \propto \left(\frac{\tau_0}{t}\right)^{\gamma}, \tag{2.755}$$

where τ_0 is the characteristic time and $0 < \alpha < 1$, then the modified diffusive equation is given by the expression

$$\frac{\partial^{\gamma} n}{\partial t^{\gamma}} = D_{\text{eff}} \frac{\partial^2 n}{\partial r^2}. \tag{2.756}$$

The particle does not disappear in the trap but only, with some probability, is kept in every trap; this leads to the nonlocal fractional form of the differential equation. In the case of double diffusion $\gamma = 1/2$, the expression for $\Phi(t)$ can be easily explained from the physical point of view. Indeed, if we use the Gaussian expression for the probability of finding a particle in a small vicinity Δ of the point r at the moment t,

$$P(r,t) \approx \frac{\Delta}{\sqrt{4\pi D_q t}} \exp\left(-\frac{r^2}{4D_q t}\right), \tag{2.757}$$

then the probability of a particle returning to the initial point $r = 0$, in the framework of one-dimensional diffusion, is written as

$$P(0,t) \approx \frac{\Delta}{\sqrt{4\pi D_q t}}. \tag{2.758}$$

Here D_q is the particle's collisional diffusivity.

In the case of moving charged particles in a braided magnetic field, the constant return of charges to the initial point, which is caused their one-dimensional diffusive motion along force lines, prevents significant transverse displacements. Therefore, in the model of transport in the braided magnetic field it is natural to use the estimate for the probability

$$\Phi(t) \approx P(0,t) \approx \frac{\Delta}{\sqrt{4\pi D_q t}}. \tag{2.759}$$

A corresponding fractional differential equation with the exponent $\gamma = 1/2$ for the electron density was obtained in [20], where careful calculations of correlation functions were carried out, but the direct relation to the probability of returns at the initial point $P(0,t)$ was not established. In the presence of strong anisotropy several spatial and temporal correlation scales describe the stochastic magnetic field and they differ from correlation scales, which correspond to particle transport. Therefore, scaling arguments (2.117) look oversimplified. Nevertheless, the development of methods to describe anomalous transport in stochastic magnetic and electric fields in the conditions of anisotropy allows one to obtain visual estimates [171]. To describe transport in comb-like structures, use is made of independent estimates of characteristic times of particles staying in traps or on a bone. Then, using the approximation from [171] we can introduce the effective time of diffusion in the transverse direction:

$$t_{\mathrm{eff}} \approx \frac{\delta_\perp}{L_{\mathrm{Trap}}} t, \tag{2.760}$$

where $\delta_\perp$ is the perpendicular correlation scale related to the stochastic magnetic field and L_{Trap} is the correlation scale related to trapping mechanisms due to particle returns. The analysis of correlation effects [171] leads to a simple estimate of the value L_{Trap} through the effective time of particles staying in traps

$$L_{\mathrm{Trap}} \propto t_{\mathrm{Trap}}. \tag{2.761}$$

Based on this approximation, it is easy to obtain the expression for t_{eff} in terms of the probability of charged particles returning:

$$\Phi(t) \approx \delta_{\perp}/\sqrt{4\pi D_q t}. \tag{2.762}$$

Since

$$t_{\text{Trap}} \approx \Phi(t)t, \tag{2.763}$$

we can write

$$t_{\text{eff}} \approx \frac{\delta_{\perp}}{L_{\text{Trap}}} t \approx \frac{\delta_{\perp} l_{/\!/}}{D_q \Phi(t)} \approx 2 l_{/\!/} \sqrt{\frac{\pi t}{D_q}}, \tag{2.764}$$

where $l_{/\!/}$ is the longitudinal correlation length related to longitudinal diffusion. The expression for the transverse displacements in a static braided magnetic field is given by

$$r_{\perp}^2 \approx D_{\text{eff}} t_{\text{eff}} \approx D_m \left(\frac{D_q}{l_{/\!/}}\right) t_{\text{eff}} \approx D_m \frac{\delta_{\perp}}{\Phi(t)} \approx D_m \sqrt{4\pi D_q t}, \tag{2.765}$$

which corresponds to the scaling for double diffusion $r_{\perp}^2 \propto t^{1/2}$.

2.22 Correlation and Phase-Space

There are certainly deep connections between the conventional space approach to transport and the phase-space approach. The Hamiltonian approach gives the advantage of using degrees of freedom to treat nonlocality and memory effects in the framework of phase-space. The kinetic model provides the possibility of describing ballistic modes and establishing the relationship between different exponents and distributions.

2.22.1 The Corrsin Conjecture and Phase-Space

The models considered show the efficiency of applying the Corrsin conjecture to describe the superdiffusion behavior of a passive scalar. However, long-range correlations play a significant role in considering trapping in turbulent flows. Results of the direct numerical simulation have led Vlad et al. [158] to the conclusion that side by side with the trajectories of a percolation character there exist considerable parts of space where transport is defined by streamlines of the trapping type. By analogy with the percolation approach [17] based on a careful consideration of the structure of the percolation streamline (e.g., the hull of a percolation cluster), Vlad, Spineanu, Misguich, and Balescu suggested that the trapping of test particles could be analyzed using a model representation of the trap streamline system. Moreover, the essential modification of the Corrsin conjecture was done in [158].

Here, we describe this new approximation briefly. Thus, from the standpoint of the authors of [158] it is possible to keep the Corrsin factorization (2.76) but to considerably modify the trajectory ensemble under consideration. Indeed, the subensemble of trajectories in which the resulting displacement corresponds to some fixed value λ could be described as follows:

$$\langle V(x(0),0)V(x(t),t)\rangle\big|_{X(t)=\lambda}. \tag{2.766}$$

The author of [158] considered a system of sub-ensembles, where the value of the initial velocity is fixed in each such system:

$$C_V(V_0,t)=\langle V(x(0),0)V(x(t),t)\rangle\big|_{X'(t)=V_0}=V_0\langle V(x(t),t)\rangle\big|_{X'(t)=V_0}. \tag{2.767}$$

On the one hand, this model leads to averaging of sub-ensembles over the velocity with the kinetic distribution $f(V_0,t)$,

$$C(t)=\int_{-\infty}^{\infty} f(V_0,t)C_V(V_0,t)\,dV_0. \tag{2.768}$$

On the other hand, this gives the possibility of more detailed analysis of the streamline behavior. This is not surprising because for the new conditions the approximation of expression (2.767) by means of the specially chosen function $V_C(x,t)$ permits us to investigate the specific system of trajectories in the framework of

$$\frac{dx}{dt}=V_C(x,t)=\langle V(x(t),t)\rangle\big|_{V_0}. \tag{2.769}$$

The option of an approximating function defines the character of trajectories and makes it possible to “visualize” correlation effects, which in this formulation of the problem are also determined by the expression for V_C. Actually, in this approach the value $V_0V_C(x,t)$ replaces the expression for the Eulerian correlation function $C_E(x,t)$. The simplest example of the approximation $V_C(x,t)$ was examined in [187] in the form that allows one to easily solve (2.769) and at the same time to satisfy the trapping character of transport

$$V_C(x,t)=V_0^2\exp\left(-\frac{x}{\lambda}\right)\exp\left(-\frac{t}{\tau}\right). \tag{2.770}$$

Here, λ is the characteristic spatial scale and τ is the characteristic time. Simple transformations of (2.769) yield the expression for the displacement

$$x(V_0,t)=\operatorname{sign}(V_0)\lambda\ln\left[1+\frac{|V_0|\tau}{\lambda}\left(1-\exp\left(-\frac{t}{\tau}\right)\right)\right]. \tag{2.771}$$

Then, taking into account the estimate $x(t\to\infty)\approx\lambda\ln[1+|V_0|\tau/\lambda]\approx\lambda\ln(1+Ku)$, which mirrors trapping, Vlad, Spineanu, Misguich, and Balescu carried out calculations of the correlation function (2.768) and the diffusion coefficient using the one-dimensional Maxwellian distribution

$$f(V_0)=\frac{1}{\sqrt{\pi}V_T}\exp\left(-\frac{V_0^2}{V_T^2}\right). \tag{2.772}$$

Here, V_T is the characteristic velocity of the one-dimensional Maxwellian distribution. Calculations yield

$$D_T = \frac{\tau}{\sqrt{\pi} V_T} \int_{-\infty}^{\infty} dV_0 \frac{V_0^2}{(1 + |V_0|\tau/\lambda)^2} \exp\left(-\frac{V_0^2}{V_T^2}\right). \tag{2.773}$$

The results of the calculations allow us to obtain the quasi-linear expression $D_T \approx V_0^2 \tau_c \propto Ku^2$ for the case $Ku \ll 1$, and "flat" scaling $D_T \propto Ku^\sigma$ with $\sigma \approx 0$ for the long-range correlation case $Ku \gg 1$.

The approach considered was subsequently developed in a number of papers [158, 187–189] where the two-dimensional model is analyzed in the framework of the special Hamiltonian function Ψ (the stream function) characterizing the trapping in the flow under consideration:

$$\frac{d\vec{x}}{dt} = -\nabla \Psi(\vec{x}, t) \times \vec{e}_Z = \left\langle \vec{V}\left(\vec{x}(t), t\right)\right\rangle\Big|_{V_0, \Psi_0}. \tag{2.774}$$

Here, $\Psi_0$is the initial value of the streamline function. Streamlines obtained in this approach are closed curves, except the single streamline, which is a straight line along the initial velocity V_0. In other words, the particles moving along closed streamlines do not make an essential contribution to the transport, if considered trajectories are localized. Actually, this case is opposite to the percolation one where a percolation streamline embraces almost the whole plane. The author of [158] found the universal character of the dependence of the effective diffusion coefficient D_T on the Kubo number for $Ku \gg 1$, $D_T \approx D_0 Ku^\sigma$. Here, $\sigma \approx 0.62$ and D_0 is the conventional (seed) coefficient of diffusion. This differs from the percolation result $\sigma = 7/10$ suggested in [83]. The majority of results in the model of decorrelation trajectories [158, 187, 188] were obtained by means of simulations. This is natural for a complex model where structures play an essential role.

2.22.2 The Hamiltonian Nature of the Universal Hurst Exponent

The problem of the description of nonlocality and memory effects is important not only for conventional space but also for phase-space. Thus, in 1940 Kramers [190] pointed out the difficulties encountered in an attempt to obtain the diffusion equation in ordinary coordinate space

$$\frac{\partial n}{\partial t} = D \frac{\partial^2 n}{\partial x^2} - \frac{\partial}{\partial x}(V_0 n) \tag{2.775}$$

from the simplest kinetic equation which includes spatial nonuniformity,

$$\frac{\partial f}{\partial t} + V \frac{\partial f}{\partial x} - F(x) \frac{\partial f}{\partial V} = \frac{1}{\tau} \frac{\partial}{\partial V}\left(V f + \frac{kT}{m} \frac{\partial f}{\partial V}\right). \tag{2.776}$$

Here, $f(t, V, x)$ is the particle distribution function, V is the velocity, T is the temperature, τ is the characteristic time, and m is the mass of the particle. Even here a demand arose for a nontrivial approach with integration over a "model trajectory" $r = r_0 + V\tau$ in lieu of "conventional averaging" with the fixed value r_0. Here, r_0 is an arbitrary initial point. This corresponds to the system of characteristic lines $dV/dt = -V/\tau$ and $dr/dt = V$. From this point of view one can see that it is possible to describe the spatial nonuniformity of the distribution function f at scales $\lambda \leq V_0\tau$: $f(t, V, x) \approx f(t, V, x + \lambda)$. This means that only local effects are described by (2.776). However, this argument was not effective enough for the introduction of corrections to the kinetic equation at that time. Kramers in fact pointed out the conventional character of the diffusion equation in use and to its close relation to the notions of the behavior of correlation functions. However, there are now papers of interest where fractional differentials are recommended for use in the description of the nondiffusive kinetic effects [191–194]. Naturally, relations between kinetic models, diffusion equations, and probabilistic estimates have to exist. On the one hand, the kinetic approach makes it possible to correctly take into account ballistic effects that are related to the convective fraction of hydrodynamic flows. On the other hand, the increase in the number of degrees of freedom, which is related to the velocity incorporation as an independent variable, permits the description of nonlocal effects related to spatial nonuniformity and stochastic layers.

Thus, recently Zaslavsky and Edelman [194] suggested a fruitful approach to relate phase-space properties of the sticky island boundary to continuous time random walk scalings. A regime close to the ballistic motion was considered on the basis of the fairly universal Hamiltonian function [74]

$$H_{\text{eff}} = b_1(\Delta\phi)^2 + b_2\Delta g - b_3(\Delta g)^3. \tag{2.777}$$

Here, $\Delta\phi$ and Δg are the deviations of the phase ϕ and the energy g values on the trajectory from their special quantities ϕ_* and g_* on the ballistic trajectory, which corresponds to an initial stage when an island is born. The ballistic kind of behavior is related to long-range trapping near the boundary of the sticky island [196]. It is possible to estimate the escape probability distribution $\psi(t)$ from the boundary layer in terms of the phase volume $\Delta\Gamma$:

$$\psi(t) \propto \frac{1}{\Delta\Gamma} \approx \frac{1}{\Delta\phi\Delta g}. \tag{2.778}$$

The authors of [195] suggested a solid estimate for the relationship between $\Delta\phi$ and Δg that is based on the Hamiltonian function (2.777): $\Delta\phi \propto \Delta g^{3/2}$. Then, one can express the phase volume in the scaling form

$$\Delta\Gamma \propto \Delta g^{5/2}. \tag{2.779}$$

This simple estimate mirrors the advantages of using additional degrees of freedom, which arises in the framework of the Hamiltonian approach. Escaping from the boundary layers implies that during an initial period Δg scales with time in accordance with $\Delta g \propto t$. Simple calculations [195] yield

$$\psi(t) \propto \frac{1}{\Delta\Gamma} \approx \frac{1}{\Delta g^{5/2}} \approx \frac{1}{t^{5/2}}. \tag{2.780}$$

This means that $\gamma = 3/2$. Now it is possible to obtain the Hurst exponent that describes transport effects (2.684):

$$H = \frac{\gamma}{2} = \frac{3}{4}. \tag{2.781}$$

This approach looks very attractive due to a universal kind of assumption about the relationship between ψ and $\Delta\Gamma$ (2.778). Indeed, different models give exponents [195, 196] which are very close to $H = 3/4$.

2.22.3 The One-Flight Model and Transport

The large variety of anomalous transport models leads to a search for "hyper-scalings" and relationships between exponents. This is not surprising since the analogous situation arose in considering phase transitions and percolation models. The investigation of relationships between the kinetic and correlation approaches plays an important role here. Thus, the simplest correlation scaling is the power approximation of the Lagrangian correlation function

$$C(t) \propto \frac{1}{t^{\gamma_c}}, \tag{2.782}$$

which, in accordance with the Taylor formula (2.6), yields the scaling for the mean displacement:

$$R \propto t^{1-\gamma_c/2}, \quad 0 < \gamma_c < 2. \tag{2.783}$$

This means that the Hurst exponent is expressed in terms of the temporal correlation exponent γ_c. Note that relations between the Lagrangian correlation function and the probability density $\psi(t)$, which plays an essential role in continuous time random walks, could exist.

Indeed, Zaslavsky [195] considered a ballistic model when the velocities $V(0)$ and $V(t)$ that enter into the Lagrangian correlation function $C(t) = \langle V(0)V(t)\rangle$ belong to the same flight. The analysis of [196] was based on the approximation of the anomalous diffusion in a map model [197] where the relationship

$$H = \frac{3-\gamma}{2} \tag{2.784}$$

was proposed. Here, γ is the exit time exponent (2.678). Formal calculations make it possible to obtain from (2.784) and (2.783) the scaling

$$\gamma_c = 1 - \gamma. \tag{2.785}$$

Zaslavsky suggested an interesting interpretation of this relationship in terms of the probability density $\psi = \Phi'(t) \propto 1/t^{\gamma+1}$. Actually, in the framework of the "one-flight" model, the correlation function $C(t)$ is proportional to the probability $P_{\mathrm{esc}}(t)$ that a particle will stay in the same flight at least during the time interval t. From the formal standpoint it can be rewritten in the functional form

$$C(t) \propto P_{\mathrm{esc}}(t) \approx \int_t^\infty dt_1 \int_{t_1}^\infty dt_2\, \psi(t_2). \tag{2.786}$$

One can see that the scaling interpretation of this expression leads to $\gamma_c = 1 - \gamma$.

It is natural to consider other approximations of relaxation functions $\Phi(t)$ as well. The Kohlrausch relaxation law (2.662) is an important example:

$$\Phi(t) \propto \exp\left(-\sqrt{\frac{t}{\tau}}\right). \tag{2.787}$$

Of particular interest is the fact that the Kohlrausch slowed relaxation law is related to the Laplace transformation of the familiar Levy's law for jumps with the exponent $\alpha_L = 1/2$:

$$\exp(-\sqrt{ws}) = \int_0^\infty \exp(-sx) f_{\alpha_L}(x)\, dx, \tag{2.788}$$

$$f_{\alpha_L}(x) = \frac{1}{2x^{3/2}}\sqrt{\frac{w}{\pi}} \exp\left(-\frac{w}{4x}\right). \tag{2.789}$$

This simple formula clearly shows a close relationship between the memory and non-locality effects. Physically, this relationship is not surprising. A particle that stays in a trap in phase space is not involved in events (does not undergo collisions). However, in conventional coordinate space, such a collisionless particle is transported over a large distance during the time it stays within the phase-space trap. In this sense, collisionless particles cannot be regarded as being involved in a conventional diffusion process, in contrast to the particles that undergo collisions.

The physical meaning of formal relationship (2.788) can easily be understood by treating its integral part as the averaging procedure for the Poisson law:

$$\exp(-sx) = \exp(-x/x_0). \tag{2.790}$$

As an example, let us consider the case $x = V$, $s = 1/x_0 \approx t/L_0$, $w = V_0$, where V is the particle's velocity V_0 is the characteristic velocity, and L_0 is the size of the region over which the averaging is performed. In this case, we have

$$\exp\left(-\sqrt{\frac{V_0}{L_0}t}\right) = \int_0^\infty \exp\left(-\frac{Vt}{L_0}\right) f(V)\, dV. \tag{2.791}$$

As a result, we see that the Kohlrausch relaxation law describes the Poisson's probability for a particle not to undergo collision in a region of size L_0 during the time t, averaged by means of a Levy distribution with $\alpha_L = 1/2$:

$$f(V) = f_{1/2}(V) \propto \frac{1}{V^{3/2}} \exp\left(-\frac{V_0}{4V}\right). \tag{2.792}$$

Note that power tails play an important role in the kinetic consideration of electron anomalous transport [198, 199] in the high temperature nonuniform plasma. Actually, for strongly nonequilibrium systems where accelerating and trapping mechanisms are present, it is necessary to take into account nondiffusive effects in describing the processes in phase-space.

2.22.4 Correlations and Nonlocal Velocity Distribution

From the common standpoint, just the distortion of the Maxwellian particle velocity distribution function leads to the difference between the transport equation in coordinate space and the classical diffusion one. It is obvious that the probabilistic interpretation is also effective for this case. Thus, the ballistic particle motion can be interpreted as trapping in phase space, since if collisions (interactions) are absent then the particle has constant velocity and hence does not change its position in the velocity space. The effectiveness of the one-flight approximation [197] indicates the possibility of using the ballistic character of motion for obtaining simple scaling estimates. Thus, the probability $\Phi(t)$ of avoiding an "event" (capture by a trap, for example) during time t can become the grounds for building a simple kinetic model. It is possible to represent this probability as a result of averaging over the ensemble of particles with the velocity distribution function $f(V)$.

Indeed, if the characteristic distance between traps is R, then the probability of avoiding trapping for a particle with velocity V could be the estimate in the form

$$w(V,t) \approx 1 - \frac{t}{T} \approx 1 - \frac{Vt}{R}. \tag{2.793}$$

Here, $T = R/V$ is the characteristic time for the particle with velocity V to reach a trap. This linear estimate can be interpreted as decomposition over the small parameter $Vt/R \ll 1$ of the conventional Poisson probability of avoiding an "event" during time t, $\exp(-Vt/R) \approx 1 - Vt/R$. In the framework of the randomization method, we can obtain the integral

$$\Phi(t) = \int_0^{Vt<R} w(V,t) f(V)\, dV. \tag{2.794}$$

Note that the upper limit of the integral is not constant: $V < R/t$. Then, the simple transformations of this expression yield the functional equation [200]

$$\Phi(t) = \int_0^{R/t} \left(1 - \left(\frac{Vt}{R}\right)\right) f(V)\, dV. \tag{2.795}$$

Following the Montroll–Weiss ideas [21, 22] we can assume that the function $\Phi(t)$ is known, or could be approximated by one of the characteristic probabilistic distributions. Then, it is possible to solve this integral equation. Using a double differentiation over t, we obtain the equation for the definition of the distribution $f(V)$. Thus, after the first differentiation of the functional, we obtain

$$\frac{d}{dt}\Phi(t) = -\psi(t) = -\int_0^{R/t} \frac{V}{R} f(V)\, dV. \tag{2.796}$$

Here, we take into account that the upper limit of the considered integral depends on time: $V = R/t$. The next differentiation yields

$$f(V) = \frac{R^2}{V^3}\frac{d^2}{dt^2}\Phi(t)\bigg|_{t=R/V} = -\frac{R^2}{V^3}\frac{d}{dt}\psi(t)\bigg|_{t=R/V}. \tag{2.797}$$

It is a very simple and at the same time nontrivial relationship, which connects kinetic and probabilistic characteristic functions. Now we can use characteristic functions for $\Phi(t)$. In the first case, we assume that $\Phi(t)$ has the exponential Poisson form, which corresponds to the absence of memory effects in the framework of continuous time random walks [18–22],

$$\Phi(t) = \exp\left(-\frac{t}{\tau}\right). \tag{2.798}$$

Here, τ is the characteristic time that is the parameter of the problem. Formal calculations then permit obtaining the mean waiting time by conventional averaging:

$$\langle t \rangle = \int_0^{\infty} t\psi(t)\, dt = \tau, \quad \text{where } \psi(t) = -\frac{d}{dt}\Phi(t) = \frac{1}{\tau}\exp\left(-\frac{t}{\tau}\right). \tag{2.799}$$

As a result of simple calculations for the Poisson case, we obtain the expression for the velocity distribution function $f(V)$,which depends on two parameters R and τ,

$$f(V) = \frac{1}{V^3}\left(\frac{R}{\tau}\right)^2 \exp\left(-\frac{R}{V\tau}\right). \tag{2.800}$$

For large values of V, one deals with the scaling $f(V) \propto 1/V^3$. In addition, the exponential factor of this function is nonanalytical with $V \to 0$ and therefore it cannot be obtained by the asymptotic technique from the diffusive phase-space Fokker–Planck equation.

In the framework of the scaling approach, it is important to consider the representation of the probability $\Phi(t)$ in the power form [18–22]:

$$\Phi(t) = \frac{1}{(1 + t/\tau)^{\gamma}}. \tag{2.801}$$

Here, $\gamma < 1$ is the characteristic exponent. In the continuous time random walk approach, this corresponds to the consideration of memory effects. However, in our case it is important that the mean waiting time $\langle t \rangle$ is an infinite value [18–22]. Upon substituting (2.801) into (2.797), we obtain the velocity distribution function,

$$f(V) \approx \gamma(\gamma + 1)\left(\frac{\tau}{R}\right)^{\gamma} \frac{1}{V^{1-\gamma}}. \tag{2.802}$$

This corresponds to the relationship between both kinetic exponent β and waiting time exponent γ: $\beta = 1 - \gamma$. Note that this distribution leads to the fractal character of collisionless particles phase space $\delta N(V) \propto f(V)V \propto V^{\beta}$ with the dimensionality $d_F = \beta$. Here, δN is the collisionless particles number. These scalings characterize systems under the unconventional condition $\langle t \rangle = \infty$, which differs significantly from the conventional Poisson model, where the mean waiting time $\langle t \rangle$ is finite.

2.22.5 The Arrhenius Law and Phase-Space Distribution

An interesting example of a long-tailed distribution is found by considering a particle in a potential well of height E. Now suppose the random time the particle spends in the well is governed by Arrhenius's law:

$$\tau = \tau_0 \exp\left(\frac{E}{kT}\right), \tag{2.803}$$

where $1/\tau_0$ is the frequency, k is the Boltzmann constant, and T is the temperature. The barrier height E is a random variable governed by the probability distribution $f(E)$,

$$f(E) = \exp\left(-\frac{E}{E_0}\right), \tag{2.804}$$

where E_0 is the width of the barrier height distribution. This distribution of barrier heights introduces a distribution of trapping times

$$\psi(\tau)\, d\tau = f(E)\, dE. \tag{2.805}$$

From (2.803), (2.804), and (2.805) we find the trapping times distribution

$$\psi(\tau) = \frac{kT\tau_0^{-\gamma_A}}{\tau^{1+\gamma_A}}, \tag{2.806}$$

where $\gamma_A = \frac{kT}{E_0}$. Here, we have an exponent of long-tailed probability distribution, which could change continuously as the temperature parameter changes. If γ_A is greater than unity, the first moment of the waiting time distribution will become finite. However, for $0 < \beta < 1$, it will be infinite. In this case, the point set of jump times will look like a randomized Carton set of dimension β, hence the name "fractal time". Actually the combination of both the Arrhenius law and the Boltzmann distribution leads to a power law for escape probability. The exponent describing the escape probability in the case considered above depends on the energetic parameters of the model.

However for nonequilibrium states, the distribution function can differ significantly from the Boltzmann one [200, 201]. Thus, nontrivial distribution functions naturally lead to the necessity of considering relaxation laws different from the Arrhenius law. As an example, let us obtain a relaxation law corresponding to a Levy-like velocity distribution function:

$$\psi(\tau)\,d\tau = \frac{\tau_0}{\tau^{\gamma_A+1}}\,d\tau = \text{const}\cdot\exp\left(-\frac{E_0}{E}\right)^{\beta_A}\frac{E_0^{\beta_A}}{E^{\beta_A+1}}\,dE. \tag{2.807}$$

Simple calculations yield the relaxation law in the form

$$\tau = \left[\exp\left(\frac{E}{E_0}\right)^{\beta_A}\right]^{\frac{1}{\gamma_A}}. \tag{2.808}$$

Here, the case $\beta_A = \frac{1}{2}$ corresponds to the Levy distribution. The obtained expression also includes two parameters, β_A and γ_A, which characterize both the kinetics of particles and trapping effects. This makes it possible to consider nontrivial transport effects, where long-tailed distributions play an essential role [202].

2.23 Conclusion

Naturally, it is impossible to consider all the aspects of turbulent transport within the framework of one article. Therefore, in this paper we focused on scaling arguments that play an important role in obtaining estimates of transport effects. All necessary calculations were considered in detail. In the framework of the mean field theory, of course, many important problems cannot be considered; however, one of the main tasks is to establish the character of the dependence of the transport coefficient on such parameters as fluctuation amplitude, characteristic size, characteristic time, etc. For these purposes, the considered approach is effective.

Acknowledgments The author thanks V. Shafranov, V. Kogan, E. Yurchenko, R. Balescu, G. Zaslavsky, S. Shandarin, and T. Schep for the useful discussions and support. The author is also indebted to A. Dnestrovsky, Y. Igitchanov, V. Ilgisonis, A. Kukushkin, A. Loskutov, D. Morozov, V. Pustovitov, A. Runov, R. Shurigin and Hugo de Blank for their reviews and for their invaluable help in proofreading the manuscript.

References

[1] J. Wesson, *Tokamaks* (Clarendon, Oxford, 1987)
[2] B.B. Kadomtsev, *Tokamak Plasma: A Complex System* (IOP, Bristol, 1992)
[3] W. Horton, Y.-H. Ichikawa, *Chaos and Structures in Nonlinear Plasmas* (World Scientific, Singapore, 1994)
[4] J. Weiland, *Collective Models in Inhomogeneous Plasma: Kinetic and Advanced Fluid Theory* (IOP, Bristol, 2000)
[5] M.N. Rosenbluth, R.Z. Sagdeev (eds.), *Handbook of Plasma Physics* (North-Holland, Amsterdam, 1984)
[6] P.H. Diamond, Plasma Phys. Control. Fusion **47**, R35 (2005)
[7] J.A. Krommes, Phys. Rep. **360**, 1–352 (2002)

[8] A. Yoshizawa, S.-I. Itoh, K. Itoh, N. Yokoi, Plasma Phys. Control. Fusion **43**, R1 (2001)
[9] A. Brandenburg, Phys. Rep. **417**, 1 (2005)
[10] B. Eliasson, Phys. Rep. **422**, 225 (2006)
[11] P.W. Terry, Rev. Mod. Phys. **72**, 109 (2000)
[12] B.D. Chandran, S.C. Cowley, Phys. Rev. Lett. **80**, 3077 (1998)
[13] S. Chandrasekhar, Rev. Mod. Phys. **15**, 1 (1943)
[14] N.G. van Kampen, *Stochastic Processes in Physics and Chemistry* (North-Holland, Amsterdam, 1981)
[15] Y.B. Zel'dovich, A.D. Myshkis, *Principles of Mathematical Physics* (Nauka, Moscow, 1973)
[16] P. Résibois, M. De Leener, *Classical Kinetic Theory of Fluids* (Wiley, New York, 1977)
[17] M.B. Isichenko, Rev. Mod. Phys. **64**, 961 (1992)
[18] J.P. Bouchaud, A. Georges, Phys. Rep. **195**, 132–292 (1990)
[19] J.W. Haus, K.W. Kehr, Phys. Rep. **150**, 263 (1987)
[20] R. Balescu, *Statistical Dynamics* (Imperial College Press, London, 1997)
[21] M.F. Shlesinger, G.M. Zaslavsky, U. Frisch, *Levy Flights and Related Topics in Physics*. Lecture Notes in Physics, vol. 450 (Springer, New York, 1995)
[22] R. Metzler, J. Klafter, Phys. Rep. **339**, 1 (2000)
[23] A. Vedenov, E.P. Velikhov, R.Z. Sagdeev, Plasma Phys. Control. Nucl. Fusion Res. **2**, 82 (1962)
[24] W.E. Drummond, D. Pines, Plasma Phys. Control. Nucl. Fusion Res. **3**, 1049 (1962)
[25] A.M. Yaglom, *Correlation Theory of Time-Independent Random Functions* (Gidrometeoizdat, Leningrad, 1981)
[26] V.I. Klyatskin, *Stochastic Equations by the Physicist's Eyes* (Fizmatlit, Moscow, 2001)
[27] A.S. Monin, A.M. Yaglom, *Statistical Fluid Mechanics; Mechanics of Turbulence* (MIT Press, Cambridge, 1971)
[28] F.N. Frenkiel (ed.), *Atmospheric Diffusion and Air Pollution* (Academic Press, New York, 1959)
[29] W. Frost, T.H. Moulden (eds.), *Handbook of Turbulence* (Plenum, New York, 1977)
[30] U. Frisch, *Turbulence: The Legacy of A.N. Kolmogorov* (Cambridge University Press, Cambridge, 1995)
[31] G.I. Taylor, Proc. Lond. Math. Soc. Ser. 2 **20**, 196 (1921)
[32] H.K. Moffatt, J. Fluid Mech. **106**, 27 (1981)
[33] H.K. Moffatt, Rep. Prog. Phys. **46**, 621 (1983)
[34] S. Corrsin, Random Geometric Problems Suggested by Turbulence, in *Statistical Models and Turbulence: Proceedings of a Symposium*, ed. by M. Rosenblatt, C. van Atta. San Diego CA, USA, 15–21 July 1971. Lecture Notes in Physics, vol. 12 (Springer, Berlin, 1975), p. 300
[35] Y.B. Zel'dovich, Sov. Phys. Dokl. **27**, 797 (1982)
[36] Y.B. Zel'dovich, S.A. Molchanov, A.A. Ruzmaĭkin, D.D. Sokolov, Sov. Phys. Usp. **30**, 353 (1987)
[37] A.A. Galeev, M.M. Kuznetsova, L.M. Zelenyi, Space Sci. Rev. **44**, 1 (1986)
[38] J.A. Krommes, Prog. Theor. Phys. Suppl. **64**, 137 (1978)
[39] J.A. Krommes, J. Plasma Phys. **30**, 11 (1983)
[40] O.G. Bakunin, Plasma Phys. Control. Fusion **47**, 1857 (2005)
[41] M. Avellaneda, A.J. Majda, Phys. Fluids **4**, 41 (1992)
[42] O.G. Bakunin, J. Plasma Phys. **72**, 647 (2006)
[43] G. Falkovich, K. Gawedzki, M. Vergassola, Rev. Mod. Phys. **73**, 913 (2001)
[44] S.I. Vainshtein, *Magnetic Fields in Space* (Nauka, Moscow, 1983)
[45] L. Fradkin, Plasma Phys. Control. Fusion **33**, 685 (1991)

[46] O.G. Bakunin, Plasma Phys. Rep. **29**, 955 (2003)
[47] A. Fanjiang, J. Stat. Phys. **88**, 1033 (1997)
[48] R.J. Bickerton, Plasma Phys. Control. Fusion **39**, 339 (1997)
[49] D. Stauffer, *Introduction to Percolation Theory* (Taylor & Francis, London, 1985)
[50] H.E. Stanley, J. Stat. Phys. **34**, 843 (1984)
[51] I.M. Sokolov, Sov. Phys. Usp. **29**, 924 (1986)
[52] J.M. Ziman, *Models of Disorder: The Theoretical Physics of Homogeneously Disordered Systems* (Cambridge University Press, Cambridge, 1979)
[53] D. Stauffer, Phys. Rep. **54**, 1 (1979)
[54] R. Narayan, Phys. Rev. Lett. **42**, 1247 (1999)
[55] H.E. Stanley, J. Stat. Phys. **34**, 843 (1984)
[56] B.B. Mandelbrot, *Fractals: Form, Chance, and Dimension* (Freeman, San Francisco, 1977)
[57] J. Feder, *Fractals* (Plenum, New York, 1988)
[58] L.F. Richardson, Proc. R. Soc. Lond. Ser. A **110**, 709 (1926)
[59] G.K. Batchelor, Proc. Camb. Philos. Soc. **48**, 345 (1952)
[60] B.I. Davydov, C. R. Acad. Sci. USSR **2**, 216 (1934)
[61] A. Khintchine, P. Lévy, C. R. Acad. Sci. (Paris) **202**, 274 (1936)
[62] A.S. Monin, Dokl. Akad. Nauk SSSR **105**, 256 (1955)
[63] A.N. Kolmogorov, Dokl. Akad. Nauk SSSR **30**, 299 (1941)
[64] T.H. Dupree, Phys. Fluids **9**, 1773 (1966)
[65] T.H. Dupree, Phys. Fluids **10**, 1049 (1967)
[66] T.H. Dupree, Phys. Fluids **15**, 334 (1972)
[67] B.B. Kadomtsev, O.P. Pogutse, in *Plasma Physics and Controlled Nuclear Fusion Research, Proceedings of the 7th International Conference*, IAEA Vienna, 1978. Nuclear Fusion Supplement, vol. 1 (1979), p. 649
[68] B.J. Berne, J. Chem. Phys. **56**, 2164 (1972)
[69] G.G. Getmantsev, Sov. Astron. Rep. **6**, 477 (1962)
[70] J.R. Jokipii, E.N. Parker, Astrophys. J. **155**, 777 (1969)
[71] J.B. Taylor, B. McNamara, Phys. Fluids **14**, 1492 (1971)
[72] Yu.A. Dreizin, A.M. Dykhne, Sov. Phys. JETP **36**, 127 (1973)
[73] I.D. Howells, J. Fluid Mech. **9**, 104 (1960)
[74] G.M. Zaslavskiĭ, B.V. Chirikov, Sov. Phys. Usp. **14**, 549 (1972)
[75] A.B. Rechester, M.N. Rosenbluth, Phys. Rev. Lett. **40**, 38 (1978)
[76] B.B. Mandelbrot, J. Fluid Mech. **72**, 401 (1975)
[77] U. Frisch, P.-L. Sulem, M. Nelkin, J. Fluid Mech. **87**, 719 (1978)
[78] H.G.E. Hentschel, I. Procaccia, Phys. Rev. A **29**, 1461 (1984)
[79] M.E. Levinshtein, B.I. Shklovsky, M.S. Shur, A.L. Efros, J. Exp. Theor. Phys. **42**, 112 (1976)
[80] M.V. Osipenko, O.P. Pogutse, N.V. Chudin, Sov. J. Plasma Phys. **13**, 550 (1987)
[81] M.N. Rosenbluth, H.L. Berk, I. Doxas, W. Horton, Phys. Fluids **30**, 2636 (1987)
[82] M.B. Isichenko, Y.L. Kalda, E.V. Tatarinova, O.V. Tel'kovskaya, V.V. Yankov, Sov. Phys. JETP **69**, 517 (1989)
[83] A.V. Gruzinov, M.B. Isichenko, Y.L. Kalda, Sov. Phys. JETP **70**, 263 (1990)
[84] P.N. Yushmanov, Comments Plasma Phys. Control. Fusion **14**, 313 (1992)
[85] M.B. Isichenko, J. Kalda, J. Nonlinear Sci. **1**, 255 (1991)
[86] M.B. Isichenko, J. Kalda, J. Nonlinear Sci. **1**, 375 (1991)
[87] B.Y. Balagurov, V.G. Vaks, Sov. Phys. JETP **38**, 968 (1974)
[88] P. Langevin, C. R. Acad. Sci. (Paris) **146**, 530 (1908)
[89] A. Einstein, Ann. Phys. (Leipzig) **17**, 549 (1905)

[90] J. Kampé de Feriet, Ann. Soc. Sci. Bruxelles **59**, 145 (1939)
[91] A.M. Obukhov, C. R. Acad. Sci. URSS **32**, 19 (1941)
[92] C. Cattaneo, Atti Semin. Mat. Fis. Univ. Modena **3**, 83 (1949)
[93] S. Goldstein, Q. J. Mech. Appl. Math. **4**, 129 (1951)
[94] R.W. Davies, Phys. Rev. **93**, 1169 (1954)
[95] O.G. Bakunin, Phys. Usp. **46**, 309 (2003)
[96] G.M. Zaslavsky, B.A. Niyazov, Phys. Rep. **283**, 73 (1997)
[97] G.M. Zaslavsky, Chaos **4**, 25 (1994)
[98] A. Okubo, J. Oceanol. Soc. Jpn. **20**, 286 (1962)
[99] M. Smoluchowski, Phys. Z. **17**, 557 (1916)
[100] S. Chapman, Philos. Trans. R. Soc. Ser. A **216**, 279 (1916)
[101] A. Kolmogoroff, Math. Ann. **104**, 415 (1931)
[102] A. Cauchy, C. R. Acad. Sci. (Paris) **37**, 292 (1853)
[103] L.O. Silva, Astrophys. J. Lett. **596**, L121 (2006)
[104] O.V. Tel'kovskaya, K.V. Chukbar, J. Exp. Theor. Phys. **85**, 87 (1997)
[105] J. Weinstock, Phys. Fluids **19**, 1702 (1976)
[106] R.H. Kraichnan, J. Fluid Mech. **81**, 385 (1977)
[107] R.H. Kraichnan, Phys. Fluids **13**, 22 (1970)
[108] T.S. Lundgren, Y.B. Pointin, Phys. Fluids **19**, 355 (1976)
[109] J.S. Hay, F. Pasquill, Adv. Geophys. **6**, 345 (1959)
[110] Y. Kaneda, T. Ishida, J. Fluid Mech. **402**, 311 (2000)
[111] A.I. Smolyakov, P.N. Yushmanov, Nucl. Fusion **33**, 383 (1993)
[112] C. Cambon, F.S. Godeferd, F.C.G.A. Nicolleau, J.C. Vassilicos, J. Fluid Mech. **499**, 231 (2004)
[113] D.L. Koch, J.F. Brady, Phys. Fluids A **1**, 47 (1990)
[114] E.B. Tatarinova, P.A. Kalugin, A.V. Sokol, Europhys. Lett. **14**, 773 (1991)
[115] O.G. Bakunin, Phys. Usp. **46**, 733 (2003)
[116] M.B. Isichenko et al., Phys. Fluids B **4**, 3973 (1992)
[117] G.I. Taylor, Proc. R. Soc. Lond. Ser. A **219**, 186 (1953)
[118] G.I. Taylor, Proc. R. Soc. Lond. Ser. A **223**, 446 (1954)
[119] W.R. Young, S. Jones, Phys. Fluids A **3**, 1087 (1991)
[120] G. Matheron, G. de Marsily, Water Resour. Res. **16**, 901 (1980)
[121] J.-P. Bouchaud et al., Phys. Rev. Lett. **64**, 2503 (1990)
[122] S. Redner, Physica D **38**, 287 (1989)
[123] B.B. Kadomtsev, Cooperative effects in plasmas, in *Reviews of Plasma Physics*, vol. 22, ed. by V.D. Shafranov (Kluwer Academic/Consultants Bureau, New York, 2001), p. 1
[124] A.S. Kingsep, *Introduction to the Nonlinear Plasma Physics* (Mosk. Fiz.-Tekh. Inst., Moscow, 1996)
[125] V.N. Tsytovich, *Theory of Turbulent Plasma* (Consultants Bureau, New York, 1977)
[126] M.N. Rosenbluth, R.Z. Sagdeev, L.B. Taylor, Nucl. Fusion **6**, 297 (1966)
[127] R.W. Flynn, Phys. Fluids **14**, 956 (1971)
[128] K.N. Graham, J.A. Fejer, Phys. Fluids **19**, 1054 (1976)
[129] F. Doveil, D. Grésillon, Phys. Fluids **25**, 1396 (1982)
[130] O. Ishihara, A. Hirose, Comments Plasma Phys. Control. Fusion **8**, 229 (1984)
[131] A. Salat, Z. Naturforsch. A **38**, 1189 (1983)
[132] O. Ishihara, A. Hirose, Phys. Fluids **28**, 2159 (1985)
[133] A. Salat, Phys. Fluids **31**, 1499 (1988)
[134] O. Ishihara, H. Xia, A. Hirose, Phys. Fluids B **4**, 349 (1992)
[135] R. Balescu, H.-D. Wang, J.H. Misguich, Phys. Plasmas **1**, 3826 (1994)

[136] D. Bohm, E. Burhop, in *The Characteristics of Electrical Discharges in Magnetic Fields*, ed. by A. Guthrie, R.K. Wakerling (McGraw-Hill, New York, 1949)
[137] V.S. Ptuskin, Astrophys. Space Sci. **61**, 251 (1979)
[138] T.H. Stix, Nucl. Fusion **18**, 353 (1978)
[139] A.B. Rechester, M.N. Rosenbluth, R.B. White, Phys. Rev. Lett. **42**, 1247 (1979)
[140] B.B. Mandelbrot, *The Fractal Geometry of Nature* (Freeman, San Francisco, 1982)
[141] L.F. Richardson, in *General System Yearbook of the Society for the Advancements of General System Theory*, vol. 6 (The Society for General Systems Research, Ann Arbor, 1961), p. 139
[142] J. Klafter, A. Blumen, M.F. Shlesinger, Phys. Rev. A **35**, 3081 (1987)
[143] W.D. McComb, *The Physics of Fluid Turbulence* (Clarendon, Oxford, 1994)
[144] A. Bunde, J.F. Gouyet, J. Phys. A: Math. Gen. **18**, L285 (1985)
[145] H. Saleur, B. Duplantier, Phys. Rev. Lett. **58**, 2325 (1987)
[146] B. Sapoval, B. Rosso, J. Gouyet, J. Phys. Lett. (Paris) **46**, L149 (1985)
[147] S.A. Trugman, Phys. Rev. B **27**, 7539 (1983)
[148] O.G. Bakunin, Chaos Solitons Fractals **23**, 1703 (2005)
[149] O.G. Bakunin, Physica A **345**, 1 (2005)
[150] M.B. Isichenko, Plasma Phys. Control. Fusion **33**, 795 (1991)
[151] M.B. Isichenko, Plasma Phys. Control. Fusion **33**, 809 (1991)
[152] M. Ottaviani, Europhys. Lett. **20**, 111 (1992)
[153] J.-D. Reuss, J.H. Misguich, Phys. Rev. E **54**, 1857 (1996)
[154] G. Zimbardo, P. Veltri, P. Pommois, Phys. Rev. E **61**, 1940 (2000)
[155] Y.B. Zeldovich, JETP Lett. **38**, 57 (1983)
[156] O.G. Bakunin, Plasma Phys. Control. Fusion **45**, 1909 (2003)
[157] O.G. Bakunin, J. Plasma Phys. **71**, 435 (2005)
[158] M. Vlad, F. Spineanu, J.H. Misguich, R. Balescu, Phys. Rev. E **58**, 7359 (1998)
[159] M. Matsushita, S. Ouchi, K. Honda, J. Phys. Soc. Jpn. **60**, 2109 (1991)
[160] S. Isogami, M. Matsushita, J. Phys. Soc. Jpn. **61**, 1445 (1992)
[161] J. Kondev, C.L. Henley, Phys. Rev. Lett. **74**, 4580 (1995)
[162] J. Kondev, C.L. Henley, D.G. Salinas, Phys. Rev. E **61**, 104 (2000)
[163] J. Kondev, G. Huber, Phys. Rev. Lett. **86**, 5890 (2001)
[164] J. Kalda, Phys. Rev. E **64**, 020101 (2001)
[165] J. Kalda, Phys. Rev. Lett. **90**, 118501 (2003)
[166] O.G. Bakunin, Physica A **351**, 241 (2005)
[167] O.G. Bakunin, T.J. Schep, Phys. Lett. A **322**, 105 (2004)
[168] O.G. Bakunin, Physica A **347**, 289 (2004)
[169] V.E. Kravtsov, I.V. Lerner, V.I. Yudson, Sov. Phys. JETP **64**, 336 (1986)
[170] O.G. Bakunin, Physica A **348**, 245 (2005)
[171] I.A. Lubashevskiĭ, A.A. Zemlyanov, J. Exp. Theor. Phys. **87**, 700 (1998)
[172] P.S. Iroscnikov, Astron. J. **40**, 742 (1963)
[173] R.H. Kraichnan, Phys. Fluids **8**, 1385 (1965)
[174] E.W. Montroll, G.H. Weiss, J. Math. Phys. **6**, 167 (1965)
[175] H. Scher, E.W. Montroll, Phys. Rev. B **12**, 2455 (1975)
[176] P. Goldreich, S. Sridhar, Astrophys. J. **485**, 680 (1997)
[177] A. Compte, J. Camacho, Phys. Rev. E **56**, 5445 (1997)
[178] M.F. Shlesinger, B.J. West, J. Klafter, Phys. Rev. Lett. **58**, 1100 (1987)
[179] R. Balescu, Plasma Phys. Control. Fusion **42**, B1 (2000)
[180] R. Balescu, Phys. Rev. E **51**, 4807 (1995)
[181] O.G. Bakunin, Rep. Prog. Phys. **67**, 965 (2004)
[182] K.V. Chukbar, J. Exp. Theor. Phys. **82**, 719 (1996)

[183] O. Cardoso, P. Tabeling, Europhys. Lett. **7**, 225 (1988)
[184] O. Cardoso, P. Tabeling, Eur. J. Mech. B: Fluids **8**, 459 (1989)
[185] T.H. Solomon, E.R. Weeks, H.L. Swinney, Physica D **76**, 70 (1994)
[186] E.R. Weeks, J.S. Urbach, H.L. Swinney, Physica D **97**, 291 (1996)
[187] J.-D. Reuss, F. Spineanu, J.H. Misguich, J. Plasma Phys. **59**, 707 (1998)
[188] M. Vlad, F. Spineanu, J.H. Misguich, R. Balescu, Phys. Rev. E **63**, 066304 (2001)
[189] M. Vlad, F. Spineanu, J.H. Misguich, R. Balescu, Phys. Rev. E **66**, 038302 (2002)
[190] H.A. Kramers, Physica **7**, 284 (1940)
[191] G.M. Zaslavsky, Chaos **4**, 25 (1994)
[192] A.V. Chechkin, V.Y. Gonchar, J. Exp. Theor. Phys. **91**, 635 (2000)
[193] O.G. Bakunin, Plasma Phys. Rep. **29**, 785 (2003)
[194] O.G. Bakunin, Plasma Phys. Rep. **30**, 338 (2004)
[195] G.M. Zaslavsky, M. Edelman, Chaos **10**, 135 (2000)
[196] C.F.F. Karney, Physica D **8**, 360 (1983)
[197] O.G. Bakunin, S.I. Krasheninnikov, Plasma Phys. Rep. **21**, 502 (1995)
[198] O.G. Bakunin, S.I. Krasheninnikov, Plasma Phys. Rep. **16**, 501 (1990)
[199] O.G. Bakunin, Phys. Lett. A **330**, 22 (2004)
[200] A.S. Mikhailov, Phys. Rep. **425**, 79 (2006)
[201] T.M. Squires, Rev. Mod. Phys. **77**, 977 (2005)
[202] O.G. Bakunin, Physica A **346**, 284 (2005)